578504

Analysis Report for AP-194

Analysis Report for Evaluation and Analysis of Current and Historical WIPP Culebra Groundwater Quality Data, under Analysis Plan: AP-194 Rev.0

AP-194: Analysis Plan to Evaluate and Analyze Current and Historical WIPP Groundwater Quality Data

Task Number 4.4.2.3.1

Authored by:	*Signature on File*	11-22-2022
	Leslie Kirkes, 8882 Repository Performance, SNL	Date
	Signature on File	11-22-2022
	Mike Farinacci, 8882 Intera, Inc	Date
	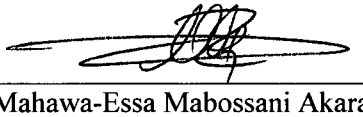	11-22-2022
	Mahawa-Essa Mabossani Akara, 8882 Repository Performance	Date
	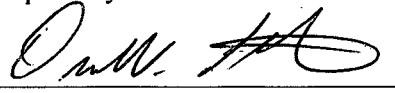	11-22-2022
	Owen Lofton, 8882 RESPEC, Inc	Date
Technical Review:	*Signature on File*	11-22-2022
	Tricia Johnson, 8882 Intera, Inc	Date
QA Review:	*Signature on File*	11-22-2022
	Shelly R. Nielsen, 8880 Edgewater, Inc	Date
Management Review:	*Signature on File*	11-22-2022
	Chammi Miller, 8882 Manager, Repository Performance	Date

WIPP:4.4.2.3.1:TD:QA-L:RECERT:578441 ~~578504~~ clh 1/6/22

Information Only

Table of Contents

1 Introduction 5
1.1 Geologic Setting/Study Area 7
1.2 Evaporite Mineral Dissolution 14
1.3 Previous Studies 20
1.4 Data Sources 22
1.5 Data Acceptability 25
2 Methods 34
2.1 Computer Codes and Programs 34
2.2 Water Types and Classifications 34
2.2.1 Correlation Matrix Analysis 34
2.2.2 Map generation 35
3 Results 37
3.1.1 Hydro-chemical Facies/Zones Updates 37
3.1.2 Correlation Analysis 38
3.1.3 Water Type Diagrams and Graphs 46
3.1.4 Saturation Indices of Key Minerals in the Culebra 50
3.1.5 Major Ion Relationships in the Culebra groundwater 61
3.1.6 Chloride vs. Bromide ratio for the Culebra 89
3.1.7 Hydrogeochemistry and Flow Patterns 93
4 Discussion/Summary 96
5 Conclusions 103
6 References 126

Table of Figures

Figure 1 Various examples of porosity and fracture structure of the Culebra Dolomite (Malama, et al. 2013) 7
Figure 2 Major hydrologic features of hydrologically closed basins (Deocampo and Jones, 2003) 8
Figure 3 Stratigraphy of the Rustler Formation, Mudstone/Halite (M/H) margins shown in color (Kuhlman and Barnhart, 2011). 9
Figure 4 M1/H1 Margin (Powers, 2007) and Culebra Wells in this Study 10
Figure 5 M2/H2 Margin (Powers, 2007) and Culebra Wells in this Study 11
Figure 6 M3/H3 Margin (Powers, 2007) and Culebra Wells in this Study 12
Figure 7 M4/H4 Margin (Powers, 2007) and Culebra Wells in this Study 13
Figure 8 Brine evolution diagram, modified from Hardie and Eguster 1978, and Lak, et al. 2022 15
Figure 9 WIPP Wells Included in This Study 18
Figure 10 WIPP Well Network 2022 19
Figure 11 Well AEC-7R in relation to the M2/H2 and M4/H4 Mudstone/Halite Margins 22
Figure 12 Contour Map Example with Equal Interval Classification 35
Figure 13 Contour Map Example with Quantile Interval Classification 36

Information Only

Figure 14 Facies/Zone Map Zone A Update (Blue oval represents the updated region of Zone A) 37
Figure 15 2022 Updated Facies/Zone Map in Relation to Well Locations 38
Figure 16 Culebra waters Ion concentration (molality) vs. Ionic Strength (molality) 40
Figure 17 Culebra waters Ion Concentration (m) vs. Ionic Strength (m) focused 40
Figure 18 Piper Diagram of the Culebra Well Network 47
Figure 19 Example of Chadha Diagram 48
Figure 20 Chadha Diagram for Culebra well data 48
Figure 21 Culebra water: (Ca^{2+}+ Mg^{2+}) vs. (HCO_3^- + SO_4^{2-}) 49
Figure 22 Culebra water: (Ca^{2+}+ Mg^{2+}) vs. (HCO_3^- + SO_4^{2-}) zoomed 49
Figure 23 Calcite Saturation Index Map for Culebra network 56
Figure 24 Dolomite Saturation Index Map of Culebra Network 59
Figure 25 Magnesite Saturation Index Map for the Culebra network 60
Figure 26 Comparison of Saturation Indices of Dolomite (left) and Magnesite (right) (Note: The legends in Figure 24 and Figure 25 apply to these subset maps) 61
Figure 27 Sodium/Chloride Molar Ratio of Culebra Network 64
Figure 28 Sodium/Chloride Molar Ratio Contour Map of Culebra Network (tan indicates presence of halite) 65
Figure 29 Magnesium/Calcium Molar Ratio of the Culebra 67
Figure 30 Magnesium/Calcium Molar Ratio Contour Maps of the Culebra Network (Data Set #1) 69
Figure 31 Magnesium/Calcium Molar Ratio Contour Map of the Culebra Network (Data Set #2) 70
Figure 32 Bicarbonate/Magnesium meq/L for the Culebra Network 72
Figure 33 Calcium/Sulfate Molar Ratio of the Culebra Network 73
Figure 34 Calcium/Sulfate Molar Ratio for Culebra (Data Set #1) 74
Figure 35 Calcium/Sulfate Molar Ratio for Culebra (Data Set #2) 75
Figure 36 Culebra Geological Areas Identified with Either Low or No Gypsum 76
Figure 37 Comparison of Low Gypsum Area and Calcium/Sulfate Molar Ratio for Data Set #1 (Note: The legend shown in Figure 34 applies to this subset map) 77
Figure 38 Comparison of Low Gypsum Area and Calcium/Sulfate Molar Ratio for Data Set #2 (low gypsum line in red) (Note: The legend shown in Figure 35 applies to this subset map) 77
Figure 39 Sulfate Molality in the Culebra Network with Diffusivity Line 78
Figure 40 Calcium meq/L versus Calcium + Sulfate meq/L 80
Figure 41 Contour map of $Ca^{2+}/(Ca^{2+}+SO_4^{2-})$ meq/L (Data Set #1) 83
Figure 42 Contour map of $Ca^{2+}/(Ca^{2+} + SO_4^{2-})$ meq/L (Data Set #2) 84
Figure 43 Cation Exchange between Sodium and Calcium Zone C 85
Figure 44 Cation Exchange between Sodium and Calcium Zone C (anomalous wells removed) 86
Figure 45 Culebra Wells that Have Undergone Cation Exchange 87
Figure 46 Culebra Wells Having Undergone Cation Exchange 89
Figure 47 Plot of Cl/Br ratio vs. Cl (in mg/L) for six main salinity acquisition processes (Alcala and Custodio, 2008) 91
Figure 48 Cl^-/Br^- Molar Ratio vs. Cl^- Observed in the Culebra Network 92
Figure 49 Culebra Groundwater Flow Map, 2020 (US DOE, 2021) 94
Figure 50 Freshwater head calculated values vs. hydrogeochemical zones 95

Information Only

Tables

Table 1 Chemical Formula of Relevant Minerals 6
Table 2 Detailed Geology Description of Rustler Formation (summarized from Holt and Powers, 1988 and Kuhlman and Barnhart, 2011) 14
Table 3 Relevant Mineral Dissolution Reactions 15
Table 4 Hydro-geochemical Zones/Facies developed by Siegel, et al. 1991 and Domski and Beauheim, 2008 21
Table 5 Hydro-geochemical Facies zones developed by Siegel, et al. 1991 and Domski and Beauheim, 2008. Updated 2022 21
Table 6 Summary of Average, CVs, and PHREEQCI Cation/Anion Percent Error for Data Set #1: Culebra_2017-2020 27
Table 7 Summary of Average, CVs, and PHREEQCI Cation/Anion Percent Error for Data Set #2: Culebra_ALL 30
Table 8 Summary of Average, CVs, and PHREEQCI Cation/Anion Percent Error for Data Set #3: WQSP_Culebra_Wells 33
Table 9 Correlation analysis for all Culebra Facies Zones A-E (Combined zones) 39
Table 10 Correlation Matrix Facies Zone A 41
Table 11 Correlation Matrix Facies Zone A/C 42
Table 12 Correlation Matrix Facies Zone B 42
Table 13 Correlation Matrix Facies Zone B/C 43
Table 14 Correlation Matrix Facies Zone C 44
Table 15 Correlation Matrix Facies Zone D/E 45
Table 16 Ionic Strength (μ) and Mineral Saturation Index Values for Key Culebra Minerals 51
Table 17 Cation Exchange Type in Relation to $Na^+/(Na^+/Cl^-)$ 66
Table 18 Cation Exchange Type in Relation to $Ca^{2+}/(Ca^{2+}+SO_4^{2-})$ 80
Table 19 Culebra wells that have undergone Cation Exchange 88
Table 20 Lowest and Highest Cl/Br Molar Ratios in WIPP Well Network 92
Table 21 Hydrogeochemical Facies zones developed by Siegel, et al. 1991, Domski and Beauheim, 2008. Updated 2022 97

Information Only

1 Introduction

This Analysis Report (AR) discusses the aqueous geochemistry associated with the Culebra Dolomite member of the Rustler Formation, in the Delaware Basin. Data in this report document the available chemical conditions that have been documented for the Waste Isolation Pilot Plant (WIPP) Monitoring Well Network, spanning a time period of 1978-2021. Data was analyzed to evaluate potential trends that may exist between groundwater chemistry data and the existing hydrogeologic setting in the subsurface, transmissivities (*T*) across the site, and groundwater flow direction. This AR serves to document and summarize the historic and recent groundwater quality data collected from the WIPP Monitoring Network. Some data have been excluded from the conclusions presented in this report due to not meeting acceptable quality assurance criteria for this study. Data acceptability is described in Section 1.5 of this AR.

The Conceptual Model Peer Review (CMPR), conducted at the time of the Compliance Certification Application (CCA), determined that the current hydrogeologic model of the Culebra was, "inadequate to define variations in the transmissivity of the Culebra at the site scale" (U.S. DOE, 1996, Appendix PEER 1, Section 3.2.2.5). The CMPR determined that the Culebra conceptual model's "inadequacy was inconsequential for performance assessment because an extensive hydrologic data base was developed and serves as an adequate substitute to support numerical modeling" (U.S. DOE, 1996, Appendix PEER 1, Section 6.0, Hansen. C, 2021). In preparation for the Compliance Recertification Application, CRA-2004, the methodology used to develop and calibrate the Culebra T-fields was changed (U.S. DOE, 2004, Appendix PA, Attachment TFIELD, Section TFIELD-1.0, Hansen. C, 2021). In 2008, an additional hydrogeologic peer review was conducted to assess the new methodology implemented in CRA-2004.

Per Hansen, C. 2021, the peer review concluded that "the RCHCM (revised Culebra hydrogeology conceptual model) is adequate to develop T-fields for application in the site flow model", but noted three weaknesses (Burgess, 2008, Section 8). Demonstrating consistency between groundwater flow patterns and geochemistry is one of the weaknesses which is addressed by this AR.

In this AR, current available geochemistry data was evaluated and compared to established hydrogeologic ideologies. Qualified data was input into PHREEQCi v.2.12.5-669 to obtain molal concentrations, saturation indices of key minerals, activity coefficients, osmotic coefficients, ionic strengths, and cation/anion percentage error.

Several of these analyses were conducted to gain a better understanding of the predominant hydrogeochemical processes that contribute to the Culebra hydrology, evaluation, and comparison of geochemistry data to established hydrogeochemical facies zones, and evaluation of geochemistry data in relation to transmissivity and flow patterns in the Culebra.

Information Only

A correlation matrix analysis was conducted to determine the predominant ions controlling hydrogeochemical processes in the Culebra. The correlation analysis was conducted on the Culebra Aquifer as a whole, and separately on each established facies zone. Analyzing facies zone chemistries separately provides a better understanding of which processes are primarily controlling the geochemistry in specific zones.

Traditional hydrologic data analysis techniques, such as Piper and Chadha diagrams, were also performed and included in this report. These diagrams help to demonstrate the primary water types for both individual facies and the greater Culebra system. Saturation indices of key minerals, molality of ions, and molar ratios were used in this study to determine absence or presence of minerals, transitions of minerology across the WIIP monitoring well network and evaluate transmissivity and flow patterns in relation to Culebra geochemistry. This work builds on work already conducted by Ramey (1985), Siegel et al. (1991), and Domski and Beauheim (2008).

Table 1 shows a relevant list of minerals and their respective formula (Bodine and Jones, 1990).

Table 1 Chemical Formula of Relevant Minerals

Anhydrite	$CaSO_4$
Arcanite	K_2SO_4
Antarcticite	$CaCl_2 \cdot 6\ H_2O$
Bischofite	$MgCl_2 \cdot 6\ H_2O$
Bloedite	$Na_2Mg(SO_4)_2 \cdot H_2O$
Burkeite	$Na_6CO_3(SO_4)_2$
Calcite	$CaCO_3$
Carnallite	$KMgCl_3 \cdot 6\ H_2O$
Dolomite	$CaMg(CO_3)_2$
Epsomite	$MgSO_4 \cdot 7\ H_2O$
Glauberite	$Na_2Ca(SO_4)$
Gypsum	$CaSO_4 \cdot 2\ H_2O$
Halite	$NaCl$
Kainite	$KMgClSO_4 \cdot 3\ H_2O$
Kalicinite	$KHCO_3$
Kieserite	$MgSO_4 \cdot H_2O$
Leonite	$K_2Mg(SO_4)_2 \cdot 4\ H_2O$
Magnesite	$MgCO_3$
Mirabilite	$Na_2SO_4 \cdot 10\ H_2O$
Nahcolite	$NaHCO_3$
Picromerite	$K_2Mg(SO_4)_2 \cdot 6\ H_2O$
Pirssonite	$Na_2Ca(CO_3)_2 \cdot 2\ H_2O$

Information Only

Polyhalite	$K_2Ca_2Mg(SO_4)_4 \cdot 2\ H_2O$
Portlandite	$Ca(OH)_2$
Sylvite	KCl
Syngenite	$K_2Ca(SO_4)_2 \cdot 2\ H_2O$
Tachyhydrite	$Mg_2CaCl_6 \cdot 12\ H_2O$
Trona	$Na_3H(CO_3)_2 \cdot 2\ H_2O$

1.1 Geologic Setting/Study Area

The WIPP repository is located 655 meters below ground in the Salado formation. The mission of WIPP is to isolate and dispose of defense related Transuranic (TRU) waste in a manner that protects public health and the environment for 10,000 years after closure. The Rustler formation overlies the Salado formation, and it has been identified as containing the only viable water sources for potential actinide transport, in the event of a human intrusion scenario. The Culebra and the Magenta are the two water bearing units in the Rustler and they both consist primarily of dolomite confined by inter-lain beds of anhydrite and mudstone preventing vertical transport between zones (Domski and Beauheim, 2008). The chemical analysis in this report will focus on the Culebra geochemistry.

Fluid flow rates and interconnection between wells in the Culebra network are primarily determined by the extensiveness of the fracture network in the formation (Holt, et al., 2005). This fracture network varies in interconnectivity and abundance, contributing to Culebra transmissivity (*T*) spanning a range of over six orders of magnitude within the WIPP vicinity. Figure 1 illustrates various examples of the types of porosity and fractures found in the Culebra Dolomite member (Malama, et al. 2013).

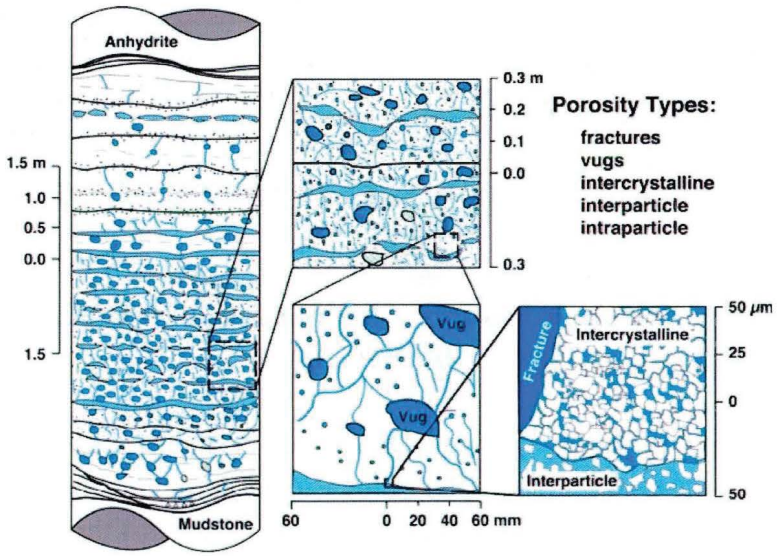

Figure 1 Various examples of porosity and fracture structure of the Culebra Dolomite (Malama, et al. 2013)

Information Only

The variation in the extensiveness of the Culebra fractures and their impact on transmissivity, have been extensively researched. Holt, et al. (2005) state, "The current conceptual model relates fracture zones to three regional-scale factors and two local scale controls. The regional-scale factors include halite dissolution from the Salado Formation, proximity to halite in other units of the Rustler and thickness of the overburden above the Culebra, while the local controls are structural deformation of the Culebra above the underlying ductile mudstone and the history of dissolution and precipitation of sulfate fracture-filling cements".

Halite persists to the west of the WIPP site in the Los Medaños member, and east of the center of the WIPP in the Tamarisk and the Forty-niner members. The halite in these members of the Rustler were formed from ancient lagoon and saline playas. The presence of this halite is likely a result of deposition, rather than dissolution (as originally thought). However, dissolution likely occurred at the edges of these playas (Holt and Powers, 1988). Figure 2, below, shows a visual representation of the major hydraulic features of a hydrologically closed basin. This image is a depiction of how the playa mudstone/halite margins would have formed, during the stratigraphic deposition of the Rustler formation.

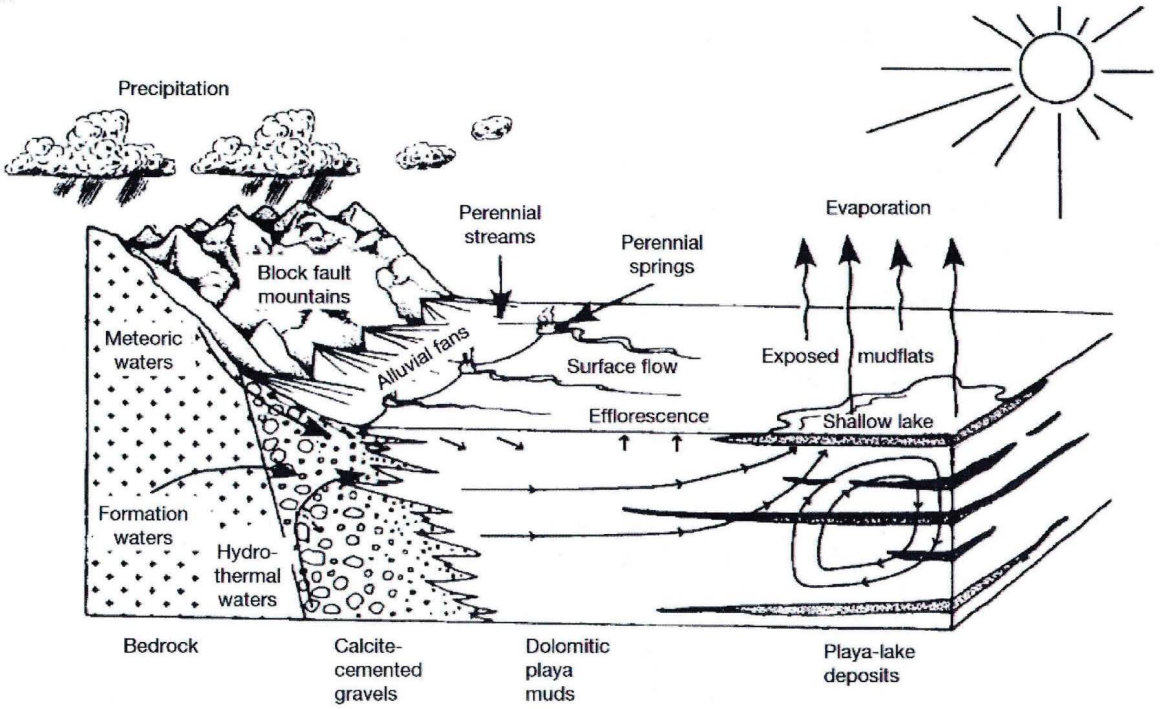

Figure 2 Major hydrologic features of hydrologically closed basins (Deocampo and Jones, 2003)

The identified mudstone/halite (M/H) margins have been designated: M1/H1, M2/H2, M3/H3 and M4/H4. Figure 3 shows the stratigraphy of the Rustler formation and the relative positions of the margins in relation to the various Rustler members. Figures 4 through 7 show the margins in relation to the well locations that are included in this study. The locations of the M/H margins and of the Salado dissolution margin impact the over-all porosity and fracture presence in the Culebra, which in turn impacts the WIPP hydrology conceptual model by influencing Culebra

Information Only

transmissivity. It is expected that the presence of halite and anhydrite below and above the Culebra member influence, the transmissivity of the Culebra. Anhydrite and halite cements are present in the pores/fractures of the formation, effectively reducing transmissivity (Holt, et. al. 2005).

The highly fractured nature of the Culebra dolomite formation would normally equate to a high hydraulic conductivity; however, the well network transmissivities vary significantly across the WIPP site. The presence or absence of halite/anhydrite cements in the Culebra member significantly contributes to the variation in transmissivity (over six orders of magnitude) across the Culebra (Holt, et al, 2005). *T* values increase westward from the eastern portion of the WIPP well network to the Salado dissolution zone and Nash Draw.

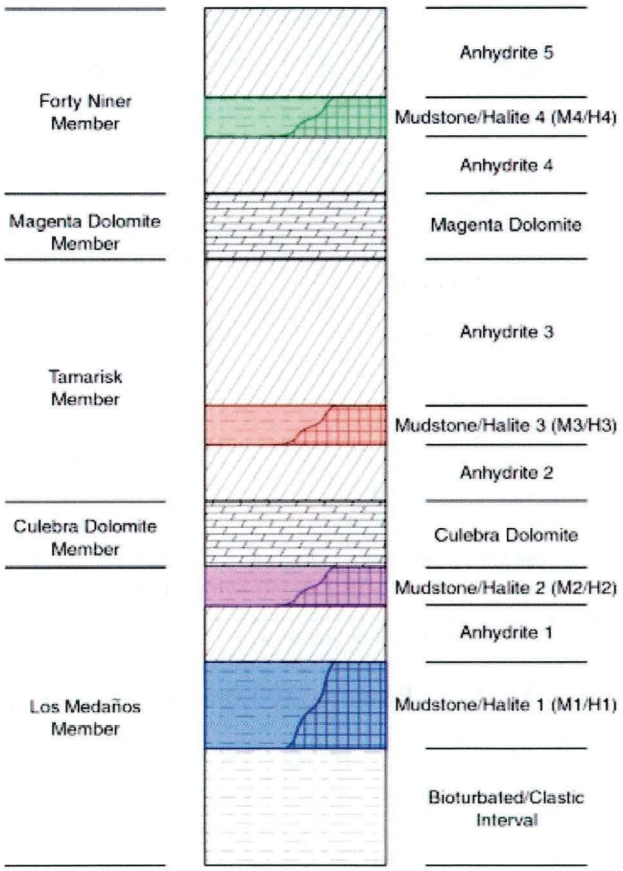

Figure 3 Stratigraphy of the Rustler Formation, Mudstone/Halite (M/H) margins shown in color (Kuhlman and Barnhart, 2011).

Information Only

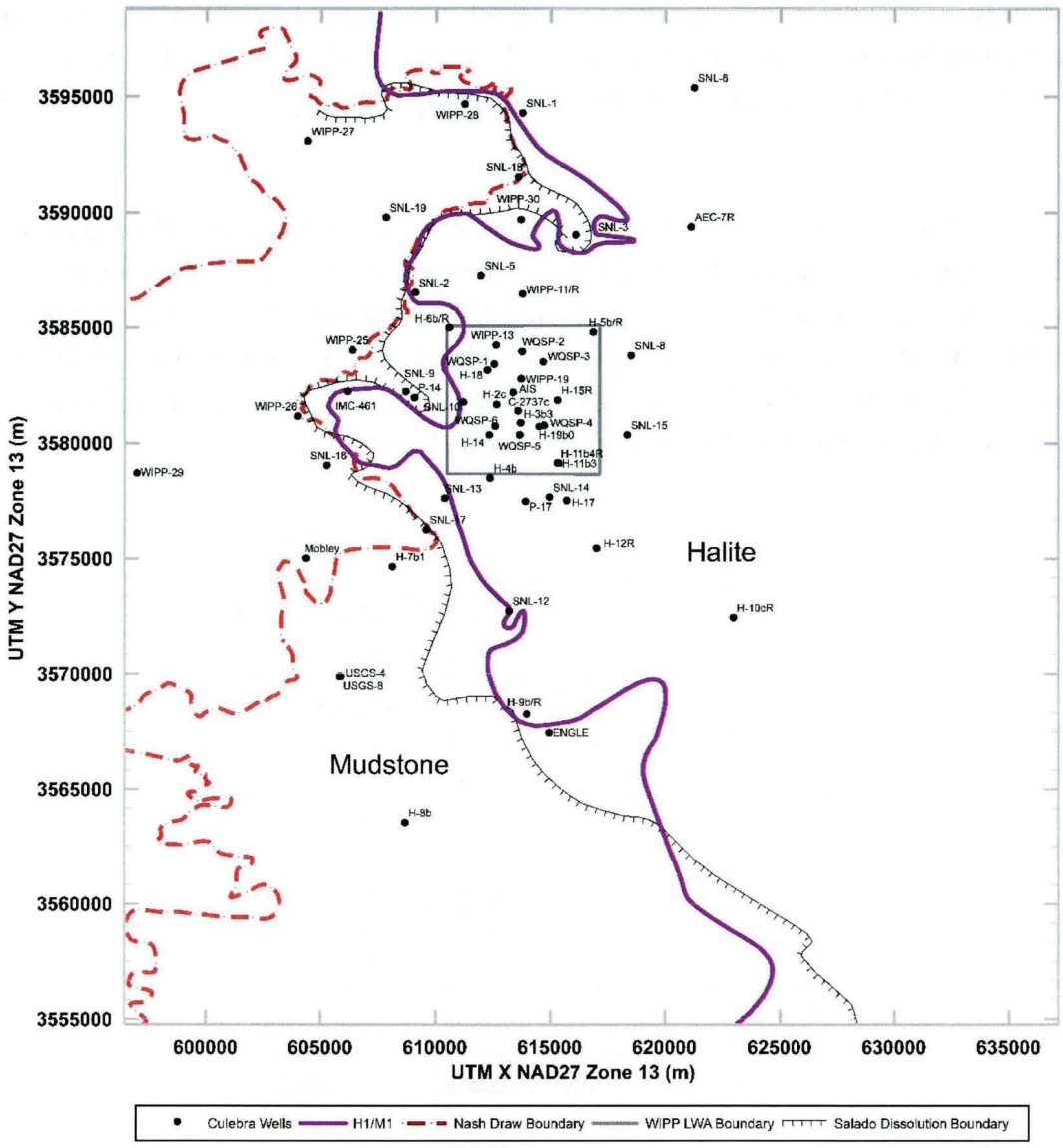

Figure 4 **M1/H1 Margin (Powers, 2007) and Culebra Wells in this Study**

Information Only

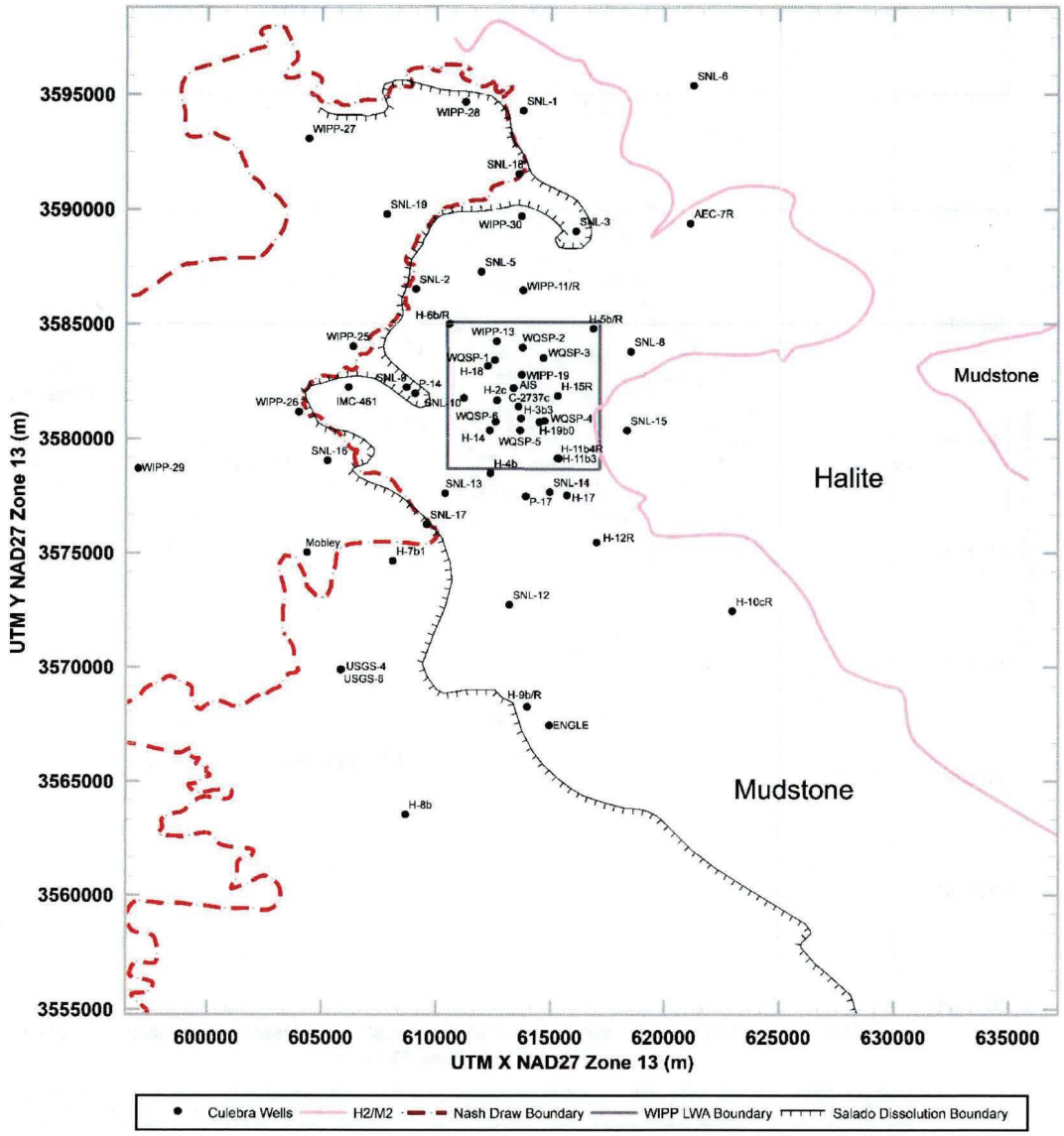

Figure 5 **M2/H2 Margin (Powers, 2007) and Culebra Wells in this Study**

Information Only

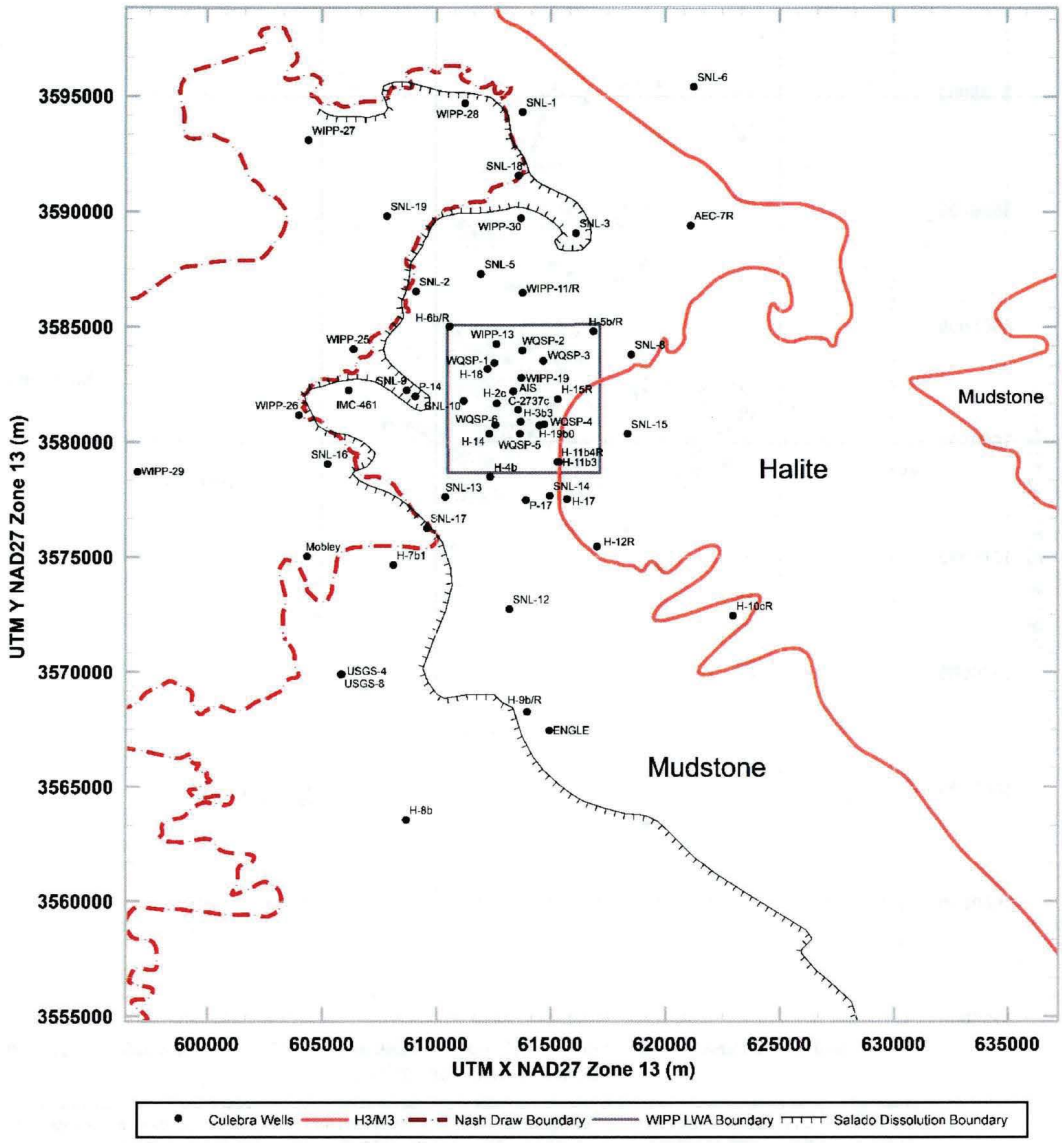

Figure 6 **M3/H3 Margin (Powers, 2007) and Culebra Wells in this Study**

Information Only

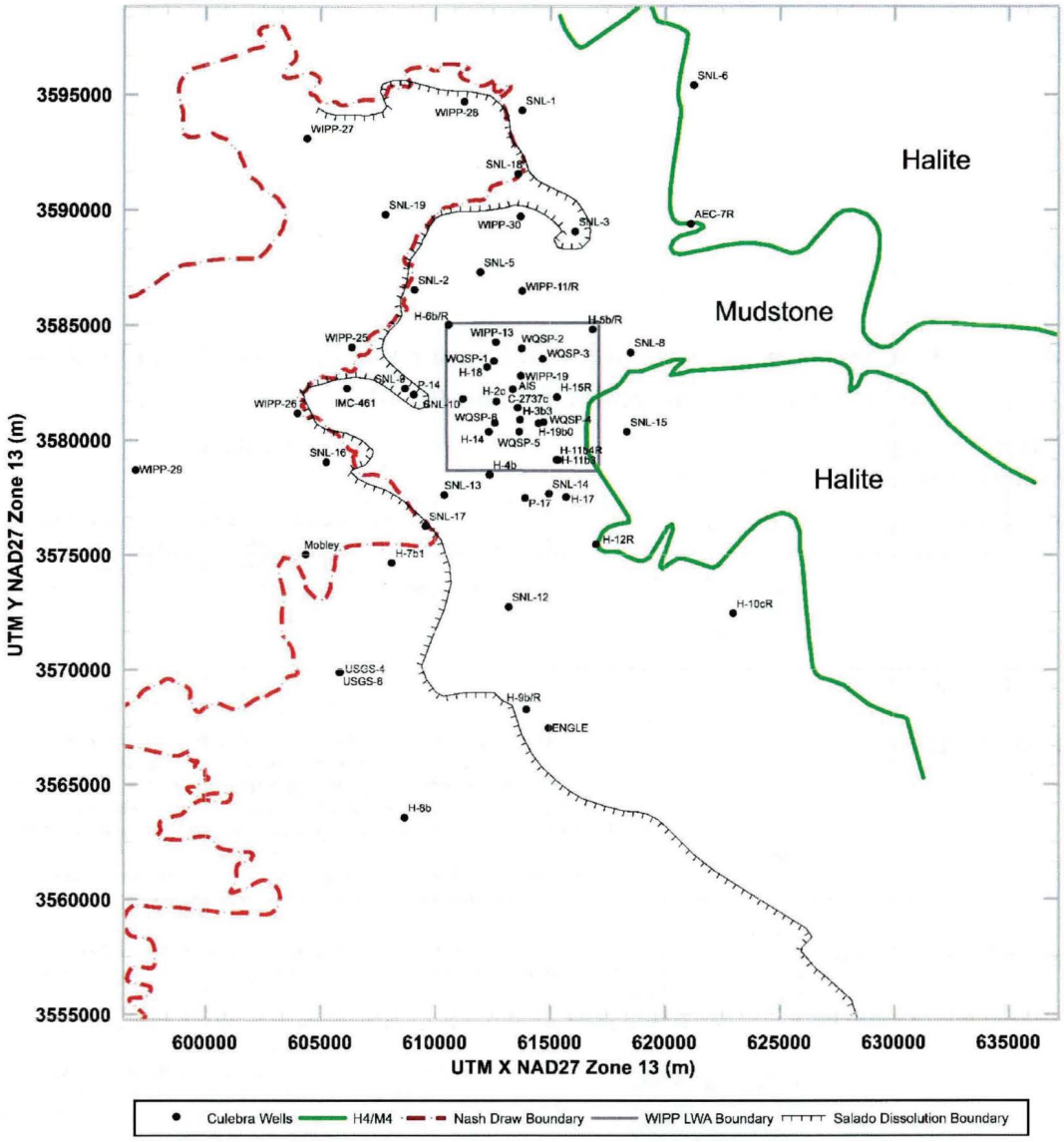

Figure 7 M4/H4 Margin (Powers, 2007) and Culebra Wells in this Study

The geologic unit components that make up the Rustler Formation are summarized in

Table 2, below.

Information Only

Table 2 Detailed Geology Description of Rustler Formation (summarized from Holt and Powers, 1988 and Kuhlman and Barnhart, 2011)

Formal Geologic Nomenclature	M/H Margins	Geology
Forty-Niner Member	A-5 M4/H4 A-4	A-4: Primarily anhydrite with some gypsum and carbonate M4/H4: Mudstone/siltstone/claystone that is commonly gypsiferous and/or calcareous. Halite zone is argillaceous with siltstone and claystone. A-5: Sulfate bed consisting of anhydrite, gypsum and carbonate.
Magenta Dolomite Member		Major: dolomite Minor: nodules of gypsum and clay-rich interbeds
Tamarisk Member	A-3 M3/H3 A-2	A-2: Anhydrite and gypsum. Divided by a bed of mudstone. Some interbedded carbonate and or claystone within the sulfate laminae. M3/H3: Halite and laterally equivalent mudstone. Areally extensive sulfate bed composed of polyhalite. Clay and sulfate occur as minor intercrystalline material in halite zone. Mudstone zone is primarily claystone and siltstone, with sulfatic and calcareous intervals. Some sulfate occurs as cements. A-3: Primarily anhydrite and gypsum, with trace claystone and carbonateCarbonate content increases upward. Anhydrite is increasingly altered to gypsum upward.
Culebra Dolomite Member	M2/H2	Major: micritic (carbonate) dolomite and finely crystalline dolomite Minor: vugs with variable gypsum and anhydrite filling. Upper area consists carbonate and organic claystone (algal origin?)
Los Medanos Member	A-1 M1/H1 BCI	Bioturbated Clastic Interval (BCI): siltstone and sandstone (argillaceous and cemented with halite), sulfatic zone at top M1/H1: bedded and argillaceous halite and equivalent mudstone, trace sulfate in the halite zone A-1: bedded anhydrite and gypsum, clay increases at top of A-1 M2/H2: argillaceous mudstone and siltstone. Interbeds of gypsum, argillaceous gypsum and carbonate are common. Holt and Powers, 1988.

1.2 Evaporite Mineral Dissolution

A primary process governing the hydrogeochemistry of the Rustler Formation is extensive dissolution of evaporite minerals (primarily halite and gypsum). Many evaporate minerals will dissolve in a congruent way, in which each ion of the mineral will dissolve equally into the solvent or water. For example, the dissolution of halite where each NaCl molecule contributes one Na^+ ion and one Cl^- ion to the solvent. Several complex evaporite minerals, however, dissolve incongruently. Consequently, the aqueous species dissolved into the solvent will be in different proportions than that found in the solid. An example of incongruent dissolution is the mineral carnallite, where the mineral dissolves and forms sylvite (KCl) as a precipitate and magnesium chloride ($MgCl_2$) in solution, as shown in the reaction below. (Braitsch, 1971).

Information Only

Equation 1 $$(KMgCl_3 \cdot 6\,H_2O) + water \rightarrow KCl + MgCl_2(aq)$$

Understanding the processes of evaporate mineral dissolution is important in recognizing the complexity of the dissolution processes and potential ion incongruency that may be presented in the geochemistry analyses. Interestingly, the formation and evolution of evaporite minerals is largely similar for many closed basin brines. The cationic evolution toward sodium dominance is primarily regulated by precipitation of alkaline earth carbonate, gypsum, and Mg-silicates. Figure 8 shows some relevant examples of evaporite evolution.

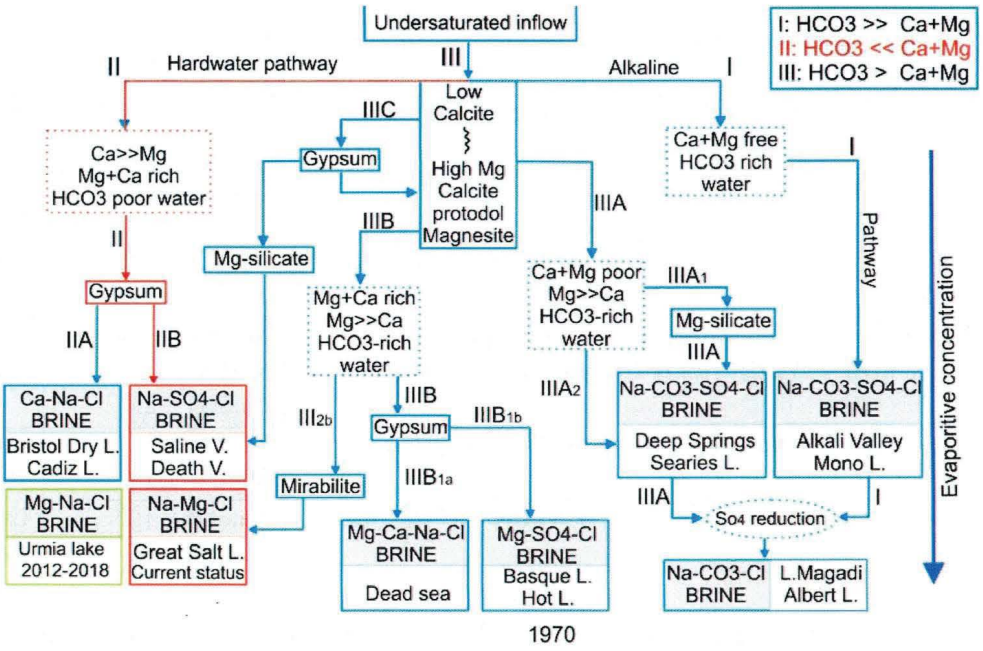

Figure 8 **Brine evolution diagram, modified from Hardie and Eguster 1978, and Lak, et al. 2022**

Based on an initial assessment, Culebra waters would most likely follow the path of the Type II waters in Figure 8. Table 3 shows a list of relevant evaporite minerals and their dissolution reactions, along with the proportional ratio of ions in the end-products.

Table 3 **Relevant Mineral Dissolution Reactions**

	Reaction	Ratio	Reference
1	$NaCl\ (halite) \rightarrow Na^+ + Cl^-$	Na:Cl = 1:1	Adams, et al. 2001
2	$CaSO_4\ (gypsum) \rightarrow Ca^{2+} + {SO_4}^{2-}$	Ca:SO_4=1:1	Adams, et al. 2001
3	$2CaAl_2Si_2O_8\ (anorthite) + 4CO_2 + 6\,H_2O \rightarrow 2Al_2Si_2O_5(OH)_4(Kaolin) + 2Ca^{2+} + 4HCO_3^-$	Ca:HCO_3 = 1:2	Walraevens et al. 2018

Information Only

	Reaction	Ratio	Reference
4	$2NaAlSi_3O_8\ (Albite) + 9H_2O + 2H_2CO_3 \rightarrow Al_2Si_2O_5(OH)_4(Kaolin) + 2Na + 2HCO_3^- + 4H_4SiO_4$	$Na:HCO_3 = 1:1$	Kim, K. 2002
5	$(Na_{0.82}Ca_{0.18})Al_{1.18}Si_{2.82}O_8\ (Plagioclase) + 1.18CO_2 + 1.77H_2O \rightarrow 0.82Na^+ + 0.18Ca^{2+} + 1.18HCO_3^- + 0.59Al_2Si_2O_5(OH)_4(Kaolin) + 1.64SiO_2$	$Na:HCO_3^-$= 0.82:1.18 $Ca:HCO_3^-$ = 0.18:0.59	Kim, K. 2002
6	$2KAlSi_3O_8\ (K-feldspar) + 9H_2O + 2H_2CO_3 \rightarrow Al_2Si_2O_5(OH)_4(Kaolin) + 2K^+ + 2HCO_3 + 4H_4SiO_4$	$K:HCO_3^-$ =1:1	Walraevens et al. 2018
7	$CaCO_3\ (calcite) + CO_3 + H_2O \rightarrow Ca^{2+} + 2HCO_3^-$	$Ca:HCO_3 = 1:2$	Walraevens et al. 2018
8	$CaMg(CO_3)_2(dolomite) + 2CO_2 + 2H_2O \rightarrow Ca^{2+} + Mg^{2+} + 4HCO_3^-$	$Ca:HCO_3 = 1:2$ $Mg:HCO_3 = 1:2$	Walraevens et al. 2018
9	$2CaCO_3\ (calcite) + Mg^{2+} + SO_4^{2-} \rightarrow CaMg(CO_3)_2\ (dolomite) + CaSO_4\ (anhydrite, gypsum)$	$Mg:HCO_3 = 1:2$ $Ca:SO_4 = 1:1$	Bodine et al. 1990
10	$2CaCO_3(calcite) + Mg^{2+} \rightarrow CaMg(CO_3)_2\ (dolomite)$	$Ca:Mg = 1:1$	Bodine et al. 1990
11	$CaSO_4^{2-}(gypsum, anhydrite) + 2HCO_3^- \rightarrow CaCO_3(calcite) + CO_2 + H_2O + SO_4^{2-}$	$Ca:HCO_3 = 1:2$	Bodine et al. 1990
12	$Ca_2K_2Mg(SO_4)_4 \cdot H_2O\ (polyhalite) \rightarrow K_2Ca(SO_4)_2 \cdot H_2O\ (syngenite) + CaSO_4^{2-}(anhydrite, gypsum) + Mg^{2+} + SO_4^{2-}$	$Mg:SO4 = 1:4$ $K:SO4 = 2:4$ $Ca:SO4 = 2:4$	Lambert, 1983
13	$(KMgCl_3 \cdot 6\,H_2O)\ (carnallite) + H_2O \rightarrow KCl + MgCl_2(aq)$	$K:Cl = 1:1$ $Mg:Cl = 1:2$	Lambert, 1983
14	$Na_2Ca(SO_4)_2\ (glauberite) \rightarrow CaSO_4^{2-} + Na(aq) + SO_4^{2-}(aq)$	$Na:SO4 = 1:2$ $Ca:SO4 = 1:2$	Lambert, 1983

In accordance with Table 3 reactions 9 and 10, when carbonate minerals such as calcite or aragonite, exchange magnesium that is in solution, the result is the formation of dolomite in a process called dolomitization. Dolomitization was a dominant process during the deposition and diagenesis of the Culebra Member of the Rustler Formation. Additionally, cation exchange reactions play a significant role in the Culebra geochemistry. This study focuses on the soluble evaporite minerals anhydrite, gypsum, halite, sylvite, polyhalite, and glauberite, due to their abundance in the Delaware basin (Lambert, 1983). While they do not play a major role in cation anion exchange reactions, silicate/clay minerals are also important to the understanding of the Culebra geochemistry, as they likely participate in cation exchange reactions, by contributing Na^+. The process of cation exchange will be discussed in this study in terms of general cation exchange, reverse ion exchange and ion exchange.

Though fractured areas of the Culebra tend to have relatively high *T,* some of the highly fractured zones have a relatively low *T* due to fracture filling gypsum cements. The formation of the gypsum cements is a result of an extensive series of cation exchange reactions. In areas where transmissivity is higher, Holt et al. (2005) proposed that the higher *T* values are due to the dissolution and/or precipitation of the gypsum cements in the fractures. Lambert, (1983)

Information Only

proposed the subsequent evaporite dissolution and evolution of the Culebra geology began with halite dissolution above and below the Culebra horizon. The dissolution of the halite below the Culebra resulted in collapses, thereby increasing the fractures in the Culebra and the effective permeability. After halite is dissolved, polyhalite becomes exposed and begins to incongruently dissolve, leaving a residue of calcium sulfate (anhydrite) and a Mg^{2+}/SO_4^{2-} rich solution. With the decrease in solute in the water, the anhydrite that was formed, begins to hydrate to gypsum. After the formation of gypsum, however, localized dissolution can occur, and permeability of the rock is increased as gypsum is dissolved. Corbet and Knupp (1996) determined that groundwater inflow to the Culebra in the vicinity of WIPP is through a combination of lateral flow within the Culebra and extremely slow vertical leakage from the overlying Tamarisk member. In addition, the inflow of water to the Culebra originated as a recharge distributed over large areas of the groundwater basin. Travel times to reach the Culebra were probably thousands or tens of thousands of years (Corbet and Knupp, 1996).

Figure 9 shows the geographic locations of the WIPP monitoring network in relation to the WIPP facility. The wells that were a part of this study are displayed on the figure along with important features such as the locations of Nash Draw and the Salado dissolution zone. Figure 10 is a map showing all the currently active wells in the WIPP monitoring network, along with the locations of the wells that have been plugged and abandoned, for reference.

Information Only

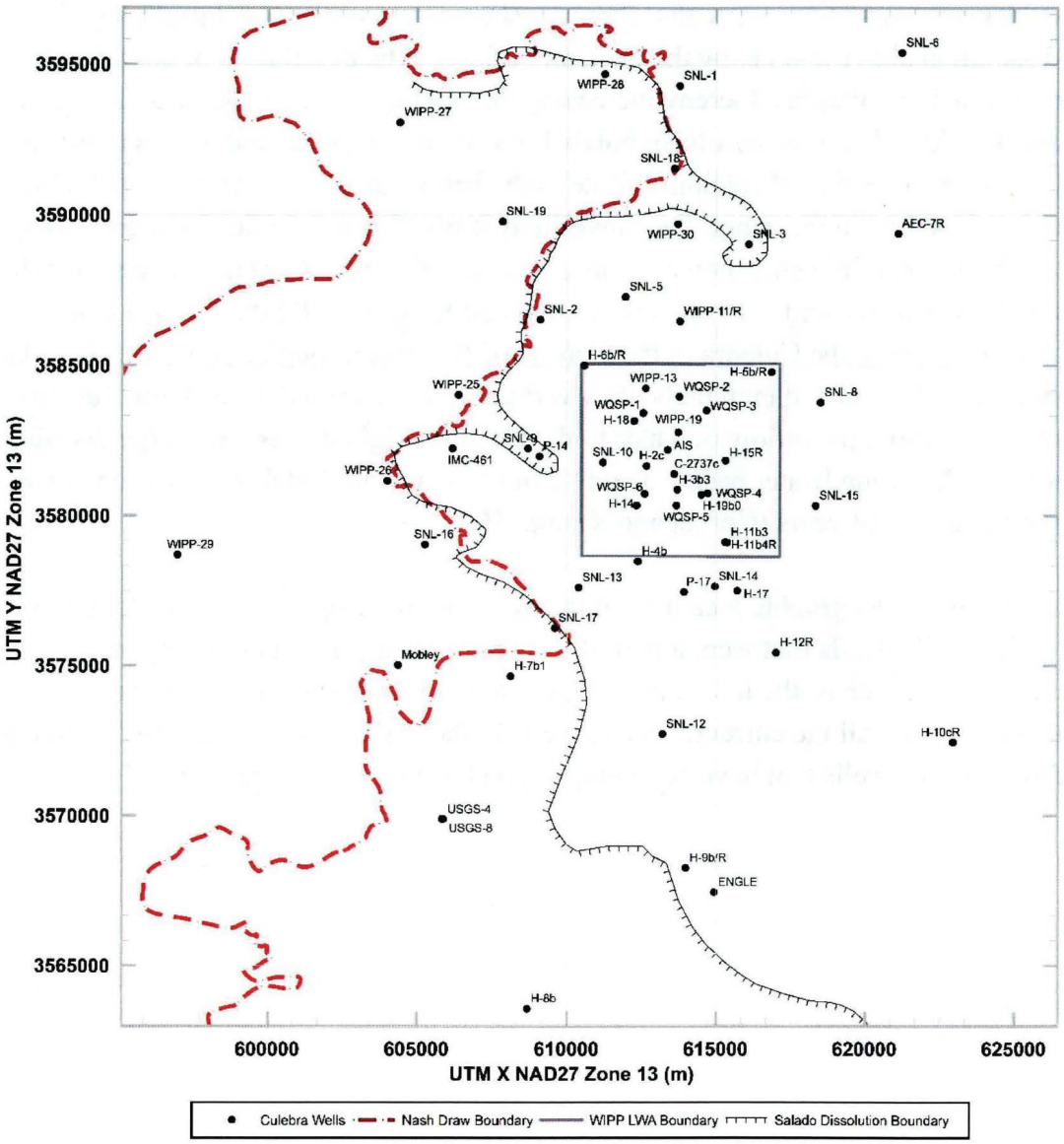

Figure 9 WIPP Wells Included in This Study

Information Only

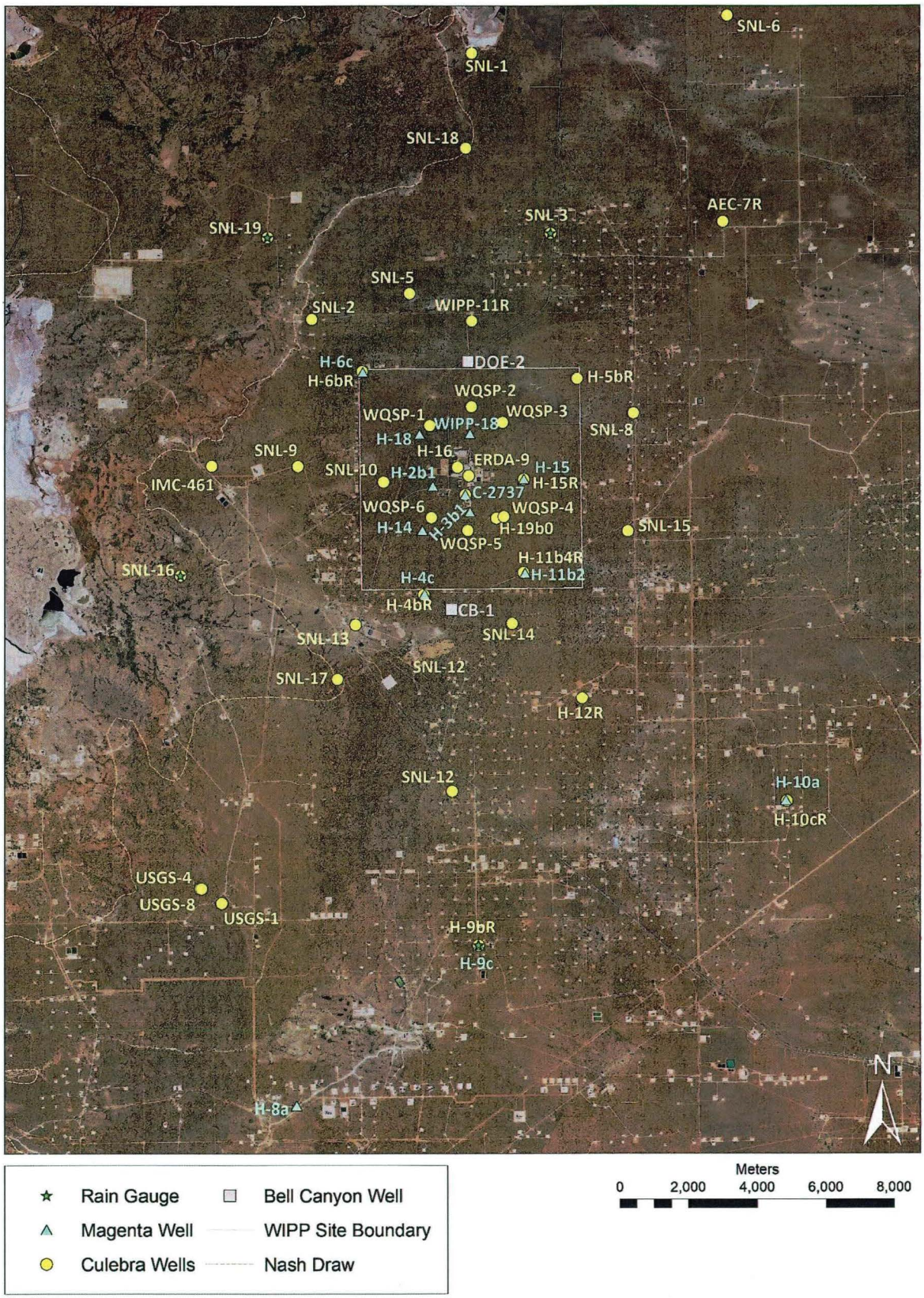

Figure 10 WIPP Well Network 2022

Information Only

1.3 Previous Studies

Culebra hydro-geochemistry has been a subject of study for decades. Siegel et al. (1991), provided a summary of the major research endeavors up to that time. Not only does Siegel et al. (1991) provide detailed background of previous studies and the geologic history of the Rustler formation, they also provide their own interpretation of the data. Siegel et al. (1991) proposed the following principals regarding the WIPP Culebra geochemistry:

- Solutes are added to the Culebra by dissolution of evaporite minerals
- The solubilities of gypsum and calcite increase as the salinity increases, and these minerals dissolve as chemical equilibrium is maintained between them and the groundwater
- Equilibrium is not maintained between the waters and dolomite; and sufficient Mg is added to the waters by dissolution of accessory carnallite or polyhalite, so that the degree of dolomite supersaturation increases with ionic strength
- Clays within the fractures and rock matrix exert some control on the distribution of Li, B, Mg, and Si via sorption, ion exchange and dissolution.

Domski and Beauheim, 2008 also provides an extensive analysis of the geochemistry of the Culebra up to the 2008 timeframe. Both studies provide a foundation for this study, which utilizes them as a framework for analyzing new data and assessing potential trends. A major product of the two combined studies was the delineation of different water-type facies zones, based on the geochemistry of the waters. Siegel et al. (1991) developed several facies zone definitions (A, B, C, D) based predominantly on ionic strength and the Ca^{2+}/Mg^{2+} molar ratio. Domski and Beauheim, 2008 contributed additional analyses to the facies classification and further defined them, adding transitional facies zones (A, A/C, B, B/C, C, D and E) between the primary originally identified facies by Siegel, et al. 1991. The well data considered in this study was mapped by facies zone based on the criteria presented by Domski & Beauheim, 2008 in Table 4.

Information Only

Table 4 **Hydro-geochemical Zones/Facies developed by Siegel, et al. 1991 and Domski and Beauheim, 2008**

Increasing Salinity ↓	Facies /Zone	Siegel et al. (1991)	Domski & Beauheim (2008)
	B	Dilute (ionic strength <0.1 molal) CaSO4 rich groundwater, from southern high transmissivity area	Same as Siegel et al. (1991) Mg/Ca molar ratio: 0.32-0.52
	B/C	Not Included	Ionic strength 0.18-0.29 molal Mg/Ca molar ratio 0.4-0.6
	C	Variable composition waters, Mg/Ca molar ratio 0.3-1.2 for waters with ionic strength <1.25 molal	Ionic strength 0.3-1.0 molal Mg/Ca molar ratio 0.4-1.1
	A/C	Not Included	Ionic strength 1.1-1.6 molal Mg/Ca molar ratio 0.5-1.2
	A	Ionic Strength ~2-3 molal, Mg/Ca molar ratio 1.2-2	Ionic strength >1.66 molal, up to 5.3 molal Mg/Ca ratio 1.2-2.4
	D	Defined based on inferred contamination related to potash refining operations. Ionic strength 3 molal, K/Na weight ratios of ~0.2	Same as Siegel et al. (1991)
	E	Not Included	Wells east of the mudstone-halite margins, ionic strength 6.4-8.6 molal, Mg/Ca molar ratio 4.1-6.6

In this study the numerical ranges, (ionic strength and Mg^{2+}/Ca^{2+} ratio) defining each zone were updated to accommodate the new well values. Zone ranges and zone lines are predominantly the same as described in the previous studies. Changes to facies zones will be discussed in Section 3.1.1 of this report. Table 5, below, summarizes the new ranges, for each facies zone.

Table 5 **Hydro-geochemical Facies zones developed by Siegel, et al. 1991 and Domski and Beauheim, 2008. Updated 2022**

Increasing Salinity ↓	Facies /Zone	Siegel et al. (1991)	Domski & Beauheim (2008)	This Study
	B	Dilute (ionic strength <0.1 molal) CaSO4 rich groundwater, from southern high transmissivity area	Same as Siegel et al. (1991) Mg/Ca molar ratio: 0.32-0.52	Same as previous Mg/Ca molar ratio: 0.28-0.51
	B/C	Not Included	Ionic strength 0.18-0.29 molal Mg/Ca molar ratio 0.4-0.6	Same as previous Mg/Ca molar ratio: 0.39-0.6
	C	Variable composition waters, Mg/Ca molar ratio 0.3-1.2 for waters with ionic strength <1.25 molal	Ionic strength 0.3-1.0 molal Mg/Ca molar ratio 0.4-1.1	Ionic strength 0.30-1.02 molal Mg/Ca molar ratio: 0.39-0.99
	A/C	Not Included	Ionic strength 1.1-1.6 molal Mg/Ca molar ratio 0.5-1.2	Ionic strength 1.07-1.6 molal Mg/Ca molar ratio: 0.85-1.25
	A	Ionic Strength ~2-3 molal, Mg/Ca molar ratio 1.2-2	Ionic strength >1.66 molal, up to 5.3 molal Mg/Ca ratio 1.2-2.4	Ionic strength 1.66-5.3 molal Mg/Ca molar ratio: 1.07-2.57
	D	Defined based on inferred contamination related to potash refining operations. Ionic strength 3 molal, K/Na weight ratios of ~0.2	Same as Siegel et al. (1991)	Same as previous
	E	Not Included	Wells east of the mudstone-halite margins, ionic strength 6.4-8.6 molal, Mg/Ca molar ratio 4.1-6.6	Wells based on location of mudstone-halite margins, Ionic strength 1.77-11.5 molal Mg/Ca molar ratio 3.81-6.6

Information Only

In previous studies, zone E was established based on the location of the wells east of the M2/H2 margin (Holt et al. 2005), as shown in Figure 11**Error! Reference source not found.**. AEC-7R was drilled in 2013 and was therefore not considered in any of the prior studies. AEC-7R is located on the boundary of the M2/H2 and M4/H4. Previous data in this region has not been available. This area was likely subject to extreme evaporation/dissolution of halite on the margin boundaries, which created a specific chemistry profile. Based on the chemistry profile similarities of AEC-7R and the other zone E wells, AEC-7R was placed in zone E. The Zone E facies boundary generated in this study, is an estimation and extends sharply toward the east. This boundary is estimated based on the sharp extension of the M2/H2 and M4/H4 boundaries, as shown in Figure 11.

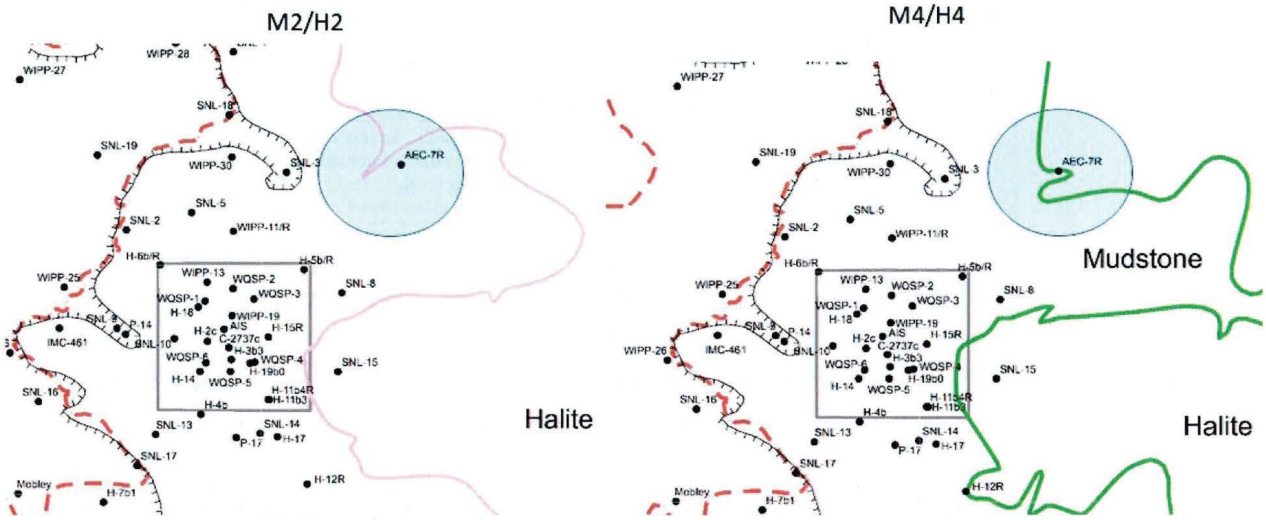

Figure 11 Well AEC-7R in relation to the M2/H2 and M4/H4 Mudstone/Halite Margins

1.4 Data Sources

Water quality analyses of Culebra groundwater samples have been performed and reported by several different laboratories and organizations over the course of the WIPP project. The available water quality chemistry data for all WIPP Culebra wells from 1978 to 2020 was analyzed and summarized for this study, and the data consisted of the three separate data sets described below:

- Data Set #1 "Culebra_2017-2020": This data set contains data collected in a focused study from 2017-2020 for all accessible Culebra wells. Water samples were collected at mid formation for all wells. Samples were collected using a depth specific sampling device for more accurate representation of the Culebra formation waters. These data were collected in a concerted effort spanning 4 years of consecutive sample collection for accessible wells. A shortcoming of this effort was that only wells that had a casing size large enough to fit the discrete depth sampling apparatus were included. In addition, some well locations were excluded for other reasons, such as depth beyond the sampling apparatus reach or deviation of the well column. A Coefficient of Variation (CV)

Information Only

between the data for each constituent analyzed for each well was calculated to ensure the data did not vary widely across the study period and then the average was calculated to report in this study. Including all the data available for a particular well provides a more complete well chemistry profile for the designated location over the time period of 2017-2020. These data are documented and summarized in milestone reports: Bowman, D. 2019 "Milestone Report for WIPP water Qualities Collected from 2017 to 2018" and Lofton, O.W. 2021, "Milestone Report for WIPP Water Qualities Collected from 2019-2020". All analyses references and data citations are provided in those two reports. The raw data, chemistry parameters, and PHREEQCI output of activity coefficients and saturation indices for key minerals, for this data set can be found in the Excel spreadsheet entitled: Culebra_Chemistry_2017-2020_AP194.xlsx and stored electronically at the file location: CVS/CVSLIB/WIPP EXTERNAL/ap194. Raw data is also summarized in Appendix A. The average value for each well analyzed in this dataset, along with the calculated CV between the collected values, are summarized in Table 6, of section 1.5 in this report.

- Data Set #2 "Culebra_ALL": This data set consists of all historical and current data available for Culebra waters for the entire WIPP monitoring program, beginning in 1978 and ending in 2021. These data contain additional samples that were not included in the focused 2017-2020 study (i.e., wells excluded for listed reasons). The well data already considered in Data Set #1 are not included. This data set is subject to variability in number of samples collected, method of sample collection and accuracy. In many cases, however, the samples in this study are the only existing data for certain wells, since the wells have since been plugged or abandoned. These data are not representative of a focused study, like the 2017-2020 data, meaning that the samples were largely collected based on circumstance (i.e., during pumping tests, well maintenance, etc.). Some of the data in this data set were considered in the Siegel et al. 1991 report and the Domski and Beauheim, 2008 report, however in those reports only the "most recent" data points were considered for analysis. In this study, all available data points throughout history were utilized in the analyses in the designated timeframe (1978-2021). With this knowledge in mind, data that were subject to deviances, such as well treatment or maintenance that would change or effect the water chemistry were not included in this study. The acceptable data results collected throughout history were averaged and those averages were used in the final analyses of this study. A CV between the data analyzed for each well was calculated to ensure the data did not vary widely through time. Including all data points available for a particular well provides a more complete well chemistry profile for the designated location over time, rather than considering only one data point at a selected time. These data have been reported and summarized in several different reports throughout the WIPP history. The raw data, chemistry parameters and PHREEQCI output of activity coefficients and saturation indices of key minerals are summarized in the Excel spreadsheet entitled: Culebra_Chemistry_ALL_AP194.xls and is stored electronically at the file location: CVS/CVSLIB/WIPP EXTERNAL/ap194.

Information Only

Raw data is summarized in Appendix B. The wells analyzed within this dataset are summarized in

Information Only

- Table 7 of section 1.5 of this report.
- Data Set #3 "WQSP_Culebra_wells": This data set contains all major cation and anion data collected from the WQSP wells (1, 2, 3, 4, 5, and 6), spanning from 1995-2020. A CV between the data analyzed for each well was calculated to ensure the data did not vary widely across the study period. Including all data points available for a particular well provide a more complete well chemistry profile for the designated locations over the time-period analyzed. These data have been reported and summarized in routine Annual Site Environmental Reports (ASERs) since WIPP began accepting waste. The raw data, chemistry parameters, and PHREEQCI output of activity coefficients and saturation indices of key minerals are summarized in the Excel spreadsheet entitled: WQSP_wells_AP194.xls and is stored electronically at the file location: CVS/CVSLIB/WIPP EXTERNAL/ap194. Raw data is summarized in Appendix C. The wells analyzed within this dataset are summarized in Table 8 of section 1.5 of this report.

1.5 Data Acceptability

In general, all data available for a certain well within the defined time periods (listed above) were utilized in this study. Exceptions to this include data that were collected early on during a multi-day pumping test/experiment or data that were subject to chemistry alteration due to mechanical/human influences. A goal of this study was to generate a complete chemistry profile of each monitoring well throughout the WIPP history. However, it is recognized that well chemistry can change over time. Averaging and reporting values that are anomalous is not good practice when developing a realistic and representative profile of a wells' chemistry. For all wells that had geochemical data spanning several years, a Coefficient of Variation (CV) between values was calculated. CV was calculated following the standard described by Abdi, H., 2010. The CV is defined as the ratio of the standard deviation to the mean and is used to describe the extent of variability in relation to the mean of the population. The higher the CV, the greater the variance of the data. The equation for calculation of CV is expressed as:

Equation 2 $$CV\% = \left(\frac{\sigma}{\mu}\right) * 100$$

Where σ is the standard deviation of the population and μ is the mean of the population.
In this study, a data set is deemed acceptable if its calculated CV is less than 30%. The CV was only used to determine the variability between the geochemical data points collected from wells spanning several years, to verify a meaningful average. A CV was not calculated for wells that only had results from one sampling event. As a note, anion/cation ratio accuracies were calculated using PHREEQCI rather than CV. All calculated CVs and subsequent deviations from the criteria are documented in Tables 6, 7 and 8.

Data that passed the CV criteria and that were deemed acceptable were input into PHREEQCI by calculated average. As mentioned previously, PHREEQCI was used to calculate the cation/anion

Information Only

percentage difference for each well. This value was deemed acceptable if it was less than 5%. The cation/anion percent difference or error is a value that shows the over-all difference between the measured cations and measured anions in a sample. A high cation/anion percent difference denotes a possible issue with the validity of the lab data calculations. A cation/anion difference value of 5% or less, indicates a well-balanced sample, where a difference of 0% denotes perfect balance. Cation/anion error is reported in Tables 6, 7 and 8.

Information Only

Table 6 Summary of Average, CVs, and PHREEQCI Cation/Anion Percent Error for Data Set #1: Culebra_2017-2020

Calculated Averages and CVs for WIPP Monitoring wells Data Set#1: Culebra_2017-2020

Well ID	Sample Date	Sample Size	pH	Density g/cm3	TDS (mg/L)	Ca^{2+} (mg/L)	Mg^{2+} (mg/L)	Na^{+} (mg/L)	K^{+} (mg/L)	Cl^{-} (mg/L)	$SO4^{2-}$ (mg/L)	Br^{-} (mg/L)	Total Alkalinity (mg/L)	$HCO3^{-}$ (mg/L)	$CO3^{2-}$ (mg/L)	PHREEQCI Cation/Anion % Error
[1]AEC-7R	2017-2020	3	7.03	1.068	91733	1733	4000	22667	1667	48333	5967	133	69	69		
CV			**1%**	**0%**	**0%**	**10%**	**9%**	**7%**	**11%**	**9%**	**1%**	**4%**	**13%**	**13%**		**-2**
H-2b2	2017-2019	3	9.30	1.012	13833	790	127	3567	110.0	5833	3067	5.6	52.4		43.9	
CV			**1%**	**0%**	**4%**	**0%**	**7%**	**1%**	**7%**	**4%**	**2%**	**6%**	**2%**		**12%**	**-5**
[2]H-4bR	2017-2020	4	7.81	1.018	15925	713	290	4100	128	5700	4375	23	64	64		
CV			**1%**	**0%**	**2%**	**2%**	**8%**	**5%**	**3%**	**6%**	**5%**	**9%**	**11%**	**11%**		**-3**
[3]H-5b	2017-2019	3	7.52	1.100	156333	1600	2033	52333	1100	92667	7667	53	50	50		
CV			**6%**	**0%**	**1%**	**5%**	**2%**	**6%**	**0%**	**4%**	**11%**	**20%**	**2%**	**2%**		**-4**
H-6bR	2017-2020	4	8.88	1.036	60975	2450	780	16250	352.5	28250	3150	27.0	39.3		29.7	
CV			**1%**	**0%**	**6%**	**4%**	**5%**	**5%**	**4%**	**10%**	**5%**	**10%**	**5%**		**17%**	**2**
[4]H-7b1	2017-2019	3	7.47	1.008	3200	593	143	283	12	423	1933		111	111		
CV			**1%**	**0%**	**34%**	**3%**	**9%**	**32%**	**21%**	**35%**	**10%**		**12%**	**12%**		**0**
H-9bR	2017-2020	4	7.64	1.002	3448	578	138	195	8	225	1875		85	85		
CV			**3%**	**0%**	**2%**	**4%**	**6%**	**6%**	**5%**	**9%**	**6%**		**8%**	**8%**		**2**
[5]H-11b4R	2017-2020	4	7.41	1.076	112250	1800	1275	36250	730	60000	7300	40	93	93		
CV			**1%**	**0%**	**2%**	**0%**	**3%**	**4%**	**3%**	**6%**	**9%**	**18%**	**8%**	**8%**		**-2**
H-12R	2017-2020	4	7.47	1.103	193500	1300	1275	63000	1225	104250	7950	61	55	55		
CV			**3%**	**0%**	**17%**	**14%**	**16%**	**13%**	**15%**	**10%**	**14%**	**17%**	**24%**	**24%**		**-3**
H-17	2017-2019	3	6.11	1.130	192667	1767	1333	69333	973	116667	7133	41				
CV			**2%**	**0%**	**4%**	**3%**	**7%**	**2%**	**3%**	**4%**	**7%**	**29%**				**-3**
[6]H-19b0	2017-2020	4	9.00	1.065	94800	1600	1038	29750	673	53250	5800	34	127	38	119	
CV			**6%**	**0%**	**14%**	**8%**	**6%**	**11%**	**10%**	**10%**	**6%**	**9%**	**24%**	**56%**	**3%**	**-5**
[7]SNL-1	2017-2020	4	7.34	1.024	36325	1400	585	10225	255	17500	3975	12	118	118		
CV			**2%**	**1%**	**4%**	**0%**	**3%**	**8%**	**3%**	**9%**	**6%**	**35%**	**12%**	**12%**		**-1**
SNL-2	2017-2020	4	7.29	1.007	9933	910	268	2075	41	3750	2175	2	158	158		
CV			**2%**	**0%**	**5%**	**3%**	**4%**	**4%**	**2%**	**4%**	**4%**	**25%**	**4%**	**4%**		**1**
[8]SNL-3	2017-2020	4	7.56	1.026	46150	1450	705	14750	370	23000	4775	19	46	46		
CV			**2%**	**0%**	**9%**	**6%**	**3%**	**7%**	**4%**	**5%**	**6%**	**9%**	**7%**	**7%**		**2**
SNL-5	2017-2020	4	7.52	1.006	15075	1550	465	2175	67	6400	1675	6	58	58		**-1**

Information Only

Well ID	Sample Date	Sample Size	pH	Density g/cm3	TDS (mg/L)	Ca^{2+} (mg/L)	Mg^{2+} (mg/L)	Na^{+} (mg/L)	K^{+} (mg/L)	Cl^{-} (mg/L)	$SO4^{2-}$ (mg/L)	Br^{-} (mg/L)	Total Alkalinity (mg/L)	$HCO3^{-}$ (mg/L)	$CO3^{2-}$ (mg/L)	PHREEQCI Cation/Anion % Error
CV			**3%**	**0%**	**6%**	**10%**	**3%**	**4%**	**6%**	**9%**	**8%**	**17%**	**9%**	**9%**		
SNL-8	2017-2020	4	7.57	1.095	140000	1875	2650	47500	1550	81750	6225	89	75	75		
CV			**2%**	**1%**	**3%**	**4%**	**4%**	**2%**	**3%**	**5%**	**13%**	**6%**	**13%**	**13%**		**0**
[9]SNL-9	2017-2020	4	6.95	1.016	26900	2875	760	5025	44	13500	1500	14	34	34		
CV			**6%**	**0%**	**6%**	**3%**	**6%**	**4%**	**6%**	**11%**	**12%**	**47%**	**14%**	**14%**		**2**
SNL-10	2017-2020	4	7.82	1.009	9058	503	180	2150	52	1375	4500	3	99	99		
CV			**1%**	**0%**	**5%**	**6%**	**4%**	**4%**	**6%**	**9%**	**4%**	**28%**	**5%**	**5%**		**0**
SNL-12	2017-2020	4	7.74	1.010	4953	660	143	505	21	790	2050	1	89	89		
CV			**1%**	**0%**	**18%**	**4%**	**3%**	**5%**	**5%**	**11%**	**4%**	**14%**	**2%**	**2%**		**0**
[10]SNL-13	2017-2020	4	8.29	1.021	20525	993	328	5575	198	8600	3575	18	41	40		
CV			**1%**	**0%**	**5%**	**1%**	**8%**	**5%**	**7%**	**4%**	**6%**	**15%**	**4%**	**9%**		**1**
SNL-14	2017-2020	4	7.38	1.044	86875	1500	978	28250	618	41750	6075	37	59	59		
CV			**1%**	**0%**	**5%**	**0%**	**2%**	**3%**	**3%**	**5%**	**5%**	**11%**	**4%**	**4%**		**3**
SNL-16	2017-2020	4	7.26	1.014	25050	1725	538	5500	295	12000	2350	3	93	93		
CV			**2%**	**0%**	**4%**	**3%**	**7%**	**5%**	**7%**	**6%**	**2%**	**27%**	**2%**	**2%**		**-2**
SNL-17	2017-2020	4	7.69	1.009	3345	605	148	155	6	278	1850		98	98		
CV			**1%**	**0%**	**0%**	**1%**	**3%**	**10%**	**13%**	**14%**	**5%**		**2%**	**2%**		**1**
SNL-18	2017-2020	4	7.73	1.009	17650	1068	355	4800	106	8275	2925	6	66	66		
CV			**1%**	**0%**	**11%**	**5%**	**9%**	**14%**	**13%**	**13%**	**8%**	**29%**	**6%**	**6%**		**0**
[11]SNL-19	2017-2020	4	7.25	1.004	8093	773	213	1600	38	2775	2200	1	76	95		
CV			**6%**	**0%**	**2%**	**3%**	**4%**	**0%**	**7%**	**5%**	**6%**	**58%**	**42%**	**2%**		**0**
[12]WIPP-11	2017-2020	4	8.43	1.034	49550	1675	718	16000	363	27750	3775	21	47	24	23	
CV			**7%**	**0%**	**6%**	**3%**	**7%**	**4%**	**3%**	**2%**	**11%**	**16%**	**24%**	**96%**	**70%**	**-1**
WIPP-13	2017-2020	4	7.74	1.033	76125	1400	1030	19000	658	35000	4700	32	34	34		
CV			**5%**	**0%**	**20%**	**5%**	**7%**	**14%**	**7%**	**6%**	**5%**	**11%**	**10%**	**10%**		**-4**
[13]WIPP-19	2017-2019	3	9.11	1.056	75333	1567	913	25000	563	40000	5700	37	128	19	109	
CV			**1%**	**0%**	**1%**	**3%**	**7%**	**3%**	**3%**	**7%**	**4%**	**23%**	**3%**	**52%**	**6%**	**0**

Notes:

- All values highlighted in red and shaded did not meet the <30% CV acceptability criteria.

Information Only

• For a detailed description of acceptance/rejection for each value, see Excel spreadsheet: Culebra_Chemistry_2017-2020_AP194.xlsx at the file location: CVS/CVSLIB/WIPP EXTERNAL/ap194. • If a cell is empty in this table, it means there were no values reported for that analyte.
[1]Historical Bicarbonate values are ~47. Historical Br values are ~165. Based on information in Lofton, 2021 milestone, data for 2020 will be excluded. Data may have been affected by well maintenance treatment.
[2]The 2017 value for Bromide is not consistent with historical data or data from 2018-2020. It will not be used to calculate the Bromide average.
[3]All Historical Bicarbonate data are ~40-50 mg/L and 2018-2019 data are also in the 40-50 mg/L range. Therefore the 2017 Alkalinity data will not be used to calculate the average.
[4]Na, Cl and TDS values, dropped dramatically in 2019. Historical data show values similar to the 2019 data. Since it cannot be determined which data are correct. All the data will still be used even though the CV is above 30%
[5]Historical data from 2012 for Bromide is 41 mg/L. Bromide data from 2017 will not be used to calculate the average. It is not consistent with historical data, or data collected 2018-2020.
[6]TDS value for 2020 was not used to calculate the average (See Lofton, 2021 report). Bicarbonate and Carbonate are very inconsistent across samplings. In this study, only the value for Total Alkalinity will be used.
[7]Bromide values are very low, this is making the CV% erroneous. Bromide data will still be used. Historical value for Bromide (2016) was 12 mg/L
[8]Historical Bicarbonate value in 2004 was 63, and in 2018-2020 Alkalinity was between 40-51. Alkalinity data for 2017 will not be used to calculate the average, due to inconsistency with other samplings.
[9]Historical data for Br are ~16. Bromide data from 2018 will not be used to calculate the average, due to its inconsistency with other collected samples. Alkalinity data from 2017 will not be used to calculate the average due to its inconsistency with data from 2018-2020
[10] Bromide data from 2017 will not be used due to inconsistency with 2018-2020
[11]Alkalinity data for 2020 will not be used to calculate the average. It is inconsistent with other samplings for this well. Bromide CV% is high because the Br concentrations are low. Br will still be used.
[12]Bicarbonate and Carbonate values are very inconsistent across samplings. Only Total alkalinity values will be used in this study
[13]Bicarbonate and Carbonate values are very inconsistent across samplings. Only Total alkalinity values will be used in this study. The CO_3^{2-} CV is below 30% however it will not be used (and is highlighted in red/gray) due to inconsistency in historical data and 2017-2020 data.

Information Only

Table 7 **Summary of Average, CVs, and PHREEQCI Cation/Anion Percent Error for Data Set #2: Culebra_ALL**

Calculated Averages and CVs for WIPP Monitoring wells Data Set #2: Culebra_ALL

Well ID	Sample Date	Sample Size	pH	TDS (mg/L)	Ca2+ (mg/L)	Mg2+ (mg/L)	Na+ (mg/L)	K+ (mg/L)	Cl- (mg/L)	SO42- (mg/L)	Br- (mg/L)	Total Alkalinity (mg/L)	HCO3- (mg/L)	CO3 2- (mg/L)	PHREEQCI Cation/Anion % Error
[1]AEC-7R	2014-2015	2	7.40	89400	1900	4515	22500	1850	57000	6500	165	48	48		
CV			**0%**	**8%**	**0%**	**4%**	**2%**	**3%**	**2%**	**2%**	**3%**	**3%**	**3%**		**-8**
[2]AIS	10/28/1988	1	7.94		1000	510	12600	400	20500	5900	22	98	98	0	**-4**
C-2737c	3/1/2018	1	9.03	9120	790	190	2200	26	3900	1800	4.8	21.64		16	**1**
ENGLE	1985-1990	2	7		590	151	210	7	211	1945		110	110		
CV			**0%**		**0%**	**1%**	**5%**	**15%**	**10%**	**2%**		**0%**	**0%**		**3**
H-2c	1989-1994	5	7.38	9922	750	181	2260	103	3204	2810	9	54	54		
CV			**6%**	**7%**	**3%**	**18%**	**15%**	**9%**	**10%**	**11%**	**28%**	**12%**	**12%**		**1**
H-3b3	1984-1995	7	7.32	55300	1463	765	16614	433	29071	4861	29	48	48		
CV			**4%**	**1%**	**7%**	**7%**	**4%**	**12%**	**5%**	**7%**	**15%**	**9%**	**9%**		**-3**
H-4b	1987-1994	5	7.17	20500	686	412	5780	206	7994	5564	41	55	55		
CV			**7%**	**6%**	**5%**	**9%**	**6%**	**12%**	**7%**	**8%**	**5%**	**14%**	**14%**		**-3**
H-5b &bR	1981-2021	8	7.42	153350	1582	1973	50800	1172	85725	7729	65	41	41		
CV			**6%**	**1%**	**8%**	**9%**	**8%**	**13%**	**5%**	**12%**	**12%**	**20%**	**20%**		**-2**
H-6b & bR	1978-2008	6	7.11	56333	1912	988	16950	438	31333	3503	31	87	87		
CV			**5%**	**8%**	**22%**	**5%**	**11%**	**22%**	**8%**	**9%**	**19%**	**10%**	**10%**		**-2**
[3]H-7b1	1986-1990	5	7.13		611	134	167	8	290	1870	2		114		
CV			**2%**		**7%**	**4%**	**23%**	**6%**	**8%**	**9%**	**46%**		**11%**		**0**
H-8b	1986-1988	3	7.50		570	167	54	4	34	1767	2	95	95		
CV			**4%**		**5%**	**3%**	**4%**	**7%**	**4%**	**5%**	**28%**	**1%**	**1%**		**6**
H-9b &bR	1980-2012	9	7.46	3290	619	146	144	8	193	1851	1	106	106		
CV			**4%**	**8%**	**6%**	**5%**	**19%**	**9%**	**24%**	**9%**		**12%**	**12%**		**3**
H-10cR	7/27/2017	2	7.49	146000	1550	2150	41500	945	70500	7050		65	65		
CV			**0%**	**0%**	**3%**	**2%**	**16%**	**2%**	**2%**	**1%**		**1%**	**1%**		**-1**
H-11b3	1985-1994	7	7.14	117600	1560	1177	38914	805	64286	6741	44	49	49		
CV			**2%**	**2%**	**9%**	**7%**	**7%**	**13%**	**7%**	**7%**	**22%**	**8%**	**8%**		**-2**
H-11b4R	6/14/2012	1	7.24	112000	1800	1500	42000	940	65000	8400	41	42	42	<2	**1**
[1]H-12R	4/22/2015	1	7.59	151000	1600	1700	51000	1100	94000	7700	99	61.8	61.8	<2	**-7**
H-14	1987-1995	7	7.40	19375	1807	541	3260	235	9106	1864	13	35	35		**-2**

Information Only

Well ID	Sample Date	Sample Size	pH	TDS (mg/L)	Ca2+ (mg/L)	Mg2+ (mg/L)	Na+ (mg/L)	K+ (mg/L)	Cl- (mg/L)	SO42- (mg/L)	Br- (mg/L)	Total Alkalinity (mg/L)	$HCO3^-$ (mg/L)	$CO3^{2-}$ (mg/L)	PHREEQCI Cation/Anion % Error
CV			**5%**	**8%**	**9%**	**7%**	**14%**	**6%**	**8%**	**11%**	**14%**	**14%**	**14%**		
H-15R	1/22/2009	1	7.53	200000	1800	2100	66000	1200	110000	6400	61	63	63	<2	**-1**
H-17	10/27/1987	1	6.64	151000	1500	1700	54700	1400	87300	7000	75	43	43	0	**0**
H-18	1988-1995	3	7.47		1163	505	7827	238	13900	4343	13	54	54		
CV			**3%**		**4%**	**4%**	**3%**	**19%**	**7%**	**14%**	**4%**	**5%**	**5%**		**-4**
H-19b0	8/31/2006	1	7.42	90000	1600	1100	27000	680	47000	4800	50	46	46	<2	**-2**
IMC-461	8/4/2006	1	6.80	9900	1000	250	1800	30	3900	2300	<5	100	100		**-3**
Mobley	4/14/1988	1	7.10		620	140	280	10	430	2100	5	140	140		**-3**
P-14	1986-1988	3	6.81		3600	850	4133	47	14433	1567	19	100	100		
CV			**2%**		**6%**	**8%**	**9%**	**5%**	**3%**	**8%**	**19%**	**0%**	**0%**		**-1**
P-17	1986-1987	2	6.62		1650	1700	29000	865	49000	5950	91	54	54		
CV			**6%**		**3%**	**6%**	**0%**	**8%**	**4%**	**8%**	**7%**	**0%**	**0%**		**0**
[4]SNL-1	2004-2016	2	7.27	36822	1500	732	10025	346	18556	3650	14	110	110		
CV			**1%**	**2%**	**7%**	**0%**	**0%**	**2%**	**2%**	**1%**	**19%**	**31%**	**31%**		**-2**
SNL-2	1/17/2004	1	7.52	11000	930	230	2600	46	4800	2400	3.1	90	90	<4	**-2**
SNL-3	4/16/2004	1	7.41	47000	1400	740	14000	360	26000	4700	32	63	63	<2	**-5**
[1]SNL-5	7/24/2004	1	7.46	13000	1400	510	1900	67	7000	1700	17	64	64	<2	**-9**
SNL-6	1/16/2008	1	6.17	320000	5500	22000	97000	4800	220000	1800	5100	170	170	<2	**1**
SNL-8	8/2/2007	1	7.26	140000	2000	3100	47000	1500	77000	6400	100	49	49	<2	**3**
SNL-9	11/19/2004	1	6.89	25000	3100	810	4700	44	14000	1600	16	140	140	<4	**-1**
SNL-10	11/3/2006	1	7.92	8500	500	170	1900	72	1100	4400	2.3	46	46	<2	**0**
SNL-12	8/14/2004	1	7.90	4200	610	120	440	15	740	1900	1.7	92	92	<4	**-2**
SNL-13	7/17/2006	1	8.49	21000	990	330	5200	190	8500	3300	31	50	50	<2	**0**
SNL-14	2005-2007	3	7.37	85333	1403	998	29700	583	45000	6467	40	47	47		
CV			**0%**	**2%**	**6%**	**8%**	**12%**	**6%**	**5%**	**9%**	**1%**	**3%**	**3%**		**2**
SNL-15	3/30/2007	1	6.64	280000	4800	12000	90000	6800	180000	1600	1100	200	200	<2	**2**
SNL-16	2006-2016	2	7.26	21851	1500	517	4801	354	9954	2402	4	96	96		
CV			**1%**	**13%**	**9%**	**13%**	**8%**	**24%**	**10%**	**3%**	**22%**	**2%**	**2%**		**0**
SNL-17	2006-2017	2	7.54	3270	612	147	152	6	264	1835	1	99	99		
CV			**0%**	**2%**	**1%**	**2%**	**14%**	**11%**	**5%**	**2%**	**0%**	**5%**	**5%**		**2**
SNL-18	8/18/2006	1	7.51	19000	1100	360	5200	120	8700	3700	5.6	75	75	<2	**-2**

Information Only

Well ID	Sample Date	Sample Size	pH	TDS (mg/L)	Ca2+ (mg/L)	Mg2+ (mg/L)	Na+ (mg/L)	K+ (mg/L)	Cl- (mg/L)	SO42- (mg/L)	Br- (mg/L)	Total Alkalinity (mg/L)	HCO3- (mg/L)	CO3 2- (mg/L)	PHREEQCI Cation/Anion % Error
SNL-19	2006-2016	2	7.69	8517	835	232	1596	60	2690	2247	2	92	92		
CV			**1%**	**5%**	**2%**	**5%**	**0%**	**28%**	**0%**	**2%**	**24%**	**2%**	**2%**		**3**
USGS-4	2006-2008	2	6.58	4200	565	120	595	15	1100	1600		33	33		
CV			**3%**	**2%**	**6%**	**0%**	**9%**	**0%**	**0%**	**13%**		**6%**	**6%**		**-1**
USGS-8	7/30/2008	1	7.75	4400	570	97	810	16	1000	1800		35	35	<2	**4**
WIPP-11 &11R	2004-2021	3	7.26	51000	1700	830	15667	363	26333	4767	28	65	65		
CV			**2%**	**4%**	**5%**	**5%**	**3%**	**1%**	**5%**	**23%**	**23%**	**14%**	**14%**		**0**
[1]WIPP-13	2/16/1987	1	6.74		1450	1010	19000	340	36000	4500	39	120	120	0	**-6**
WIPP-19	1989-1995	7	7.27	71884	1593	1089	25729	587	40914	6001	42	50	50		
CV			**2%**	**7%**	**7%**	**17%**	**15%**	**13%**	**13%**	**10%**	**21%**	**13%**	**13%**		**1**
[1]WIPP-25	9/23/2004	1	7.55	28000	1800	660	8000	720	14000	2600	<5	100	100	<4	**6**
WIPP-26	4/14/1988	1	6.87		1200	330	2600	189	5500	2500		110	110		**-1**
WIPP-27	9/3/1980	1	6.25		3210	1920	39400	8010	79000	3800		126	126		**-2**
WIPP-28	9/11/1980	1	6.5		1150	550	15200	490	24800	4460		373	373		**-1**
WIPP-29	3/11/1987	1	6.28		600	5900	89000	20000	200000	17000	54	180	180		**-10**
WIPP-30	5/5/2005	1	8.01	38000	1140	320	13000	170	18000	3900	12	44	44	<4	**5**

[1] Samples labeled in this table with a 1 superscript, have Cation/Anion % errors that are over 5%. These data will still be used in the study, since limited data is available. However, they should be considered with caution as the cations and anions are not well balanced.

[2] AIS stands for Air Intake Shaft and represents Culebra waters that were collected during drilling of the shaft.

[3]Bromide values are very low, this is making the CV% erroneous. Bromide data will still be used. Historical value for Bromide (2016) was 12 mg/L

[4] SNL-1 has values for Total Alkalinity and Bicarbonate that are above the 30% acceptance criteria (31%). The Total Alkalinity value will still be used in this study. The values that were collected were collected over a very large span (2004-2016) of time and it is possible that the chemistry evolved in that time period.

Note:

- If a cell is empty in this table, it means there were no values reported for that analyte.
- A CV percentage was not calculated for samples that only had one data collection.
- For a detailed description of acceptance/rejection for each value, see Excel spreadsheet: *Culebra_Chemistry_ALL_AP194.xlsx* at the file location CVS/CVSLIB/WIPP EXTERNAL/ap194

Information Only

Table 8 **Summary of Average, CVs, and PHREEQCI Cation/Anion Percent Error for Data Set #3: WQSP_Culebra_Wells**

Calculated Averages and CVs for WIPP Monitoring wells: Data Set #3: WQSP_Culebra_Wells

Well ID	Sample Date	Sample Size	pH	Ca^{2+} (mg/L)	Mg^{2+} (mg/L)	Na^{+} (mg/L)	K^{+} (mg/L)	Cl^{-} (mg/L)	$SO4^{2-}$ (mg/L)	Br^{-} (mg/L)	Total Alkalinity (mg/L)	$HCO3^{-}$ (mg/L)	$CO3^{2-}$ (mg/L)	PHREEQCI Cation/Anion % Error
WQSP-1	1995-2020	32	7.17	1734	1136	19719	596	37097	4801	38	51	51		
CV			**2%**	**6%**	**7%**	**10%**	**25%**	**7%**	**7%**	**15%**	**9%**	**2%**		-4
WQSP-2	1995-2020	32	7.24	1534	1067	19810	578	35663	5586	40	47	48		
CV			**1%**	**6%**	**6%**	**10%**	**27%**	**7%**	**8%**	**24%**	**5%**	**1%**		-4
WQSP-3	1995-2020	32	6.84	1470	2288	78307	1868	131656	7543	95	36	39		
CV			**2%**	**12%**	**11%**	**20%**	**29%**	**7%**	**7%**	**21%**	**15%**	**11%**		-2
WQSP-4	1995-2020	32	7.16	1595	1193	33950	922	60100	6889	54	39	39		
CV			**2%**	**6%**	**7%**	**9%**	**27%**	**8%**	**9%**	**18%**	**8%**	**2%**		-5
WQSP-5	1995-2020	32	7.53	1059	496	9577	367	15738	5103	26	48	48		
CV			**2%**	**8%**	**17%**	**9%**	**24%**	**7%**	**9%**	**25%**	**7%**	**4%**		-3
[1]WQSP-6	1995-2020	32	7.72	684	214	4406	183	5818	4814	9	48	50		
CV			**1%**	**5%**	**7%**	**12%**	**22%**	**32%**	**8%**	**27%**	**7%**	**4%**		-3

[1]The data from this sample will still be used even though the CV is above the 30% cut-off criteria. It is only 2 % above the criteria and it spans a 32-year period and the Cl- concentration is low and contains more error because it is close to the limit of detection for the instrumentation.

Notes:

- All values highlighted in red and shaded did not meet the <30% CV acceptability criteria.
- For a detailed description of acceptance/rejection for each value, see Excel spreadsheet: Culebra_wells_AP194.xlxs at the file location: CVS/CVSLIB/WIPP EXTERNAL/ap194.
- If a cell is empty in this table, it means there were no values detected for that analyte.

Information Only

2 *Methods*

2.1 Computer Codes and Programs

PHREEQCI version 2.12.5-669, (Parkhurst and Appelo, 1999) was used to perform basic speciation and saturation index calculations. All molalities, activity coefficients, ionic strengths, osmotic coefficients, cation/anion percent error and saturation indices for all well data in this study were calculated using PHREEQCI 2.12.5-669 code.

PHREEQCI version 2.12.5-669 is a computer program that is written in the C programming language. It is designed to perform various aqueous geochemistry calculations. There are several databases that can be used to accompany the calculations and PHREEQCI code. This study will use the *pitzer.dat* database. This database contains parameters that allow interpretation of geochemistry parameters, in higher ionic strength environments.

2.2 Water Types and Classifications

Several techniques were used to explore and evaluate water types in this study. Data was plotted in Microsoft Excel and displayed in diagrams such as Piper plots, Chadha plots and ion/element ratio spatial distribution contour maps. A correlation matrix analysis was also conducted to establish predominant ions contributing to and controlling the water characteristics and processes.

2.2.1 Correlation Matrix Analysis

A correlation matrix analysis was performed for all data sets, to determine the primary correlations (r, correlation coefficients) between ions in the Culebra waters. Correlation analysis was performed using the Microsoft Excel Analyze feature: Data analysis (correlation). A correlation analysis was performed on all three data sets combined and an individual correlation analysis was also completed for each identified facies zone to determine the dominant correlations for each individual zone.

Microsoft Excel computes the Correlation Coefficient (r), using the equation for the Pearson's Correlation Coefficient, given as:

Equation 3

$$r = \frac{n(\sum x_i y_i) - (\sum x_i)(\sum y_i)}{\sqrt{[n\sum x_i^2 - (\sum x_i)^2][n\sum y_i^2 - (\sum y_i)^2]}}$$

where,

r = Correlation Coefficient
x = values of the variable x
y = values of the variable y
n = number of samples in the data set
Numerator = Covariance of x and y

Information Only

Denominator = Product of Standard Deviation of x and Standard Deviation of y

2.2.2 Map generation

Maps for this study were generated using ArcGIS 10.8 and the ArcGIS extensions spatial analyst. Contour maps were generated for several different components, such as saturation index for key minerals, molar ratio spatial distribution and ion concentration spatial distribution. For all the molality concentration maps, a quantile classification method was used to generate the contour ranges. The quantile classification method is such that, the ArcGIS software will statistically analyze the data and generate contour intervals based on the percentages of data at various concentrations rather than equally dividing the ranges across the entire data range. This type of classification will help better delineate similarities and differences between the data points and hopefully allow unique areas to be identified. An example of equal range distribution is shown in Figure 12.

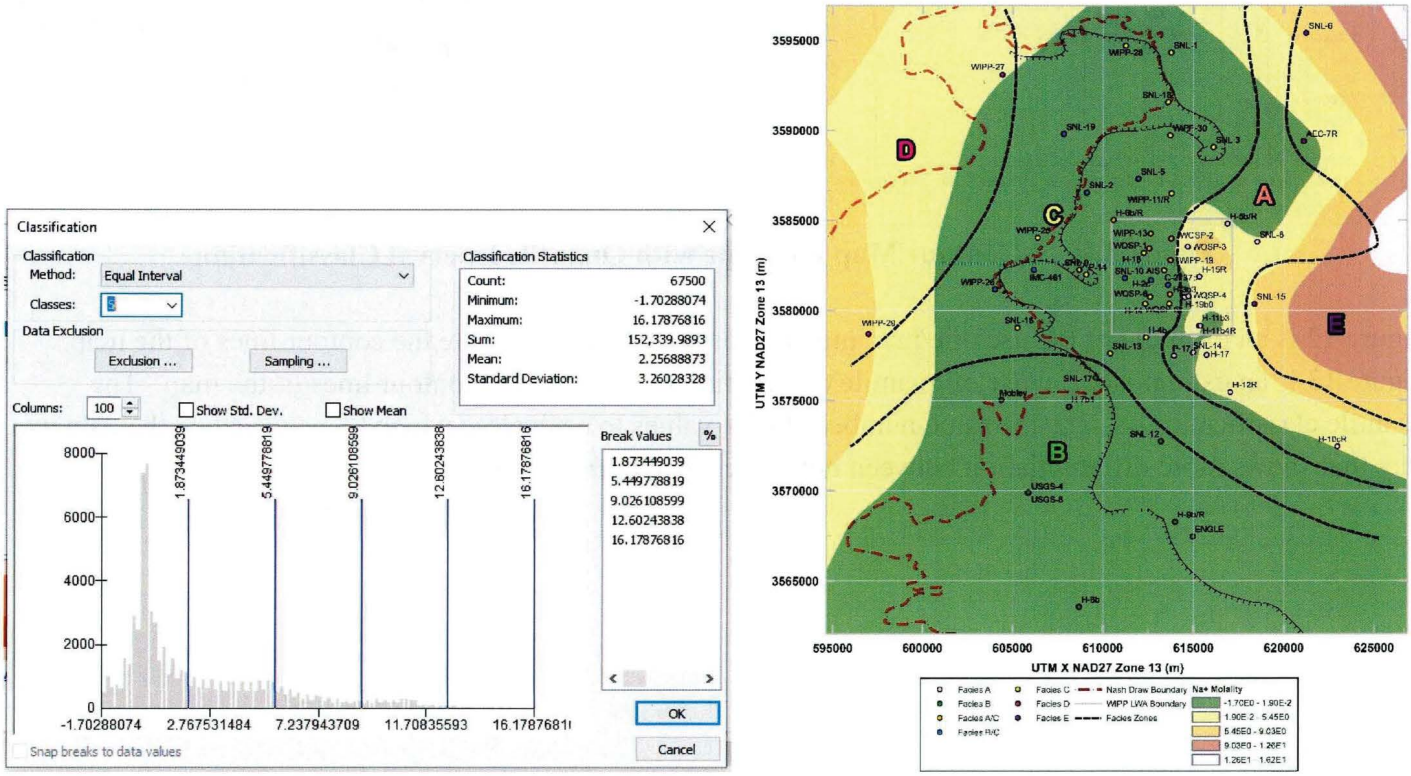

Figure 12 Contour Map Example with Equal Interval Classification

Information Only

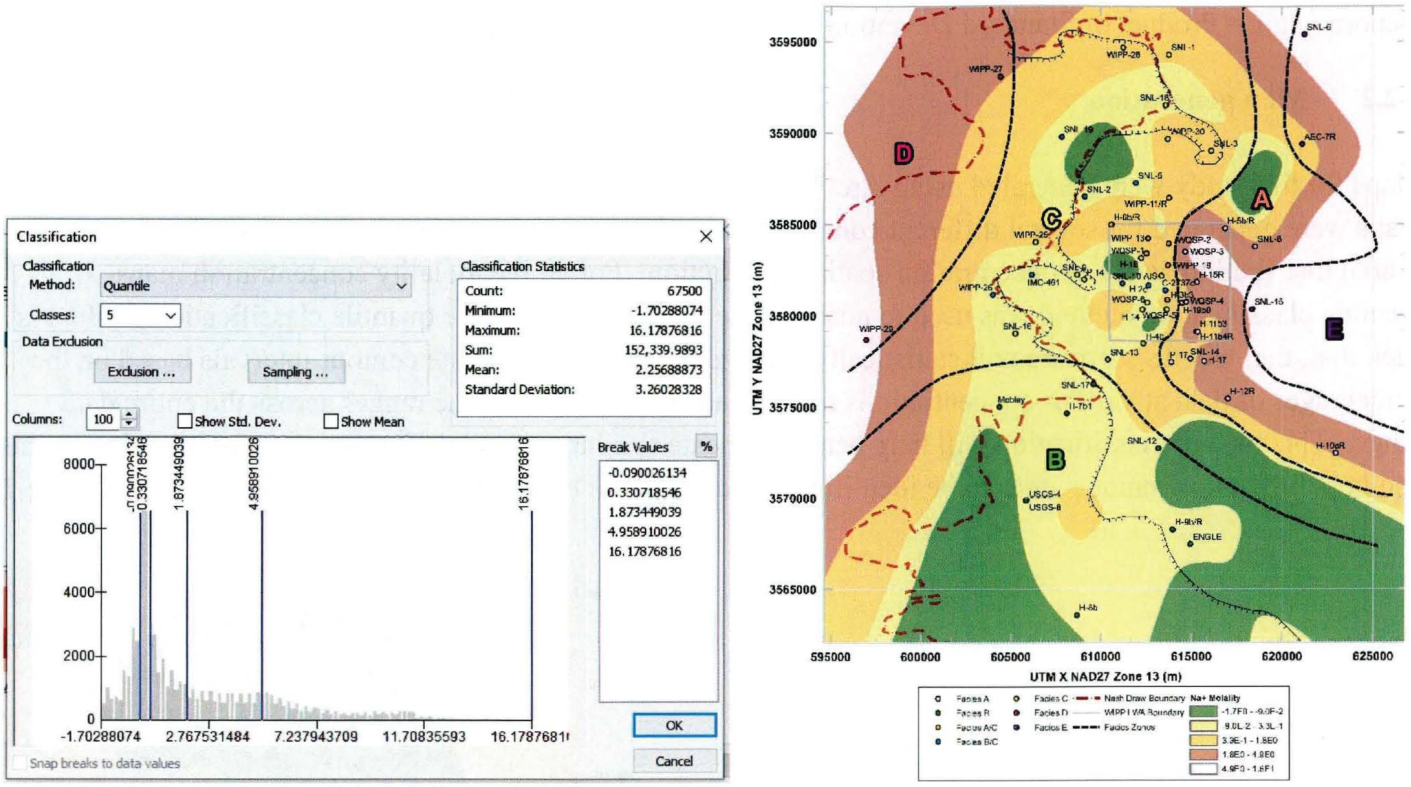

Figure 13 Contour Map Example with Quantile Interval Classification

Figure 12 is an example of the use of equal interval classification to generate the contour lines of the map. Figure 13 is an example of the use of quantile distribution to generate the contour lines of the map. The quantile classification assigns the same number of data values to each class which helps visualize the data in a way that shows more differentiation between notable changes between wells.

Information Only

3 *Results*

3.1.1 Hydro-chemical Facies/Zones Updates

As described in section 1.3 of this report, wells were separated into zones based on previous studies (Siegel, 1991, and Domski and Beauheim, 2008). Three data sets are considered, including all located geochemistry data for Culebra wells from 1978-2021. The incorporation of new geochemical data warranted a change in the facies zone A facies division, from Siegel et al. (1991). The current data suggests that wells WQSP-2 and WIPP-19 should be mapped in faces zone A/C rather than facies zone A. This same classification was determined in Domski and Beauheim, 2008; however, their study did not re-draw the Siegel et al. 1991 facies divisions. The division was "straightened" to allow these two wells to be represented in facies zone A/C. Figure 14 below shows the change to the zone A facies division. The image on the left, is the zone A facies division drawn to the Siegel, 1991 criteria, and the figure on the right is the zone A facies division re-drawn to encompass the current data values. Facies zone A division was extended to include the full area of the map. The facies zone A division in the northern region of the map, however, is an approximation, because there are no data points in that region. Figure 15 shows the updated map with all the Culebra well locations considered in this study.

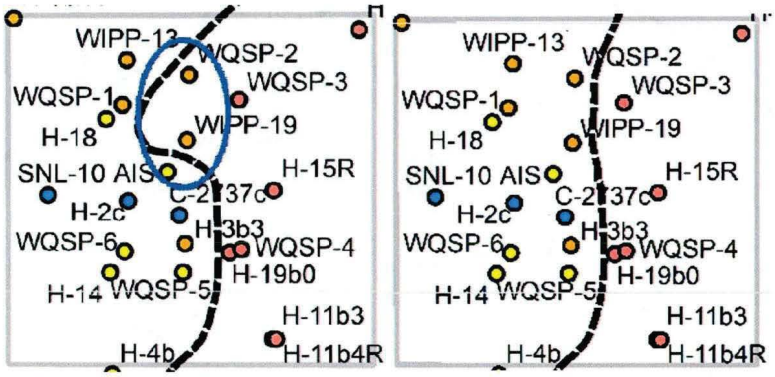

Figure 14 Facies/Zone Map Zone A Update (Blue oval represents the updated region of Zone A)

Another update that was made to the facies zone map, was the addition of a facies division for facies E. This was estimated/approximated based on wells with similar chemistry (wells SNL-6, SNL-15 and AEC-7R) and based on the locations of the Mudstone/Halite (M/H) margins.

New geochemical data have been collected from wells since 2008, and these data were not included in the Domski and Beauheim, 2008 study. For this analysis, more modern data and data added from wells not considered in either of the previous studies were considered. Additional wells added in this study include AEC-7R, H-2b2, H-3b3, H-4bR, H-5b, H-5bR, H-6bR, H-7b1, H-9bR, H-10cR, H-11b4R, H-12R, H-15R, USGS-8, and WIPP-11R. The majority of these new study wells are replacement wells (wells with R designation) that have been installed since 2007.

Information Only

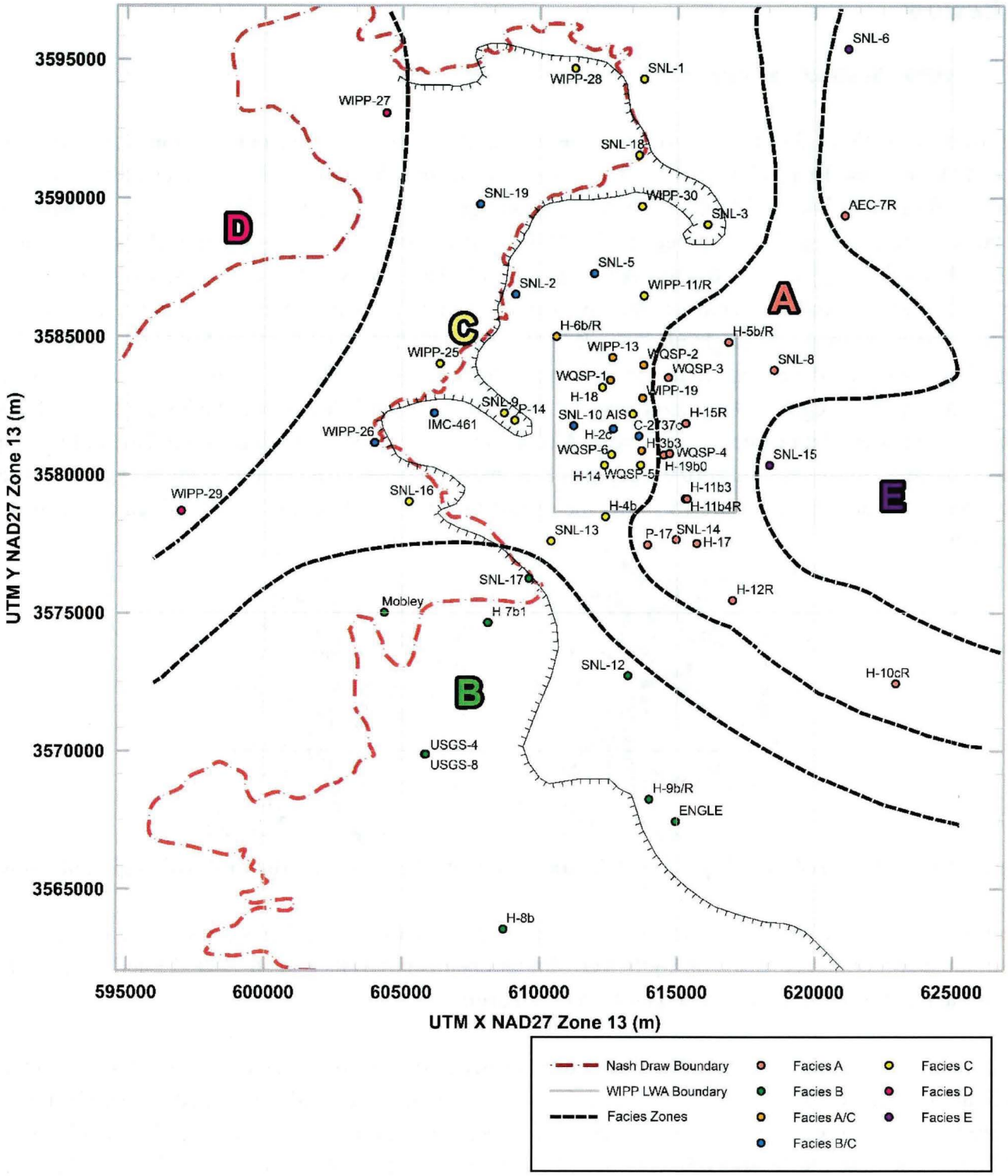

Figure 15 2022 Updated Facies/Zone Map in Relation to Well Locations

3.1.2 Correlation Analysis

A correlation analysis was performed to determine correlations between primary hydrochemical parameter interactions. Correlation analysis for the entire Culebra well study area is summarized in Table 9. In this study all correlation values ≥0.5 and ≤-0.5 will be considered relevant and any correlation value ≥0.7 and ≤-0.7 will

Information Only

be considered highly correlated. Waters that have a very high correlation between geologically paired ions, such as Na^+ and Cl^-, indicate that a mineral containing those ions, in this case halite, is likely present in the water. These analyses do not give information about over-all concentration of the parameters or their percentage in the whole but show that the parameters are highly correlated and likely both present in the water. Another example of this is the effect or correlation that Na^+ has on ionic strength. If Na^+ and Cl^- are highly correlated (i.e halite) and Na^+ and Cl^- are both also highly correlated to ionic strength, then there is a high likelihood that halite (or another Na^+/Cl^- salt) is contributing significantly to the ionic strength of the waters. The correlation of individual parameters to ionic strength can be very helpful in understanding the contribution of a parameter to the whole, while the correlations between individual ions are helpful in determining what types of minerals may be contributing to that water type. In Table 9 and Table 10, Φ symbol is used to denote osmotic coefficient or the relative ion activity of the water.

Table 9 Correlation analysis for all Culebra Facies Zones A-E (Combined zones)

All Culebra Wells (Facies Zones A-E) (n = 86)

	pH	*Alk*	*mu*	*m_Ca+2*	*m_Mg+2*	*m_Na+*	*m_K+*	*m_Cl-*	*m_SO4-2*	*m_Br-*	*m_HCO3-*	*m_CO3-2*	Φ
pH	1.00												
Alk	-0.32	1.00											
mu	-0.40	0.40	1.00										
m_Ca+2	-0.36	0.39	**0.75**	1.00									
m_Mg+2	-0.34	0.49	**0.85**	**0.83**	1.00								
m_Na+	-0.39	0.34	**0.98**	**0.66**	**0.74**	1.00							
m_K+	-0.35	0.47	**0.67**	0.31	0.49	**0.66**	1.00						
m_Cl-	-0.40	0.38	**1.00**	**0.74**	**0.83**	**0.99**	**0.65**	1.00					
m_SO4-2	-0.20	0.07	**0.57**	0.03	0.16	**0.66**	**0.66**	**0.57**	1.00				
m_Br-	-0.29	**0.52**	**0.68**	**0.77**	**0.93**	**0.54**	0.26	**0.66**	-0.07	1.00			
m_HCO3-	-0.52	**0.88**	0.12	0.06	0.12	0.10	0.39	0.11	0.07	0.09	1.00		
m_CO3-2	**0.58**	0.09	0.06	0.04	0.00	0.08	-0.01	0.07	0.09	-0.02	-0.18	1.00	
Φ	-0.37	0.41	**0.97**	**0.82**	**0.90**	**0.93**	**0.60**	**0.97**	0.46	**0.77**	0.09	0.06	1.00

The comprehensive Culebra water chemistry shows strong positive correlations between ionic strength (*mu*) and ions (Ca^{2+}, Mg^{2+}, Na^+, K^+, Cl^-, SO_4^{2-}, and Br^-). This result suggests an important role between these ions and the geochemistry of the Culebra. In Table 9, any correlation value at or above 0.5 or at or below -0.5 was considered significant and bolded. The high correlation between the Na^+/Cl^- and Ca^{2+}/Mg^{2+} ions indicates that these waters are possibly being heavily influenced by the mineral halite (0.99 Na^+/Cl^- correlation), and dolomite (0.83 Ca^{2+}/Mg^{2+} correlation). Interestingly, there is also a very high correlation between Mg^{2+} and Br^- molality (0.93), which suggests that these minerals are likely to occur together. The moderately high correlation between K^+ and Cl^- and SO_4^{2-} (0.65 and 0.66, respectively), alludes to a presence of minerals with those ions, such as polyhalite and/or carnallite. A final observation for the over-all correlation matrix analysis of the Culebra is that pH is affected primarily by the carbonate in the system (CO_3^{2-}). The ion concentrations of major ions in the system are plotted against ionic strength in Figure 16.

Information Only

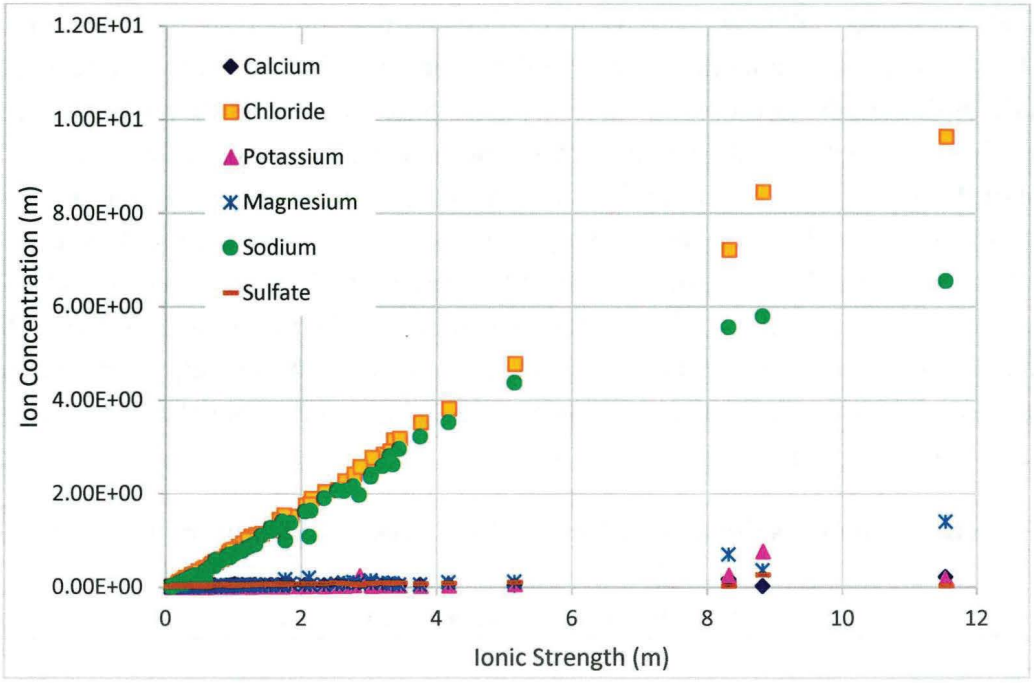

Figure 16 Culebra waters Ion concentration (molality) vs. Ionic Strength (molality)

The correlation matrix analysis and Figure 16 both identify the same primary ions contributing to ionic strength of the waters. This figure makes it clear that the predominant ions in the waters are Na^+ and Cl^-, however, with this method it is more difficult to clearly identify the influences of concentration of the other ions in the system.

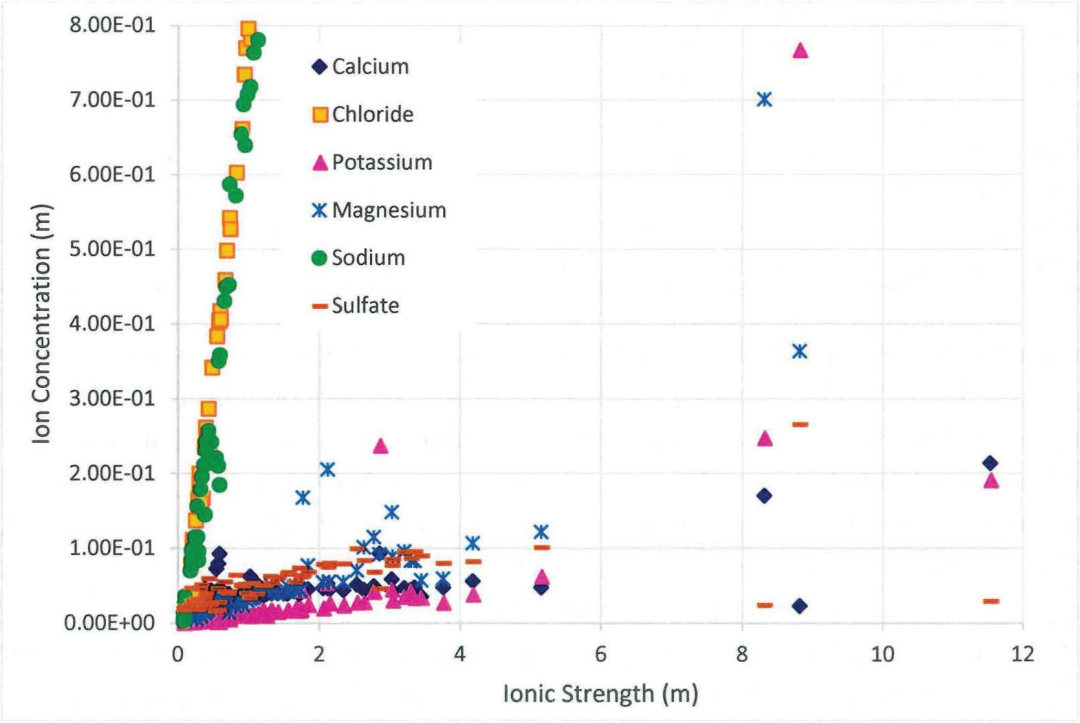

Figure 17 Culebra waters Ion Concentration (m) vs. Ionic Strength (m) focused

Figure 17 plots ion concentration vs. ionic strength with a focus on a narrower ion concentration range. Based on Figure 17, the ions influencing the ionic strength the most follow the order; $Cl>Na>Mg>SO_4>Ca>K$. While

Information Only

these ions are influencing the ionic strength the most, it does not necessarily mean that they are influencing the hydrogeochemistry in the same way. Many processes other than ionic strength play a much bigger role in the chemistry of a system than just ionic strength. Activity of an ion and the solubility of a mineral both play major roles in hydrogeochemistry processes of a water system. Ionic strength can influence the ions and minerals in the water to make them more or less soluble. The solubility of a mineral, when it is exposed to different solvents, directly correlates to dissolution rates of the host rock and the order in which dissolution occurs.

While these data give us information about the combined ionic strength of the Culebra water as a whole, it does not reveal the specific minerals or waters that make up the various facies individually or their specific dissolution/solubility rates. To compensate for this lack of information, each of the designated facies zones was analyzed in a focused correlation matrix study, to determine the primary correlations of ions for each facies water. An important thing to note about these types of data, however, are that they can be heavily influenced by sample size. If the sample size is very small for a data set, the correlation coefficient can be easily affected by small differences in the data values. For this reason, data may show false or misleading trends. The sample size (n) for each of the facies in this correlation matrix is listed in the facies title heading. Facies zones D and E have very small sample sizes (2 and 4 respectively), so their correlation data and any conclusions derived from the data, should be considered with discernment. Table 10 shows the correlation analyses of the various zones.

Table 10 Correlation Matrix Facies Zone A

Zone A (n = 19)													
	pH	*Alk*	*mu*	*m_Ca+2*	*m_Mg+2*	*m_Na+*	*m_K+*	*m_Cl-*	*m_SO4-2*	*m_Br-*	*m_HCO3-*	*m_CO3-2*	Φ
pH	1.00												
Alk	**0.82**	1.00											
mu	-0.33	-0.32	1.00										
m_Ca+2	-0.20	-0.08	0.33	1.00									
m_Mg+2	-0.12	-0.04	**0.58**	**0.67**	1.00								
m_Na+	-0.36	-0.34	**1.00**	0.29	**0.53**	1.00							
m_K+	-0.27	-0.19	**0.84**	0.42	**0.81**	**0.82**	1.00						
m_Cl-	-0.30	-0.32	**1.00**	0.28	**0.53**	**0.99**	**0.81**	1.00					
m_SO4-2	-0.27	-0.30	**0.67**	0.16	0.32	**0.67**	**0.54**	**0.65**	1.00				
m_Br-	-0.25	-0.07	**0.53**	0.40	**0.80**	0.48	**0.79**	**0.51**	0.33	1.00			
m_HCO3-	-0.14	0.36	-0.08	0.19	0.07	-0.09	-0.11	-0.10	-0.09	0.05	1.00		
m_CO3-2	**0.86**	**0.82**	-0.23	-0.21	-0.25	-0.24	-0.27	-0.20	-0.36	-0.33	-0.24	1.00	
Φ	-0.31	-0.30	**1.00**	0.33	**0.59**	**0.99**	**0.84**	**0.99**	**0.62**	**0.54**	-0.09	-0.21	1.00

Facies Zone A

A relevant correlation between ionic strength and ions Mg^{2+}, Na^{+}, K^{+}, Cl^{-}, SO_4^{2-}, and Br^{-} was identified in the correlation analysis. This is different from the combined analysis in that Ca^{2+} is not influencing the ionic strength in this facies zone (0.33), while in the combined analysis the Ca^{2+} correlation to ionic strength was (0.75). Mg^{2+} and Ca^{2+} are still highly correlated in this facies zone (0.67) but not nearly as strong (0.83) as in the combined analysis. In addition, Mg^{2+} is the only ion that is highly correlated with Ca^{2+} for this zone. These correlations indicate that a Ca^{2+}/Mg^{2+} containing mineral such as dolomite is likely present and a mineral, such as gypsum or calcite (minerals without magnesium) are not as prevalent in this zone. Another relevant

Information Only

correlation in this zone is the relatively high correlation between K^+/Cl^- (0.81), K^+/SO_4^{2-} (0.54) and K^+/Br^- (0.79). This correlation likely indicates the presence of minerals such as, polyhalite and/or carnallite.

Table 11 Correlation Matrix Facies Zone A/C

Zone A/C (n = 9)													
	pH	*Alk*	*mu*	*m_Ca+2*	*m_Mg+2*	*m_Na+*	*m_K+*	*m_Cl-*	*m_SO4-2*	*m_Br-*	*m_HCO3-*	*m_CO3-2*	Φ
pH	1.00												
Alk	0.29	1.00											
mu	0.23	0.02	1.00										
m_Ca+2	-0.24	0.16	-0.33	1.00									
m_Mg+2	-0.41	-0.23	0.39	0.16	1.00								
m_Na+	0.31	0.04	**0.98**	-0.38	0.20	1.00							
m_K+	0.33	**-0.65**	**0.53**	-0.27	0.38	0.49	1.00						
m_Cl-	0.18	0.08	**0.98**	-0.35	**0.52**	**0.92**	0.49	1.00					
m_SO4-2	0.26	-0.23	**0.81**	**-0.63**	0.13	**0.82**	**0.55**	**0.75**	1.00				
m_Br-	-0.18	0.10	**0.69**	-0.20	**0.71**	**0.55**	0.19	**0.78**	**0.60**	1.00			
m_HCO3-	**-0.60**	**0.58**	-0.21	0.32	0.12	-0.25	**-0.82**	-0.12	-0.46	0.15	1.00		
m_CO3-2	**0.93**	**0.60**	0.23	-0.13	-0.38	0.29	0.04	0.21	0.19	-0.03	-0.30	1.00	
Φ	0.15	0.16	**0.95**	-0.15	**0.52**	**0.90**	0.42	**0.96**	**0.59**	**0.68**	-0.01	0.19	1.00

Facies Zone A/C

A relevant correlation between ionic strength in zone A/C and ions Na^+, K^+, Cl^-, SO_4^{2-} and Br^- was identified in the correlation analysis. Neither Mg^{2+} (0.39) or Ca^{2+} (-0.33) are highly correlated to ionic strength in this zone. In fact, Ca^{2+} is showing a weak negative correlation (-0.33) with ionic strength, indicating the low presence of calcium containing minerals. Additionally, Ca^{2+} is negatively correlated with SO_4^{-2} (-0.63), further indicating that the mineral gypsum is not likely present in this zone. There is a relatively higher negative correlation between K^+/HCO_3^- (-0.82) and K^+/Alkalinity (-0.65) and a positive correlation between K^+/SO_4^{2-} (0.55). There is also a very strong correlation between Na^+/SO_4^{2-} (0.82) and Na^+/Cl^- (0.92) in this zone, suggesting that minerals gypsum/anhydrite and halite could be major components in this zone. There is also a positive correlation between Mg^{2+}/Br^- (0.71) and Mg^{2+}/Cl^- (0.52), suggesting that minerals such as carnallite and/or magnesium chloride dominant minerals could be present.

Table 12 Correlation Matrix Facies Zone B

Zone B (n = 13)													
	pH	*Alk*	*mu*	*m_Ca+2*	*m_Mg+2*	*m_Na+*	*m_K+*	*m_Cl-*	*m_SO4-2*	*m_Br-*	*m_HCO3-*	*m_CO3-2*	Φ
pH	1.00												
Alk	0.35	1.00											
mu	0.13	-0.10	1.00										

Information Only

m_Ca+2	0.45	**0.54**	0.42	1.00									
m_Mg+2	-0.05	**0.56**	**-0.67**	0.11	1.00								
m_Na+	0.01	-0.46	**0.86**	-0.05	**-0.88**	1.00							
m_K+	0.13	-0.28	**0.93**	0.29	**-0.65**	**0.85**	1.00						
m_Cl-	-0.11	-0.51	**0.84**	-0.05	**-0.83**	**0.96**	**0.87**	1.00					
m_SO4-2	0.29	**0.65**	0.30	**0.81**	0.22	-0.16	0.13	-0.23	1.00				
m_Br-	**-0.62**	0.35	0.19	0.02	-0.07	0.04	-0.07	0.03	**0.64**	1.00			
m_HCO3-	**-0.72**	**1.00**	-0.30	0.29	**0.65**	**-0.66**	-0.40	**-0.57**	**0.57**	**0.86**	1.00		
m_CO3-2	**0.77**	-0.11	0.23	0.38	-0.15	0.11	0.39	0.30	-0.02	-0.44	-0.16	1.00	
Φ	-0.08	-0.44	**0.87**	0.01	**-0.87**	**0.96**	**0.87**	**0.99**	-0.15	0.08	**-0.52**	0.26	1.00

Facies Zone B

A relevant correlation between ionic strength in zone B and ions Mg^{2+}, Na^{+}, K^{+}, and Cl^{-} was identified in the correlation analysis. Mg^{2+} has a moderately negative correlation (-0.67), while Na^{+}, K^{+}, and Cl^{-} have a highly positive correlation with ionic strength (0.86, 0.93 and 0.84 respectively). The negative correlation of Mg^{2+} would indicate that magnesium is not contributing significantly to the ionic strength in this zone. The predominant ion contributors to ionic strength, are Na^{+}, K^{+}, and Cl^{-}. There is also a very high positive correlation between Ca^{2+} and SO_4^{2-} (0.81), in this zone indicating that a mineral containing both calcium and sulfate (i.e., gypsum) is present. There is a very high positive correlation between Na^{+}/K^{+} (0.85), Na^{+}/Cl^{-} (0.96) and K^{+}/Cl^{-} (0.87). These high correlations indicate that minerals such as sylvite or halite may predominate this zone, along with smaller amounts of gypsum. There is a very high positive correlation between Br^{-}/HCO_3^{-} (0.86), and a significantly negative correlation between pH/Br^{-} (-0.62) and pH/HCO_3^{-}(-0.72). A final relevant observation for this zone, is a very high positive correlation between pH/CO_3^{2-} (0.77). All these final observations suggest that a carbonate containing mineral, such as calcite or dolomite, has a dominant presence in this zone.

Table 13 Correlation Matrix Facies Zone B/C

	Zone B/C (n = 13)											
	pH	*Alk*	*mu*	*m_Ca+2*	*m_Mg+2*	*m_Na+*	*m_K+*	*m_Cl-*	*m_SO4-2*	*m_Br-*	*m_HCO3-*	*m_CO3-2*	Φ
pH	1.00												
Alk	**-0.61**	1.00											
mu	-0.01	-0.03	1.00										
m_Ca+2	-0.35	0.08	**0.78**	1.00									
m_Mg+2	-0.43	0.11	**0.67**	**0.91**	1.00								
m_Na+	**0.51**	-0.15	**0.56**	0.02	-0.23	1.00							
m_K+	-0.11	0.04	**0.51**	0.21	0.11	**0.51**	1.00						
m_Cl-	0.01	-0.06	**0.91**	**0.86**	**0.69**	0.44	0.31	1.00					
m_SO4-2	0.16	-0.03	-0.33	**-0.74**	**-0.58**	0.13	0.14	**-0.68**	1.00				

Information Only

m_Br-	-0.05	-0.31	**0.65**	**0.58**	**0.64**	0.09	0.38	**0.65**	-0.34	1.00			
m_HCO3-	**-0.74**	**0.98**	-0.08	0.11	0.18	-0.30	0.00	-0.12	-0.04	-0.29	1.00		
m_CO3-2	**0.79**	-0.30	0.26	-0.20	-0.39	**0.78**	0.18	0.24	0.15	0.00	-0.49	1.00	
Φ	0.10	-0.05	**0.56**	**0.66**	0.39	0.36	0.09	**0.84**	**-0.87**	0.41	-0.11	0.25	1.00

Facies Zone B/C

A relevant correlation between ionic strength in zone B/C and ions Ca^{2+}, Mg^{2+}, Na^{+}, K^{+}, Cl^{-} and Br^{-} was identified in the correlation analysis. Ca^{2+}/mu (0.78) and Cl^{-}/mu (0.91) have the highest positive correlations, while ions for Mg^{2+}, Na^{+}, K^{+}, Cl^{-} and Br^{-} have only moderately high positive correlations with ionic strength (0.67, 0.56, 0.51, 0.65 respectively). This would indicate that Ca^{2+} and Cl^{-} are both predominant in contributing to ionic strength for this zone. The correlations between Ca^{2+}/Mg^{2+} (0.91) and Ca^{2+}/Cl^{-} (0.86) are also very high. These ion correlations would indicate that dolomite and $CaCl_2$ may be present in this zone. Furthermore, there is a highly negative correlation between Ca^{2+}/SO_4^{2-} (-0.74), indicating a lack of gypsum in this zone. There is a high positive correlation between Na^{+}/CO_3^{2-} (0.78), along with a very high positive correlation between pH $/CO_3^{2-}$ (0.79). There is a relatively high correlation between Cl^{-}/Br^{-} (0.65). A final observation for this zone is the rather low positive correlation (compared to the other zones), of the ionic strength and the osmotic coefficient (0.56). All other facies zones have ionic strength/osmotic coefficient correlations that are 0.87 or higher, signifying that ionic strength and osmotic coefficient are directly influenced by each other. Having a lower ionic strength/osmotic coefficient correlation suggests that the mineral controlling the ionic strength and osmotic coefficient is not very soluble.

Table 14 Correlation Matrix Facies Zone C

	Zone C (n = 26)												
	pH	*Alk*	*mu*	*m_Ca+2*	*m_Mg+2*	*m_Na+*	*m_K+*	*m_Cl-*	*m_SO4-2*	*m_Br-*	*m_HCO3-*	*m_CO3-2*	Φ
pH	1.00												
Alk	**-0.54**	1.00											
mu	0.09	0.24	1.00										
m_Ca+2	-0.29	0.05	0.22	1.00									
m_Mg+2	-0.30	0.15	**0.67**	**0.77**	1.00								
m_Na+	0.22	0.22	**0.96**	-0.05	0.43	1.00							
m_K+	0.07	0.32	**0.52**	-0.20	0.25	**0.58**	1.00						
m_Cl-	0.08	0.26	**1.00**	0.24	**0.68**	**0.94**	**0.51**	1.00					
m_SO4-2	0.17	0.05	0.34	**-0.72**	-0.27	**0.51**	0.34	0.28	1.00				
m_Br-	0.19	-0.27	0.38	-0.06	0.22	0.37	0.24	0.34	0.48	1.00			
m_HCO3-	**-0.59**	**1.00**	0.21	0.04	0.13	0.19	0.30	0.22	0.05	-0.30	1.00		
m_CO3-2	**0.84**	-0.18	0.41	0.02	0.08	0.45	0.22	0.42	0.08	0.26	-0.25	1.00	
Φ	0.12	0.25	**0.93**	0.35	**0.70**	**0.86**	0.49	**0.95**	0.04	0.15	0.21	0.44	1.00

Information Only

Facies Zone C

A relevant correlation between ionic strength in zone C and ions Mg^{2+}, Na^{+}, K^{+}, and Cl^{-} was identified in the correlation analysis. Ca^{2+} was not an ion that was identified to contribute to the ionic strength, however, Ca^{2+} has a very high positive correlation with Mg^{2+}(0.77), indicating the likely presence of the mineral dolomite. There is also a very high negative correlation between Ca^{2+}/SO_4^{2-} (-0.72), which diminishes the likelihood of gypsum being present in this zone. The Mg^{2+}/Cl^{-} ion correlation has a relatively high positive correlation (0.68). There is a positive correlation between Na^{+}/SO_4^{2-} (0.51) and Na^{+}/K^{+} (0.58) ions. Due to the negative correlation between Ca^{2+}/SO_4^{2-} (-0.72) and the positive correlation between Na^{+}/SO_4^{2-} (0.51), it is most likely that the SO_4^{2-} in the waters of this zone are contributed by a mineral containing both Na^{+} and SO_4^{2-}, since SO_4^{2-} only has one relevant positive correlation with another cation. There is also a positive correlation between K^{+}/Cl^{-} (0.51). There is a strong positive correlation between CO_3^{2-}/pH (0.84) and a negative correlation between HCO_3^{-}/pH (-0.59), suggesting the dissolution of a mineral contributing carbonate to the system, and that mineral controlling the pH of these waters.

Table 15 Correlation Matrix Facies Zone D/E

Zone D (n = 2)

	pH	*Alk*	*mu*	*m_Ca+2*	*m_Mg+2*	*m_Na+*	*m_K+*	*m_Cl-*	*m_SO4-2*	*m_Br-*	*m_HCO3-*	*m_CO3-2*	Φ
pH	1.00												
Alk	**-0.79**	1.00											
mu	**-0.61**	**0.97**	1.00										
m_Ca+2	-0.24	-0.41	**-0.62**	1.00									
m_Mg+2	-0.19	**0.76**	**0.89**	**-0.91**	1.00								
m_Na+	**-0.63**	**0.98**	**1.00**	**-0.60**	**0.88**	1.00							
m_K+	**-0.68**	**0.99**	**1.00**	**-0.55**	**0.85**	**1.00**	1.00						
m_Cl-	**-0.66**	**0.98**	**1.00**	**-0.57**	**0.87**	**1.00**	**1.00**	1.00					
m_SO4-2	-0.40	**0.88**	**0.97**	**-0.79**	**0.98**	**0.96**	**0.94**	**0.95**	1.00				
m_Br-	**1.00**	**-1.00**	**-1.00**	**1.00**	**-1.00**	**-1.00**	**-1.00**	**-1.00**	**-1.00**	1.00			
m_HCO3-	**-0.81**	**1.00**	**0.96**	-0.37	**0.73**	**0.96**	**0.98**	**0.97**	**0.86**	**-1.00**	1.00		
m_CO3-2	0.43	0.22	0.45	**-0.98**	**0.80**	0.43	0.37	0.40	**0.65**	**-1.00**	0.17	1.00	
Φ	**-0.61**	**0.97**	**1.00**	**-0.62**	**0.90**	**1.00**	**1.00**	**1.00**	**0.97**	**-1.00**	**0.96**	0.45	1.00

Zone E (n = 4)

	pH	*Alk*	*mu*	*m_Ca+2*	*m_Mg+2*	*m_Na+*	*m_K+*	*m_Cl-*	*m_SO4-2*	*m_Br-*	*m_HCO3-*	*m_CO3-2*	Φ
pH	1.00												
Alk	**-0.88**	1.00											
mu	**-0.94**	**0.94**	1.00										
m_Ca+2	**-0.93**	**0.96**	**1.00**	1.00									
m_Mg+2	**-0.94**	**0.83**	**0.97**	**0.95**	1.00								
m_Na+	**-0.93**	**0.98**	**0.99**	**1.00**	**0.93**	1.00							

Information Only

m_K+	**-0.77**	**0.98**	**0.87**	**0.91**	**0.73**	**0.93**	1.00						
m_Cl-	**-0.94**	**0.95**	**1.00**	**1.00**	**0.96**	**0.99**	**0.89**	1.00					
m_SO4-2	**0.89**	**-0.99**	**-0.91**	**-0.93**	**-0.80**	**-0.95**	**-0.96**	**-0.92**	1.00				
m_Br-	**-0.89**	**0.66**	**0.88**	**0.84**	**0.97**	**0.80**	**0.54**	**0.86**	**-0.64**	1.00			
m_HCO3-	**-0.50**	**0.81**	**0.56**	**0.61**	0.35	**0.67**	**0.87**	**0.58**	**-0.83**	0.11	1.00		
m_CO3-2	0.01	0.47	0.19	0.26	-0.04	0.32	**0.63**	0.23	-0.45	-0.28	**0.81**	1.00	
Φ	**-0.95**	**0.91**	**1.00**	**0.99**	**0.98**	**0.98**	**0.84**	**1.00**	**-0.89**	**0.91**	**0.50**	0.13	1.00

Facies Zones D & E

Due to the very small sample sizes for these two zones, it is difficult to make any definitive correlations; however, some information can be gleaned. In zone D there is a strong negative correlation between Ca^{2+}/Mg^{2+} (-0.91) and Ca^{2+}/SO_4^{2-} (-0.79), indicating that dolomite and gypsum may be lacking in this zone. Similarly, there are also strong correlations between Ca^{2+}/Mg^{2+} (0.95), indicating the possible presence of dolomite in zone E. There is also highly negative correlation between the SO_4^{2-} (-0.91) ion and ionic strength, indicating the absence of any SO_4^{2-} minerals in zone E.

3.1.3 Water Type Diagrams and Graphs

Traditional diagrams, often used in hydrogeochemical analysis, such as a Piper (1944) diagram can be helpful in visualizing the predominant water types within a water network. Piper diagrams, plot the percentages of the major solutes in a water network (Ca^{2+}, Mg^{2+}, Na^{+}, K^{+}, Cl^{-}, SO_4^{2-}, and HCO_3^{2-}). The Piper diagram is comprised of two triangles at the bottom and one diamond in the center. The percentages of the primary cations are plotted on the bottom left triangle and the percentages of the primary anions are plotted in the bottom right triangle. Water sample data for a well network is plotted on both the cation triangle and the anion triangle. Based on the location that the sample falls in these two triangles, a correlation or combined projection of the cation and anion information can be displayed on the center diagram, where a primary water type can then be defined. Figure 18 shows a Piper diagram of the Culebra water network with the samples plotted by zones. The diagram shows a primary grouping of the wells in the Ca(Mg)-Cl(SO_4) type and the Na-Cl type. There does not seem to be a distinctive correlation between the designated facies zones and the water types defined in the Piper diagram. However, this information is consistent with the correlation matrix in that both analyses identified the dominant cations as being Ca^{2+} and Na^{+}, and the dominant anions being SO_4^{2-} and Cl^{-}.

Information Only

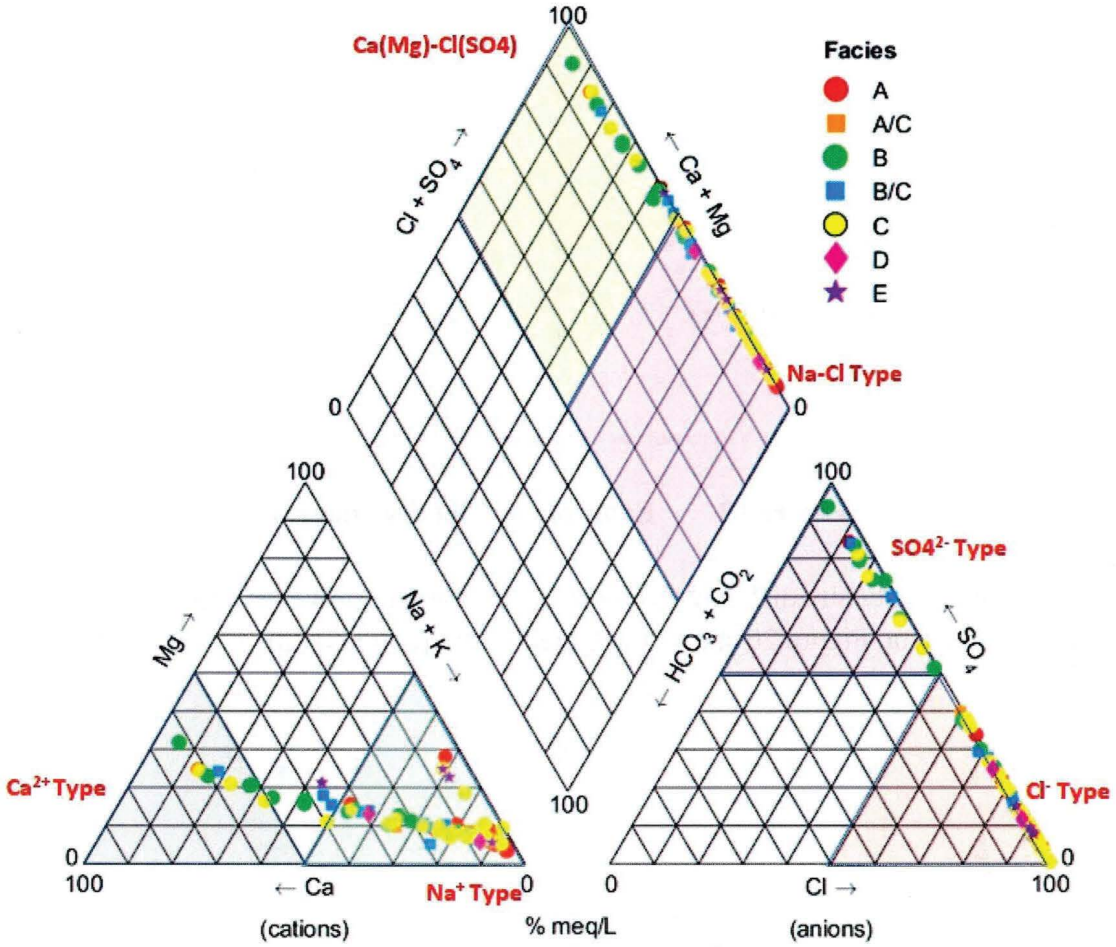

Figure 18 Piper Diagram of the Culebra Well Network

Another useful diagram to help define water types is the Chadha (1999) diagram. The Chadha diagram is a form of modified Piper diagram proposed by Chadha, D.K. in 1999. The diagram evaluates the difference in milliequivalent (meq) percentage of the cations, alkaline earth metals (Ca + Mg) vs. alkali metals (Na + K), by plotting them on the X-axis. The meq percentage (meq %) of the anionic constituents including weak acidic anions (CO_3^{2-} + HCO_3^-) and strong acidic anions (Cl + SO_4^{2-}), are plotted on the Y-axis. Each graphed quadrant represents a water type including Na-HCO_3 type, Ca-Mg-HCO_3 type, Na-Cl water type and Ca-Mg-Cl water type. Figure 19 shows an example of the Chadha diagram template.

Information Only

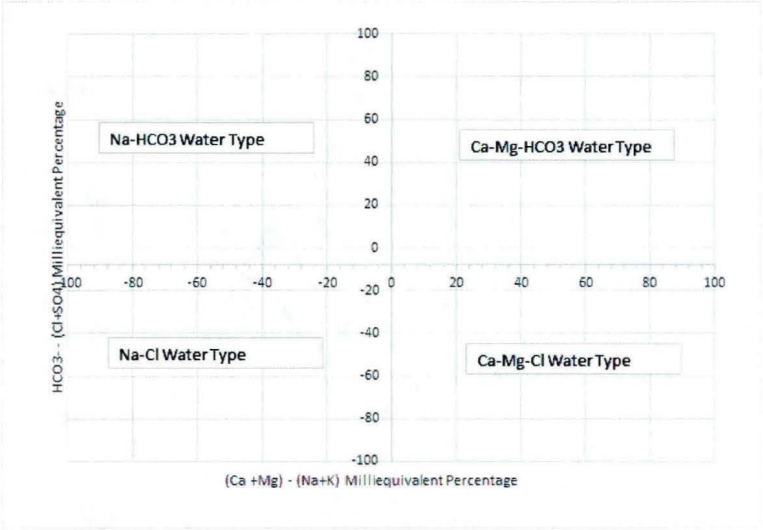

Figure 19 Example of Chadha Diagram

These water types are not drastically different from the Piper diagram; however, this type of diagram allows a better visualization of the data. Figure 20 shows the Culebra data plotted on the Chadha diagram.

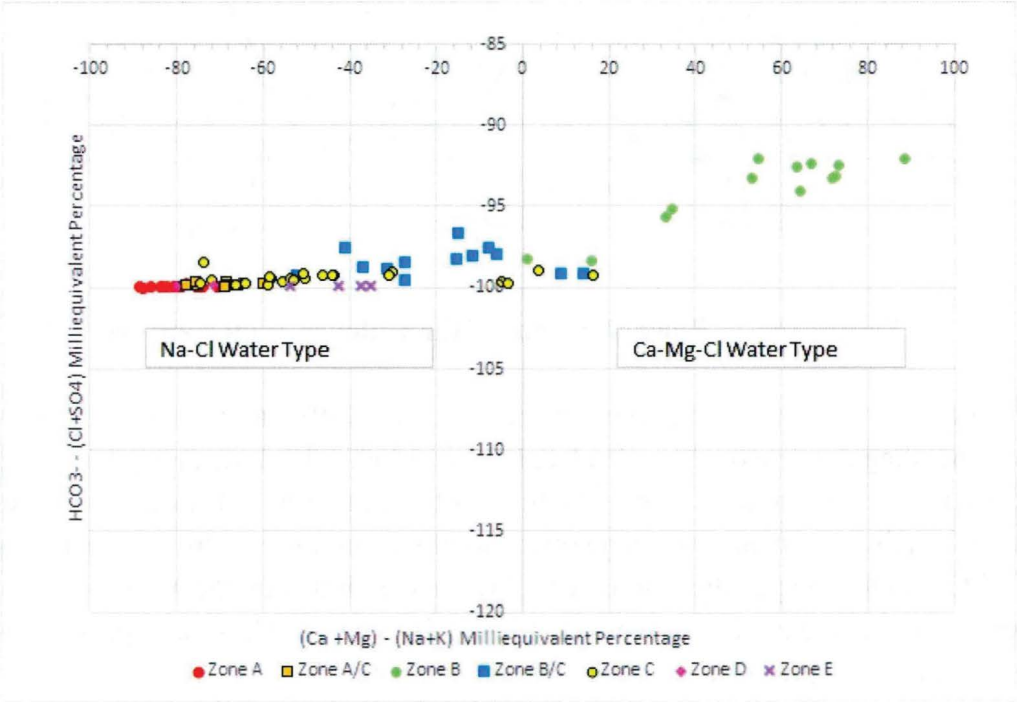

Figure 20 Chadha Diagram for Culebra well data

From the Chadha diagram, it is evident that the majority of zone B samples fall in the Ca-Mg-Cl water type with a few of the zone C and zone B/C samples as well. The diagram also shows grouping of the majority of the zone B/C samples at the center of the X-axis, indicating mixed water types. Finally, the zones A, A/C, D, E and the majority of zone C, are at the far left/bottom quadrant of the diagram, indicating the primary water type as Na-Cl.

Determining the major water types of a network is beneficial, but it is also beneficial to understand the various hydrogeochemical processes that are primary to the network. Plotting the meq/L of the major alkaline earth

Information Only

metals (Ca^{2+} +Mg^{2+}) vs the meq/L of the anions associated with silicate weathering (HCO_3^- +SO_4^{2-}), can provide information about the major weathering processes that are occurring within the system. Figure 21 shows the data for the Culebra network plotted as described.

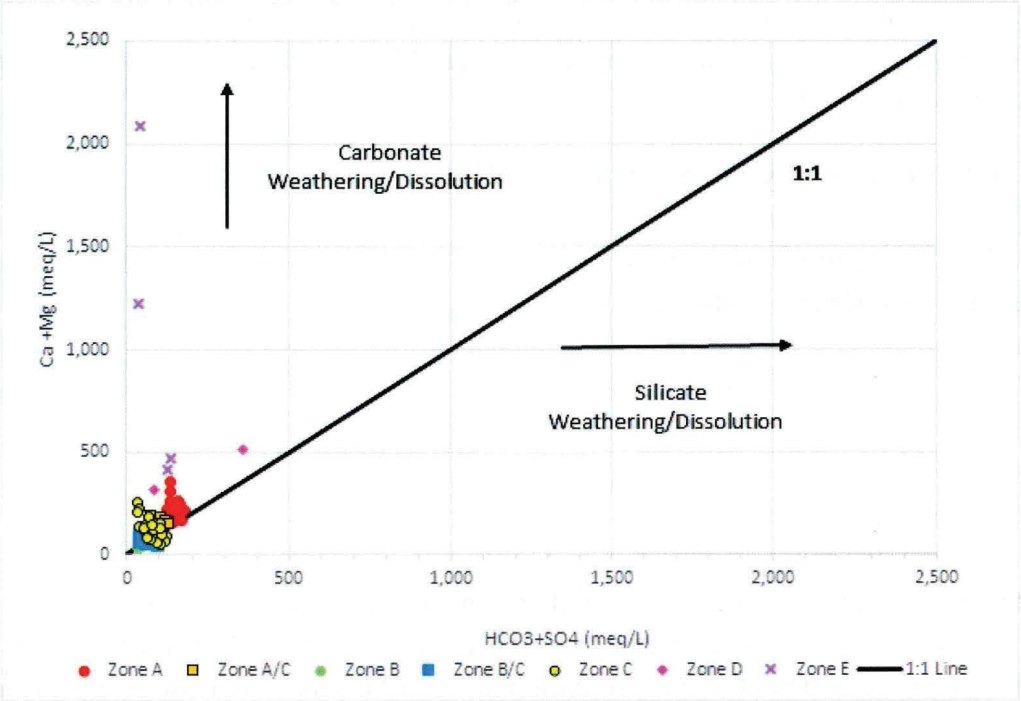

Figure 21 Culebra water: (Ca^{2+}+ Mg^{2+}) vs. (HCO_3^- + SO_4^{2-})

Due to the very high ionic strength of zone E wells, the data of Figure 21 is not displayed in a useful way. These data were re-plotted in Figure 22, with the axes zoomed to show the major portion of the data.

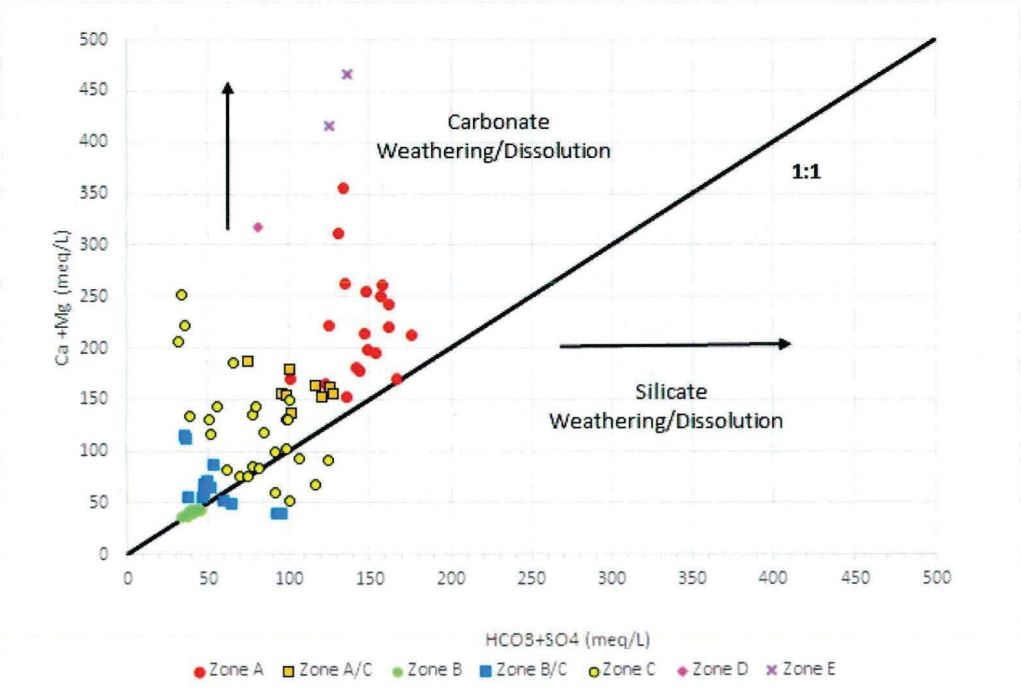

Figure 22 Culebra water: (Ca^{2+}+ Mg^{2+}) vs. (HCO_3^- + SO_4^{2-}) zoomed

Information Only

With the data re-plotted on Figure 22, the primary hydrogeochemical process that is influencing the Culebra waters is carbonate weathering or dissolution, rather than silicate weathering or dissolution. This is demonstrated by the data plotting above the 1:1 line, indicating carbonate weathering. Data that plots below the 1:1 line will be predominantly dominated by silicate weathering. This is consistent with the initial results obtained from the correlation matrix analysis, in that Ca^{2+} and Mg^{2+} ions are major contributors to the hydrogeochemical processes of the Culebra.

3.1.4 Saturation Indices of Key Minerals in the Culebra

The Saturation Index (SI) measures the relative amount of a mineral that can be dissolved into a specific solvent. SI value can be classified as follows:

Undersaturated	= < -0.5
Saturated	= -0.5 – 0.5
Supersaturated	= 0.51 – 1.0
Very Supersaturated (Scaling)	= > 1.0

In a geologic context, saturated values cease dissolution, undersaturation promotes mineral dissolution, and supersaturation promotes precipitation. A caution in evaluating saturation indices for minerals, is that the SI is only an indicator of the state of potential transformation of the solid (dissolution or precipitation) but does not indicate the presence of a solid/mineral. The SI value is essentially more descriptive of the chemistry of the water, so it is used as a hypothetical tool rather than a known component. To get a clearer understanding of whether the mineral is present or not in the formation at a particular location, a molality of the ion or molar ratio of joint ions in a mineral would need to be determined.

The contour maps that are generated for this section are not facies zone based; however, the zone lines are still present for reference. All the contours on the SI maps that are presented in this section utilize the actual SI index determined by PHREEQCI and the designated ranges of saturation specified above. This approach allows the SI to be independent from a "perceived zone" and is an effort to better understand the geology and hydrogeology of the WIPP network, without the constraint of a label. Understanding when a particular mineral will dissolve versus precipitate can be helpful in determining the water trend for chemical equilibrium. Due to the diverse mineralogy of the WIPP study area and of the water compositions, it is likely that different areas could have vastly different SIs for a particular mineral. Minerals may dissolve in some areas, creating fast paths for water flow, but may also precipitate in other areas, creating cements that inhibit water flow. The general ranges defined above will help in distinguishing between potential spatial differences in the mineralogy and dissolution/precipitation characteristics of the Culebra network. SI values and ionic strength were calculated by PHREEQCI, and the results are summarized for key Culebra minerals per well in Table 16.

Information Only

Table 16 Ionic Strength (μ) and Mineral Saturation Index Values for Key Culebra Minerals

Estimated Zone	Well_ID	Date	Ionic Strength (μ)	Saturation Indices from PHREEQCI												
				Color Key	Undersaturated	Saturated	Super-Saturated	Very Super-Saturated								
					< -0.50	-0.50-0.50	0.51-1.0	>1.0								
			Molal	Anhydrite	Calcite	Aragonite	Dolomite	Magnesite	Gypsum	Halite	Polyhalite	Carnallite	Leonite	Bischofite	Sylvite
A	H-5b & bR	1981-2021	3.21E+00	-0.02	0.35	0.17	1.42	0.22	0.10	-1.00	-5.10	-6.83	-6.19	-5.52	-2.34
A	H-10cR	2017	2.64E+00	-0.11	0.50	0.32	1.75	0.40	0.04	-1.24	-5.49	-7.30	-6.39	-5.77	-2.55
A	H-11b3	1985-1994	2.35E+00	-0.12	0.03	-0.16	0.52	-0.35	0.04	-1.33	-5.89	-7.81	-6.77	-6.15	-2.68
A	H-11b4R	2012	2.53E+00	0.01	0.10	-0.08	0.72	-0.23	0.16	-1.28	-5.28	-7.62	-6.40	-6.05	-2.60
A	H-12R	2015	3.36E+00	0.04	0.77	0.58	2.18	0.58	0.16	-0.94	-5.06	-6.72	-6.28	-5.42	-2.32
A	H-15R	2009	4.18E+00	0.06	0.87	0.69	2.46	0.74	0.14	-0.66	-5.02	-6.18	-6.31	-5.05	-2.15
A	H-17	1987	3.31E+00	-0.09	-0.38	-0.57	-0.09	-0.55	0.03	-0.95	-5.24	-6.78	-6.20	-5.56	-2.25
A	H-19b0	2006	1.67E+00	-0.22	0.21	0.02	0.82	-0.23	-0.04	-1.68	-6.42	-8.42	-7.07	-6.54	-2.91
A	P-17	1986-1987	1.84E+00	-0.15	-0.50	-0.68	-0.41	-0.76	0.02	-1.62	-5.77	-8.08	-6.56	-6.32	-2.78
A	SNL-8	2005-2007	3.03E+00	-0.06	0.31	0.13	1.42	0.26	0.08	-1.10	-4.97	-6.75	-5.98	-5.49	-2.29
A	SNL-14	2007	1.72E+00	-0.18	0.07	-0.12	0.55	-0.36	0.00	-1.66	-6.29	-8.63	-7.02	-6.66	-3.00
A	WQSP-3	1995-2020	5.15E+00	0.19	0.14	-0.05	1.14	0.16	0.23	-0.38	-4.07	-5.41	-5.67	-4.63	-1.80
A	WQSP-4	1995-2020	2.14E+00	-0.08	-0.05	-0.24	0.35	-0.44	0.08	-1.44	-5.65	-7.86	-6.58	-6.22	-2.66
A	H-5b	2017-2019	3.04E+00	-0.09	0.45	0.27	1.62	0.33	0.04	-1.06	-5.47	-6.97	-6.42	-5.57	-2.43
A	H-11b4R	2017-2020	2.06E+00	-0.09	0.51	0.33	1.46	0.10	0.08	-1.48	-5.93	-8.13	-6.86	-6.33	-2.83
A	H-12R	2017-2020	3.46E+00	-0.13	0.43	0.25	1.49	0.21	-0.02	-0.88	-5.63	-6.87	-6.51	-5.59	-2.30
A	H-17	2017-2019	3.77E+00	-0.03	NA	NA	NA	NA	0.07	-0.77	-5.73	-6.75	-6.83	-5.43	-2.35
A	H-19b0	2017-2020	1.74E+00	-0.19	1.50	1.31	3.38	1.04	-0.01	-1.63	-6.37	-8.41	-7.09	-6.52	-2.92
A	SNL-8	2017-2020	2.78E+00	-0.15	0.67	0.48	2.08	0.57	-0.01	-1.17	-5.37	-6.95	-6.19	-5.63	-2.34
A/C	H-3b3	1984-1995	1.07E+00	-0.16	0.04	-0.14	0.35	-0.54	0.03	-2.13	-6.61	-9.46	-7.35	-7.17	-3.32
A/C	H-6b & bR	1978-2008	1.13E+00	-0.20	0.24	0.05	0.73	-0.35	-0.01	-2.08	-6.89	-9.23	-7.56	-6.97	-3.28
A/C	WIPP-13	1987	1.25E+00	-0.22	-0.09	-0.28	0.20	-0.55	-0.03	-1.97	-6.97	-9.14	-7.59	-6.83	-3.33
A/C	WIPP-19	1989-1995	1.56E+00	-0.14	0.05	-0.14	0.49	-0.40	0.04	-1.77	-6.18	-8.72	-6.99	-6.71	-3.04
A/C	WQSP-1	1995-2020	1.33E+00	-0.14	0.03	-0.16	0.42	-0.45	0.04	-1.94	-6.26	-8.81	-7.05	-6.76	-3.08
A/C	WQSP-2	1995-2020	1.31E+00	-0.13	-0.01	-0.20	0.37	-0.46	0.06	-1.96	-6.15	-8.92	-6.96	-6.83	-3.11
A/C	SNL-14	2017-2020	1.55E+00	-0.20	0.15	-0.04	0.66	-0.33	-0.02	-1.76	-6.39	-8.83	-7.07	-6.81	-3.05

Information Only

Estimated Zone	Well_ID	Date	Ionic Strength (μ)	Saturation Indices from PHREEQCI											
				Color Key	Undersaturated	Saturated	Super-Saturated	Very Super-Saturated							
					< -0.50	-0.50-0.50	0.51-1.0	>1.0							
			Molal	Anhydrite	Calcite	Aragonite	Dolomite	Magnesite	Gypsum	Halite	Polyhalite	Carnallite	Leonite	Bischofite	Sylvite
A/C	WIPP-13	2017-2020	1.20E+00	-0.25	0.26	0.07	0.93	-0.17	-0.06	-2.01	-6.44	-8.96	-7.02	-6.90	-3.09
A/C	WIPP-19	2017-2019	1.41E+00	-0.19	1.63	1.44	3.58	1.11	0.00	-1.85	-6.50	-8.98	-7.20	-6.88	-3.12
B	ENGLE	1985-1990	9.14E-02	-0.23	0.07	-0.12	0.07	-0.84	-0.01	-6.03	-10.29	-17.85	-10.88	-11.80	-7.08
B	H-7b1	1986-1990	8.97E-02	-0.22	0.14	-0.05	0.15	-0.84	0.00	-5.99	-10.25	-17.42	-10.85	-11.56	-6.88
B	H-8b	1986-1988	8.18E-02	-0.25	0.41	0.22	0.81	-0.44	-0.03	-7.41	-10.82	-20.38	-11.36	-13.31	-8.10
B	H-9b & bR	1980-2012	8.87E-02	-0.22	0.44	0.25	0.78	-0.50	0.00	-6.23	-10.21	-17.90	-10.82	-11.88	-7.05
B	Mobley	1988	1.00E-01	-0.20	0.18	-0.01	0.24	-0.78	0.02	-5.61	-9.94	-16.83	-10.59	-11.23	-6.62
B	SNL-12	2004	1.01E-01	-0.25	0.77	0.58	1.36	-0.25	-0.03	-5.18	-9.84	-16.01	-10.39	-10.82	-6.21
B	SNL-17	2006-2017	8.92E-02	-0.23	0.48	0.30	0.87	-0.45	-0.01	-6.07	-10.49	-17.62	-11.07	-11.60	-7.04
B	USGS-4	2006	1.01E-01	-0.34	-0.99	-1.18	-2.13	-1.98	-0.12	-4.88	-10.17	-15.49	-10.54	-10.47	-6.04
B	USGS-8	2008	1.07E-01	-0.31	0.17	-0.02	0.09	-0.92	-0.09	-4.79	-10.06	-15.70	-10.49	-10.67	-6.06
B	H-7b1	2017-2019	9.45E-02	-0.24	0.43	0.24	0.77	-0.51	-0.02	-5.61	-9.92	-16.76	-10.48	-11.23	-6.55
B	H-9bR	2017-2020	8.76E-02	-0.24	0.48	0.30	0.87	-0.45	-0.02	-6.04	-10.26	-17.74	-10.82	-11.77	-6.99
B	SNL-12	2017-2020	1.10E-01	-0.21	0.61	0.43	1.09	-0.37	0.00	-5.10	-9.42	-15.75	-10.03	-10.72	-6.05
B	SNL-17	2017-2020	8.86E-02	-0.23	0.61	0.42	1.14	-0.32	-0.02	-6.05	-10.50	-17.57	-11.08	-11.56	-7.03
B/C	C-2737c	2018	1.98E-01	-0.34	1.01	0.82	1.91	0.06	-0.13	-3.81	-9.79	-13.58	-10.15	-9.30	-5.31
B/C	H-2c	1989-1994	2.09E-01	-0.21	-0.01	-0.19	-0.11	-0.94	0.01	-3.89	-7.99	-13.31	-8.62	-9.54	-4.80
B/C	IMC-461	2006	2.16E-01	-0.17	-0.15	-0.33	-0.38	-1.07	0.04	-3.90	-9.08	-13.42	-9.78	-9.20	-5.25
B/C	SNL-2	2004	2.44E-01	-0.22	0.45	0.27	0.82	-0.48	0.00	-3.66	-8.85	-13.04	-9.46	-9.08	-4.98
B/C	SNL-5	2004	2.93E-01	-0.26	0.45	0.27	0.98	-0.32	-0.04	-3.64	-8.74	-12.04	-9.27	-8.40	-4.67
B/C	SNL-10	2006	1.90E-01	-0.20	0.20	0.01	0.47	-0.57	0.01	-4.43	-7.87	-14.93	-8.51	-10.54	-5.42
B/C	SNL-19	2006-2016	1.83E-01	-0.21	0.62	0.43	1.20	-0.26	0.00	-4.10	-8.50	-13.60	-9.12	-9.53	-5.10
B/C	WIPP-26	1988	2.80E-01	-0.14	0.01	-0.18	-0.03	-0.88	0.07	-3.61	-7.40	-12.12	-8.16	-8.83	-4.32
B/C	H-2b2	2017-2019	2.76E-01	-0.23	1.41	1.23	2.56	0.30	-0.02	-3.46	-8.25	-12.75	-8.83	-9.23	-4.55
B/C	SNL-2	2017-2020	2.13E-01	-0.24	0.48	0.30	0.95	-0.38	-0.02	-3.86	-8.95	-13.33	-9.52	-9.21	-5.14
B/C	SNL-5	2017-2020	2.91E-01	-0.23	0.50	0.31	0.98	-0.36	-0.02	-3.63	-8.76	-12.22	-9.34	-8.53	-4.71
B/C	SNL-10	2017-2020	2.01E-01	-0.21	0.42	0.24	0.94	-0.33	0.00	-4.29	-8.18	-14.79	-8.80	-10.34	-5.48

Information Only

Estimated Zone	Well_ID	Date	Ionic Strength (μ)	Saturation Indices from PHREEQCI												
				Color Key	Undersaturated	Saturated	Super-Saturated	Very Super-Saturated								
					< -0.50	-0.50-0.50	0.51-1.0	>1.0								
			Molal	Anhydrite	Calcite	Aragonite	Dolomite	Magnesite	Gypsum	Halite	Polyhalite	Carnallite	Leonite	Bischofite	Sylvite
B/C	SNL-19	2017-2020	1.78E-01	-0.25	0.08	-0.11	0.11	-0.81	-0.03	-4.09	-9.00	-13.80	-9.55	-9.54	-5.28
C	AIS	1988	8.18E-01	-0.18	0.75	0.56	1.74	0.15	0.02	-2.41	-6.54	-10.15	-7.24	-7.67	-3.50
C	H-4b	1987-1994	4.35E-01	-0.20	-0.39	-0.58	-0.48	-0.92	0.01	-3.14	-6.89	-11.68	-7.54	-8.54	-4.17
C	H-14	1987-1995	3.83E-01	-0.20	0.20	0.01	0.39	-0.65	0.01	-3.31	-7.60	-11.20	-8.25	-8.20	-4.03
C	H-18	1988-1995	5.76E-01	-0.14	0.15	-0.03	0.48	-0.52	0.07	-2.77	-6.97	-10.81	-7.74	-7.96	-3.88
C	P-14	1986-1988	5.92E-01	-0.15	0.37	0.18	0.63	-0.58	0.06	-3.02	-9.21	-11.18	-9.97	-7.65	-4.55
C	SNL-1	2004-2016	7.22E-01	-0.17	0.38	0.20	0.98	-0.24	0.03	-2.54	-6.85	-10.13	-7.56	-7.56	-3.60
C	SNL-3	2004	9.50E-01	-0.16	0.24	0.05	0.74	-0.34	0.04	-2.25	-6.73	-9.69	-7.47	-7.27	-3.45
C	SNL-9	2004	5.70E-01	-0.18	0.52	0.33	0.98	-0.39	0.03	-2.98	-9.29	-11.27	-9.98	-7.70	-4.59
C	SNL-13	2006	3.88E-01	-0.21	1.00	0.81	2.04	0.20	0.01	-3.14	-7.45	-11.66	-8.09	-8.53	-4.16
C	SNL-16	2006-2016	4.26E-01	-0.20	0.38	0.19	0.81	-0.41	0.01	-3.11	-7.07	-10.98	-7.73	-8.18	-3.82
C	SNL-18	2006	4.07E-01	-0.13	0.34	0.16	0.73	-0.46	0.08	-3.13	-7.60	-11.80	-8.39	-8.48	-4.35
C	WIPP-11 & 11R	2004-2021	1.02E+00	-0.11	0.17	-0.02	0.57	-0.44	0.09	-2.20	-6.62	-9.64	-7.46	-7.23	-3.44
C	WIPP-25	2004	5.96E-01	-0.20	0.70	0.51	1.48	-0.06	0.01	-2.75	-6.50	-10.20	-7.16	-7.84	-3.39
C	WIPP-28	1980	9.30E-01	-0.26	0.01	-0.17	0.24	-0.62	-0.06	-2.24	-6.81	-9.76	-7.36	-7.46	-3.33
C	WIPP-30	2005	7.30E-01	-0.27	0.52	0.34	1.02	-0.34	-0.07	-2.44	-7.94	-10.88	-8.47	-7.98	-3.92
C	WQSP-5	1995-2020	6.57E-01	-0.16	0.09	-0.10	0.39	-0.55	0.05	-2.64	-6.57	-10.51	-7.31	-7.89	-3.64
C	WQSP-6	1995-2020	3.38E-01	-0.18	0.12	-0.07	0.26	-0.70	0.03	-3.38	-7.20	-12.38	-7.88	-9.07	-4.34
C	H-4bR	2017-2020	3.22E-01	-0.20	0.35	0.16	0.84	-0.35	0.02	-3.43	-7.50	-12.44	-8.15	-8.95	-4.51
C	H-6bR	2017-2020	1.02E+00	-0.16	1.33	1.14	2.69	0.52	0.03	-2.18	-7.22	-9.65	-7.97	-7.23	-3.45
C	SNL-1	2017-2020	6.81E-01	-0.17	0.42	0.24	0.99	-0.27	0.03	-2.58	-7.14	-10.49	-7.86	-7.74	-3.77
C	SNL-3	2017-2020	8.97E-01	-0.17	0.20	0.01	0.63	-0.42	0.03	-2.31	-6.75	-9.94	-7.48	-7.46	-3.51
C	SNL-9	2017-2020	5.42E-01	-0.24	-0.09	-0.27	-0.23	-0.99	-0.03	-2.98	-9.47	-11.37	-10.05	-7.78	-4.62
C	SNL-13	2017-2020	3.96E-01	-0.20	0.73	0.54	1.50	-0.07	0.01	-3.13	-7.39	-11.69	-8.04	-8.56	-4.16
C	SNL-16	2017-2020	4.77E-01	-0.19	0.41	0.23	0.84	-0.42	0.02	-2.99	-7.33	-10.84	-8.00	-8.03	-3.84
C	SNL-18	2017-2020	3.70E-01	-0.21	0.51	0.32	1.05	-0.30	0.00	-3.19	-8.04	-11.91	-8.66	-8.51	-4.43
C	WIPP-11	2017-2020	9.81E-01	-0.22	1.36	1.18	2.90	0.69	-0.03	-2.19	-7.14	-9.69	-7.77	-7.28	-3.44

Information Only

Estimated Zone	Well_ID	Date	Ionic Strength (μ)	Saturation Indices from PHREEQCI											
				Color Key	Undersaturated	Saturated	Super-Saturated	Very Super-Saturated							
					< -0.50	-0.50-0.50	0.51-1.0	>1.0							
			Molal	Anhydrite	Calcite	Aragonite	Dolomite	Magnesite	Gypsum	Halite	Polyhalite	Carnallite	Leonite	Bischofite	Sylvite
D	WIPP-27	1980	2.86E+00	-0.05	0.01	-0.18	0.38	-0.47	0.09	-1.18	-4.12	-6.20	-5.15	-5.66	-1.56
D	WIPP-29	1987	8.82E+00	0.83	0.57	0.38	2.98	1.57	0.70	0.33	1.14	-2.32	-1.92	-3.03	-0.31
E	AEC-7R	2017-2020	1.77E+00	-0.20	-0.03	-0.22	0.86	0.05	-0.02	-1.79	-5.10	-7.58	-5.78	-6.04	-2.56
E	AEC-7R	2014-2015	2.12E+00	-0.07	0.32	0.13	1.59	0.43	0.10	-1.64	-4.55	-7.04	-5.50	-5.68	-2.38
E	SNL-6	2008	1.15E+01	1.22	1.40	1.21	4.30	2.06	0.91	0.87	-0.50	-1.49	-4.51	-1.89	-0.62
E	SNL-15	2007	8.31E+00	0.48	1.58	1.40	4.33	1.90	0.37	0.27	-2.65	-2.79	-4.97	-2.99	-0.83

*Cells that have NA in the Table above are due to missing ion data. i.e. Those samples did not have carbonate data, therefore SI for carbonate minerals cannot be calculated

Information Only

Highlighted in Table 16 are the various SIs of the wells analyzed in this study, separated by undersaturated (green), saturated (tan), supersaturated (red) and very supersaturated (scaling) (light pink). All of the wells in the study were saturated to the mineral's gypsum and anhydrite, except for SNL-6 and WIPP-29, which were supersaturated and very supersaturated (scaling) for both the minerals.

All wells were undersaturated to the minerals halite, polyhalite, carnallite, leonite, bischofite and sylvite, with minor exceptions (WQSP-3, WIPP-29, SNL-6 and SNL-15). WQSP-3 and SNL-15 were saturated rather than undersaturated to halite. SNL-6 was supersaturated in terms of halite and saturated in terms of polyhalite. WIPP-29 was very supersaturated (scaling) in terms of polyhalite and saturated in terms of sylvite and halite. This is an expected result, as both previous studies identified this well as one that had been influenced by potash mining operations, and are contaminated with high concentrations of K^+, and Cl^- (Siegal, et al. 1991).

All Culebra wells are either saturated, supersaturated or very supersaturated (scaling) to the mineral calcite, except for one exception, USGS-4, which is undersaturated (-0.99) to calcite. Figure 23 shows a contour map of the spatial distribution of the calcite SI. The tan area indicates where calcite is at equilibrium, meaning it will neither precipitate or dissolve in these areas. The red and light pink areas are supersaturated/very supersaturated (scaling) and indicate where calcite would precipitate from solution. An important observation about the calcite supersaturated areas is the distinct pattern in the east/central region of the LWB. There is a distinct area that protrudes into the LWB and ends precisely at well C-2737(c). C-2737 is an important landmark because it is positioned at the location directly above the center of the current WIPP waste panels (CRA-2014, Appendix TFIELDS). This is also the start location used in the particle-tracking simulations performed by PA in APPENDIX T-FIELD (CRA-2014). As mentioned in section 1.1 of this report, transmissivity is thought to be directly related to the amount of gypsum and halite cement dissolution that has occurred in the formation. The calcite precipitation pattern seen in Figure 23, is a direct result of gypsum dissolution. Table 3, reaction 11, shows that a direct product of gypsum dissolution is calcite precipitate and CO_2, H_2O, Mg and SO_4 ions in solution. The dissolution reaction of gypsum/anhydrite is shown below:

$$\boldsymbol{CaSO_4\,(gypsum, anhydrite) + 2HCO_3^- \rightarrow CaCO_3(calcite) + CO_2 + H_2O + SO_4^{2-}}$$

While the presence of the calcite precipitate indicates gypsum dissolution has occurred, it does not mean that all gypsum in the region has been dissolved. The location at which the calcite supersaturation is, in the LWB, is closely aligned with the high transmissivity zone that has been described by Beauheim, 2007. This indicates that gypsum has dissolved in the indicated (high diffusivity) area, and has been replaced by calcite, which as shown by Figure 23, it is at saturation/equilibrium and supersaturated/very supersaturated (scaling) (precipitating) in the eastern and east/central region of the WIPP. In areas where the calcite is saturated (at

Information Only

equilibrium) it is likely that an additional reaction played a role in converting the precipitated calcite to dolomite and possibly gypsum.

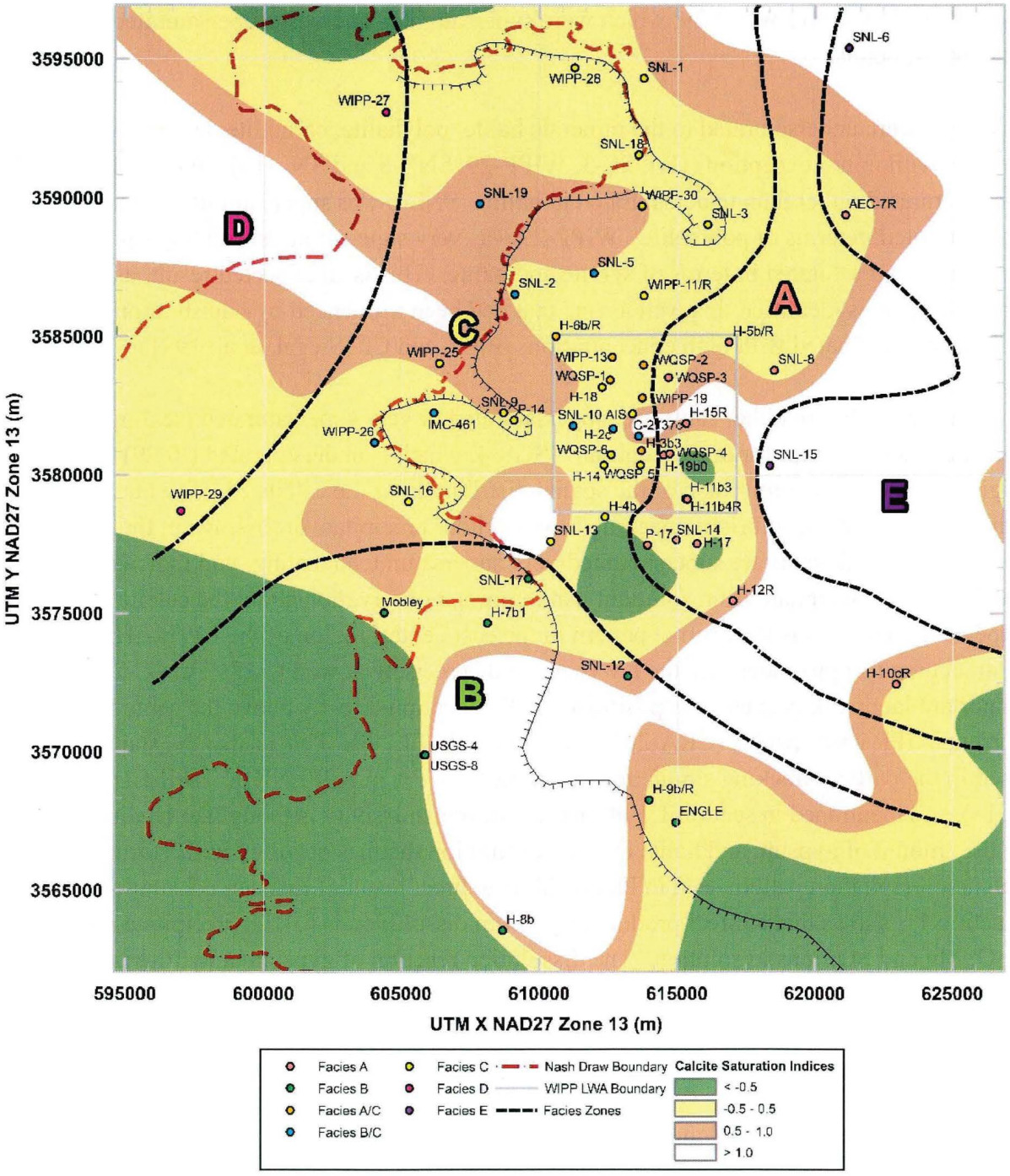

Figure 23 Calcite Saturation Index Map for Culebra network

All the wells in the Culebra network were either saturated, supersaturated or very supersaturated (scaling) in terms of dolomite, except for USGS-4, which was undersaturated (-2.13). As shown in Figure 24, the tan area is where dolomite is at equilibrium and will neither precipitate nor dissolve. The red and light pink areas are where dolomite is supersaturated and very

Information Only

supersaturated (scaling) and will precipitate if present. Interestingly, there are a few areas in the calcite SI map that are undersaturated (green), near or in the LWB. Many of these areas are where there are no wells located in the area and should be considered with caution. H-17 has a unique chemistry in that compared to the other wells in zone A, it has a reported non-detect for all carbon ions. This is interesting because wells adjacent to H-17, namely P-17 and SNL-14 have carbon ion concentrations of ~47-54 mg/L, as shown in

Information Only

Table 7.

As with the calcite precipitation, the dolomite precipitation is directly related to the reaction processes governing the geochemistry of the Culebra. Calcite precipitation in the presence of Mg^{2+} and SO_4^{2-}, produced by the dissolution of gypsum, allows the formation of dolomite in the reaction:

$$2CaCO_3\ (calcite) + Mg^{2+} + SO_4^{2-} \rightarrow CaMg(CO_3)_2\ (dolomite) + CaSO_4\ (anhydrite, gypsum)$$

In this reaction, dolomite is formed, and some gypsum is re-precipitated. This reaction will continue until the available Mg^{2+} and SO_4^{2-} are exhausted. Therefore, not all the calcite will convert to the new minerals (hence the reason there are supersaturated/very supersaturated (scaling) zones in Figure 23). The reaction is limited by the availability of the reactants in the system. This is represented by Figure 23 and Figure 24, with both dolomite and calcite being supersaturated in several of the same zones. For example, dolomite and calcite are both supersaturated in the high diffusivity zone discussed previously (Beauheim, 2007). The diffusivity line identified by Beauheim, 2007 closely coincides with the area where gypsum was dissolved. The dissolved gypsum was replaced by dolomite in subsequent reactions. Dolomite will remain the dominant mineral in this area unless new reactants, particularly CO_2 and H_2O, become available.

Information Only

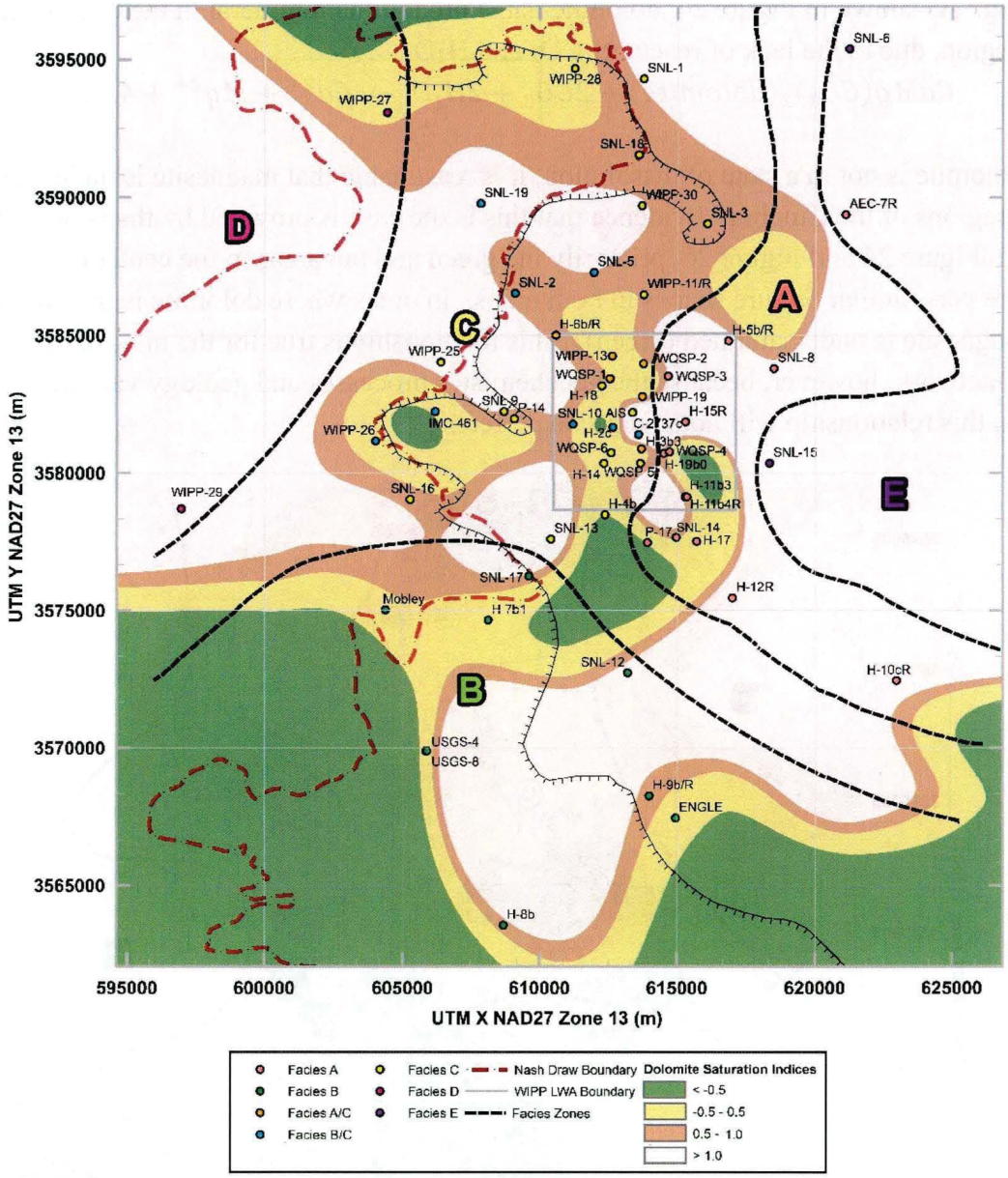

Figure 24 Dolomite Saturation Index Map of Culebra Network

Magnesite saturation index is plotted in Figure 25. As with the previous saturation indices maps, the tan area represents areas where magnesite is at equilibrium and will not precipitate or dissolve. The red and light pink areas are where magnesite is supersaturated or very supersaturated (scaling). In these areas magnesite will precipitate. Magnesite is precipitated when dolomite reacts with excess CO_2 and H_2O. As discussed earlier, there is a limitation in these reactants and therefore it is unlikely that magnesite will be a predominant mineral in the direct WIPP vicinity. This is confirmed by the fact that magnesite is undersaturated (green) in several areas of the WIPP area. As shown in the reaction below, magnesite is the product of the dissolution of dolomite. Therefore, it will only begin to precipitate if dolomite dissolution is

Information Only

occurring. As shown in Figure 24, dolomite is the predominant mineral in the Culebra in the WIPP region, due to the lack of reactants CO_2 and H_2O.

$$CaMg(CO_3)_2(dolomite) + 2CO_2 + 2H_2O \rightarrow Ca^{2+} + Mg^{2+} + 4HCO_3^-$$

Since dolomite is not in a state of dissolution, it is reasonable that magnesite is undersaturated in several regions of the Culebra. Evidence that this is the case is provided by the contour lines shown in Figure 24 and Figure 25, primarily the green and tan areas in the center of the LWB. There are very similar feature shapes in both maps. In areas where dolomite is in equilibrium (tan), magnesite is undersaturated (green). This relationship is true for the majority of the Culebra network; however, because the geochemistry processes and geology vary across the network, this relationship will not always be perfect.

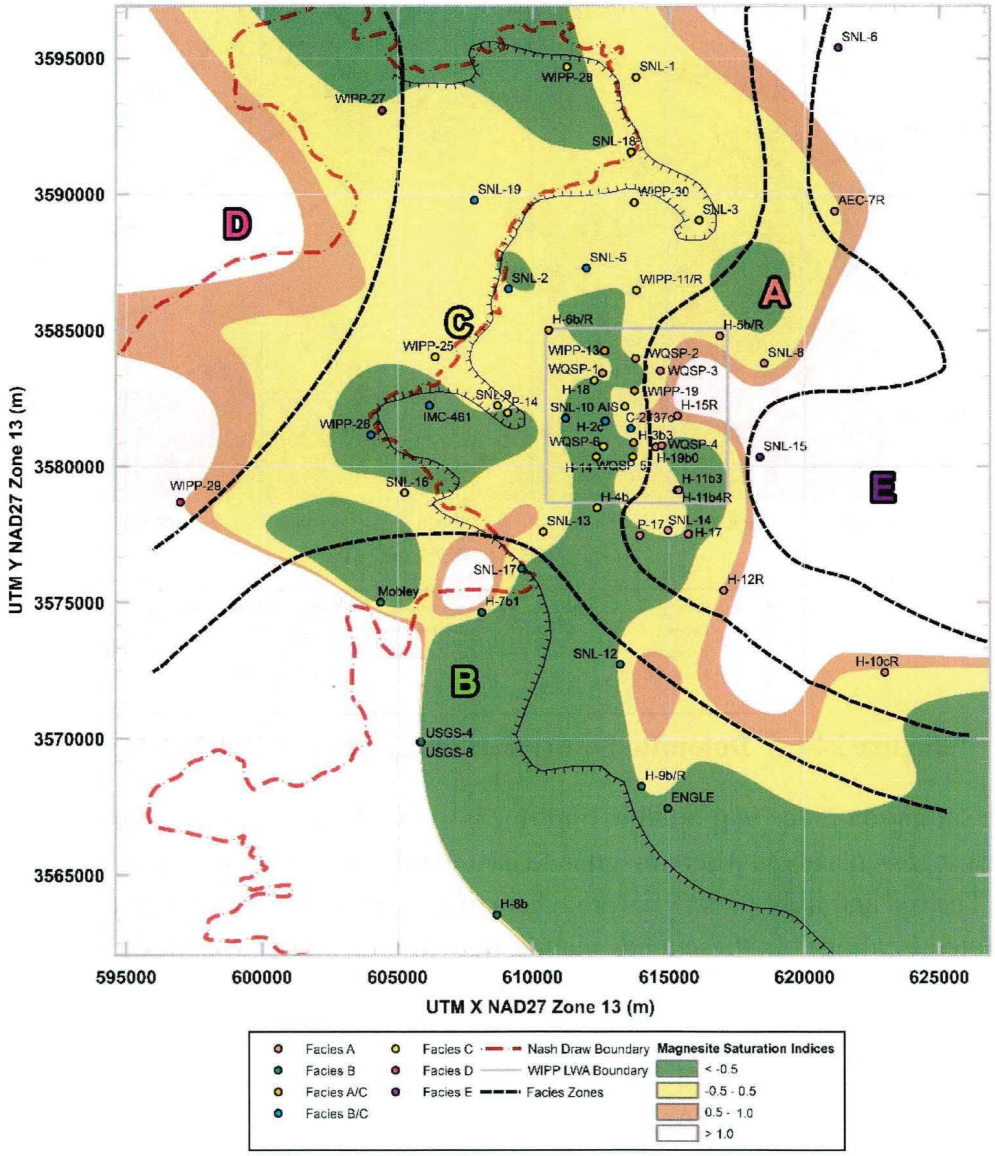

Figure 25 Magnesite Saturation Index Map for the Culebra network

Information Only

Figure 26 shows a focused illustration of the relationship between magnesite SI and dolomite SI. Note, particularly, the relationship between the tan areas of the dolomite SI and the green areas of the magnesite SI, within the LWB.

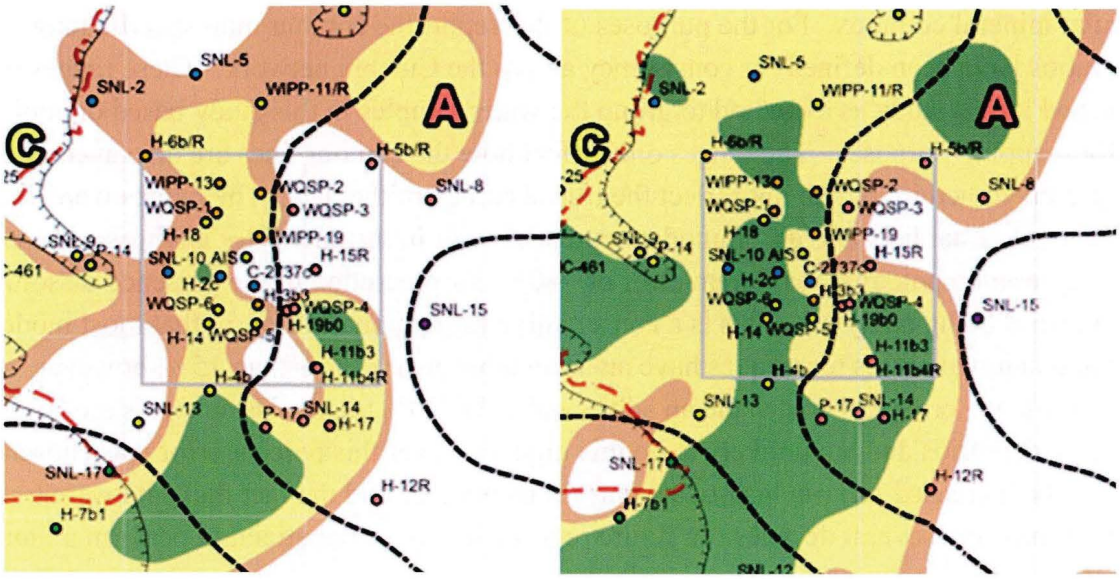

Figure 26 Comparison of Saturation Indices of Dolomite (left) and Magnesite (right) (Note: The legends in Figure 24 and Figure 25 apply to these subset maps)

As described previously, since magnesite is a product of dolomite dissolution, it will be undersaturated in locations where dolomite is in equilibrium or saturated. In addition, in areas where dolomite is supersaturated, magnesite will likely be at equilibrium.

Saturation indices of key minerals are useful tools to better understand and visualize the reaction processes controlling the Culebra geochemistry. The presented data, align with previous analyses by Holt, et al. 2005 and conclusions raised by Beauheim, 2007, regarding diffusivity. A limitation of analyses using saturation indices is that they do not verify with certainty that the mineral is present, it only indicates the ease with which the mineral will dissolve or precipitate if it is present.

3.1.5 Major Ion Relationships in the Culebra groundwater

Studying the major ion relationships in terms of molality concentration and meq/L in a water system can provide detail regarding the dominant hydrogeochemical processes controlling a water system. These data are relevant because they reveal what is currently present in the water at a specific location in time (i.e., there cannot be Mg^{2+} in the water system, unless there is a mineral contributing Mg^{2+}, excluding contamination scenarios). These relationships can help the further understanding of the water-rock interactions of the system when paired with correlation matrix and saturation indices analyses. Molar ratios are useful in that, if two ions are in a mineral at a 1:1 ratio, they will most often dissolve in a congruent way at a 1:1 ratio. Some

Information Only

complex minerals, such as polyhalite and carnallite, dissolve in an incongruent way (see discussion in Section 1.2 of this report). The dissolution habits of minerals determine the appropriate ratios for molal ratio comparisons. In the following section several contour maps have been provided to show a visual and spatial representation of the molar or meq/L ratios for a particular mineral complex. For the purposes of this report the contour map specific ranges for molar ratios have been defined for consistency across the Culebra network. These ranges were established in this study as a method to group the water samples in this study based on molar ratio for mapping purposes. The ranges only affect how the contour lines are displayed on the maps presented herein, but do not reflect the true accuracy of the data. The ranges were conservatively established to accommodate potential error in the chemistry analysis. The current ranges represent a potential maximum error of ~40%, for prediction of the presence/dissolution of the mineral being analyzed. This is a conservative estimation of error, in that most modern cation and anion analyses techniques have an acceptable error of less than 15%, however estimated human error can contribute an additional 15% (30% total). These errors are based on worst case scenarios and are unlikely to be this high, however this percent error was chosen based on the increased error in historical analyses techniques and the fact that data were collected spanning several decades. In future reports, it may be beneficial to perform a more in-depth statistical analyses of the data, in order to determine if the percent error in this study can be lowered. Since a molar ratio of 1 indicates the presence of or the primary ion contribution of the mineral, the ranges are established as follows for this study:

Description	Molar Ratio Ranges for this Study
Mineral is contributing ions un-equally, with the first ion being contributed at a greater concentration	<0.6
Mineral is contributing ions equally to the solvent	0.6 to 1.4
Mineral is contributing ions un-equally, with the second ion being contributed at a greater concentration	>1.4

Consider the molar ratio of a Na^+/Cl^- mineral that dissolves in a congruent habit. If the molar ratio is 1, then a mineral such as halite that contains Na^+ and Cl^- in a 1:1 ratio is contributing both Na^+ and Cl^- to the waters. If the molar ratio is <0.6 then it means that Na^+ and Cl^- are not at a 1:1 ratio in the dissolved mineral, and that Na^+ is higher in concentration than Cl^-. Likewise, if the molar ratio is >1.4 then it means that Na^+ and Cl^- are not at a 1:1 ratio in the mineral and that Cl^- is higher in concentration than Na^+.

This theory holds true for minerals that dissolve incongruently as well, however the molar ratio for comparison will be different. Information about how the mineral incongruently dissolves is necessary to compare ions using molar ratios for incongruently dissolving minerals. For example, consider the dissolution of the mineral calcite. The reaction for this dissolution in water is:

Information Only

$$CaCO_3\,(calcite) + CO_3 + H_2O \rightarrow Ca^{2+} + 2HCO_3^-$$

In this reaction, the calcite dissolves incongruently, in that the products of the reaction are 1 ion of Ca^{2+} and 2 ions of HCO_3^-. Therefore, the molar ratio for this dissolution reaction would be a 1:2 ratio for comparison. Application of this would mean that for calcite to be considered present in the system the final molal concentrations of Ca^{2+} and HCO_3^- would be in a 1:2 ratio. The ranges presented earlier of (<0.6, 0.6-1.4 and >1.4) are still relevant to this scenario, because if it is present the ratio will calculate to be between 0.6-1.4.

Combining molar ratio analysis with other analyses such as correlation matrix analyses helps to elucidate which minerals are present and which minerals are dominant in a water system. In other words, if Na^+/Cl^- are at a 1:1 ratio, it does not necessary mean that halite is present. Any mineral that has a Na^+/Cl^- ratio of 1:1 could be present. Therefore, utilizing a variety of analysis techniques and geologic knowledge of the area can help to pinpoint the minerals present. The following will be assumed about the molar ratios considered in this study:

1:1 ratio of Na^+/Cl^-	= Halite
1:1 ratio of Mg^{2+}/Ca^{2+}	= Dolomite
1:2 ratio of Mg^{2+}/HCO_3^-	= Dolomite
1:2 ratio of Ca^{2+}/HCO_3^-	= Dolomite or Calcite
1:1 ratio of Ca^{2+}/SO_4^{2-}	= Gypsum

These assumptions are based on current geologic knowledge of the area and on the Correlation Analysis conducted previously in this study.

Halite

Consistent with historical studies, this study further verified that a predominant mineral in the Culebra waters in the WIPP area is halite. The molar ratio of Na^+/Cl^- was used to determine information about halite dissolution. If the molar ratio of Na^+/Cl^- is 1 then that would indicate that halite is the primary mineral contributing to the Na^+ content of that water. Hounslow (1995) suggests that in a plot of Na^+ vs. Cl^-, if groundwater data plots close to the 1:1 ratio line, the sodium source is from sea aerosol/halite. If the data plots above the 1:1 line it indicates ion-exchange and if the data plots below the 1:1 line, the sodium contribution is from reverse ion-exchange. Figure 27 shows a plot of the molar ratio of Na^+ to Cl^-.

Information Only

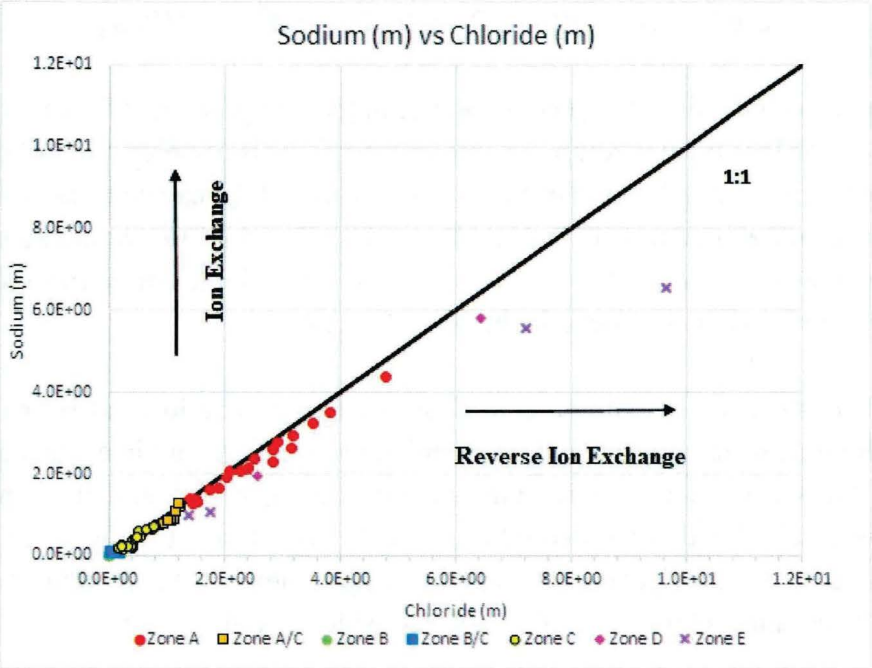

Figure 27 Sodium/Chloride Molar Ratio of Culebra Network

Most of the samples in this study plotted along the 1:1 Na^+/Cl^- line as shown in Figure 27. This result indicates that halite is contributing the Na^+ and Cl^- ions in a 1:1 ratio to the Culebra waters. Many of the higher ionic strength samples (zone A, zone E, zone D) have molar ratios that are plotting slightly below the 1:1 Na^+/Cl^- ratio line, indicating that some reverse ion exchange may be occurring in these zones. Figure 28 shows a contour map of the Na^+/Cl^- molar ratio.

Information Only

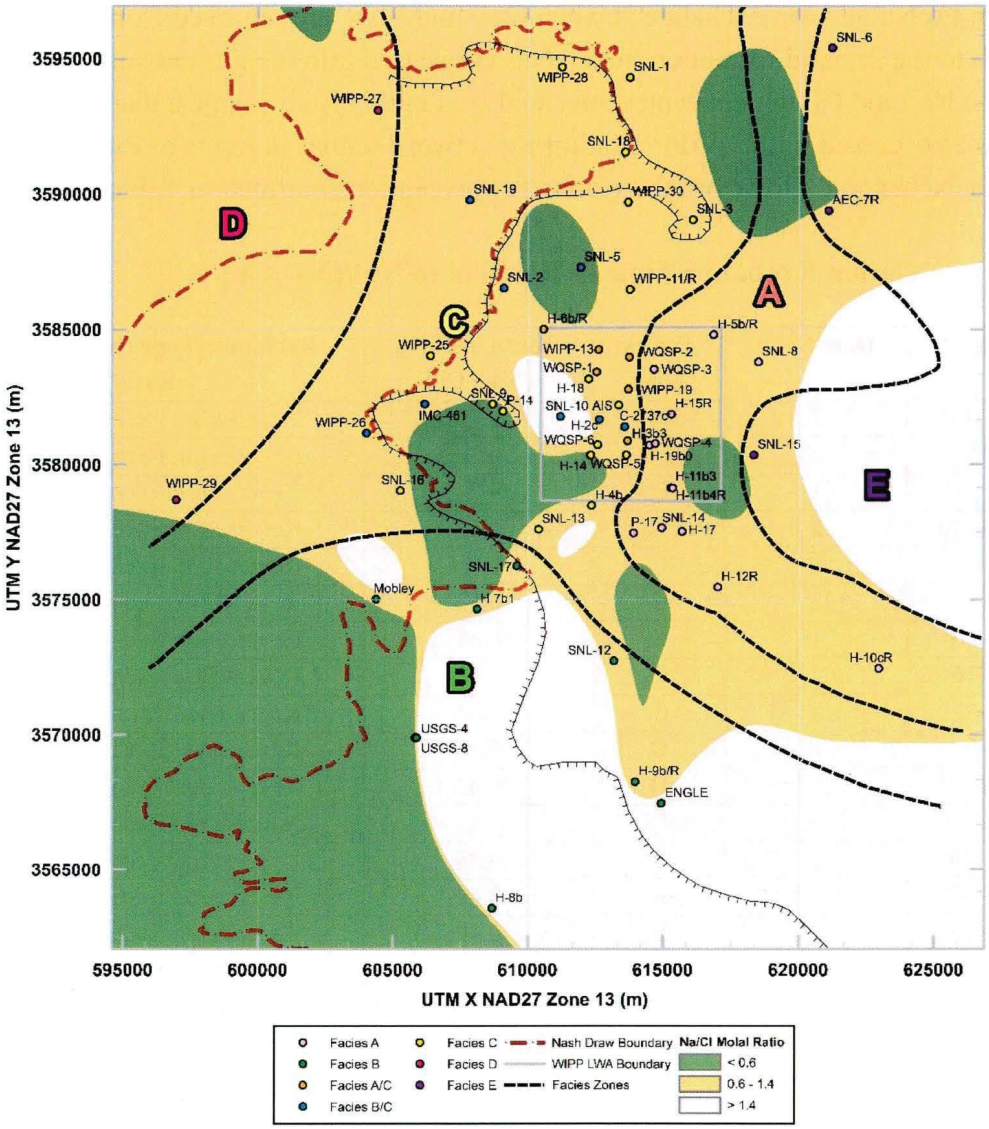

Figure 28 Sodium/Chloride Molar Ratio Contour Map of Culebra Network (tan indicates presence of halite)

The Na^+/Cl^- molar ratio map shows the presence of halite in tan. The light pink portions of the map indicate that reverse ion exchange may have taken place. Reverse ion exchange is when Na^+ from the solution adsorbs to the formation rock and displaces another major cation, such as Ca^{2+} (Mg^{2+} can also undergo this exchange), creating a Ca^{2+} rich water. The area in zone E that is highlighted in light pink is likely an artifact of the algorithm in the software creating the contour lines. There are no data in that area that would indicate reverse ion exchange. Primarily all the wells in the WIPP monitoring network showed evidence of having very little exchange, in that all the well data was very near the Na^+/Cl^- 1:1 ratio line. A few wells however, showed deviations that are relevant. Hounslow (1995) and Tay, C.K. (2021) state that for groundwater with major ion ratios of $Na^+/(Na^+ + Cl^-) > 0.5$, the origin of the sodium is either albite (or other plagioclase feldspar mineral) or ion-exchange, while ratios <0.5 indicate the presence of halite or

Information Only

reverse ion exchange. Ion exchange is when Ca^{2+} and Mg^{2+} are removed from the groundwater and adsorb to the mineral formation, while Na^{+} is released into the groundwater (Hounslow, 1995). The Na^{+} and Cl^{-} ion concentrations analyzed in this study suggest that very little cation exchange has occurred in the WIPP monitoring network (either in terms of ion exchange or reverse ion exchange). However, there are a few exceptions outlined in Table 17 below:

Table 17 Cation Exchange Type in Relation to $Na^{+}/(Na^{+}/Cl^{-})$

Well_ID	Data Set #	Facies Zone	Ratio of $Na^{+}/(Na^{+}+Cl^{-})$	Exchange Type ($Na^{+}/(Na^{+}+Cl^{-})$ Ratio)
IMC-461	2	B/C	0.42	Reverse Ion Exchange (< 0.5)
SNL-5	2	B/C	0.30	Reverse Ion Exchange (< 0.5)
SNL-5	1	B/C	0.34	Reverse Ion Exchange (< 0.5)
WIPP-26	2	B/C	0.42	Reverse Ion Exchange (< 0.5)
H-14	2	C	0.36	Reverse Ion Exchange (< 0.5)
P-14	2	C	0.31	Reverse Ion Exchange (< 0.5)
SNL-16	1	C	0.41	Reverse Ion Exchange (< 0.5)
SNL-16	2	C	0.43	Reverse Ion Exchange (< 0.5)
SNL-9	2	C	0.34	Reverse Ion Exchange (< 0.5)
SNL-9	1	C	0.36	Reverse Ion Exchange (< 0.5)
WIPP-27	2	D	0.43	Reverse Ion Exchange (< 0.5)
WIPP-29	2	D	0.41	Reverse Ion Exchange (< 0.5)
AEC-7R	2	E	0.38	Reverse Ion Exchange (< 0.5)
AEC-7R	1	E	0.42	Reverse Ion Exchange (< 0.5)
SNL-15	2	E	0.44	Reverse Ion Exchange (< 0.5)
SNL-6	2	E	0.40	Reverse Ion Exchange (< 0.5)
*NOTE: Data that are considered to be participating in Reverse Ion Exchange are < 0.45				
ENGLE	2	B	0.61	Ion Exchange (> 0.5)
H-8b	2	B	0.71	Ion Exchange (> 0.5)
H-9bR	1	B	0.57	Ion Exchange (> 0.5)
USGS-8	2	B	0.56	Ion Exchange (> 0.5)
SNL-10	1	B/C	0.71	Ion Exchange (> 0.5)
SNL-10	2	B/C	0.73	Ion Exchange (> 0.5)
*NOTE: Data that are considered to be participating in Ion Exchange are > 0.55				

The wells in Table 17 that have been identified as participating in reverse ion exchange are primarily located in the Northwestern region of the WIPP monitoring network. Several of these wells including P-14 and WIPP-26 have been identified in historical analyses as having brine signatures that support the idea of reverse ion exchange (Bodine and Jones, 1990). The Bodine and Jones study distinctly identified geochemical signatures in these wells with higher calcium concentrations in the groundwater and lower sodium concentrations. Bodine and Jones surmised this signature could be attributed to simple dissolution of calcium sulfate (and possibly dolomite), followed by dilution of primitive-diagenetic fluids.

Information Only

The wells that have been identified as participating in ion exchange, are primarily located in the southern region of the will monitoring network. The Bodine and Jones, 1990 study confirmed the idea of ion exchange in several of the identified wells including Engle, H-8, and H-9. It was recognized in the Bodine and Jones study that these wells yield salt norm signatures containing sodium rich groundwaters, likely contributed by sodium-bearing sulfates. This information supports the idea of ion exchange.

Dolomite

The molar ratio of Mg^{2+}/Ca^{2+} can be used to determine if the mineral dolomite is the primary source of these ions in solution. As shown in Figure 24, dolomite is saturated, supersaturated or very supersaturated (scaling), throughout the Culebra network indicating it is a predominant mineral contributing to the hydrogeochemistry of the system. A 1:1 ratio of Mg^{2+}/Ca^{2+} would indicate the dissolution or equilibrium of dolomite in the system. Figure 29 shows the plot of Mg^{2+}/Ca^{2+}(m), without zones D or E (due to their high ionic strength).

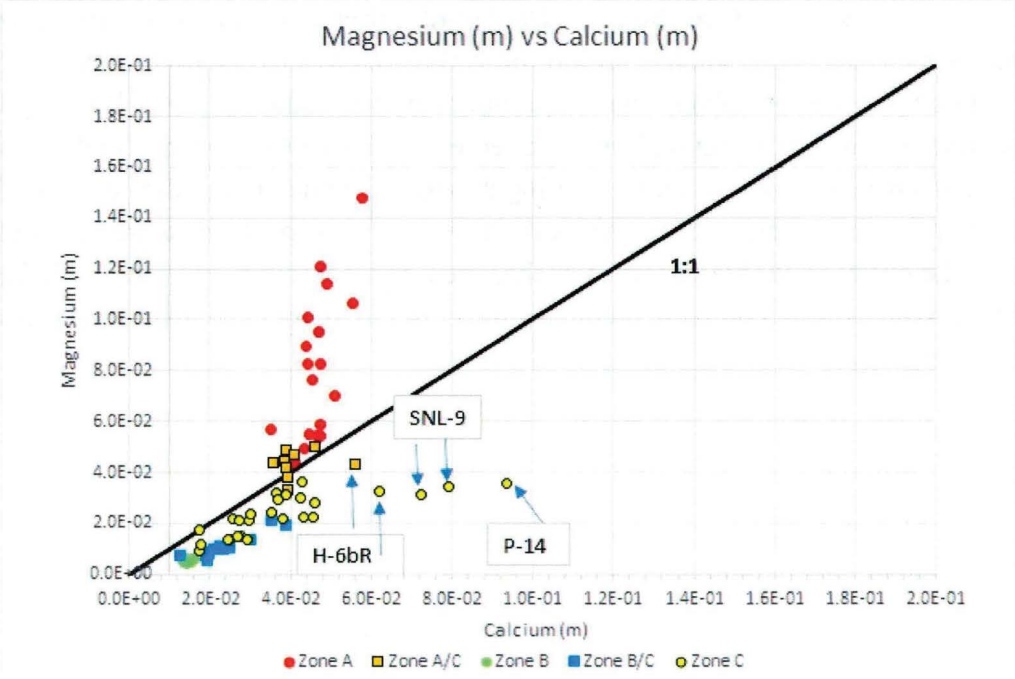

Figure 29 Magnesium/Calcium Molar Ratio of the Culebra

The general trend of Mg^{2+}/Ca^{2+} is positively correlated in zones B, B/C and C, with a higher Ca^{2+} concentration than Mg^{2+}, indicated by the fact that the data is below the 1:1 line. There are several samples in zone C and one sample in zone A/C that do not follow the trend of the other samples in the zone. Many of the wells in zone A do not follow the 1:1 Mg^{2+}/Ca^{2+} ratio line, suggesting that dolomite is not significant in this area.

Information Only

Zone A waters clearly have an excess of Mg^{2+} ion compared to Ca^{2+}, indicating that Ca^{2+} may not be present in abundance in zone A. This interpretation is consistent with the previous assertion that cation exchange may be occurring, creating Ca^{2+} depleted waters and Na^{+} rich waters. Hounslow, 1995 also suggests that a higher Mg concentration than Ca in groundwater could indicate dedolomitization and/or ion exchange. Another possible process contributing to the higher Mg concentration in this area, could be Silicate weathering.

Zone A/C is grouped primarily around the 1:1 line with a few anomalies, indicating that a Mg^{2+}/Ca^{2+} mineral such as dolomite may be in a state of dissolution or equilibrium. This result is in alignment with Figure 24, where dolomite is primarily shown to be in equilibrium for zone A/C.

There are 3 zone C wells that are obviously divergent from the Mg^{2+}/Ca^{2+} 1:1 line and one A/C well. The zone C wells are P-14 (Data Set #2), SNL-9 (Data Set #1&2), and H-6bR (Data Set #1). The anomalous zone A/C well was also H-6bR (Data Set #2). Note: H-6bR water chemistry changed from Data Set #2 (1978-2008) to the 2017-2020 study, therefore it is in a different zone.

Figure 30 shows the Mg^{2+}/Ca^{2+} molar ratio for both Data Set #1 (2017-2020 study) and Data Set #2, for direct comparison. Both maps have limitations in their data analyses. The map for Data Set #1 has more recent data, meaning it is more representative of the current Culebra waters; however, it has fewer wells in the study, limiting its spatial application to the network. Data Set #2 has excellent spatial coverage of the network; however, some of the data are very old and may not represent the current Culebra waters. For these reasons, contour maps from both data sets are presented to provide a more complete picture of the current Culebra chemistry in terms of Mg^{2+}/Ca^{2+} molar ratio.

Information Only

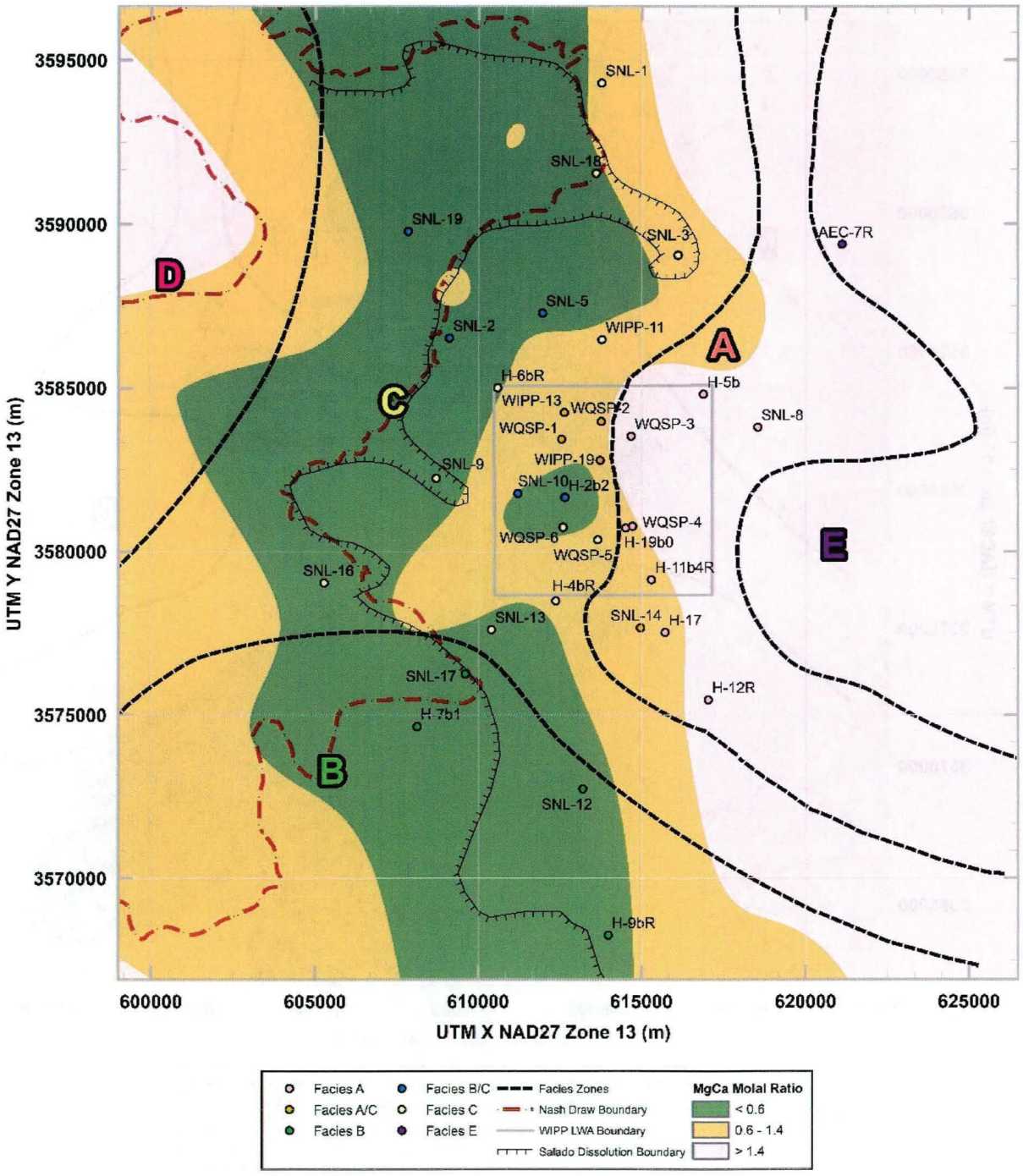

Figure 30 **Magnesium/Calcium Molar Ratio Contour Maps of the Culebra Network (Data Set #1)**

Information Only

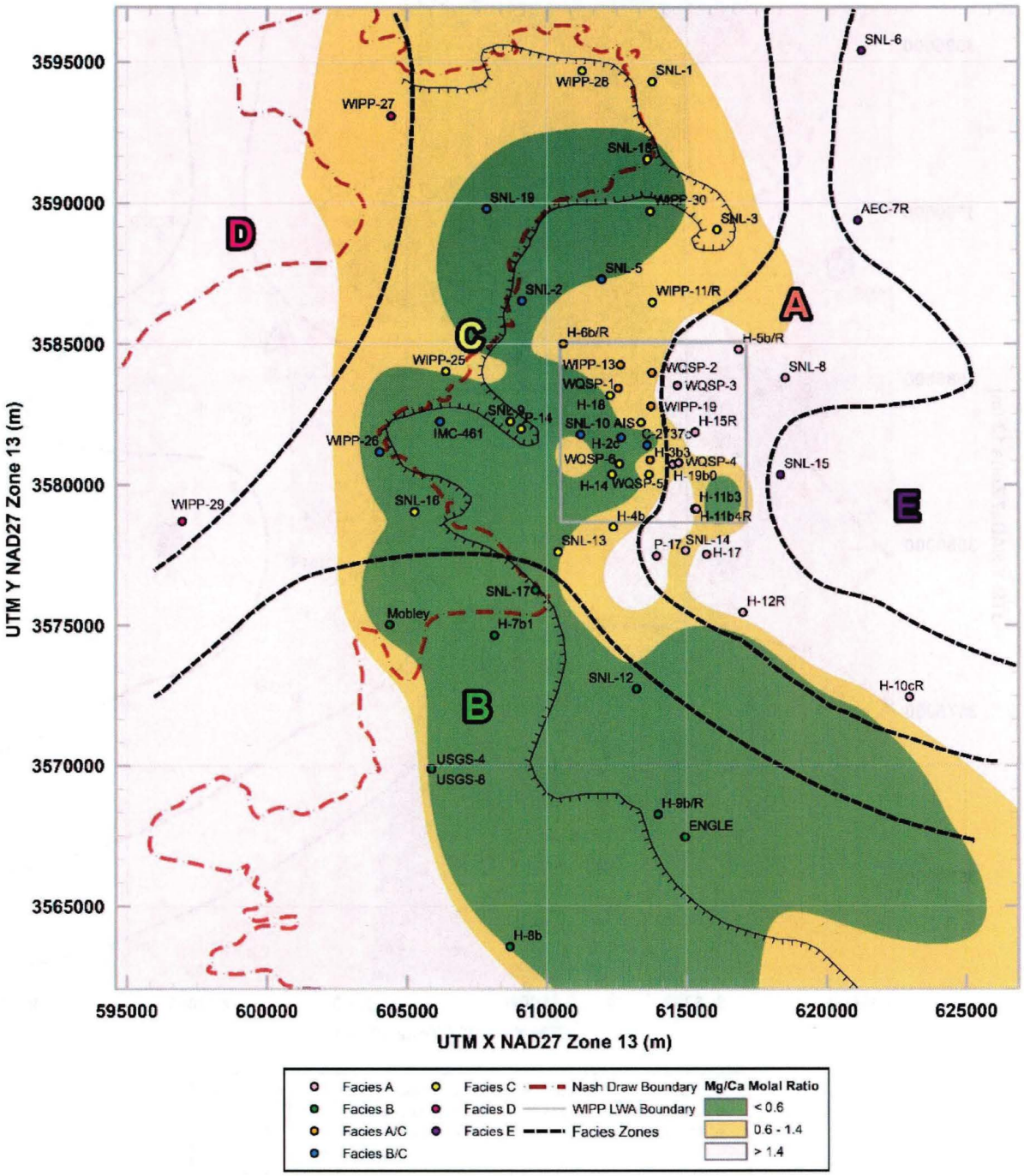

Figure 31 **Magnesium/Calcium Molar Ratio Contour Map of the Culebra Network (Data Set #2)**

The Mg^{2+}/Ca^{2+} contour maps for each data set in Figure 30, show similar patterns for dolomite presence. The tan color on the map represents where Mg^{2+}/Ca^{2+} are at a 1:1 ratio, indicating the presence of dolomite, because both Mg^{2+} and Ca^{2+} are being contributed to the Culebra water at an equal rate. A ratio that is higher than 1.4 (light pink area of map) has concentrations of Mg^{2+} that are higher than the Ca^{2+} concentration.

Information Only

Since dolomite is a mineral that dissolves in a congruent way in terms of Mg^{2+}/Ca^{2+}, this would indicate that an additional mineral is contributing to the Mg^{2+} ion contributed to this area, or that Ca^{2+} is precipitating. The Mg^{2+} in this area is likely contributed by a potash type mineral such as polyhalite or carnallite. These data are consistent with the reaction path simulations with PHRQPITZ reported by Seigel and Anderholm, 1994. In the Seigel and Anderhom study, it was proposed that, although dolomite solubility increases with ionic strength, the supply of Mg^{2+} from other sources (cation exchange or evaporite salts) effectively prevents the dissolution of dolomite and allows the dolomite to remain saturated or supersaturated in the majority of the WIPP vicinity. It is further proposed that the excess Mg^{2+} is being contributed by accessory carnallite or polyhalite. Figure 24, showing the saturation indices of dolomite, confirm the assertion that dolomite remains saturated and/or supersaturated in the majority of the WIPP vicinity.

A Mg^{2+}/Ca^{2+} molar ratio of 0.6 or less (green areas of map) indicate the abundance of Ca^{2+} compared to Mg^{2+} and suggest that the Ca^{2+} in these areas is not contributed by dolomite. The Ca^{2+} ions in the groundwater in these areas are likely contributed by dissolution of minerals such as calcite, calcium chloride or gypsum. These data are also supported by the Siegel and Anderholm, 1994 study where, it was concluded that the solubilities of gypsum and calcite increase with increasing ionic strength, and the minerals begin to dissolve as chemical equilibrium is maintained between them and the groundwater. Figure 23, of this study shows the correlation of the calcite saturation indices and the idea of calcite remaining at chemical equilibrium with the groundwater, in that a significant portion of the map is "tan", indicating calcite chemical equilibrium.

Graphing the HCO_3^- vs. Mg^{2+} meq/L, can help determine if dissolution of dolomite is occurring in a system. As shown in Table 3, the Mg^{2+}/HCO_3^- ratio is 1:2. This means that if the Mg^{2+}/HCO_3^- meq/L concentrations are plotted against each other and they fall along the 1:2 ratio line, then dolomite dissolution is likely occurring in those zones. Figure 32 shows the meq/L ratio of HCO_3^- to Mg^{2+}.

Information Only

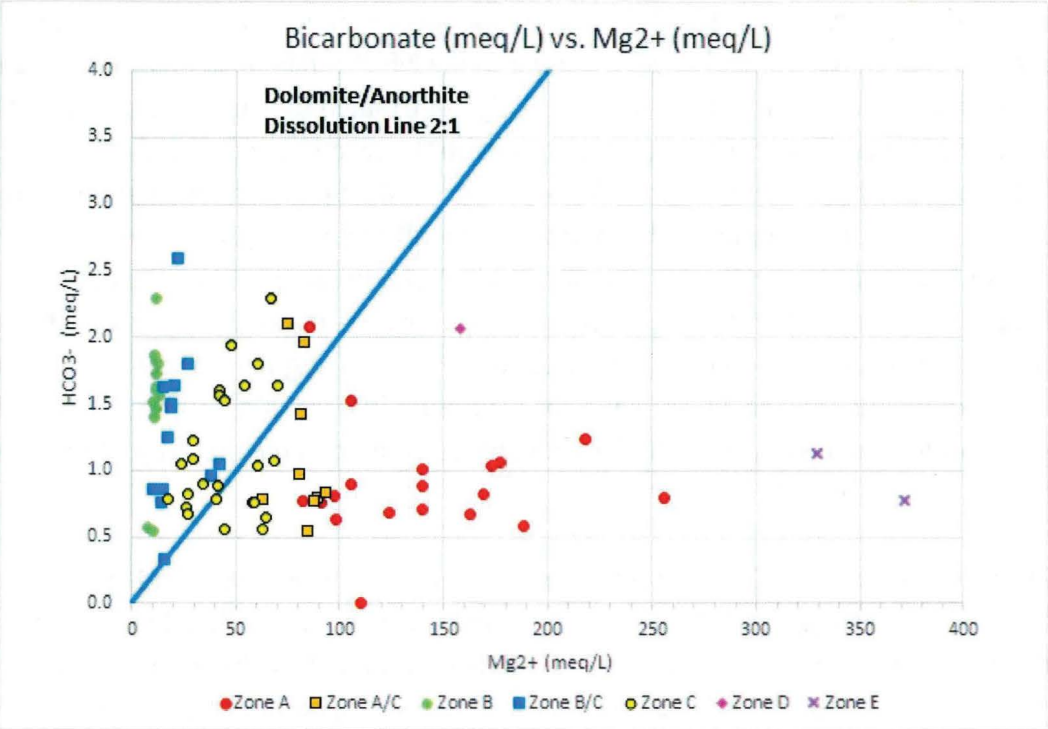

Figure 32 Bicarbonate/Magnesium meq/L for the Culebra Network

Figure 32 does not show a distinct pattern of any facies zone having dolomite dissolution. Many of the zone C and A/C wells are near the dolomite dissolution line, while zones A, B, and B/C are far from the dolomite dissolution line. This would indicate that dolomite dissolution is unlikely occurring in any part of the Culebra network and the concept is reinforced by the saturation index map in Figure 24. Dolomite being at equilibrium is consistent with the historical assertion that the Culebra is composed of 80-99% dolomite (Sewards, 1991), based on core analyses for several boreholes in the WIPP network (Bodine and Jones, 1990).

Gypsum

Ca^{2+} and SO_4^{2-} play a major role in the hydrogeochemical processes controlling the Culebra waters. If the Ca^{2+} and SO_4^{2-} molar ratio is 1:1, it is an indication that the primary contribution of Ca^{2+} and SO_4^{2-} ions are due to the dissolution of gypsum. Data that plots above the 1:1 gypsum trend line, indicates a higher Ca^{2+} concentration than SO_4^{2-}, suggesting that a mineral other than gypsum is contributing to the excess Ca^{2+} ions. If the data plots below the 1:1 trend line, it indicates that the SO_4^{2-} concentration is higher than the Ca^{2+} concentration and is being contributed by a SO_4^{2-} rich mineral. Figure **33** shows the Ca^{2+}/SO_4^{2-} molar ratio of the Culebra well network, excluding the very high ionic strength wells in zones D and E.

Information Only

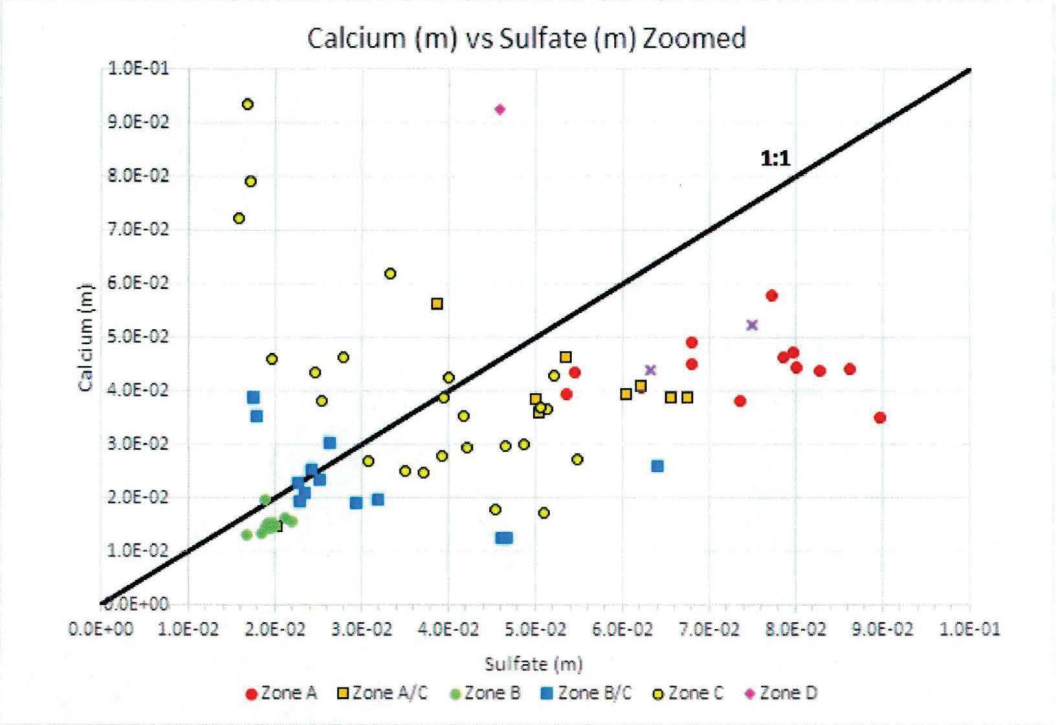

Figure 33 **Calcium/Sulfate Molar Ratio of the Culebra Network**

Figure **33** shows a positive trend toward gypsum dissolution, but there are several anomalies. Several wells in zone C are above the 1:1 ratio line for gypsum, indicating that the Ca^{2+} is being contributed by a different mineral other than gypsum. The majority of the wells in the Culebra network plot below the gypsum 1:1 line, indicating that the SO_4^{2-} may be contributed by a different mineral other than gypsum, or that the Ca^{2+} is precipitating. Figure 34 and Figure 35 show the contour maps of the spatial distribution of the Ca^{2+}/SO_4^{2-} molar ratios across the Culebra network for both Data Set #1 and Data Set #2 (Data Set #3 is included in both maps).

Information Only

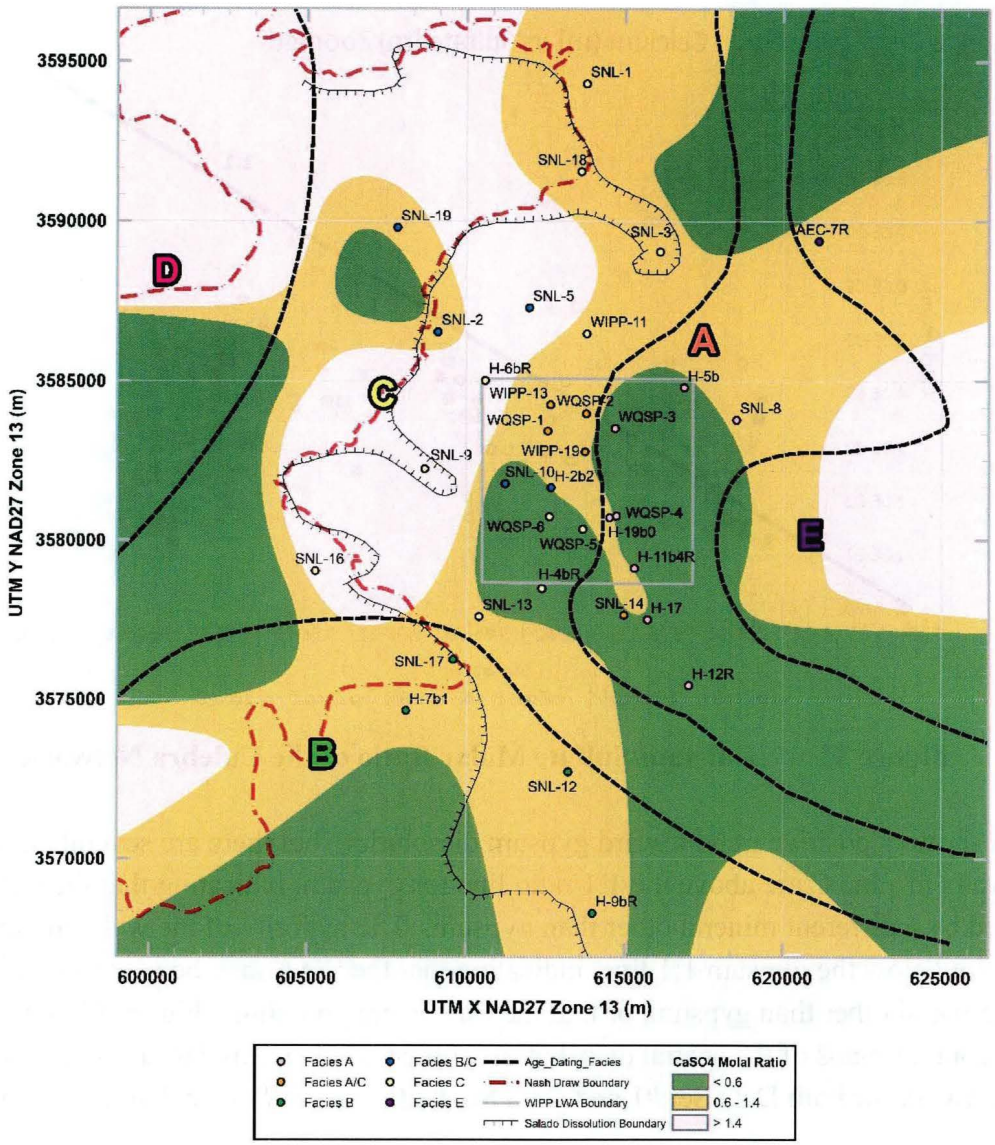

Figure 34 Calcium/Sulfate Molar Ratio for Culebra (Data Set #1)

Information Only

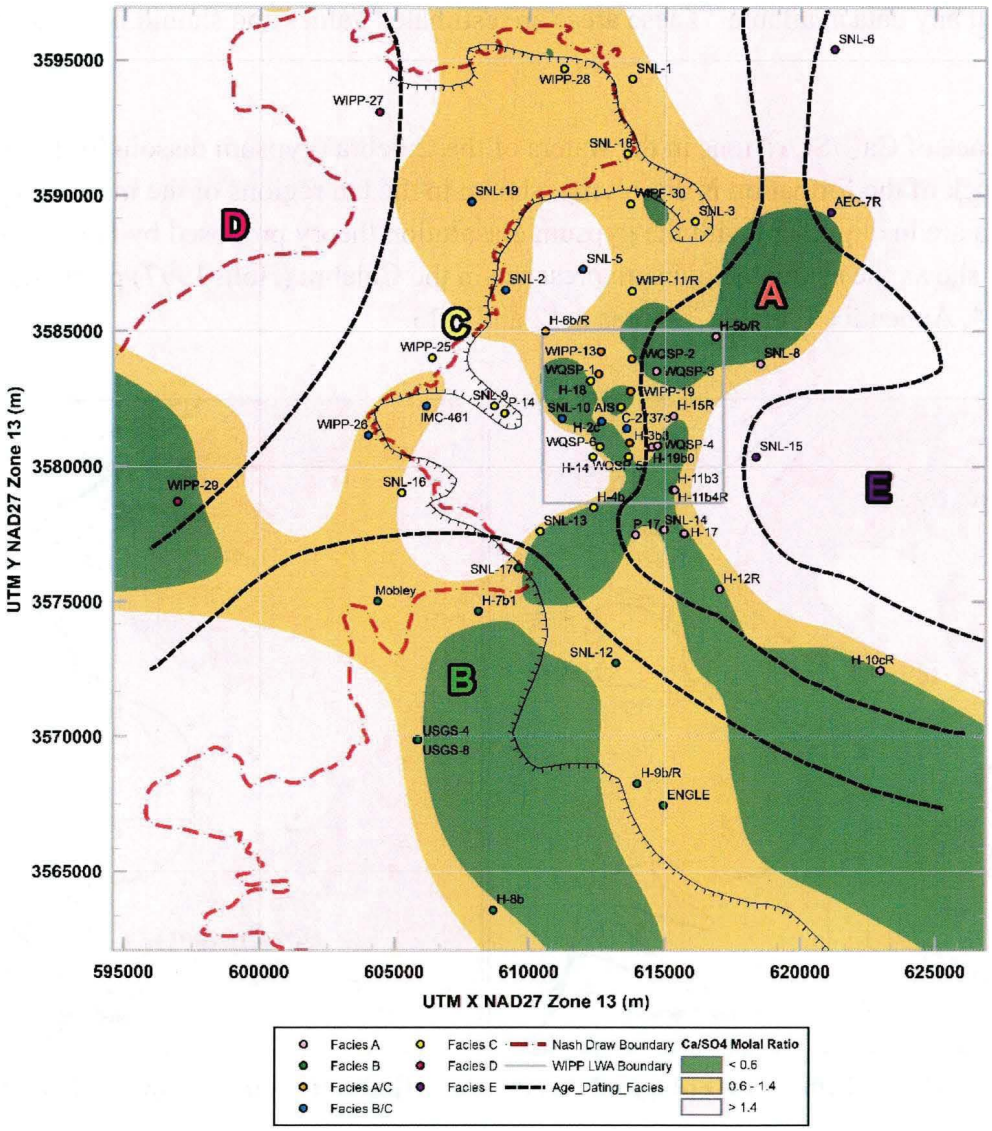

Figure 35 Calcium/Sulfate Molar Ratio for Culebra (Data Set #2)

The tan area of the maps, indicate that Ca^{2+} and SO_4^{2-} are being contributed to the waters equally suggesting the presence of gypsum. Since Ca^{2+} and SO_4^{2+} ions are in solution, it is also an indication of gypsum equilibrium or dissolution. The light pink areas of the map, suggest that another Ca^{2+} containing mineral is contributing to the Ca^{2+}. The green areas indicate that the SO_4^{2-} ion is being contributed by an additional SO_4^{2-} containing mineral, other than gypsum. There are differences between the two datasets; however, the general trend of the data is very similar. The dataset differences are likely due to an analysis error in the data (some of the historical data is not as accurate as current), the sample size (more data points/locations in the Data Set #2) and spatial location of the well data etc. Data Set #1 has the most recent data available for the wells in this study, however Data Set #2, has a more comprehensive spatial and historical analyses of wells across the Culebra well network. Another important caution is that the map generation software and calculation technique, will often generate contour lines where

Information Only

there is not any data available. These areas are estimated values and should be considered with caution.

The presence of Ca^{2+}/SO_4^{2-} ions in the waters of the Culebra (gypsum dissolution) indicates that the host rock of the formation is dissolving, shown in the tan regions of the map in Figure 34. These data are in alignment with the gypsum dissolution theory proposed by Holt et al. 2005. Figure 36 shows the estimated gypsum presence in the Culebra (Holt, 1997) presented in WIPP-CRA-2014, Appendix T-Fields, Figures 2-12 and 2-13.

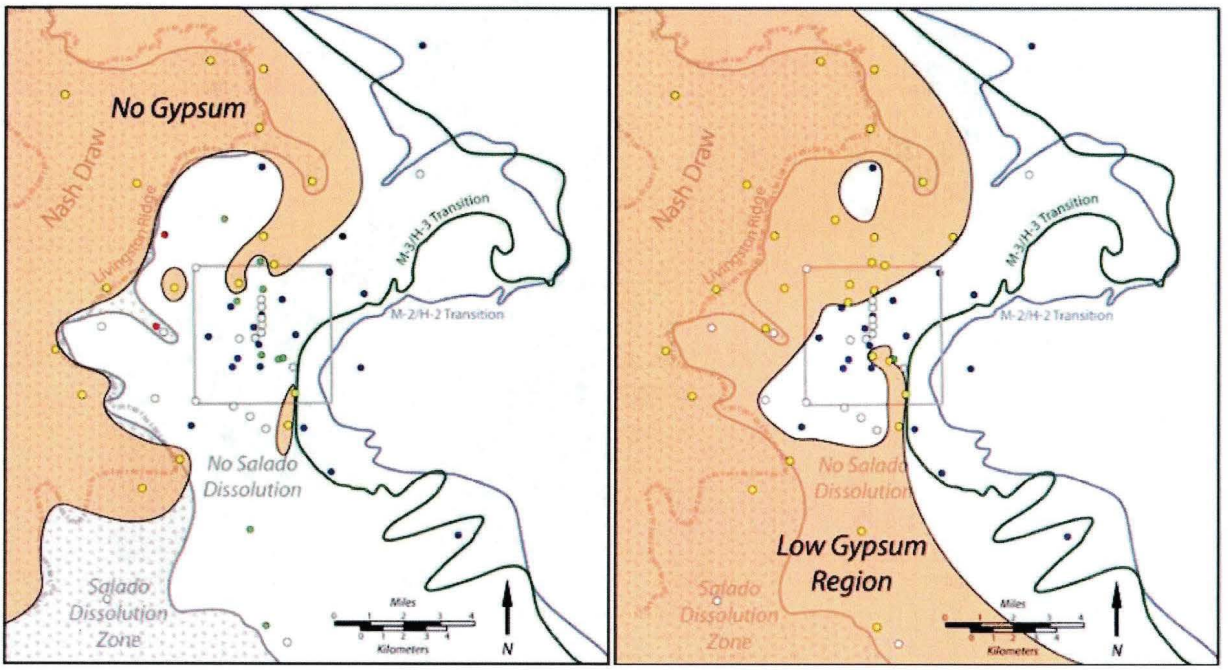

Figure 36 Culebra Geological Areas Identified with Either Low or No Gypsum

The mapping of the Low Gypsum Region in Figure 36 compliments the Ca^{2+}/SO_4^{2-} molar ratios map from 2017-2020. The region identified as low gypsum in the formation, where gypsum has been dissolved, has an inverse relationship to the dissolved gypsum present in the water. In this case, the water chemistry data and the geology data are directly supporting each other, further supporting the previous geological analyses by Holt (1997) and Holt, et. al., (2005). Figure 37 shows the Low Gypsum map on the left and the Ca^{2+}/SO_4^{2-} molar ratio map on the right. Both maps indicate dissolution of gypsum in the center of the LWB and to the west of the region.

Information Only

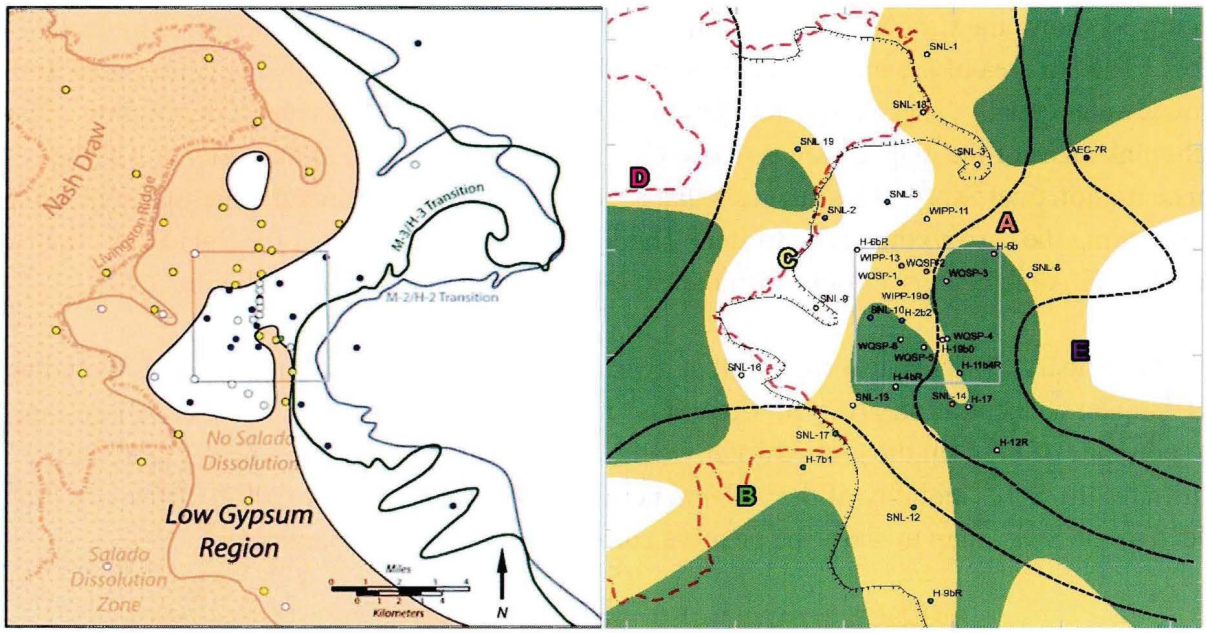

Figure 37 Comparison of Low Gypsum Area and Calcium/Sulfate Molar Ratio for Data Set #1 **(Note: The legend shown in Figure 34 applies to this subset map)**

The dissolution of gypsum in the Culebra Formation, provides a pathway for fluid flow through the formation, as fractures are relieved of gypsum cements (Holt, 1997). The map from Data Set #2, does not show the "high diffusivity pathway" in the southern portion of the LWB, as well as Data Set #1; however, the general trends and lack of gypsum in the western and south-central area of the WIPP monitoring network are still consistent.

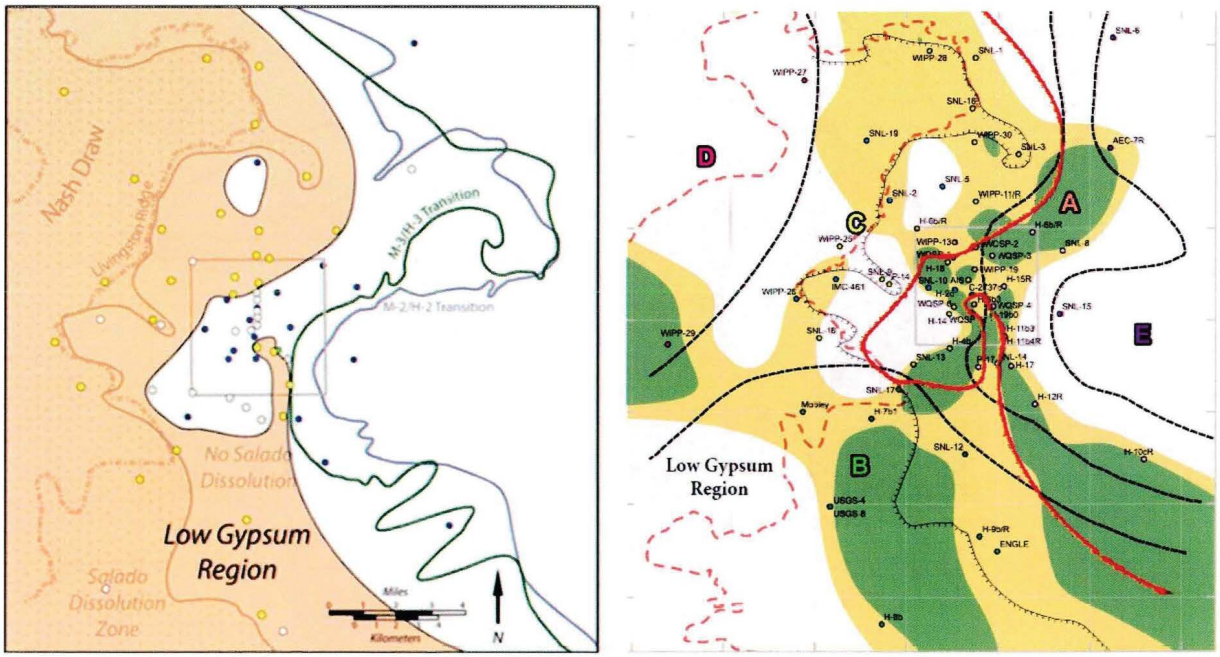

Figure 38 Comparison of Low Gypsum Area and Calcium/Sulfate Molar Ratio for Data Set #2 (low gypsum line in red) **(Note: The legend shown in Figure 35 applies to this subset map)**

Information Only

Figure 38 shows the Ca^{2+}/SO_4^{2-} molar ratio and the Low Gypsum region, identified by Holt, 1997. The tan area of the map indicates areas where Ca^{2+} and SO_4^{2-} are being contributed to the groundwater equally, suggesting that gypsum is at equilibrium or in a state of dissolution. The light pink areas of the map are areas where Ca^{2+} is being contributed to the water at a higher concentration than SO_4^{2-}. This suggests that a calcium containing mineral other than gypsum is contributing the Ca^{2+} to the groundwater. The light pink areas identified for Data Set #1 and Data Set #2 coincide very closely with the No Gypsum region identified in Figure 36.

Other chemistry analyses also support that gypsum dissolution creates a high T zone, including SO_4^{2-} molal concentration. As with Ca^{2+}/SO_4^{2-} molar ratio indicating the presence of gypsum, the presence of SO_4^{2-} in the groundwater would also indicate gypsum presence. Figure 39 illustrates the SO_4^{2-} molality of the Culebra network with the Beauheim (2007) diffusivity line added to the SO_4^{2-} map to show the positive correlation between the parameters.

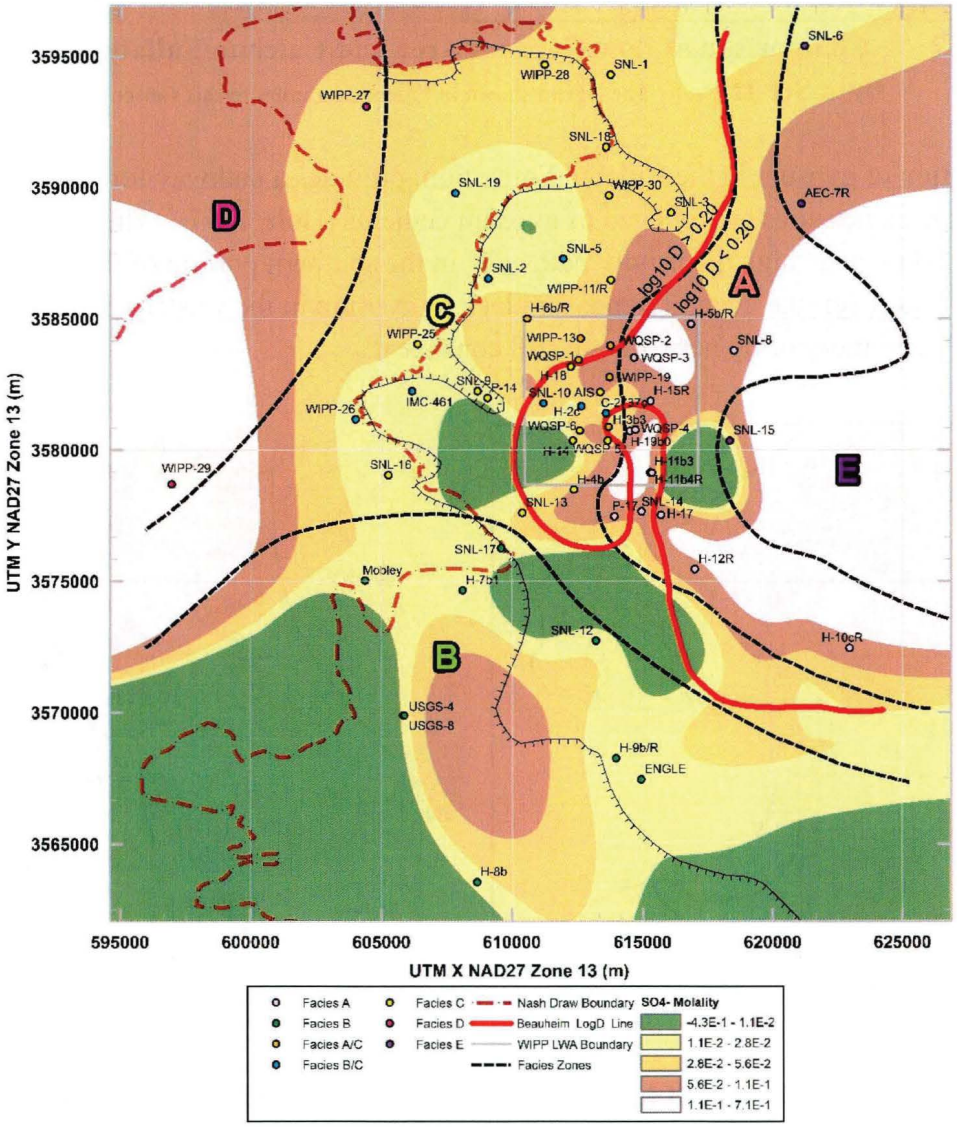

Figure 39 Sulfate Molality in the Culebra Network with Diffusivity Line

Information Only

The Beauheim, 2007 diffusivity line was added to Figure 39 in red. Wells that are to the left side of the line are considered high diffusivity, and wells to the right side of the line are considered low diffusivity. The dissolution of gypsum cements is likely the reason for the increased SO_4^{2-} concentration and the higher diffusivity.

Three wells in zone C have anomalously high calcium concentrations (>2400 mg/L), including SNL-9, P-14 and H-6bR, as shown in Figure 29 and Figure 40 of this AR. The unique chemistry in these wells suggests there is a change in geology or hydrogeologic processes in this area. SNL-13, H-4b and WQSP-6 all have the lowest Ca^{2+} concentrations in zone C (<1000 mg/L). All the low Ca^{2+} wells are located in the south-western portion of the LWB. The differences between the high Ca^{2+} wells and the low Ca^{2+} wells would indicate that there is a mineral change or transition between these wells. Wells SNL-9 and P-14 are lower in SO_4^{2-} than other wells in this zone, however WIPP-13 and H-6bR have higher SO_4^{2-} than Ca^{2+}. SNL-9 and P-14 also have anomalously low K^+ concentrations. Several wells in zone B/C also have anomalously low K^+ concentrations, and there is a possible connection.

The ratio of $Ca^{2+}/(Ca^{2+}+SO_4^{2-})$ meq/L can be used as an indicator of gypsum presence (Tay, 2021, Hounslow, 1995). A value of > 0.5 indicates the Ca^{2+} ion is contributed by a mineral source other than gypsum, while a value < 0.5 indicates that the Ca^{2+} in the water is from a gypsum mineral source. $Ca^{2+}/ (Ca^{2+} + SO_4^{2-})$ can also be used to determine if cation exchange is occurring. Figure 40 shows a graph of Ca^{2+} versus $Ca^{2+} + SO_4^{2-}$, along with the 0.5 ratio line. If the data plot near the 0.5 line, then it is likely that Ca^{2+} is being contributed by gypsum. Additionally, if the data plot above the 0.5 line, it suggests that reverse ion exchange is occurring, while if data plot below the 0.5 line, then ion exchange is likely occurring. It is important to note that this comparison is exactly opposite to the relationship seen earlier with $Na^+/ (Na^+ + Cl^-)$. This is because, in reverse ion exchange, Ca^{2+} is elevated in the groundwater while Na^+ is lower and in ion exchange, Ca^{2+} is lowered while Na^+ is elevated. Unlike the $Na^+/ (Na^+ + Cl^-)$ graph in Figure 27, the $Ca^{2+}/ (Ca^{2+} + SO_4^{2-})$, shows a more definitive pattern for determining the type of cation exchange that is occurring. Several of the previously identified wells, are above the 0.5 line indicating reverse ion exchange, while the predominant trend was for Culebra waters to plot under the 0.5 line, indicating ion exchange.

Information Only

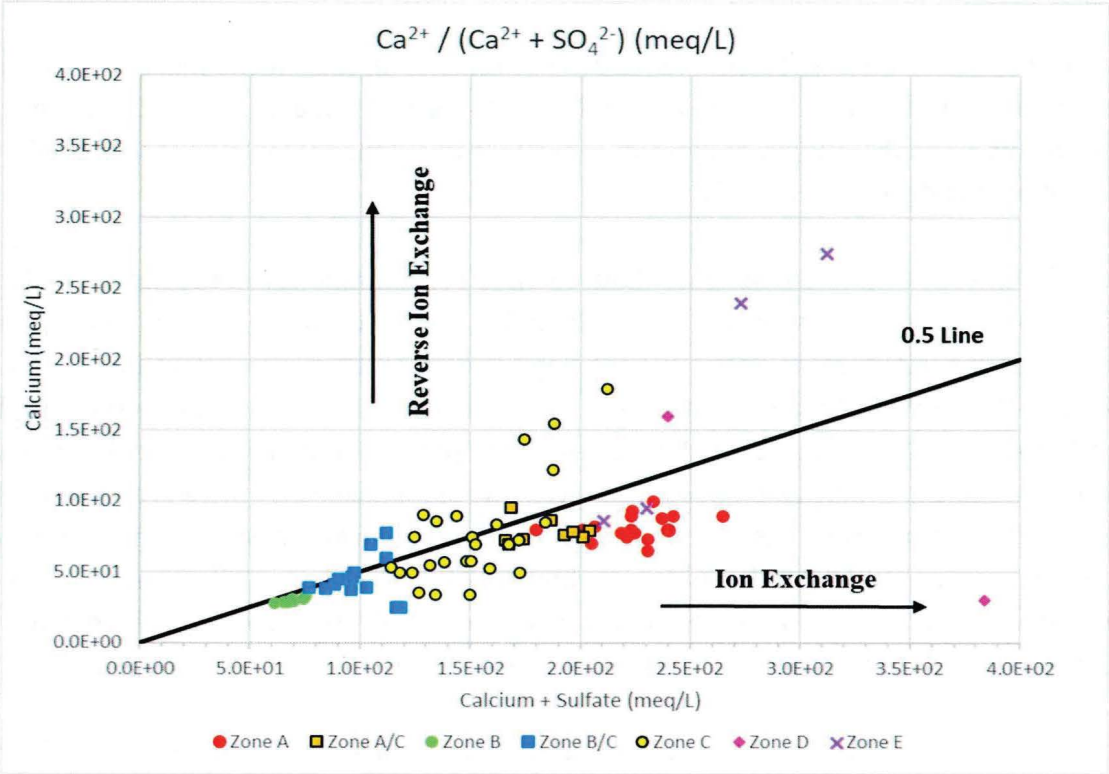

Figure 40 Calcium meq/L versus Calcium + Sulfate meq/L

Table 18 below summarizes the wells identified to be undergoing cation exchange.

Table 18 Cation Exchange Type in Relation to $Ca^{2+}/(Ca^{2+}+SO_4^{2-})$

Well_ID	Data Set #	Facies Zone	Ratio of $Ca^{2+}/(Ca^{2+}+SO_4^{2-})$	Exchange Type $(Ca^{2+}/(Ca^{2+}+SO_4^{2-})^{-})$ Ratio
SNL-5	2	B/C	0.66	Reverse Ion Exchange (> 0.5)
SNL-5	1	B/C	0.69	Reverse Ion Exchange (> 0.5)
H-6b & bR	2	A/C	0.57	Reverse Ion Exchange (> 0.5)
H-14	2	C	0.70	Reverse Ion Exchange (> 0.5)
H-6bR	1	C	0.65	Reverse Ion Exchange (> 0.5)
P-14	2	C	0.85	Reverse Ion Exchange (> 0.5)
SNL-16	2	C	0.60	Reverse Ion Exchange (> 0.5)
SNL-16	1	C	0.64	Reverse Ion Exchange (> 0.5)
SNL-9	1	C	0.82	Reverse Ion Exchange (> 0.5)
SNL-9	2	C	0.82	Reverse Ion Exchange (> 0.5)
WIPP-25	2	C	0.62	Reverse Ion Exchange (> 0.5)
WIPP-27	2	D	0.67	Reverse Ion Exchange (> 0.5)
SNL-15	2	E	0.88	Reverse Ion Exchange (> 0.5)
SNL-6	2	E	0.88	Reverse Ion Exchange (> 0.5)
*NOTE: Data are considered participating in Reverse Ion Exchange if the value is > 0.55				
H-10cR	2	A	0.35	Ion Exchange (< 0.5)
H-11b3	2	A	0.36	Ion Exchange (< 0.5)
H-11b4R	2	A	0.34	Ion Exchange (< 0.5)

Information Only

Well_ID	Data Set #	Facies Zone	Ratio of Ca^{2+}/ (Ca^{2+}+SO_4^{2-})	Exchange Type (Ca^{2+}/ (Ca^{2+}+SO_4^{2-})) Ratio
H-11b4R	1	A	0.37	Ion Exchange (< 0.5)
H-12R	1	A	0.28	Ion Exchange (< 0.5)
H-12R	2	A	0.33	Ion Exchange (< 0.5)
H-15R	2	A	0.40	Ion Exchange (< 0.5)
H-17	2	A	0.34	Ion Exchange (< 0.5)
H-17	1	A	0.37	Ion Exchange (< 0.5)
H-19b0	1	A	0.40	Ion Exchange (< 0.5)
H-19b0	2	A	0.44	Ion Exchange (< 0.5)
H-5b	1	A	0.33	Ion Exchange (< 0.5)
H-5b & bR	2	A	0.33	Ion Exchange (< 0.5)
P-17	2	A	0.40	Ion Exchange (< 0.5)
SNL-14	2	A	0.34	Ion Exchange (< 0.5)
SNL-8	1	A	0.42	Ion Exchange (< 0.5)
SNL-8	2	A	0.43	Ion Exchange (< 0.5)
WQSP-3	3	A	0.32	Ion Exchange (< 0.5)
WQSP-4	3	A	0.36	Ion Exchange (< 0.5)
H-3b3	2	A/C	0.42	Ion Exchange (< 0.5)
SNL-14	1	A/C	0.37	Ion Exchange (< 0.5)
WIPP-13	1	A/C	0.42	Ion Exchange (< 0.5)
WIPP-13	2	A/C	0.44	Ion Exchange (< 0.5)
WIPP-19	2	A/C	0.39	Ion Exchange (< 0.5)
WIPP-19	1	A/C	0.40	Ion Exchange (< 0.5)
WQSP-2	3	A/C	0.40	Ion Exchange (< 0.5)
ENGLE	2	B	0.42	Ion Exchange (< 0.5)
H-7b1	1	B	0.42	Ion Exchange (< 0.5)
H-7b1	2	B	0.44	Ion Exchange (< 0.5)
H-8b	2	B	0.44	Ion Exchange (< 0.5)
H-9b & bR	2	B	0.44	Ion Exchange (< 0.5)
H-9bR	1	B	0.42	Ion Exchange (< 0.5)
Mobley	2	B	0.41	Ion Exchange (< 0.5)
SNL-12	2	B	0.43	Ion Exchange (< 0.5)
SNL-12	1	B	0.44	Ion Exchange (< 0.5)
SNL-17	1	B	0.44	Ion Exchange (< 0.5)
SNL-17	2	B	0.44	Ion Exchange (< 0.5)
USGS-8	2	B	0.43	Ion Exchange (< 0.5)
H-2b2	1	B/C	0.38	Ion Exchange (< 0.5)
H-2c	2	B/C	0.39	Ion Exchange (< 0.5)
SNL-10	1	B/C	0.21	Ion Exchange (< 0.5)
SNL-10	2	B/C	0.21	Ion Exchange (< 0.5)
AIS	2	C	0.29	Ion Exchange (< 0.5)
H-18	2	C	0.39	Ion Exchange (< 0.5)
H-4b	2	C	0.23	Ion Exchange (< 0.5)
H-4bR	1	C	0.28	Ion Exchange (< 0.5)
SNL-13	1	C	0.40	Ion Exchange (< 0.5)
SNL-13	2	C	0.42	Ion Exchange (< 0.5)

Information Only

Well_ID	Data Set #	Facies Zone	Ratio of Ca^{2+}/ (Ca^{2+}+SO_4^{2-})	Exchange Type (Ca^{2+}/ (Ca^{2+}+SO_4^{2-})$^-$) Ratio
SNL-18	2	C	0.42	Ion Exchange (< 0.5)
SNL-3	2	C	0.42	Ion Exchange (< 0.5)
SNL-3	1	C	0.42	Ion Exchange (< 0.5)
WIPP-28	2	C	0.38	Ion Exchange (< 0.5)
WIPP-30	2	C	0.41	Ion Exchange (< 0.5)
WQSP-5	3	C	0.33	Ion Exchange (< 0.5)
WQSP-6	3	C	0.25	Ion Exchange (< 0.5)
WIPP-29	2	D	0.08	Ion Exchange (< 0.5)
AEC-7R	1	E	0.41	Ion Exchange (< 0.5)
AEC-7R	2	E	0.41	Ion Exchange (< 0.5)
Note: Data are considered participating in Ion Exchange if value is below 0.45				

Several of the wells identified in Table 17 as participating in reverse ion exchange in terms of Na^+ and Cl^- are also identified as participating in reverse ion exchange in terms of Ca^{2+} and SO_4^{2-}, including SNL-5, H-14, P-14, SNL-16, SNL-9, WIPP-27, SNL-15 and SNL-6.

Figure 41 and **Error! Reference source not found.**Figure 42 show the Ca^{2+}/(Ca^{2+}+SO_4^{2-}) meq/L for the Culebra water samples for Data Set #1 and Data Set #2 (Data Set #3 is included in both maps). The light pink areas in both maps suggest where reverse ion exchange may be occurring causing Ca^{2+} to be elevated and Na^+ to precipitate, while the green areas of both maps suggest where ion exchange may be occurring, causing an elevated Na^+ concentration and Ca^{2+} precipitation.

Information Only

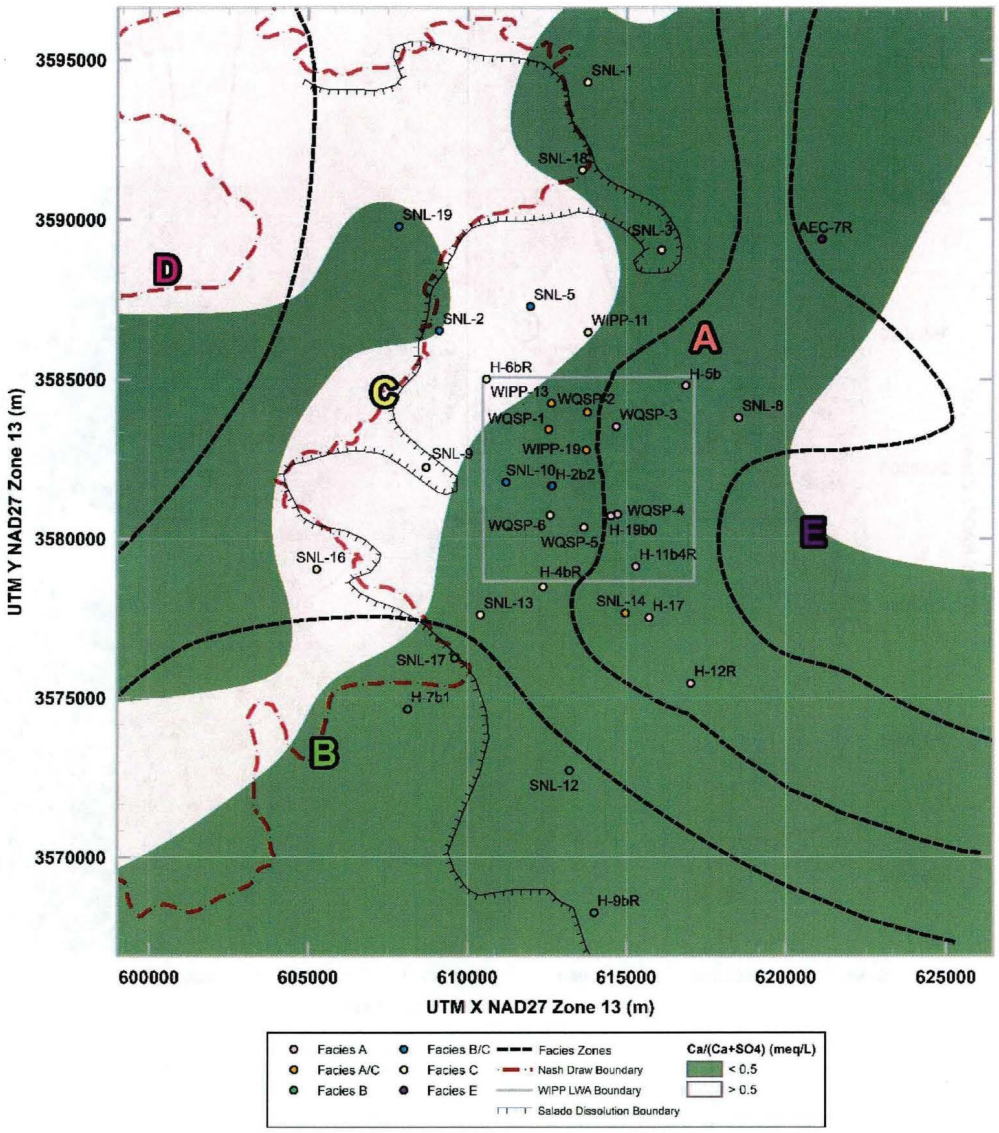

Figure 41 **Contour map of $Ca^{2+}/(Ca^{2+}+SO_4^{2-})$ meq/L (Data Set #1)**

Information Only

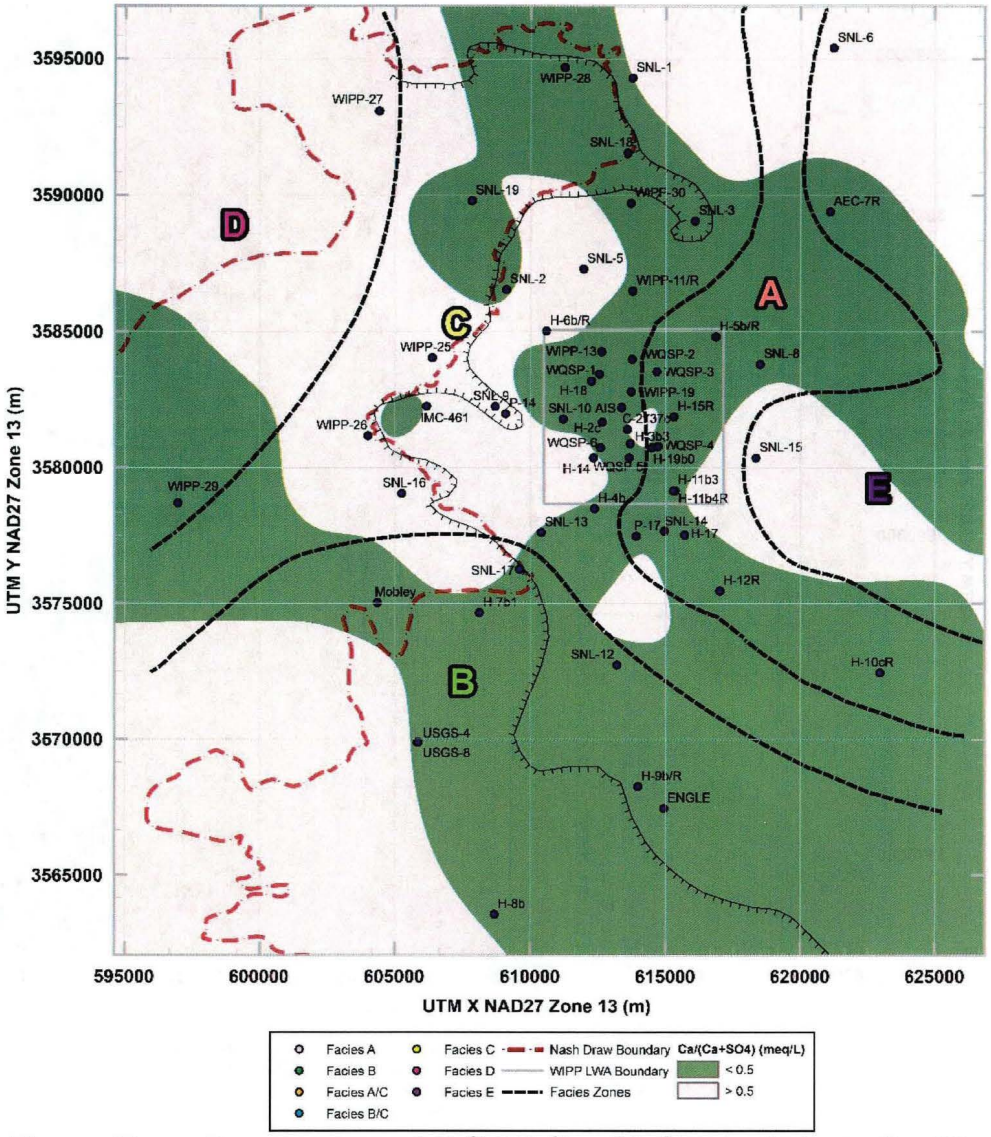

Figure 42 Contour map of $Ca^{2+}/(Ca^{2+} + SO_4^{2-})$ meq/L (Data Set #2)

Several of the wells identified as participating in reverse ion exchange (light pink areas of Figure 41 and 42), have been previously noted for their anomalous characteristics in historical studies. Bodine and Jones, 1990 noted that well P-14 has a markedly high Ca/Mg ratio when comparted to other primitive-diagenetic samples. This high Ca/Mg ratio can be contributed to the high Ca concentration produced from reverse ion exchange. Another notable study that confirmed anomalies in some of these wells was Siegel et al. 1990. The Siegel et al. study noted that between 8/1980 and 2/1986, there was a marked increase in Ca^{2+} concentration in well, WIPP-25 and P-14 had an anomalously high Ca^{2+} concentration compared to what was expected. At the time of the report, this anomaly was attributed to erroneous sampling or analysis techniques, however this study suggests that it may have been due to reverse ion exchange processes.

There are different Na^{+} concentrations across the zone C area, ranging from 3260 mg/L to 16,250 mg/L. This large range of Na^{+} concentrations is likely a result of cation exchange of Na^{+}

Information Only

and Ca^{2+}. Wu, C. et al 2021, proposed that plotting the $(Mg^{2+}+Ca^{2+})$ - $(HCO_3^{-}+SO_4^{2-})$ vs. $(Na^{+}+K^{+})$ – Cl^{-}, can confirm if cation exchange has occurred between Ca^{2+} and Na^{+}. **Error! Reference source not found.** Figure 43 plots the zone C values. The slope of the line from the data is positively correlated at -0.9164. This value is very near -1, which would indicate that several of the wells in zone C have undergone cation exchange between Na^{+} and Ca^{2+}. Several zone C wells did not plot along the normal trend of the other wells in this zone. These wells were H-6bR, WIPP-25, SNL-3, AIS and WIPP-30.

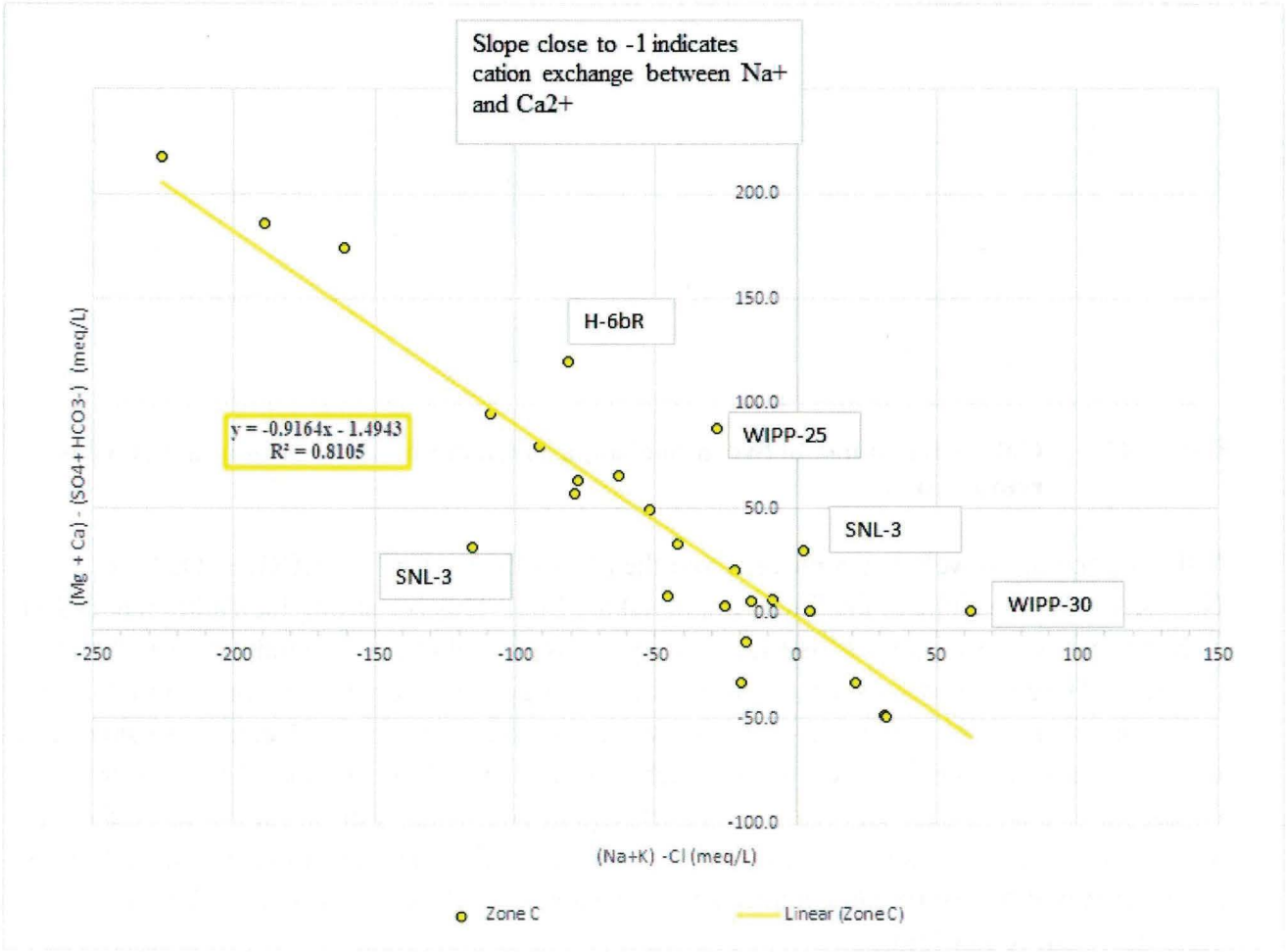

Figure 43 Cation Exchange between Sodium and Calcium Zone C

To understand the relationship of the wells in zone C, the anomalous wells (H-6bR, WIPP-25, SNL-3, AIS, H-18 and WIPP-30) were removed from this data set and the data in Figure 43 was re-plotted.

Information Only

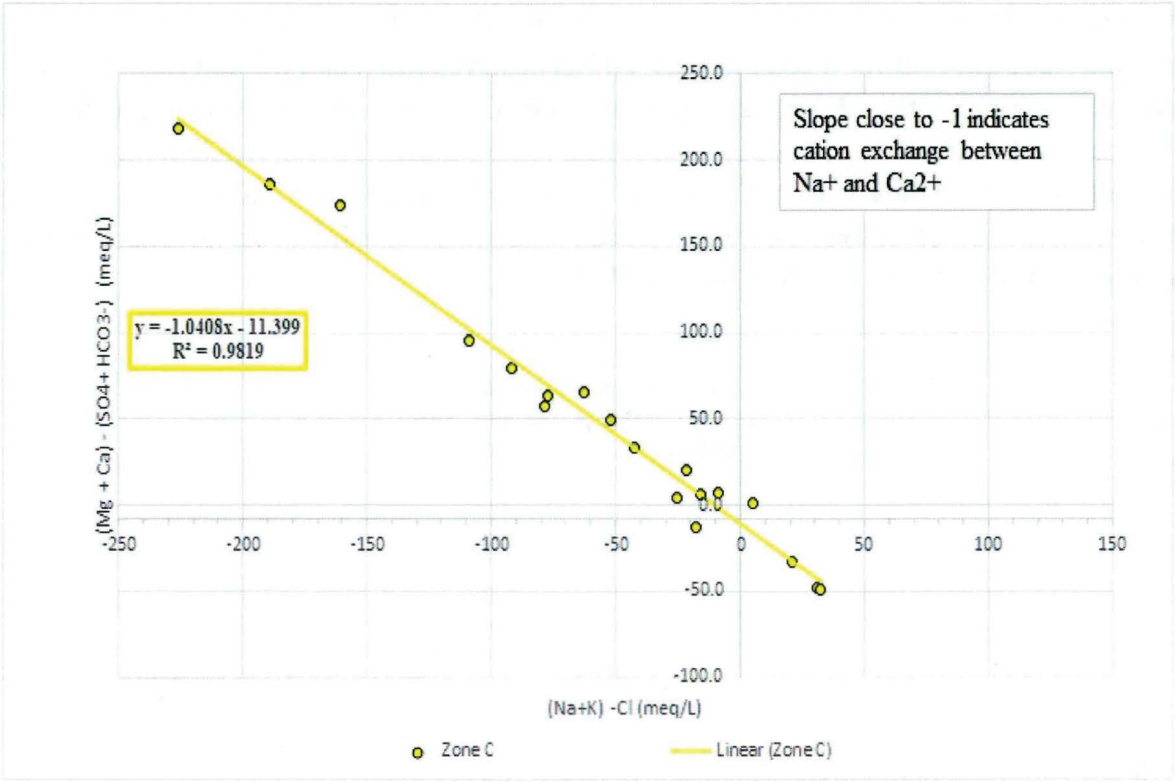

Figure 44 **Cation Exchange between Sodium and Calcium Zone C (anomalous wells removed)**

With the anomalous well data removed from the plot of $(Mg^{2+}+Ca^{2+})$ - $(HCO_3^-+SO_4^{2-})$ vs. (Na^++K^+) – Cl^-, the slope of the line is improved to -1.04. This is a strong indication that cation exchange between Na^+ and Ca^{2+} is a dominant process controlling the groundwater geochemistry in zone C. Based on previous data presented in this study, it is likely that the predominant cation exchange reaction occurring in this zone is reverse ion exchange. **Error! Reference source not found.** was used to calculate the slope for each well in the Culebra network. As discussed previously, a -1 slope indicates that cation exchange has occurred. For this study, all wells that fall within a range of, -0.8 to -1.2 will be considered as participating in cation exchange. Figure 45**Error! Reference source not found.** shows the results of the calculation from **Error! Reference source not found.**.

Equation 4

$$\frac{(Mg^{2+}+Ca^{2+})-(HCO_3^-+SO_4^{2-})}{(Na^++K^+)-Cl^-}$$

Information Only

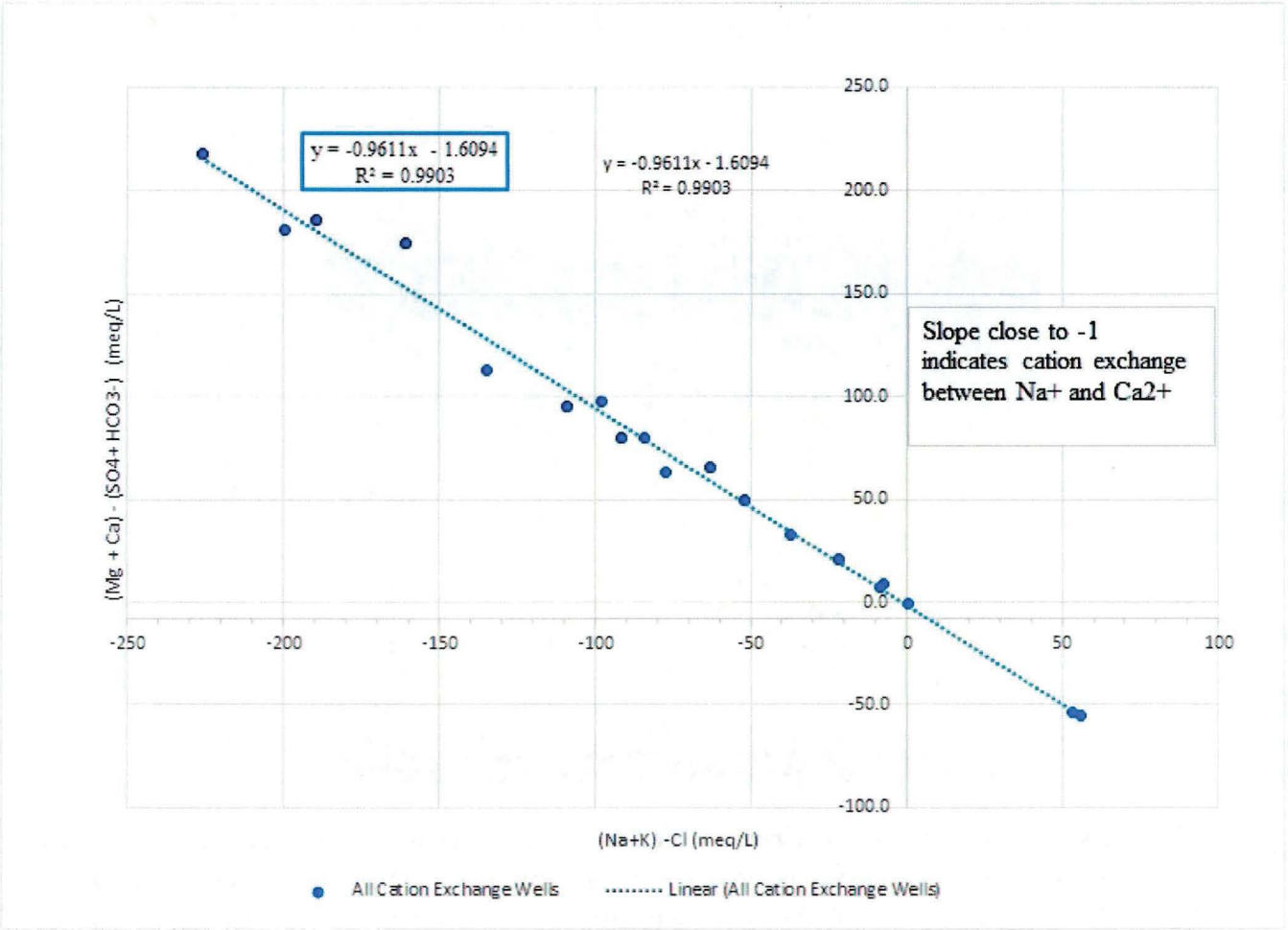

Figure 45 Culebra Wells that Have Undergone Cation Exchange

Based on the information presented in Figure 45, wells in several different zones have undergone cation exchange. The slope of the line has an excellent correlation, with an R^2 of 0.9903, and a slope of -0.9611. **Error! Reference source not found.** summarizes the wells and their subsequent zones, that are plotted in Figure 45**Error! Reference source not found.**.

Information Only

Table 19 Culebra wells that have undergone Cation Exchange

Estimated Zone	Well_ID	Date	(Na+K)-Cl meq/L	(Mg+Ca)-(SO4+HCO3) meq/L	Cation Exchange Equation 4 Slope
A	P-17	1986-1987	-98.02	97.46	-0.99
A	SNL-8	2017-2020	-199.21	180.79	-0.91
A/C	H-6b & bR	1978-2008	-134.99	113.25	-0.84
B	H-7b1	2017-2019	0.70	-0.66	-0.94
B/C	SNL-10	2006	53.50	-53.42	-1.00
B/C	WIPP-26	1988	-37.16	33.18	-0.89
B/C	SNL-5	2017-2020	-84.15	79.78	-0.95
B/C	SNL-10	2017-2020	56.11	-55.43	-0.99
B/C	SNL-19	2017-2020	-7.68	8.98	-1.17
C	H-14	1987-1995	-108.96	95.31	-0.87
C	P-14	1986-1988	-226.03	217.83	-0.96
C	SNL-9	2004	-189.24	185.74	-0.98
C	SNL-13	2006	-8.61	7.03	-0.82
C	SNL-16	2006-2016	-62.79	65.80	-1.05
C	WIPP-11 & 11R	2004-2021	-51.72	49.47	-0.96
C	SNL-9	2017-2020	-161.00	174.22	-1.08
C	SNL-16	2017-2020	-91.59	79.86	-0.87
C	SNL-18	2017-2020	-21.83	20.50	-0.94
C	WIPP-11	2017-2020	-77.20	63.27	-0.82
E	AEC-7R	2017-2020	-334.32	290.29	-0.87
E	SNL-6	2008	-1861.57	2044.53	-1.10

The wells identified in Table 19**Error! Reference source not found.** that have undergone cation exchange, are uniquely spatially correlated. Figure 46**Error! Reference source not found.**, below shows the wells identified as having undergone cation exchange (reverse ion exchange) of Na^+ for Ca^{2+} (i.e. creating a Ca^{2+} rich water).

Information Only

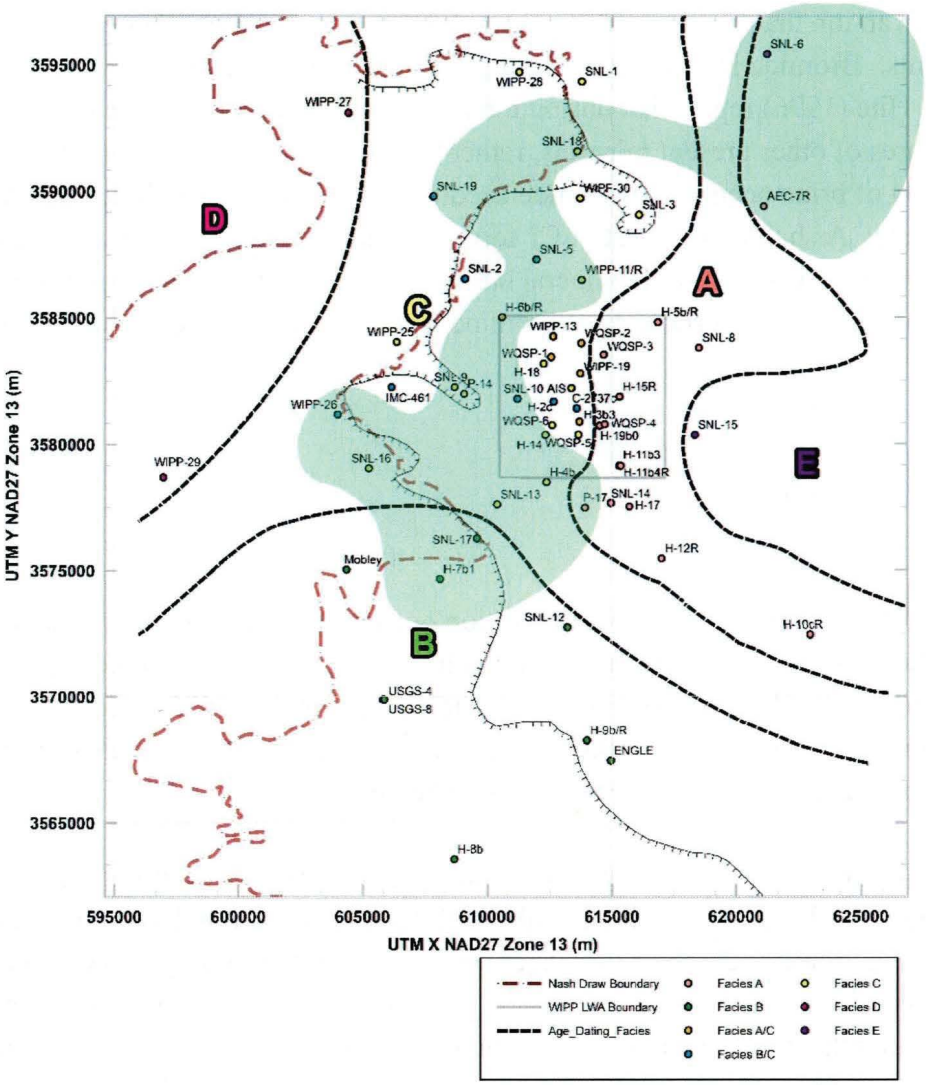

Figure 46 Culebra Wells Having Undergone Cation Exchange

The wells in Figure 46 that are shaded by the green area are the wells in the Culebra network that have undergone cation exchange. The wells configured in this way, suggests that there is a flow path of some kind (from north to south), that is contributing to the cation exchange reaction of the shaded wells.

3.1.6 Chloride vs. Bromide ratio for the Culebra

The Cl^-/Br^- ratio of a water system can provide essential information about water age and the hydrogeochemical processes of a water network. Cl^-/Br^- ratios have been useful in research for a) estimation of aquifer recharge from precipitation (Alcala and Custodio, 2008 & 2004; Cartwright et al. 2006) b) identification of groundwater flow system and understanding interaction between rock and water (Park, et al. 2002), and c) determination of the origin and evolution of groundwater and surface water (Freeman, 2007).

Information Only

Bromide is an ion that has a relatively low solubility compared to other evaporite mineral components. Bromide is a known and common component in evaporite mineral assemblages. Raup and Hite (1996) report that during the formation of evaporites, bromide is incorporated into the structures of other present minerals, rather than forming its own assemblages. As evaporation of brine occurs, the bromide becomes concentrated in solution and halite will begin to precipitate. As halite precipitates, Cl^- ions are removed and the Br^- is added to the chloride minerals present. Each chloride mineral has a different amount of Br^- that can be incorporated into its structure. The coefficients of bromine incorporation for each chloride mineral are:

Halite	= 1
Sylvite	= 10
Kainite	= 3.5
Carnallite	= 7

as reported by Braitsch, 1971. As evaporation occurs, if two or more chloride minerals are present, the bromine ion will be incorporated into the solid at the reported ratio. Polyhalite, does not incorporate the Br^- ion into its structure, however, Combs (1975) reported a positive correlation between Br^- concentration and presence of polyhalite. It is unclear what causes this positive correlation and further research could be beneficial.

Because Cl^- is relatively soluble and Br^- is not, as dissolution or evaporation occurs, the chloride concentration will vary across time, while the Br^- concentration will remain relatively the same. As the over-all ionic strength of the system changes, the Br^- will begin to incorporate itself into other chloride dominant minerals, displacing Cl- and incorporating into the structures of existing chloride minerals. Br^- in a water system can originate from several different sources, including atmospheric sources (precipitation), recrystallization of evaporite minerals, diffusion of ions, intrusion of sea water, and contamination (Heston, 2015). Each of these sources and processes has been shown to have different Cl^-/Br^- mass ratios. The Cl^-/Br^- mass ratio is calculated by dividing the molality of Cl^- by the molality of Br^-. Alcala and Custodio (2008), describe the processes impacting Cl^-/Br^- ratios in the context of evaporite dissolution. They propose that Cl^-/Br^- ratios will not be changed from sea water values until the halite becomes concentrated enough to precipitate, because the Br^- is not easily incorporated into the crystalline structures of the chloride minerals. At this stage the Cl^-/Br^- ratio compared to the Cl^- concentration will be low (655 or less).

Gypsum that is precipitated in this early stage of crystallization my contain halite of this type. During the last stages of halide crystallization from brine, at the time K^+ replaces Na^+, Br^- will begin to replace Cl^- in the precipitate minerals. These minerals will have a relative Cl^-/Br^- ratio of ~800 or less. In cases where more complex chloride minerals are present such as carnallite and sylvite, the Cl^-/Br^- ratio will be even lower because these minerals can incorporate more Br^- into their structure than simple halite. In environments where halite dissolution occurs and there

Information Only

are very high concentrations of Cl^-, the Cl^-/Br^- ratios will be extremely high (Kloppman, et al. 2001) Figure 47 shows common types of salinity and the associated relative Cl^-/Br^- molar ratios. The processes that control the Cl^-/Br^- ratio of the Culebra would most likely be represented as "leaching of natural evaporites" and possibly "leaching of potassium halides" (categories 3 and 6 in Figure 47) (Alcala and Custodio, 2008).

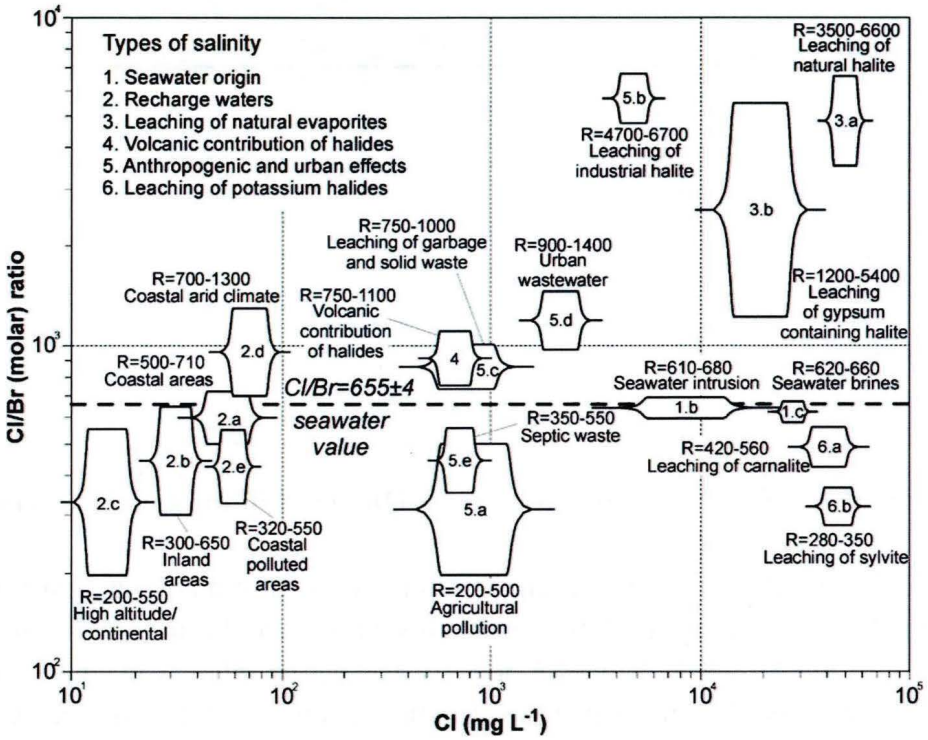

Figure 47 Plot of Cl/Br ratio vs. Cl (in mg/L) for six main salinity acquisition processes (Alcala and Custodio, 2008)

Figure 48 is a plot of the Cl^-/Br^- molar ratios vs. Cl^- concentration for the Culebra well network. Data are plotted by facies zone (scale is log base 10 for both axes). Based on the diagram in Figure 47, it appears that the majority of the water samples fall within category 3.b, which is "leaching of gypsum containing halite" with a Cl^-/Br^- molar ratio between 1200-5400.

Information Only

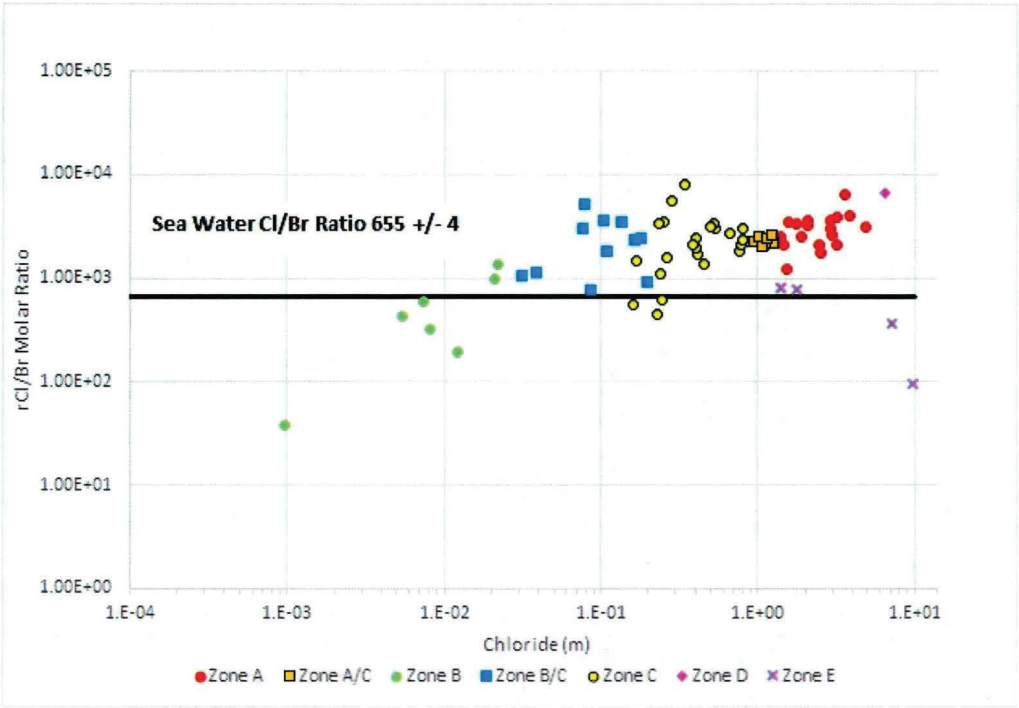

Figure 48 Cl^-/Br^- Molar Ratio vs. Cl^- Observed in the Culebra Network

Some of the Culebra well waters fall within the salinity classification of 3.a, "leaching of natural halite", with a Cl^-/Br^- ratio range of 3500-6600. Most of the samples in zones B and E had Cl^-/Br^- ratios below 800. All wells in zones A and A/C had Cl^-/Br^- ratios well above 800 with the lowest value being 1214. The majority of the samples in zones A, A/C and E had Cl^-/Br^- ratios higher than 2000. These data are mostly congruent with the Siegal, et al, 1991 historical data, with the Cl^-/Br^- ratio being the highest in/near Nash Draw and SNL-16 (5609-9015), intermediate through the center of the WIPP Site (1214-4226), and lowest in H-4 (the low salinity region south of the LWB) and in the very high salinity wells SNL-15 and SNL-6, on the east side of the LWB. The Siegal report identified P-14 and H-4 having the lowest Cl^-/Br^- molar ratios, while in this study, P-14 had a Cl^-/Br^- molar ratio of 1712, which is moderate compared to the other well data analyzed. Table 20 summarizes the wells with the lowest Cl^-/Br^- molar ratios, in green and the highest Cl^-/Br^- molar ratios in red. All other wells in this study fell within the "intermediate" category ranging from 1214-4226.

Table 20 Lowest and Highest Cl/Br Molar Ratios in WIPP Well Network

Well_ID	Estimated Zone (Domski)	Date	Cl/Br molal Ratio
H-8b	B	1986-1988	38
SNL-6	E	2008	97
Mobley	B	1988	194
H-7b1	B	1986-1990	327
SNL-15	E	2007	369

Information Only

H-9b & bR	B	1980-2012	435
H-4b	C	1987-1994	439
H-4bR	C	2017-2020	559
SNL-17	B	2006-2017	595
SNL-13	C	2006	618
AEC-7R	E	2014-2015	779
H-2c	B/C	1989-1994	802
AEC-7R	E	2017-2020	819
SNL-12	B	2004	834
SNL-5	B/C	2004	928
SNL-10	B/C	2017-2020	1033
SNL-13	C	2017-2020	1077
SNL-16	C	2006-2016	5609
SNL-19	B/C	2017-2020	6254
H-17	A	2017-2019	6413
WIPP-29	D	1987	8347
SNL-16	C	2017-2020	9015

Cl^-/Br^- ratios are useful in the determination of groundwater origins, in that atmospheric chloride contribution can be distinguished from other origins, then used to estimate aquifer recharge from precipitation through the chloride mass balance method (Alcala and Custodio, 2008). Utilizing this technique may also be useful to facilitate WIPP research to better elucidate where recharge from precipitation is occurring, if at all.

3.1.7 Hydrogeochemistry and Flow Patterns

In past studies, it has been purported that the steady-state confined-flow hydrologic model and the geochemical interpretations were inconsistent (Ramey, 1985, Chapman, 1988 and Siegal et al., 1991). Lambert, 1991, utilized isotope tracers to better define the Culebra water age, based on zone. Lambert (1991) and Siegal et al. 1991, proposed that the inconsistency between the steady state hydrologic model and the geochemistry could be explained by change in flow direction in the last 30,000 to 12,000 years (Siegal et al., 1991).

Steady-state freshwater heads are calculated each year for key wells in the Culebra network. These calculations are reported in the Annual Site Environmental Report (ASER), that is issued annually. Figure 49 shows the most recent (2020 data) Culebra flow contour map (US DOE, 2021).

Information Only

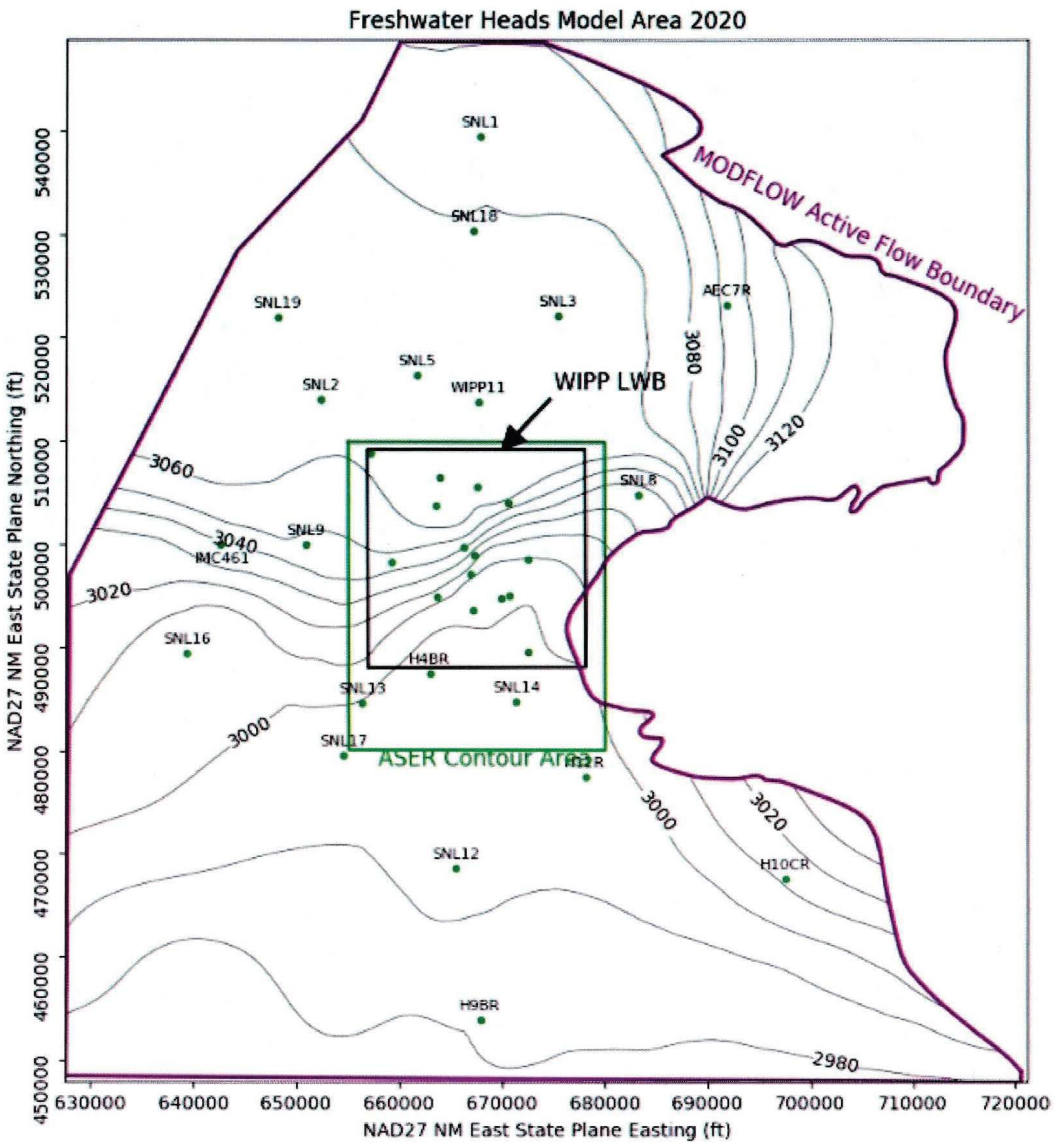

Figure 49 Culebra Groundwater Flow Map, 2020 (US DOE, 2021)

Freshwater heads are calculated utilizing calculated densities at mid-formation for each well. The densities are calculated as per SP 9-11 Rev.3 (Johnson, P. 2015). Freshwater head calculations capture the mean flow behavior of the Culebra and are based on water level measurements in the well column. Figure 50 is the generated freshwater-heads superimposed on the hydrogeochemical facies/zones.

Information Only

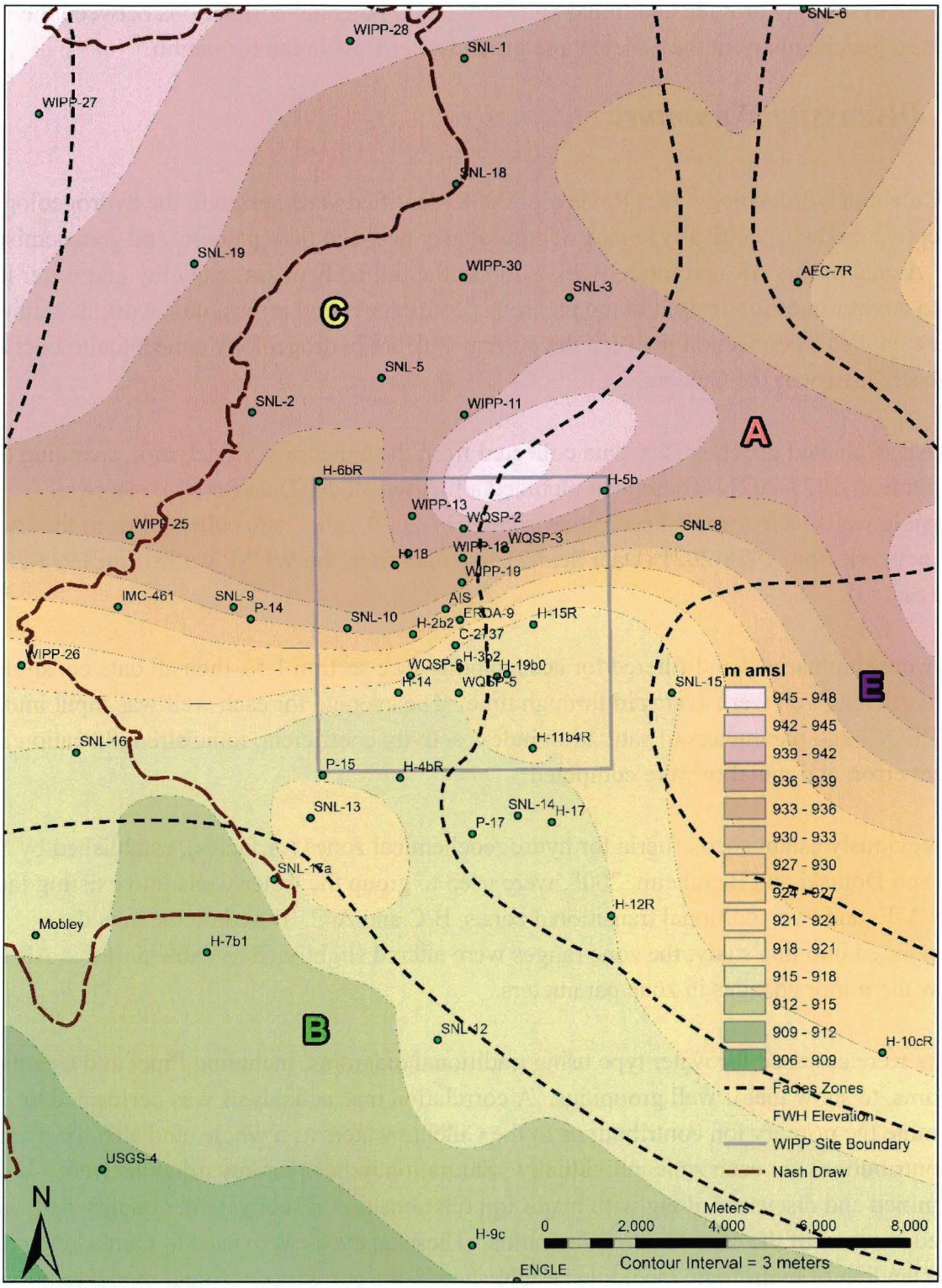

Figure 50 Freshwater head calculated values vs. hydrogeochemical zones

As shown in Figure 50, groundwater elevations in the Culebra are higher in the northern portion of the network, with a higher mound in the north north/east portion of the LWB. More detailed

Information Only

future analyses may provide additional knowledge into potential correlations between the observed geochemistry in the Culebra and groundwater flow in the formation.

4 *Discussion/Summary*

The Culebra Hydrogeology Peer Review of 2008 identified weaknesses in the hydrogeologic conceptual model, specifically, a lack of consistency between flow patterns and geochemistry data. A goal of this AR and future work is to use the full body of water quality and water level data to answer questions raised in the previous peer reviews and inform new work that may better establish a connection between the current Culebra hydrogeology conceptual model and the geochemistry of the Culebra.

This AR evaluated geochemistry data collected from the Culebra Well network, spanning the timeframe of 1978-2021. These data included a focused study (Data Set #1), where all accessible wells were sampled each year from 2017-2020, other data collected from the Culebra Well network from 1978-2021 (Data Set #2), and data from the WQSP wells from 1995-2020 (Data Set #3).

Data were summarized and filtered for acceptability (see section 1.5), then all data constituents for a particular well were averaged through time. The average for each well was input into PHREEQCI and parameters of saturation index, activity coefficient, ionic strength, cation/anion percent error, and molality were computed.

The previously established criteria for hydrogeochemical zones (or facies), established by Siegel, 1991 and Domski and Beauheim, 2008, were used to group the water wells into existing facies zones A-E, and two additional transitional zones, B/C and A/C. Based on the new data incorporated into this study, the zone ranges were altered slightly. See Table 5 of this AR to review the minor changes in zone parameters.

Waters were assessed for water type using traditional diagrams, including Piper and Chadha diagrams, to show major well groupings. A correlation matrix analysis was performed to determine the primary ion contributions to the Culebra waters as a whole, and also the primary ion contributions for each zone individually. Saturation indices for key minerals were determined and discussed along with major ion relationships. Finally, water quality data were studied in terms of the chloride/bromide ratios. These analyses were used to gain a better understanding of hydrologic ideologies established in the current conceptual model relating to transmissivity, geology of the Rustler formation, hydrogeochemical processes and flow patterns. The geochemistry of the Culebra is directly associated to these concepts and this AR explores those relationships. The following discussion includes the findings of this report and comparisons to past analyses, by established zones/facies, and recommends areas for future work.

Information Only

Facies Zones

Summaries of the groundwater chemistry in the Culebra network and the established facies zones are shown in Table 5 and Table 21, below.

Table 21 Hydrogeochemical Facies zones developed by Siegel, et al. 1991, Domski and Beauheim, 2008. Updated 2022

Increasing Salinity ↓	Facies /Zone	Siegel et al. (1991)	Domski & Beauheim (2008)	This Study
	B	Dilute (ionic strength <0.1 molal) CaSO4 rich groundwater, from southern high transmissivity area	Same as Siegel et al. (1991) Mg/Ca molar ratio: 0.32-0.52	Same as previous Mg/Ca molar ratio: 0.28-0.51
	B/C	Not Included	Ionic strength 0.18-0.29 molal Mg/Ca molar ratio 0.4-0.6	Same as previous Mg/Ca molar ratio: 0.39-0.6
	C	Variable composition waters, Mg/Ca molar ratio 0.3-1.2 for waters with ionic strength <1.25 molal	Ionic strength 0.3-1.0 molal Mg/Ca molar ratio 0.4-1.1	Ionic strength 0.30-1.02 molal Mg/Ca molar ratio: 0.39-0.99
	A/C	Not Included	Ionic strength 1.1-1.6 molal Mg/Ca molar ratio 0.5-1.2	Ionic strength 1.07-1.6 molal Mg/Ca molar ratio: 0.85-1.25
	A	Ionic Strength ~2-3 molal, Mg/Ca molar ratio 1.2-2	Ionic strength >1.66 molal, up to 5.3 molal Mg/Ca ratio 1.2-2.4	Ionic strength 1.66-5.3 molal Mg/Ca molar ratio: 1.07-2.57
	D	Defined based on inferred contamination related to potash refining operations. Ionic strength 3 molal, K/Na weight ratios of ~0.2	Same as Siegel et al. (1991)	Same as previous
	E	Not Included	Wells east of the mudstone-halite margins, ionic strength 6.4-8.6 molal, Mg/Ca molar ratio 4.1-6.6	Wells based on location of mudstone-halite margins, Ionic strength 1.77-11.5 molal Mg/Ca molar ratio 3.81-6.6

Facies Zone A

Facies zone A is located in the eastern portion of the Culebra network, where transmissivity is relatively low and ionic strength has been established as high. Zone A parameters established in this study are ionic strength 1.66 to 5.3 molal and Mg^{2+}/Ca^{2+} molar ratios of 1.07-2.57. A molar ratio of Mg^{2+}/Ca^{2+} in this range indicates, dolomite in various states of saturated to very supersaturated (scaling). The Piper diagram plotted this zone as the Na-Cl water type and this assessment was confirmed by the Chadha diagram. The correlation matrix analysis showed strong positive (>0.7) correlations between: Mg^{2+}/K^{+}, Mg^{2+}/Br^{-}, Na^{+}/K^{+}, Na^{+}/Cl^{-}, K^{+}/ Cl^{-}, and K^{+}/ Br^{-}. The primary ions contributing to ionic strength were: Mg^{2+}, Na^{+}, K^{+}, Cl^{-}, SO_4^{2-} and Br^{-}. These ion correlations would suggest a presence of minerals such as: halite, sylvite, polyhalite, and carnallite. Siegel, et al., 1991 also concluded that significant Mg^{2+} is added to the waters by dissolution of accessory carnallite or polyhalite, so that the degree of dolomite supersaturation increases with ionic strength. The findings in this study, correlate with this assessment. Carbonate was also shown to have a very high correlation with pH and alkalinity (0.86 and 0.82, respectively). This is in alignment with the assumption discussed in section 3.1.4 of this AR,

Information Only

showing the relationship of the dominant geochemical reactions. These being the dissolution of gypsum to form the mineral calcite and a SO_4^{2-}/CO_2 rich water, then the dissolution of calcite, to form dolomite and gypsum and finally the dissolution of dolomite to form magnesite. The reactions are displayed in order of progression below:

$$CaSO_4\ (gypsum, anhydrite) + 2HCO_3^- \rightarrow CaCO_3(calcite) + CO_2 + H_2O + SO_4^{2-}$$

$$2CaCO_3\ (calcite) + Mg^{2+} + SO_4^{2-} \rightarrow CaMg(CO_3)_2\ (dolomite) + CaSO_4\ (anhydrite, gypsum)$$

$$CaMg(CO_3)_2(dolomite) + 2CO_2 + 2H_2O \rightarrow Ca^{2+} + Mg^{2+} + 4HCO_3^-$$

Dolomite dissolution, step 3, will only continue if reactants are available to keep the reaction moving forward. In addition, the reaction of calcite dissolution is limited by the presence of necessary reactants. These reactions and analyses support the previous data generated by the correlation matrix analyses. Molal concentrations and molar ratios were evaluated for key ions in the region. A higher Mg^{2+} concentration was found than Ca^{2+}, indicating that dolomite is not a mineral that is significantly contributing to the geochemistry in this region, since the Mg^{2+} and Ca^{2+} are not at a 1:1 ratio. This result is consistent with the correlation matrix analyses. Calcite, dolomite and magnesite were primarily, all found to be at equilibrium or supersaturated in the majority of this zone, indicating these minerals may precipitate in this region, but not dissolve. Molal carbonate concentrations were also found to be higher in this zone when compared to other zones, which could indicate dissolution of a carbon containing mineral (i.e. calcite shown in the reaction above). The predominant minerals that were identified as contributing to the hydrogeochemical processes in this zone are: halite, polyhalite and carnallite. These data are consistent with previous studies conducted by Siegal, et al. 1991 and Bodine and Jones, 1990, which stated that all zone A waters have appreciable $MgCl_2$, $MgSO_4$, and KCl, indicating dissolution of the assemblage halite/carnallite/polyhalite or mixing of primitive brine with halite-dissolution water. In the far eastern portion of this region gypsum is likely present but does not show significant signs of dissolution. This is in alignment with the Holt, et al. 2005 study in that gypsum is present, but has not begun to dissolve. However, geochemistry data do show gypsum dissolution occurring inside the LWB, primarily to the south. Finally, Cl^-/Br^- ratios in zone A were in the range of 1214-6413, suggesting primarily leaching of gypsum containing halite and possibly some leaching of natural halite.

The data collected in this study support the previously concluded analyses by Siegel et al., 1991 and Domski and Beauheim, 2008, in addition to the geology analysis and hypotheses presented by Holt, et al. 2005; however, a significant amount of additional analysis and comparisons could be made to more clearly define the hydrogeochemical processes of this zone. Future research into the listed topics could help improve the knowledge of this zone:

Information Only

- Improve the definition of the separation/boundary between zone A and zone E, by evaluating available core and geochemistry data (WIPP and Non-WIPP) in that vicinity, that has not been previously analyzed.
- Several wells classified in zone A, have a unique chemistry when compared to the rest of the zone A wells. H-12R, SNL-14, H-19b0, WQSP-4, H-11b4R and H-17, all wells in or near the high T zone, have low Mg^{2+} and K^{+} concentrations compared to the other wells in zone A, while H-15R (directly north of WQSP-4 and H-19b0), has a significant increase in Mg^{2+} and K^{+} (~500-1000 mg/L) along with SNL-8 (farther north and east) which has the highest Mg^{2+} and K^{+} in the entire zone. These data indicate that there is a transition in the minerology between wells WQSP-4 and H-15R, and this could be further researched by collecting more samples from these wells and re-evaluating established relationships between core data and groundwater geochemistry.
- H-17 has a unique chemistry compared to the other wells in this zone because it has a non-detect for all carbon ions, while wells P-17 and SNL-14 have values ~47-54 mg/L and they are right next to H-17. The chemistry for these three well should be re-collected to verify the lack of carbon in H-17.

Facies Zone A/C

Facies zone A/C is located in the north-central region of the LWB. Zone A/C parameters are established in this study as having an ionic strength of 1.07-1.6 molal and a Mg^{2+}/Ca^{2+} molar ratio of 0.85-1.25. A molar ratio of Mg^{2+}/Ca^{2+} in this range indicates, dolomite saturation and supersaturation. The Piper diagram for this zone, showed the waters falling into the Na-Cl water type and this assessment was confirmed by the Chadha diagram. The correlation matrix analysis showed strong positive (>0.7) correlations between: Mg^{2+}/Br^{-}, Na^{+}/Cl^{-}, Na^{+}/SO_4^{2-}, Cl^{-}/SO_4^{2-} and Cl^{-}/Br^{-}. The primary ions contributing to ionic strength are, Na^{+}, K^{+}, Cl^{-}, SO_4^{2-} and Br^{-}. These ion correlations suggest the presence of minerals such as: halite, carnallite and possibly a mineral with elevated concentrations of, Na^{+} and SO_4^{2-}. Ca^{2+} does not have a significant presence in this zone and has a negative correlation with SO_4^{2-} (-0.63). This result is consistent with Domski and Beauheim, 2008, in that WIPP-19 and other wells in this zone have a low anhydrite signature. The most positive correlation that Ca^{2+} has in this zone is with HCO_3^{-}, which could indicate the presence of calcite in the waters. There is a strong correlation between CO_3^{2-} and pH (0.93), which could indicate the dissolution of gypsum, through reaction 11 in Table 3. There is a strong negative correlation between K^{+}/HCO_3^{2-} (-0.82), however there is a weak positive correlation between K^{+}/SO_4^{2-}. The high correlation between Na^{+}, Mg^{2+} and SO_4^{2-}, could indicate a mineral such as bloedite, and the high correlation between K^{+}/SO_4^{2-} would indicate trace presence of a K^{+}/SO_4^{2-} rich mineral. There was not a significant correlation between Mg^{2+}/Ca^{2+}, meaning dolomite is not likely a predominant mineral in this zone. Dolomite and calcite were not shown to be present in significant quantities but were saturated or supersaturated in the majority of the region. Magnesite was shown to be both, undersaturated and at equilibrium in this region. The majority of the wells in zone A/C had Ca^{2+}/SO_4^{2+} molar ratios lower than 1,

Information Only

meaning the SO_4^{2-} is higher concentration than the Ca^{2+}. Finally, Cl^-/Br^- ratios in this area were in the range of 2009-2578 mg/L. This range is in the range of "leaching of gypsum containing halite". This is the most tightly grouped set of Cl^-/Br^- in the Culebra. Future research into the listed topics could help improve the knowledge of this zone:

- Definition of the facies zone A/C boundary, by collecting water samples consistently for wells in this zone and correlating the results with available core data.
- H-6b/bR has a much higher Ca^{2+}/SO_4^{2-} molar ratio than any other well in this zone. Possibly consider re-zoning this and other wells in this zone.
- H-6b/bR, WIPP-19 and WIPP-13 are all at equilibrium or supersaturated to dolomite, however all other wells in the zone are undersaturated to dolomite. Propose consistent collection of water samples for the three wells to verify these data.

Facies Zone B

Facies zone B is located in the southern most area of the Culebra well network. It is the zone with the most dilute ionic strength in the network, with parameters of <0.1 m ionic strength and Mg^{2+}/Ca^{2+} molar ratios of 0.28-0.51. A molar ratio of Mg^{2+}/Ca^{2+} in this range indicates, dolomite is in undersaturated conditions, and will dissolve if present. The Piper and Chadha diagrams for this zone, plot the samples in the Ca-Mg-Cl water type. The correlation matrix analysis showed strong positive (>0.7) correlations between: Ca^{2+}/SO_4^{2-}, Na^+/K^+, Na^+/Cl^-, K^+/Cl^- and Br^-/CO_3^{2-}. The primary ions contributing to ionic strength are, Na^+, K^+, Cl^-. There is a strong negative correlation between HCO_3^{2-} and pH, but a high correlation between CO_3^{2-} and pH, indicating the carbonate is controlling the pH in this zone. These data suggest possible dissolution of gypsum and calcite precipitation, through reaction 11 of Table 3. These ion correlations suggest the presence of minerals such as: halite and sylvite. Ca^{2+} and Mg^{2+} are both equally contributing to alkalinity. Transmissivity is high for this zone, likely due to the dissolution of gypsum and the low ionic strength. Mg^{2+} has a strong negative correlation between many ions, including, Na^+, K^+, Cl^- and Br^-, but Mg has a positive correlation to HCO_3^-. Confirming the hypotheses presented in section 3.1.4, and reaction 8, in Table 2 for dolomite dissolution. Dolomite and calcite were shown to be saturated or over-saturated for all wells, however magnesite was undersaturated (see discussion in section 3.1.4). The Cl^-/Br^- ratios in this zone are, 38-1370. This zone showed the lowest Cl^-/Br^- ratios in the Culebra study, however many of the wells were missing Br^- data. Future research into the listed topics could help improve the knowledge of this zone:

- Collect more Br^- data in this area. It could help determine if anthropogenic effects such as precipitation are affecting the Culebra in this region. The only well that had a low Cl^-/Br ratio was H-8b, the most southern well in the network, and a well most likely affected by anthropogenic effects.

Information Only

Facies Zone B/C

Facies zone B/C is one of the designated transition zones, by Domski and Beauheim, 2008, and is located scattered throughout the area Siegal, 1991, designated as zone C. Many of the zone B/C wells are located along the Salado dissolution line and the Nash Draw boundary. Transmissivity has been designated as both high and low in this region, with wells SNL-10, SNL-5, C-2737 and H-2c being low transmissivity, and all other wells in this zone being high. All the wells designated with the "low" transmissivity are farther from the Salado dissolution line than the other wells in this zone. The parameters that designate this zone are an ionic strength from 0.18-0.29 molal and a Mg^{2+}/Ca^{2+} molar ratio of 0.39-0.6. The Piper diagram for this zone is non-specific and wells are scattered between water types $Ca^{2+}$and Na^{+} type. The Chadha diagram provided clearer definition of this zone and plots the wells primarily in the Na-Cl water type with two wells in the Ca-Mg-Cl type. That being said, most of the wells plot in the center of the Chadha diagram, meaning a mixed water type. The correlation matrix analysis shows a strong positive (>0.7) correlation between: Ca^{2+}/ Mg^{2+}, Ca^{2+}/Cl^{-}, Na^{+}/CO_3^{2-}, pH/CO_3^{2-} and HCO_3^{-}/Alkalinity. The primary ions contributing to ionic strength are: Ca^{2+}, Mg^{2+}, Na^{+}, K^{+}, Cl^{-} and Br^{-}. These ion correlations suggest a presence of minerals such as: dolomite, calcium chloride, halite and possibly carnallite. There is a very negative relationship between Ca^{2+} and SO_4^{2-}, indicating the absence of gypsum. This result is consistent with the analyses by Holt, et al. 2005.

SNL-10, H-2c and C-2737 have chemistry profiles, especially regarding Na^{+}, that are different than many of the other wells in this zone. All other wells in zone B/C show that Na^{+} is being contributed by halite. These three wells are also the only wells in this zone located within the LWB. All wells in this zone were either at equilibrium or supersaturated to calcite and dolomite, with mixed saturation (undersaturated and saturated) results for magnesite. There is a high correlation between Ca^{2+}/ Mg^{2+} in this zone, however there is a negative/no relationship between both Ca^{2+}/Mg^{2+} and HCO_3^{2-}, indicating dolomite is not a significant contributor to ion water chemistry in this zone. K^{+}/Na^{+} and Na^{+}/CO_3^{2-} have a positive correlation. In addition, SO_4^{2-}/Cl^{-} have a negative correlation and Na^{+}/ Ca^{2+} have no relationship. This indicates that there is a mineral that contains Na^{+}+ CO_3^{2-} and possibly K^{+} and a different mineral that contains, Ca^{2+}+ Mg^{2+}+ Cl^{-}, with the Ca^{2+}/ Mg^{2+}/Cl^{-} mineral being the dominant mineral in the zone. The Ca^{2+}/ Mg^{2+}/Cl^{-} mineral also has a positive correlation with Br^{-}. These data suggest the possible reaction for the dissolution of a Br-rich carnallite mineral (reaction 13 in Table 2) and also $CaCl_2$ presence. The Cl^{-}/ Br^{-} ratios in this zone are wide-spread and not consistent. SNL-5, SNL-10 and SNL-19 (northern region of network), all have very high Cl^{-}/ Br^{-} ratios in the 2017-2020 study (2400-5200). Cl^{-}/ Br^{-} ratios of SNL-5 and H-2 vary significantly between Data Set #1 and Data Set #2, with the older data having much lower ratios. Future research into the listed topics could help improve the knowledge of this zone:

Information Only

- Collect updated Br^- data in this area. It could help determine if anthropogenic effects such as precipitation are affecting the Culebra and determine if these ratios have possibly changed over-time.
- SNL-5 and WIPP-26 have much higher Ca^{2+} concentrations than other wells in this zone. Collect additional water samples to verify this result and then complete an analysis to potentially re-zone these wells.
- Establish clear B/C zone boundary facies divisions, by collecting additional water samples and correlating them with available core data.

Facies Zone C

Facies zone C is one of the original zones identified by Siegal, et al., 1991. It is the largest zone in the Culebra network and was divided into transitional zones B/C and A/C by Domski and Beauheim, 2008. Even with the divisions of the additional zones, this zone still has the largest number of wells in it. The parameters designated for this zone are ionic strength of 0.30-1.02 and a Mg^{2+}/Ca^{2+} molar ratio of 0.39-0.99. The Piper and Chadha diagrams for this zone plotted the wells predominantly in the Na-Cl water type. The correlation matrix analysis shows strong positive (>0.7) correlations between: Ca^{2+}/Mg^{2+}, Na^+/ Cl^-, pH/CO_3^{2-} and a strong negative correlation between, Ca^{2+}/ SO_4^{2-} and HCO_3^-/Alkalinity. The primary ions contributing to ionic strength are: Mg^{2+}, Na^+, K^+, and Cl^-. These ion correlations suggest a presence of minerals such as halite, and carnallite. There is a negative correlation between Ca^{2+} and SO_4^{2-} indicating an absence of gypsum. The absence of gypsum in this area of the Culebra is consistent with the analysis by Holt, et al. 2005. The strong correlations between pH and the carbon ions shows that CO_3^{2-} is controlling the pH of the water system. All wells in this zone are at equilibrium or supersaturated to calcite and dolomite and there are mixed saturation states (undersaturation and saturated) for magnesite.

Future research into the listed topics could help improve the knowledge of zone C:

- Establish defined facies zone C boundaries, by collecting additional water samples in this area and correlating the data to available core data.
- Research the high Ca^{2+}, low K^+ region surrounding P-14 and SNL-9, by collecting water samples and optimally drilling new wells in this region to better understand mineral transformations.
- Research the zone where cation exchange has occurred and the transition between wells, by collecting consistent water samples and comparing the data to available core data.
- Evaluate whether wells that have undergone cation exchange have a correlation to established Culebra flow patterns.

Information Only

Facies Zone D and E

Facies zone D is located in the far western portion of the Culebra network and has two wells in the zone, including: WIPP-27 and WIPP-29. These data were collected in 1980 and 1987, respectively, and the wells have since been abandoned. These wells are purported to be contaminated with potash mining operations (Siegal, et al. 1991) and were not considered extensively in this AR. No additional physical data can be collected from these wells because they have been plugged and abandoned.

Facies Zone E is located in the far eastern portion of the Culebra network and includes 3 wells, including SNL-6, SNL-15 and AEC-7R. Previously only SNL-6 and SNL-15 were included in zone E (Domski and Beauheim, 2008). In this study AEC-7R was added to the zone, as it has very similar chemical characteristics to the other zone E well. AEC-7R has a lower ionic strength than the other two wells in the zone, however the chemistry profile as a whole is more consistent with zone E than any other zone.

5 Conclusions

- Culebra waters are classified as Na-Cl and Ca-Mg-Cl waters based on Piper and Chadha diagrams
- The predominant hydrogeochemical processes are carbonate mineral dissolution and cation exchange
- Cation exchange processes include both reverse ion exchange and ion exchange across the Culebra network.
- Mg^{2+} primarily in the eastern region of the Culebra network are added to the waters by dissolution of accessory carnallite/polyhalite so that dolomite supersaturation increases with ionic strength
- The majority of wells in the Culebra network are at equilibrium or supersaturated to calcite and dolomite. Magnesite saturation varies across the Culebra network, and it is limited based on available reactants: CO_2 and H_20
- Gypsum dissolution zones established by Holt et al. 2005 are confirmed in geochemistry analysis of this study
- High diffusivity zones in the southern portion of the LWB established by Beauheim, 2007are confirmed through geochemistry in this study
- There is a significant cation exchange region in zone C of the Culebra network that may have significant implications for Culebra hydrologic flow patterns.

Information Only

Appendix A (Data Set #1, Raw Data)

Well ID	Sample Date	pH	Density g/cm3	TDS (mg/L)	Chg Bal Error (%)	Ca2+ (mg/L)	Mg2+ (mg/L)	Na+ (mg/L)	K+ (mg/L)	Cl- (mg/L)	SO42- (mg/L)	Br- (mg/L)	Total Alkalinity (mg/L)	HCO3- (mg/L)	CO32- (mg/L)
AEC-7R	5/10/2017	7.06	1.066	91800	1	1500	3500	21000	1400	43000	6000	130	57	57	ND
AEC-7R	6/20/2018	7.11	1.075	91900	2	1900	4300	22000	1800	49000	5900	130	72	72	ND
AEC-7R	6/12/2019	6.93	1.063	91500	2	1800	4200	25000	1800	53000	6000	140	78	78	ND
AEC-7R	6/24/2020	**7.17**	**1.065**	**95600**	**5**	**1800**	**4400**	**24000**	**1800**	**46000**	**4700**	**9**	**139**	**139**	**ND**
Average	**2017-2020**	**7.03**	**1.068**	**91733.3**	**3**	**1733.3**	**4000.0**	**22666.7**	**1667**	**48333**	**5967**	**133**	**69**	**69**	**ND**
CV		**1%**	**0%**	**0%**		**10%**	**9%**	**7%**	**11%**	**9%**	**1%**	**4%**	**13%**	**13%**	
	Notes: Historical bicarbonate values are ~47 mg/L. Historical Br values are ~165 mg/L. Based on information in Lofton, 2021 milestone, data for 2020 will be excluded. Data may have been affected by well maintenance treatment.														
H-2b2	9/7/2017	9.19	1.011	14600	7	790	140	3600	120	6200	3100	6	53	ND	46
H-2b2	9/19/2018	9.43	1.011	13100	3	790	120	3600	100	5600	3100	6	51	ND	37
H-2b2	9/5/2019	9.28	1.013	13800	5	790	120	3500	110	5700	3000	5	53	ND	48
H-2b2	No DATA for 2020														
Average	**2017-2019**	**9.30**	**1.012**	**13833**	**5**	**790**	**127**	**3567**	**110**	**5833**	**3067**	**6**	**52**	**ND**	**44**
CV		**1%**	**0%**	**4%**		**0%**	**7%**	**1%**	**7%**	**4%**	**2%**	**6%**	**2%**		**12%**
H-4bR	3/9/2017	7.82	1.018	16500	0	710	320	4400	130	5700	4400	**41**	72	72	ND
H-4bR	3/28/2018	7.81	1.016	15600	4	730	300	4200	130	6200	4500	25	70	70	ND
H-4bR	3/7/2019	7.87	1.018	15700	6	690	260	3900	130	5700	4600	20	58	58	ND
H-4bR	3/5/2020	7.73	1.018	15900	0	720	280	3900	120	5200	4000	24	56	56	ND
Average	**2017-2020**	**7.81**	**1.018**	**15925**	**3**	**713**	**290**	**4100**	**128**	**5700**	**4375**	**23**	**64**	**64**	**ND**
CV		**1%**	**0%**	**2%**		**2%**	**8%**	**5%**	**3%**	**6%**	**5%**	**9%**	**11%**	**11%**	
	Note: The 2017 value for bromide is not consistent with historical data or data from 2018-2020. It will not be used to calculate the bromide average.														
H-5b	9/7/2017	6.84	1.096	155000	2	1500	2000	57000	1100	88000	8000	41	**ND**	**ND**	ND
H-5b	9/19/2018	7.81	1.100	155000	9	1600	2100	50000	1100	97000	8500	67	49	49	ND
H-5b	8/16/2019	7.90	1.103	159000	6	1700	2000	50000	1100	93000	6500	50	51	51	ND
H-5b	No DATA for 2020														
Average	**2017-2019**	**7.52**	**1.100**	**156333**	**6**	**1600**	**2033**	**52333**	**1100**	**92667**	**7667**	**53**	**50**	**50**	**ND**
CV		**6%**	**0%**	**1%**		**5%**	**2%**	**6%**	**0%**	**4%**	**11%**	**20%**	**2%**	**2%**	

Information Only

Well ID	Sample Date	pH	Density g/cm3	TDS (mg/L)	Chg Bal Error (%)	Ca2+ (mg/L)	Mg2+ (mg/L)	Na+ (mg/L)	K+ (mg/L)	Cl- (mg/L)	SO42- (mg/L)	Br- (mg/L)	Total Alkalinity (mg/L)	HCO3- (mg/L)	CO32- (mg/L)
	NOTE: All Historical Bicarbonate data is ~40-50 mg/L and 2018-2019 data is also in the 40-50 mg/L range. Therefore the 2017 Alkalinity data will not be used to calculate the average.														
H-6bR	8/9/2017	8.75	1.037	60000	7	2400	830	16000	340	25000	3400	26	39	ND	25
H-6bR	8/8/2018	9.01	1.033	64800	0	2600	780	15000	360	28000	3100	30	42	ND	36
H-6bR	8/7/2019	8.81	1.037	63500	4	2400	730	17000	340	33000	3100	23	36	ND	25
H-6bR	9/23/2020	8.95	1.037	55600	6	2400	780	17000	370	27000	3000	29	41	ND	33
Average	**2017-2020**	**8.88**	**1.036**	**60975**	**4**	**2450**	**780**	**16250**	**353**	**28250**	**3150**	**27**	**39**	**ND**	**30**
CV		**1%**	**0%**	**6%**		**4%**	**5%**	**5%**	**4%**	**10%**	**5%**	**10%**	**5%**		**17%**
H-7b1	7/12/2017	7.45	1.005	4240	4	610	160	410	16	630	2200	ND	127	127	ND
H-7b1	7/25/2018	7.42	1.009	3640	0	570	130	230	10	350	1800	ND	108	108	ND
H-7b1	7/23/2019	7.54	1.011	1720	3	600	140	210	11	290	1800	ND	96	96	ND
H-7b1	No DATA for 2020														
Average	**2017-2019**	**7.47**	**1.008**	**3200**	**2**	**593**	**143**	**283**	**12**	**423**	**1933**	**ND**	**111**	**111**	**ND**
CV		**1%**	**0%**	**34%**		**3%**	**9%**	**32%**	**21%**	**35%**	**10%**		**12%**	**12%**	
	NOTE: Na, Cl and TDS values decreased in 2019. Historical data show values similar to the 2019 data. Since it cannot be determined which data are correct, all the data will still be used even though the CV is above 30%														
H-9bR	6/7/2017	7.87	1.002	3360	1	580	140	180	7	210	1900	ND	90	90	ND
H-9bR	5/23/2018	7.45	1.003	3440	4	570	130	190	8	220	1700	ND	91	91	ND
H-9bR	5/8/2019	7.41	1.003	3510	1	610	150	210	8	260	2000	ND	87	87	ND
H-9bR	5/28/2020	7.82	1.000	3480	0	550	130	200	7	210	1900	ND	73	73	ND
Average	**2017-2020**	**7.64**	**1.002**	**3448**	**2**	**578**	**138**	**195**	**8**	**225**	**1875**	**ND**	**85**	**85**	**ND**
CV		**3%**	**0%**	**2%**		**4%**	**6%**	**6%**	**5%**	**9%**	**6%**		**8%**	**8%**	
H-11b4R	3/9/2017	7.33	1.076	113000	4	1800	1300	37000	710.0	64000	7700	**170.0**	91.3	91.3	ND
H-11b4R	3/28/2018	7.42	1.076	114000	3	1800	1300	37000	770.0	63000	8200	45.0	89.7	89.7	ND
H-11b4R	3/7/2019	7.47	1.076	114000	1	1800	1200	34000	720.0	56000	6600	30.0	105.2	105.2	ND
H-11b4R	3/5/2020	7.42	1.077	108000	2	1800	1300	37000	720.0	57000	6700	46.0	85.2	85.2	ND
Average	**2017-2020**	**7.41**	**1.076**	**112250**	**3**	**1800**	**1275**	**36250**	**730.0**	**60000**	**7300**	**40.3**	**92.9**	**92.9**	**ND**
CV		**1%**	**0%**	**2%**		**0%**	**3%**	**4%**	**3%**	**6%**	**9%**	**18%**	**8%**	**8%**	
	NOTE: Historical data from 2012 for Bromide is 41 mg/L. Bromide data from 2017 will not be used to calcuate the average. It is not consistent with historical, or data collected 2018-2020.														

Information Only

Well ID	Sample Date	pH	Density g/cm3	TDS (mg/L)	Chg Bal Error (%)	Ca2+ (mg/L)	Mg2+ (mg/L)	Na+ (mg/L)	K+ (mg/L)	Cl- (mg/L)	SO42- (mg/L)	Br- (mg/L)	Total Alkalinity (mg/L)	HCO3- (mg/L)	CO32- (mg/L)
H-12R	5/10/2017	7.34	1.102	225000	7	1200	1100	66000	1100	118000	9400	75	47	47	ND
H-12R	5/23/2018	7.39	1.108	204000	5	1100	1100	63000	1400	110000	8300	63	47	47	ND
H-12R	5/8/2019	7.33	1.102	208000	8	1300	1300	73000	1400	97000	6300	46	46	46	ND
H-12R	5/20/2020	7.80	1.101	137000	7	1600	1600	50000	1000	92000	7800	58	77	77	ND
Average	**2017-2020**	**7.47**	**1.103**	**193500**	**7**	**1300**	**1275**	**63000**	**1225**	**104250**	**7950**	**61**	**55**	**55**	**ND**
CV		**3%**	**0%**	**17%**		**14%**	**16%**	**13%**	**15%**	**10%**	**14%**	**17%**	**24%**	**24%**	
H-17	9/7/2017	6.00	1.131	194000	1	1700	1200	68000	940	110000	6500	27	ND	ND	ND
H-17	9/19/2018	6.29	1.130	182000	3	1800	1400	71000	980	120000	7600	56	ND	ND	ND
H-17	9/5/2019	6.04	1.129	202000	5	1800	1400	69000	1000	120000	7300	40	ND	ND	ND
H-17	No DATA in 2020														
Average	**2017-2019**	**6.11**	**1.130**	**192667**	**3**	**1767**	**1333**	**69333**	**973**	**116667**	**7133**	**41**	**ND**	**ND**	**ND**
CV		**2%**	**0%**	**4%**		**3%**	**7%**	**2%**	**3%**	**4%**	**7%**	**29%**			
H-19b0	5/10/2017	8.18	1.064	97700	8	1400	950	25000	560	47000	6100	37	74	**74**	**ND**
H-19b0	5/23/2018	9.38	1.065	93200	5	1600	1000	28000	690	51000	5500	36	140	**26**	**114**
H-19b0	5/8/2019	9.01	1.064	93500	0	1700	1100	33000	710	54000	5400	29	150	**30**	**120**
H-19b0	5/20/2020	9.42	1.065	**64300**	6	1700	1100	33000	730	61000	6200	35	143	**21**	**122**
Average	**2017-2020**	**9.00**	**1.065**	**94800**	**5**	**1600**	**1038**	**29750**	**673**	**53250**	**5800**	**34**	**127**	**38**	**119**
CV		**6%**	**0%**	**14%**		**8%**	**6%**	**11%**	**10%**	**10%**	**6%**	**9%**	**24%**	**56%**	**3%**
	Notes: TDS value for 2020 was not used to calculate the average (See Lofton, 2021 report). Bicarbonate and Carbonate are very inconsistent across samplings. In this study, only the value for Total Alkalinity will be used. Bicarbonate values were determined by subtracting CO32- from the Total Alkalinity														
SNL-1	8/8/2017	7.10	1.029	36600	2	1400	590	9800	260	17000	4200	12	137	137	ND
SNL-1	8/7/2018	7.29	1.029	36800	1	1400	560	9100	260	16000	3600	19	106	106	ND
SNL-1	8/7/2019	7.48	1.008	38100	4	1400	590	11000	240	20000	3900	7	104	104	ND
SNL-1	8/26/2020	7.49	1.030	33800	3	1400	600	11000	260	17000	4200	12	126	126	ND
Average	**2017-2020**	**7.34**	**1.024**	**36325**	**3**	**1400**	**585**	**10225**	**255**	**17500**	**3975**	**12**	**118**	**118**	**ND**
CV		**2%**	**1%**	**4%**		**0%**	**3%**	**8%**	**3%**	**9%**	**6%**	**35%**	**12%**	**12%**	
	Note: Bromide values are very low, making the CV% erroneous. Bromide data will still be used. Historical value for Bromide (2016) was 12 mg/L														
SNL-2	7/11/2017	7.30	1.006	10600	2	900	270	2100	41	3700	2200	3	168	168	ND
SNL-2	7/24/2018	7.41	1.006	9490	1	870	250	2000	39	3600	2100	3	157	157	ND

Information Only

Well ID	Sample Date	pH	Density g/cm3	TDS (mg/L)	Chg Bal Error (%)	Ca2+ (mg/L)	Mg2+ (mg/L)	Na+ (mg/L)	K+ (mg/L)	Cl- (mg/L)	SO42- (mg/L)	Br- (mg/L)	Total Alkalinity (mg/L)	HCO3- (mg/L)	CO32- (mg/L)
SNL-2	7/10/2019	7.09	1.008	9540	2	930	280	2000	41	4000	2300	1	152	152	ND
SNL-2	7/22/2020	7.35	1.007	10100	5	940	270	2200	41	3700	2100	2	156	156	ND
Average	**2017-2020**	**7.29**	**1.007**	**9933**	**3**	**910**	**268**	**2075**	**41**	**3750**	**2175**	**2**	**158**	**158**	**ND**
CV		**2%**	**0%**	**5%**		**3%**	**4%**	**4%**	**2%**	**4%**	**4%**	**25%**	**4%**	**4%**	
SNL-3	9/6/2017	7.84	1.025	51500	9	1600	730	16000	380	22000	4300	18	94	94	ND
SNL-3	9/5/2018	7.49	1.026	48100	4	1400	680	13000	350	23000	5000	18	51	51	ND
SNL-3	9/25/2019	7.54	1.027	40900	4	1400	690	15000	360	22000	4800	18	46	46	ND
SNL-3	8/25/2020	7.37	1.027	44100	1	1400	720	15000	390	25000	5000	22	43	43	ND
Average	**2017-2020**	**7.56**	**1.026**	**46150**	**5**	**1450**	**705**	**14750**	**370**	**23000**	**4775**	**19**	**46**	**46**	**ND**
CV		**2%**	**0%**	**9%**		**6%**	**3%**	**7%**	**4%**	**5%**	**6%**	**9%**	**7%**	**7%**	
	NOTE: Historical Bicarbonate value in 2004 was 63, and in 2018-2020 Alkalinity was between 40-51. Alkalinity data for 2017 will not be used to calculated the average, due to inconsistency with other samplings.														
SNL-5	4/12/2017	7.42	1.010	14800	3	1700	490	2300	62	6400	1500	7	65	65	ND
SNL-5	4/25/2018	7.94	1.005	13800	3	1400	460	2100	73	5500	1600	5	50	50	ND
SNL-5	4/24/2019	7.28	1.005	15900	3	1700	460	2100	66	6800	1800	5	61	61	ND
SNL-5	5/28/2020	7.44	1.004	15800	7	1400	450	2200	68	6900	1800	7	58	58	ND
Average	**2017-2020**	**7.52**	**1.006**	**15075**	**4**	**1550**	**465**	**2175**	**67**	**6400**	**1675**	**6**	**58**	**58**	**ND**
CV		**3%**	**0%**	**6%**		**10%**	**3%**	**4%**	**0**	**0**	**0**	**0**	**0**	**0**	
SNL-8	9/6/2017	7.61	1.099	139000	4	2000	2500	48000	1600	75000	5200	92	69	69	ND
SNL-8	9/5/2018	7.65	1.104	146000	3	1800	2600	47000	1500	84000	6600	85	69	69	ND
SNL-8	9/4/2019	7.68	1.089	139000	2	1800	2700	49000	1600	87000	7300	82	71	71	ND
SNL-8	9/23/2020	7.35	1.088	136000	3	1900	2800	46000	1500	81000	5800	95	93	93	ND
Average	**2017-2020**	**7.57**	**1.095**	**140000**	**3**	**1875**	**2650**	**47500**	**1550**	**81750**	**6225**	**89**	**75**	**75**	**ND**
CV		**2%**	**1%**	**3%**		**4%**	**4%**	**2%**	**3%**	**5%**	**13%**	**6%**	**13%**	**13%**	
SNL-9	6/7/2017	7.43	1.015	29100	4	3000	820	5300	39	16000	1600	24	75	75	ND
SNL-9	6/20/2018	7.15	1.015	27300	3	2900	700	5100	46	13000	1500	58	36	36	ND
SNL-9	6/12/2019	6.96	1.016	26800	2	2800	760	5000	44	13000	1700	10	39	39	ND
SNL-9	6/24/2020	6.25	1.016	24400	6	2800	760	4700	45	12000	1200	9	28	28	ND

Information Only

Well ID	Sample Date	pH	Density g/cm3	TDS (mg/L)	Chg Bal Error (%)	Ca2+ (mg/L)	Mg2+ (mg/L)	Na+ (mg/L)	K+ (mg/L)	Cl- (mg/L)	SO42- (mg/L)	Br- (mg/L)	Total Alkalinity (mg/L)	HCO3- (mg/L)	CO32- (mg/L)
Average	**2017-2020**	**6.95**	**1.016**	**26900**	**4**	**2875**	**760**	**5025**	**44**	**13500**	**1500**	**14**	**34**	**34**	**ND**
CV		**6%**	**0%**	**6%**		**3%**	**6%**	**4%**	**6%**	**11%**	**12%**	**47%**	**14%**	**14%**	
	NOTE: Historical data has Br is ~16. Bromide data from 2018 will not be used to calculate the average, due to its inconsistency with other collected samples. Alkalinity data from 2017 will not be used to calculate the average due to its inconsistency with data from 2018-2020														
SNL-10	6/7/2017	7.98	1.008	9670	2	480	170	2100	47	1300	4600	4	106	106	ND
SNL-10	6/20/2018	7.83	1.009	8350	4	550	180	2300	54	1300	4500	2	101	101	ND
SNL-10	6/12/2019	7.73	1.009	9280	5	480	180	2100	52	1600	4700	3	95	95	ND
SNL-10	6/24/2020	7.72	1.010	8930	3	500	190	2100	56	1300	4200	2	94	94	ND
Average	**2017-2020**	**7.82**	**1.009**	**9058**	**4**	**503**	**180**	**2150**	**52**	**1375**	**4500**	**3**	**99**	**99**	**ND**
CV		**1%**	**0%**	**5%**		**6%**	**4%**	**4%**	**6%**	**9%**	**4%**	**28%**	**5%**	**5%**	
SNL-12	4/11/2017	7.66	1.011	4310	4	660	140	460	19	670	1900	1	91	91	ND
SNL-12	5/28/2018	7.90	1.013	6500	1	690	150	520	21	910	2100	1	90	90	ND
SNL-12	4/24/2019	7.68	1.008	4450	NA	670	140	510	22	810	2100	1	86	86	ND
SNL-12	5/27/2020	7.70	1.008	4550	1	620	140	530	21	770	2100	2	89	89	ND
Average	**2017-2020**	**7.74**	**1.010**	**4953**	**2**	**660**	**143**	**505**	**21**	**790**	**2050**	**1**	**89**	**89**	**ND**
CV		**1%**	**0%**	**18%**		**4%**	**3%**	**5%**	**5%**	**11%**	**4%**	**14%**	**2%**	**2%**	
SNL-13	3/8/2017	8.31	1.022	22300	2	990	310	5400	180	8100	3400	39	40	42	2.0
SNL-13	3/28/2018	8.23	1.020	19800	3	1000	370	6000	220	9000	3400	19	44	44	ND
SNL-13	3/6/2019	8.27	1.022	19700	1	980	310	5300	200	8600	3600	14	41	41	ND
SNL-13	3/5/2020	8.36	1.020	20300	0	1000	320	5600	190	8700	3900	20	40	34	5.3
Average	**2017-2020**	**8.29**	**1.021**	**20525**	**2**	**993**	**328**	**5575**	**198**	**8600**	**3575**	**18**	**41**	**40**	**ND**
CV		**1%**	**0%**	**5%**		**1%**	**8%**	**5%**	**7%**	**4%**	**6%**	**15%**	**4%**	**9%**	
	NOTE: Bromide data from 2017 will not be used due to inconsistency with 2018-2020														
SNL-14	8/9/2017	7.40	1.044	86900	3	1500	990	29000	640	43000	6200	39	58	58	ND
SNL-14	8/8/2018	7.39	1.045	85100	3	1500	990	27000	600	41000	5600	37	55	55	ND
SNL-14	9/25/2019	7.30	1.045	82200	6	1500	940	28000	600	39000	6100	30	60	60	ND
SNL-14	8/26/2020	7.44	1.043	93300	2	1500	990	29000	630	44000	6400	40	62	62	ND
Average	**2017-2020**	**7.38**	**1.044**	**86875**	**4**	**1500**	**978**	**28250**	**618**	**41750**	**6075**	**37**	**59**	**59**	**ND**
CV		**1%**	**0%**	**5%**		**0%**	**2%**	**3%**	**3%**	**5%**	**5%**	**11%**	**4%**	**4%**	

Information Only

Well ID	Sample Date	pH	Density g/cm3	TDS (mg/L)	Chg Bal Error (%)	Ca2+ (mg/L)	Mg2+ (mg/L)	Na+ (mg/L)	K+ (mg/L)	Cl- (mg/L)	SO42- (mg/L)	Br- (mg/L)	Total Alkalinity (mg/L)	HCO3- (mg/L)	CO32- (mg/L)
SNL-16	8/8/2017	7.20	1.012	24000	1	1700	500	5100	280	11000	2400	4	94	94	ND
SNL-16	9/5/2018	7.41	1.014	24100	2	1700	510	5500	280	12000	2300	3	94	94	ND
SNL-16	8/7/2019	7.43	1.015	26700	4	1800	550	5600	290	13000	2300	2	94	94	ND
SNL-16	9/23/2020	7.00	1.016	25400	0	1700	590	5800	330	12000	2400	5	89	89	ND
Average	**2017-2020**	**7.26**	**1.014**	**25050**	**2**	**1725**	**538**	**5500**	**295**	**12000**	**2350**	**3**	**93**	**93**	**ND**
CV		**2%**	**0%**	**4%**		**3%**	**7%**	**5%**	**7%**	**6%**	**2%**	**27%**	**2%**	**2%**	
SNL-17	3/8/2017	7.60	1.004	3350	2	610	150	170	6	320	1800	1	96	96	ND
SNL-17	3/28/2018	7.85	1.007	3360	1	600	140	170	7	310	1800	1	102	102	ND
SNL-17	3/6/2019	7.68	1.012	3320	2	600	150	140	6	240	1800	ND	97	97	ND
SNL-17	3/5/2020	7.62	1.012	3350	2	610	150	140	6	240	2000	ND	96	96	ND
Average	**2017-2020**	**7.69**	**1.009**	**3345**	**2**	**605**	**148**	**155**	**6**	**278**	**1850**	**ND**	**98**	**98**	**ND**
CV		**1%**	**0%**	**0%**		**1%**	**3%**	**10%**	**13%**	**14%**	**5%**		**2%**	**2%**	
SNL-18	7/12/2017	7.69	1.008	19500	1	1100	380	5500	120	9500	3100	8	61	61	ND
SNL-18	8/8/2018	7.81	1.011	14400	2	970	300	3700	82	6700	2700	7	65	65	ND
SNL-18	7/11/2019	7.75	1.009	17700	3	1100	370	4800	110	8800	3200	4	70	70	ND
SNL-18	7/23/2020	7.67	1.008	19000	5	1100	370	5200	110	8100	2700	4	70	70	ND
Average	**2017-2020**	**7.73**	**1.009**	**17650**	**3**	**1068**	**355**	**4800**	**106**	**8275**	**2925**	**6**	**66**	**66**	**ND**
CV		**1%**	**0%**	**11%**		**5%**	**9%**	**14%**	**13%**	**13%**	**8%**	**29%**	**6%**	**6%**	
SNL-19	7/11/2017	7.48	1.005	8180	0	790	210	1600	40	2800	2200	ND	98	98	ND
SNL-19	7/24/2018	7.52	1.004	8050	1	740	200	1600	37	2700	2100	2	94	94	ND
SNL-19	7/10/2019	7.46	1.004	8230	3	800	220	1600	41	3000	2400	1	93	93	ND
SNL-19	7/22/2020	6.53	1.002	7910	4	760	220	1600	34	2600	2100	2	20	20	ND
Average	**2017-2020**	**7.25**	**1.004**	**8093**	**2**	**773**	**213**	**1600**	**38**	**2775**	**2200**	**2**	**76**	**95**	**ND**
CV		**6%**	**0%**	**2%**		**3%**	**4%**	**0%**	**7%**	**5%**	**6%**	**8%**	**42%**	**2%**	
	Notes: Alkalinity data for 2020 will not be used to calculate the average. It is inconsistent with other samplings for this well. Bromide CV% is high because the Br concentrations are low. Br will still be used.														
WIPP-11	4/12/2017	8.59	1.034	54000	3	1600	660	17000	380	27000	3300	22	31	15	16
WIPP-11	4/24/2018	8.88	1.037	49400	3	1700	700	15000	360	28000	3400	17	47	5	42
WIPP-11	4/24/2019	8.79	1.034	46300	2	1700	720	16000	360	28000	4200	18	46	12	34

Information Only

Well ID	Sample Date	pH	Density g/cm3	TDS (mg/L)	Chg Bal Error (%)	Ca2+ (mg/L)	Mg2+ (mg/L)	Na+ (mg/L)	K+ (mg/L)	Cl- (mg/L)	SO42- (mg/L)	Br- (mg/L)	Total Alkalinity (mg/L)	HCO3- (mg/L)	CO32- (mg/L)
WIPP-11	5/28/2020	7.44	1.029	48500	1	1700	790	16000	350	28000	4200	25	63	63	0
Average	**2017-2020**	**8.43**	**1.034**	**49550**	**2**	**1675**	**718**	**16000**	**363**	**27750**	**3775**	**21**	**47**	**24**	**23**
CV		**7%**	**0%**	**6%**		**3%**	**7%**	**4%**	**3%**	**2%**	**11%**	**16%**	**24%**	**96%**	**70%**
	NOTE: Bicarbonate and Carbonate values are very inconsistent across samplings. Only Total alkalinity values will be used in this study. Bicarbonate value was calculated by subtracting the CO3- from the Total Alkalinity														
WIPP-13	5/10/2017	8.04	1.034	65400	12	1300	930	15000	590	33000	4500	34	32	32	ND
WIPP-13	5/23/2018	8.22	1.032	68300	12	1400	990	18000	690	33000	4400	35	33	33	ND
WIPP-13	5/8/2019	7.26	1.033	68800	3	1400	1100	21000	640	37000	4900	26	39	39	ND
WIPP-13	5/20/2020	7.43	1.032	102000	0	1500	1100	22000	710	37000	5000	31	30	30	ND
Average	**2017-2020**	**7.74**	**1.033**	**76125**	**7**	**1400**	**1030**	**19000**	**658**	**35000**	**4700**	**32**	**34**	**34**	**ND**
CV		**5%**	**0%**	**20%**		**5%**	**7%**	**14%**	**7%**	**6%**	**5%**	**11%**	**10%**	**10%**	
WIPP-19	6/7/2017	9.13	1.053	75000	2	1600	1000	25000	590	42000	5900	49	126	7	119
WIPP-19	6/20/2018	9.25	1.057	74700	3	1600	850	24000	550	36000	5400	31	125	18	106
WIPP-19	6/12/2019	8.96	1.059	76300	1	1500	890	26000	550	42000	5800	31	134	31	103
WIPP-19	No DATA for 2020														
Average	**2017-2019**	**9.11**	**1.056**	**75333**	**2**	**1567**	**913**	**25000**	**563**	**40000**	**5700**	**37**	**128**	**19**	**109**
CV		**1%**	**0%**	**1%**		**3%**	**7%**	**3%**	**3%**	**7%**	**4%**	**23%**	**3%**	**52%**	**6%**
	NOTE: Bicarbonate and Carbonate values are very inconsistent across samplings. Only Total alkalinity values will be used in this study. Bicarbonate value was calculated by subtracting the CO3- from the Total Alkalinity														

Data excluded from Average NEW Domski

Notes:

- Some wells in this study were plugged and abandoned between 2019 and 2020, and therefore no data are available for 2020.
- All data and References are summarized at file path: CVS/CVSLIB/WIPP EXTERNAL/ap194

Information Only

Appendix B (Data Set #2)

Well ID	Sample Date	pH	TDS (mg/L)	Chg Bal Error (%)	Ca2+ (mg/L)	Mg2+ (mg/L)	Na+ (mg/L)	K+ (mg/L)	Cl- (mg/L)	SO42- (mg/L)	Br- (mg/L)	ALKALINITY Total (mg/L)	Bicarbonate (HCO3-) (mg/L)	Carbonate (CO32-) (mg/L)
AEC-7R	7/15/2014	7.38	96300	7	1900	4330	23000	1800	56000	6400	170	46	46	>2
AEC-7R	3/11/2015	7.41	82500		1900	4700	22000	1900	58000	6600	160	49	49	>2
Average	**2014-2015**	**7.40**	**89400**		**1900**	**4515**	**22500**	**1850**	**57000**	**6500**	**165**	**48**	**48**	
CV	**2014-2015**	**0%**	**8%**		**0%**	**4%**	**2%**	**3%**	**2%**	**2%**	**3%**	**3%**	**3%**	
AIS	10/28/1988	7.94			1000	510	12600	400	20500	5900	22	98	98	0
C-2737c	3/1/2018	9.03	9120	1	790	190	2200	26	3900	1800	4.8	21.64		16
ENGLE	3/5/1985			1	590	152	200	5.6	231	1990	0.27	110	110	0
ENGLE	1/31/1990	7.10			588	150	220	7.6	190	1900		110	110	0
Average	**1985-1990**	**7.10**			**590**	**151**	**210**	**7**	**211**	**1945**		**110**	**110**	
CV	**1985-1990**	**0%**			**0%**	**1%**	**5%**	**15%**	**10%**	**2%**		**0%**	**0%**	
H-2c	12/13/1989	6.65	10500		720	150	2700	110	3700	3200	6	56	56	0
H-2c	7/25/1990	7.44	9300			160	2000	100	2700	2900	12	60	60	0
H-2c	8/14/1991	7.93	9410		772	165	2590	105	3330	2320	6.1	59.8		0
H-2c	6/28/1993	7.26	9300			187	1800	87	3070	2570	9.39	44	44	0
H-2c	6/21/1994	7.63	11100		759	241	2210	112	3220	3060	10.8	48.3	48.3	0
Average	**1989-1994**	**7.38**	**9922**		**750**	**181**	**2260**	**103**	**3204**	**2810**	**9**	**54**	**52**	
CV	**1989-1994**	**6%**	**7%**		**3%**	**18%**	**15%**	**9%**	**10%**	**11%**	**28%**	**12%**	**12%**	
H-3b3	6/11/1984	7.40		<1.4	1550	829	17400	495	29500	5130	29	52	52	0
H-3b3	5/5/1986	7.42			1500	780	17000	360	31000	4600	39	52	52	0
H-3b3	8/24/1987	6.73			1300	830	17000	450	28000	4800	28	47	47	0
H-3b3	3/2/1989	7.33			1500	750	17000	500	27700	4300	25	51	51	0
H-3b3	8/15/1990	7.16				700	16000	450	27000	4700	27	49	49	0
H-3b3	7/19/1994	7.74	55000			773	16700	412	31100	5080	27.1	39.6	39.6	0
H-3b3	5/23/1995	7.44	55600			690	15200	366	29200	5420	26.5	43.3	43.3	0

Information Only

Well ID	Sample Date	pH	TDS (mg/L)	Chg Bal Error (%)	Ca2+ (mg/L)	Mg2+ (mg/L)	Na+ (mg/L)	K+ (mg/L)	Cl- (mg/L)	SO42- (mg/L)	Br- (mg/L)	ALKALINITY Total (mg/L)	Bicarbonate (HCO3-) (mg/L)	Carbonate (CO32-) (mg/L)
Average	**1984-1995**	**7.32**	**55300**		**1463**	**765**	**16614**	**433**	**29071**	**4861**	**29**	**48**	**48**	
CV	**1984-1995**	**4%**	**1%**		**7%**	**7%**	**4%**	**12%**	**5%**	**7%**	**15%**	**9%**	**9%**	
H-4b	9/25/1987	6.14			*640*	430	6300	240	7500	5100	42	58	58	
H-4b	4/6/1989	7.46			*730*	400	5500	220	7600	5000		66	66	0
H-4b	9/17/1992	7.55	21400		688	438	5990	198	8370	5810	43.4	51.8	51.8	0
H-4b	9/13/1993	7.39	21200			337	5230	172	7350	6280	39.3	49.4	49.4	0
H-4b	11/8/1994	7.30	18900			453	5880	199	9150	5630	38.9	48	48	0
Average	**1987-1994**	**7.17**	**20500**		**686**	**412**	**5780**	**206**	**7994**	**5564**	**41**	**55**	**55**	
CV	**1987-1994**	**7%**	**6%**		**5%**	**9%**	**6%**	**12%**	**7%**	**8%**	**5%**	**14%**	**14%**	
H-5b	6/1/1981	*7.90*	154400	<2.1	*1710*	2140	52400	1290	89500	7360	*62.5*			
H-5b	8/26/1985	7.50		1.5	*1700*	2170	54100	1350	85400	7840	*48.6*	41	41	
H-5b	5/21/1986	6.84			*1400*	2200	53000	1100	89000	7000	59	46	46	
H-5b	2/24/1988	7.03			*1500*	1800	52000	1340	84100	7000	73	42	42	
H-5b	5/2/1990	8.33				1800	55200	1200	92100	7900	69	41	41	
H-5b	5/24/1993	7.08	150000			1710	42400	904	84000	9170	69.1	30.9	30.9	
H-5b	4/26/1994	7.07	156000			2060	47300	1190	85700	9160	70.3	31.1	31.1	
H-5bR	10/20/2021	7.58	153000		1600	1900	50000	1000	76000	6400	ND	57.2	57.2	
Average	**1981-2021**	**7.42**	**153350**		**1582**	**1973**	**50800**	**1172**	**85725**	**7729**	**65**	**41**	**41**	
CV	**1981-2021**	**6%**	**1%**		**8%**	**9%**	**8%**	**13%**	**5%**	**12%**	**12%**	**20%**	**20%**	
H-6b	12/20/1978	7.30	*52500*		*1200*	970	18000	500	28000	3800		85	85	
H-6b	7/28/1986	7.06			*1800*	970	17000	350	33000	3300	35	100	100	
H-6b	7/24/1989	6.70			*2100*	940	14600	350	31600	3100	35	91	91	
H-6b	2/12/1990	6.90				1000	15000	600	28000	3400	23	93	93	
H-6b	3/29/1994	6.98	62500		2460	1100	20100	479	35400	*3415*	24	75.9	75.9	
H-6bR	12/10/2008	7.73	54000		*2000*	950	17000	350	32000	4000	36	77	77	
Average	**1978-2008**	**7.11**	**56333**		**1912**	**988**	**16950**	**438**	**31333**	**3503**	**31**	**87**	**87**	

Information Only

Well ID	Sample Date	pH	TDS (mg/L)	Chg Bal Error (%)	Ca2+ (mg/L)	Mg2+ (mg/L)	Na+ (mg/L)	K+ (mg/L)	Cl- (mg/L)	SO42- (mg/L)	Br- (mg/L)	ALKALINITY Total (mg/L)	Bicarbonate (HCO3-) (mg/L)	Carbonate (CO32-) (mg/L)
CV	**1978-2008**	**5%**	**8%**		**22%**	**5%**	**11%**	**22%**	**8%**	**9%**	**19%**	**10%**	**10%**	
H-7b1	3/26/1986	*7.20*		0.4	*587*	130	207	7	320	1850	*0.57*	120	120	
H-7b1	2/25/1987	7.38			580	140	*160*	*7.7*	310	1700	2	130	130	
H-7b1	4/25/1988	6.95			*570*	130	200	8.2	290	2000	2	120	120	
H-7b1	5/19/1989	7.00			*650*	130	170	7.2	250	1700	3	110	110	
H-7b1	11/9/1990	7.14			*670*	140	100		280	2100		92	92	
Average	**1986-1990**	**7.13**			**611**	**134**	**167**	**8**	**290**	**1870**	**2**		**114**	
CV	**1986-1990**	**2%**			**7%**	**4%**	**23%**	**6%**	**8%**	**9%**	**46%**		**11%**	
H-8b	1/22/1986	7.90			540	170	51	3.7	*33*	1700	1	94	94	
H-8b	2/11/1987	7.45			*560*	160	55	4	36	1700	2	96	96	
H-8b	6/8/1988	7.15			*610*	170	55	4.4	33	1900	2	95	95	
Average	**1986-1988**	**7.50**			**570**	**167**	**54**	**4**	**34**	**1767**	**2**	**95**	**95**	
CV	**1986-1988**	**4%**			**5%**	**3%**	**4%**	**7%**	**4%**	**5%**	**28%**	**1%**	**1%**	
H-9b	2/5/1980	7.30	3590			150	210		320	2000		90	90	
H-9b	11/14/1985	7.50			560	140	150	7.7	200	1600	1	120	120	
H-9b	1/28/1987	7.44			*630*	150	150	7	190	1700	1	120	120	
H-9b	6/21/1988	7.03			*690*	140	140	8.2	180	1600	2	120	120	
H-9b	1/19/1990	7.41				160	100	8.3	160	1800	2	120	120	
H-9b	9/27/1994	7.16	2800		634	144	130	6.49	173	2060	2	92.8	92.8	
H-9bR	6/28/2011	7.98	3330		590	150	140	6.9	170	2000		100	100	<2
H-9bR	8/7/2012	7.60	3350		620	140	130	8.3	160	1900	*ND*	94	94	<2
H-9bR	8/20/2012	7.68	3380		610	140	150	7.4	180	2000	*ND*	94	94	<2
Average	**1980-2012**	**7.46**	**3290**		**619**	**146**	**144**	**8**	**193**	**1851**	**2**	**106**	**106**	
CV	**1980-2012**	**4%**	**8%**		**6%**	**5%**	**19%**	**9%**	**24%**	**9%**	**NA**	**12%**	**12%**	
H-10cR	7/26/2017	7.50	146000	9	1600	2200	35000	960	72000	7100	58	65.44	65.44	<2
H-10cR	7/27/2017	7.48	146000	6	1500	2100	48000	930	69000	7000	60	63.64	63.64	<2

Information Only

Well ID	Sample Date	pH	TDS (mg/L)	Chg Bal Error (%)	Ca2+ (mg/L)	Mg2+ (mg/L)	Na+ (mg/L)	K+ (mg/L)	Cl- (mg/L)	SO42- (mg/L)	Br- (mg/L)	ALKALINITY Total (mg/L)	Bicarbonate (HCO3-) (mg/L)	Carbonate (CO32-) (mg/L)
Average	**7/27/2017**	**7.49**	**146000**		**1550**	**2150**	**41500**	**945**	**70500**	**7050**		**65**	**65**	
CV	**7/27/2017**	**0%**	**0%**		**3%**	**2%**	**16%**	**2%**	**2%**	**1%**		**1%**	**1%**	
H-11b3	6/3/1985			0.9	1700	1320	40400	943	65900	7180	47			
H-11b3	6/4/1986	7.18	121000			1100	38000	720	65000	6100	48	52	52	0
H-11b3	9/15/1987	6.87	120000		*1370*	1080	44000	980	63000	6200	52	52	52	0
H-11b3	10/25/1989	7.07	116000		*1500*	1200	35000	780	73400	6200	21	54	54	0
H-11b3	10/17/1990	7.06	113000			1100	40000	680	56000	7400	51	44	44	0
H-11b3	10/6/1992	7.39				1170	35400	728	61200	6980	46.5	46	46	0
H-11b3	8/30/1994	7.24	118000		1670	1270	39600	803	65500	7130	45.3	47.4	47.4	0
Average	**1985-1994**	**7.14**	**117600**		**1560**	**1177**	**38914**	**805**	**64286**	**6741**	**44**	**49**	**49**	
CV	**1985-1994**	**2%**	**2%**		**9%**	**7%**	**7%**	**13%**	**7%**	**7%**	**22%**	**8%**	**8%**	
H-11b4R	6/14/2012	7.24	112000		1800	1500	42000	940	65000	8400	41	42	42	<2
H-12R	4/22/2015	7.59	151000		1600	1700	51000	1100	94000	7700	99	61.8	61.8	<2
H-14	5/26/1987	7.50			1800	530	3300	250	8200	1500	14	40	40	
H-14	1/27/1988	6.54			1700	500	3300	240	7900	1900	11	39	39	0
H-14	2/14/1989	7.48			2000	570	3800	250	9000	1900	15	37	37	0
H-14	8/28/1991	7.60	21800		2110	612	2460	239	9740	1920	15	*40*	40	
H-14	8/27/1992	7.58	19300		1630	535	3830	242	9850	1660	13	30.1	30.1	
H-14	8/30/1993	7.54	18200		1640	512	2930	209	9050	2060	13	28.2	28.2	
H-14	6/19/1995	7.59	18200		1770	527	3200	217	10000	2110	10	29.9	29.9	
Average	**1987-1995**	**7.40**	**19375**		**1807**	**541**	**3260**	**235**	**9106**	**1864**	**13**	**35**	**35**	
CV	**1987-1995**	**5%**	**8%**		**9%**	**7%**	**14%**	**6%**	**8%**	**11%**	**14%**	**14%**	**14%**	
H-15R	1/22/2009	7.53	200000		1800	2100	66000	1200	110000	6400	61	63	63	<2
H-17	10/27/1987	6.64	ND		1500	1700	54700	1400	87300	7000	75	43	43	0
H-18	4/7/1988	7.16			1100	480	8000	220	12500	3800	14	50	50	
H-18	4/10/1990	7.59			1200	520	8000	300	14600	5200	13	56	56	

Information Only

Well ID	Sample Date	pH	TDS (mg/L)	Chg Bal Error (%)	Ca2+ (mg/L)	Mg2+ (mg/L)	Na+ (mg/L)	K+ (mg/L)	Cl- (mg/L)	SO42- (mg/L)	Br- (mg/L)	ALKALINITY Total (mg/L)	Bicarbonate (HCO3-) (mg/L)	Carbonate (CO32-) (mg/L)
H-18	4/4/1995	7.66			1190	515	7480	194	14600	4030	13	55	55	
Average	**1988-1995**	**7.47**			**1163**	**505**	**7827**	**238**	**13900**	**4343**	**13**	**54**	**54**	
CV	**1988-1995**	**3%**			**4%**	**4%**	**3%**	**19%**	**7%**	**14%**	**4%**	**5%**	**5%**	
H-19b0	8/31/2006	7.42	90000		1600	1100	27000	680	47000	4800	50	46	46	<2
IMC-461	8/4/2006	6.80	9900		1000	250	1800	30	3900	2300	<5	100	100	
Mobley	4/14/1988	7.10			620	140	280	10	430	2100	5	140	140	
P-14	2/27/1986	7.01			3900	760	3700	44	14000	1700	24	100	100	
P-14	6/18/1987	6.75			*3500*	910	4100	50	15000	1400	17	100	100	
P-14	3/16/1988	6.68			3400	880	4600	48	14300	1600	16	100	100	
Average	**1986-1988**	**6.81**			**3600**	**850**	**4133**	**47**	**14433**	**1567**	**19**	**100**	**100**	
CV	**1986-1988**	**2%**			**6%**	**8%**	**9%**	**5%**	**3%**	**8%**	**19%**	**0%**	**0%**	
P-17	3/17/1986	7.02			1700	1600	29000	800	51000	6400	97	54	54	
P-17	10/21/1987	6.22			1600	1800	29000	930	47000	5500	84	54	54	
Average	**1986-1987**	**6.62**			**1650**	**1700**	**29000**	**865**	**49000**	**5950**	**91**	**54**	**54**	
CV	**1986-1987**	**6%**			**3%**	**6%**	**0%**	**8%**	**4%**	**8%**	**7%**	**0%**	**0%**	
SNL-1	5/29/2004	7.22	36000		1400	730	10000	340	19000	3700	17	76	76	<2
SNL-1	6/15/2016	7.31	37644	1	1600	734	10050	351	18112	3599	12	144	144	<2
Average	**2004-2016**	**7.27**	**36822**		**1500**	**732**	**10025**	**346**	**18556**	**3650**	**14**	**110**	**110**	
CV	**2004-2016**	**1%**	**2%**		**7%**	**0%**	**0%**	**2%**	**2%**	**1%**	**19%**	**31%**	**31%**	
SNL-2	1/17/2004	7.52	11000		930	230	2600	46	4800	2400	3.1	90	90	<4
SNL-3	4/16/2004	7.41	47000		1400	740	14000	360	26000	4700	32	63	63	<2
SNL-5	7/24/2004	7.46	13000		1400	510	1900	67	7000	1700	17	64	64	<2
SNL-6	1/16/2008	6.17	320000		5500	22000	97000	4800	220000	1800	5100	170	170	<2
SNL-8	8/2/2007	7.26	140000		2000	3100	47000	1500	77000	6400	100	49	49	<2
SNL-9	11/19/2004	6.89	25000		3100	810	4700	44	14000	1600	16	140	140	<4
SNL-10	11/3/2006	7.92	8500		500	170	1900	72	1100	4400	2.3	46	46	<2

Information Only

Well ID	Sample Date	pH	TDS (mg/L)	Chg Bal Error (%)	Ca2+ (mg/L)	Mg2+ (mg/L)	Na+ (mg/L)	K+ (mg/L)	Cl- (mg/L)	SO42- (mg/L)	Br- (mg/L)	ALKALINITY Total (mg/L)	Bicarbonate (HCO3-) (mg/L)	Carbonate (CO32-) (mg/L)
SNL-12	8/14/2004	7.90	4200		610	120	440	15	740	1900	1.7	92	92	<4
SNL-13	7/17/2006	8.49	21000		990	330	5200	190	8500	3300	31	50	50	<2
SNL-14	8/26/2005	7.33	83000		1400	980	34000	590	42000	5600		45	45	<2
SNL-14	7/30/2007	7.37	86000		1310	915	25100	538	46000	6900	40.6	48	48	<2
SNL-14	8/21/2007	7.41	87000		1500	1100	30000	620	47000	6900	40	48	48	<2
Average	**2005-2007**	**7.37**	**85333**		**1403**	**998**	**29700**	**583**	**45000**	**6467**	**40**	**47**	**47**	
CV	**2005-2007**	**0%**	**2%**		**6%**	**8%**	**12%**	**6%**	**5%**	**9%**	**1%**	**3%**	**3%**	
SNL-15	3/30/2007	6.64	280000		4800	12000	90000	6800	180000	1600	1100	200	200	<2
SNL-16	6/9/2006	7.19	18000		1400	430	4400	290	8600	2500	<5	97	97	<2
SNL-16	11/9/2015	7.27	24200		1700	530	5300	300	11000	2400	2.9	96.4	96.4	<2
SNL-16	6/15/2016	7	23353	1	1399	590	4703	473	10263	2306	5	94	94	<2
Average	**2006-2016**	**7.26**	**21851**		**1500**	**517**	**4801**	**354**	**9954**	**2402**	**4**	**96**	**96**	
CV	**2006-2016**	**1%**	**13%**		**9%**	**13%**	**8%**	**24%**	**10%**	**3%**	**22%**	**2%**	**2%**	
SNL-17	9/15/2006	7.55	3200		620	150	130	5.3	250	1800	<1	94	94	<2
SNL-17	3/8/2017	7.52	3340		603	144	174	6.64	277	1870	0.62	104	104	<1
Average	**2006-2017**	**7.54**	**3270**		**612**	**147**	**152**	**6**	**264**	**1835**	**1**	**99**	**99**	
CV	**2006-2017**	**0%**	**2%**		**1%**	**2%**	**14%**	**11%**	**5%**	**2%**	**0%**	**5%**	**5%**	
SNL-18	8/18/2006	7.51	19000		1100	360	5200	120	8700	3700	5.6	75	75	<2
SNL-19	7/28/2006	7.74	8100		850	220	1600	43	2700	2300	1.6	90	90	<2
SNL-19	6/14/2016	8	8933	1	820	245	1591	77	2680	2194	3	94	94	<2
Average	**2006-2016**	**7.69**	**8517**		**835**	**232**	**1596**	**60**	**2690**	**2247**	**2**	**92**	**92**	
CV	**2006-2016**	**1%**	**5%**		**2%**	**5%**	**0%**	**28%**	**0%**	**2%**	**24%**	**2%**	**2%**	
USGS-4	7/19/2006	6.80	4300		530	120	540	15	1100	1800	<2.5	35	35	<2
USGS-4	7/30/2008	6.36	4100		*600*	120	650	15	1100	1400	<1	31	31	<2
Average	**2006-2008**	**6.58**	**4200**		**565**	**120**	**595**	**15**	**1100**	**1600**		**33**	**33**	
CV	**2006-2008**	**3%**	**2%**		**6%**	**0%**	**9%**	**0%**	**0%**	**13%**		**6%**	**6%**	

Information Only

Well ID	Sample Date	pH	TDS (mg/L)	Chg Bal Error (%)	Ca2+ (mg/L)	Mg2+ (mg/L)	Na+ (mg/L)	K+ (mg/L)	Cl- (mg/L)	SO42- (mg/L)	Br- (mg/L)	ALKALINITY Total (mg/L)	Bicarbonate (HCO3-) (mg/L)	Carbonate (CO32-) (mg/L)
USGS-8	7/30/2008	7.75	4400		570	97	810	16	1000	1800		35	35	<2
WIPP-11	12/15/2004	7.47	50000		*1800*	890	16000	370	28000	4200	23	56	56	<2
WIPP-11	2/20/2005	7.03	49000		1600	810	15000	360	26000	6300	37	78	78	<4
WIPP-11R	9/16/2021	*7.28*	54000		1700	790	16000	360	25000	3800	24	62	62	
Average	**2004-2021**	**7.26**	**51000**		**1700**	**830**	**15667**	**363**	**26333**	**4767**	28	**65**	**65**	
CV	**2004-2021**	**2%**	**4%**		**5%**	**5%**	**3%**	**1%**	**5%**	**23%**	**23%**	**14%**	**14%**	
WIPP-13	2/16/1987	6.74			1450	1010	19000	340	36000	4500	39	120	120	0
WIPP-19	10/18/1989	7.27			*1700*	1400	23000	600	38400	5600	21	54	54	
WIPP-19	6/13/1990	7.24				1000	31000	600	37900	5000	49	56	56	
WIPP-19	7/31/1991	7.29	76020		*1640*	1120	24100	707	52600	6610	47.7	*61.2*		
WIPP-19	6/29/1992	7.19	66000			944	22800	528	39700	5790	42.8	44.6	44.6	
WIPP-19	5/11/1993	6.98	75600			933	23200	520	42400	5830	41.2	45.3	45.3	
WIPP-19	5/24/1994	7.32	76200			1330	32800	669	40900	6600	45	44.4	44.4	
WIPP-19	5/2/1995	7.60	65600		1440	899	23200	485	34500	6580	48	*43.3*	45.3	
Average	**1989-1995**	**7.27**	**71884**		**1593**	**1089**	**25729**	**587**	**40914**	**6001**	**42**	**50**	**48**	
CV	**1989-1995**	**2%**	**7%**		**7%**	**17%**	**15%**	**13%**	**13%**	**10%**	**21%**	**13%**	**10%**	
WIPP-25	9/23/2004	7.55	28000		1800	660	8000	720	14000	2600	<5	100	100	<4
WIPP-26	4/14/1988	6.87			1200	330	2600	189	5500	2500		110	110	
WIPP-27	9/3/1980	6.25			3210	1920	39400	8010	79000	3800		126	126	
WIPP-28	9/11/1980	6.5			1150	550	15200	490	24800	4460		373	373	
WIPP-29	3/11/1987	6.28			600	5900	*89000*	*20000*	*200000*	17000	54	180	180	
WIPP-30	5/5/2005	8.01	38000		1140	320	13000	170	18000	3900	12	44	44	<4

Data excluded from Average NEW Domski

Notes:

- Where a specific Sample Date is not available, the year is provided instead.
- All data and References are summarized at file path: CVS/CVSLIB/WIPP EXTERNAL/ap194

Information Only

Appendix C (Data Set #3)

Well ID	Sample Date	ALKALINITY Total (mg/L)	Br	Percent Error	Cl (mg/L)	Mg (mg/L)	pH	K (mg/L)	Na (mg/L)	SO4 (mg/L)	Ca (mg/L)	Bicarbonate (HCO3-) (mg/L)	Carbonate (CO32-) (mg/L)
WQSP-1	8/17/1995	46.5	44.9	2	34500	1110	7.09	497	20100	5230	1700		
WQSP-1	4/11/1996	53	35.6	4	33000	1050	7.29	476	18500	5480	1710		
WQSP-1	7/25/1996	50	39	8	37200	1020	7.24	471	18900	4920	1740		
WQSP-1	4/24/1997	51	40.6	4	34200	928	7.42	443	17700	4760	1410		
WQSP-1	7/24/1997	50	44.4	5	35700	1180	7.295	499	19400	4260	1720		
WQSP-1	3/5/1998				37600	1160		467	19800	4400	1610		
WQSP-1	7/15/1998	50	42	6	34000	1140		710	17550	4900	1710		
WQSP-1	3/3/1999	55	42	1	33000	993	7.2	661	19700	4600	1770		
WQSP-1	9/1/1999	46	42	10	40000	1100	7.2	700		5000	1710		
WQSP-1	3/2/2000	49	29	3	36000	1112	7.1	442	16446	4800	1800		
WQSP-1	9/7/2000	50	44	6	36000	1200	7.3	717	19000	4800	1760		
WQSP-1	3/1/2001	51	33	6	37000	1255	7.1	767	19170	4900	1854		
WQSP-1	9/6/2001	50	26.8	2	35900	1262	7.31	896	18450	4730	1828		
WQSP-1	3/6/2002	50	35.6	11	36600	1240	7.1	695	18400	4270	1630		
WQSP-1	2003	52			35100	1170	6.8	539	19600	4910	1730		
WQSP-1	2004	54			36400	978	7.18	606	16900	4460	1600		
WQSP-1	2005	52			38800	1150	7.07	934	19100	4840	1700		
WQSP-1	2006	50			38500	1230	7.56	1050	17500	4780	1780		
WQSP-1	2007	72			44000	1220	6.97	588	24700	5340	1890		
WQSP-1	2008	50			37000	1220	6.87	767	23500	5470	1890		
WQSP-1	2009	46.3			40000	1020	7.26	470	19800	4940	1490		
WQSP-1	2010	48.7			40400	1220	7.19	530	20500	5030	1870		
WQSP-1	2011	51.3			41000	1120	7.17	498	20100	4570	1710		
WQSP-1	2012	51			37500	1190	7.16	528	22000	5130	1820		
WQSP-1	2013				36200	1130	7.05	515			1850		

Information Only

Well ID	Sample Date	ALKALINITY Total (mg/L)	Br	Percent Error	Cl (mg/L)	Mg (mg/L)	pH	K (mg/L)	Na (mg/L)	SO4 (mg/L)	Ca (mg/L)	Bicarbonate (HCO3-) (mg/L)	Carbonate (CO32-) (mg/L)
WQSP-1	2014				37200	1140	7.19	508			1790		
WQSP-1	2015				41400	1180	7.12	534			1820		
WQSP-1	2016				30700	1110	7.2	575			1720		
WQSP-1	2017	50			39800	1130	7.10	480	21200	4700	1760	50	
WQSP-1	2018	52			39000	1130	7.18	531	24000	4700	1700	52	
WQSP-1	2019	51			36800	1130	7.18	481	19400	4380	1740	51	
WQSP-1	2020	50			36600	1120	7.27	500	21000	4140	1660	50	
Ave.	**1995-2020**	**51**	**38**		**37097**	**1136**	**7**	**596**	**19719**	**4801**	**1734**	**51**	
CV		**9%**	**15%**		**7%**	**7%**	**2%**	**25%**	**10%**	**7%**	**6%**	**2%**	
WQSP-2	8/17/1995	52.5	33.3	10	38500	1110	7.33	497	20100	5540	1460		
WQSP-2	4/11/1996	48	30	7	34200	1050	7.12	476	18500	5610	1480		
WQSP-2	7/25/1996	48	37	7	36000	1020	7.34	471	18900	5700	1440		
WQSP-2	4/24/1997	50	61.3	5	33000	928	7.415	443	17700	6360	1320		
WQSP-2	7/24/1997	46	38.8	0	32500	1180	7.225	499	19400	4990	1540		
WQSP-2	3/5/1998	43	36.2	2	35500	1160	7.3	467	19800	5280	1540		
WQSP-2	7/15/1998	46	42	19	37000	1140	7.3	710	17550	5400	1380		
WQSP-2	3/3/1999	47	32	2	34000	993	7.3	661	19700	5000	1510		
WQSP-2	9/1/1999			0	36000	1100	7.3	700			1509		
WQSP-2	3/15/2000	44	28	14	37000	1033	7.1	333	15374	6000	1619		
WQSP-2	9/20/2000	51	48	1	37000	982	7.3	815	19800	5600	1460		
WQSP-2	3/14/2001	48	42	1	35000	1199	7.2	706	19790	5200	1651		
WQSP-2	9/19/2001	46	55.8	0	34900	1175	7.2	841	20910	5160	1689		
WQSP-2	3/20/2002	48		11	34500	1093	7.2	759	20240	5570	1662		
WQSP-2	2003	44			39000	1130	7.1	455	17100	6570	1350		
WQSP-2	2004	48			34400	1010	7.3	610	17100	5370	1500		
WQSP-2	2005	46			39800	1110	7.28	944	19200	5920	1580		
WQSP-2	2006	52			37500	1060	7.42	992	17000	6300	1520		
WQSP-2	2007	46			37300	1100	7.17	513	22200	6140	1650		

Information Only

Well ID	Sample Date	ALKALINITY Total (mg/L)	Br	Percent Error	Cl (mg/L)	Mg (mg/L)	pH	K (mg/L)	Na (mg/L)	SO4 (mg/L)	Ca (mg/L)	Bicarbonate (HCO3-) (mg/L)	Carbonate (CO32-) (mg/L)
WQSP-2	2008	46			34200	1080	7.04	701	24500	5810	1590		
WQSP-2	2009	46.3			40000	1020	7.26	470	19800	4940	1490		
WQSP-2	2010	45.3			38200	1050	7.26	498	21700	5710	1500		
WQSP-2	2011	47.8			35000	1110	7.24	484	21500	5760	1690		
WQSP-2	2012	47.8			33000	1110	7.29	499	21900	5560	1670		
WQSP-2	2013				36100	1020	7.18	463			1400		
WQSP-2	2014				34400	1060	7.23	496			1600		
WQSP-2	2015				38200	1030	7.19	528			1550		
WQSP-2	2016				33800	998	7.23	546			1520		
WQSP-2	2017	48			33900	1080	7.20	460	21600	5140	1640	48	
WQSP-2	2018	49			29000	1040	7.22	514	22800	5560	1530	49	
WQSP-2	2019	47			37800	950	7.21	454	19700	5370	1590	47	
WQSP-2	2020	48			34500	1020	7.24	481	21000	5250	1450	48	
Ave.	**1995-2020**	**47**	**40**		**35663**	**1067**	**7**	**578**	**19810**	**5586**	**1534**	**48**	
CV		**5%**	**24%**		**7%**	**6%**	**1%**	**27%**	**10%**	**8%**	**6%**	**1%**	
WQSP-3	9/19/1995	44	100	3	130000	2210	7.12	1380	79100	6710	1420		
WQSP-3	5/9/1996	35	81	9	144000	2000	6.81	1710	74200	6760	1480		
WQSP-3	8/22/1996	36	70.1	5	129000	1960	6.86	1360	76700	7650	1300		
WQSP-3	5/22/1997	33	127	6	128000	1890	6.845	1370	71200	7230	1100		
WQSP-3	8/21/1997	32	93	1	121000	1910	6.745	1530	75700	7400	1210		
WQSP-3	4/22/1998	33	78.8	1	125000	2340	6.9	1460	74900	6770	1380		
WQSP-3	8/26/1998	31	82	9	120000	2100	6.8	1300	58000	7400	1200		
WQSP-3	4/8/1999	31		27	120000	2070	6.9	2140	146800	7300	1400		
WQSP-3	10/6/1999	36	76	11	140000	2290	6.9	2870	66600	7500	1500		
WQSP-3	3/23/2000	55	110	1	123000	2110	7.1	2700	75200	7500	1390		
WQSP-3	10/5/2000	35	120	1	130000	2120	6.9	2880	77900	7000	1410		
WQSP-3	3/29/2001	34	80	7	130000	2120	6.6	2180	68300	7200	1310		
WQSP-3	10/4/2001	32	127	1	131000	2455	6.77	3035	81600	7460	1537		

Information Only

Well ID	Sample Date	ALKALINITY Total (mg/L)	Br	Percent Error	Cl (mg/L)	Mg (mg/L)	pH	K (mg/L)	Na (mg/L)	SO4 (mg/L)	Ca (mg/L)	Bicarbonate (HCO3-) (mg/L)	Carbonate (CO32-) (mg/L)
WQSP-3	4/4/2002	36		2	125000	2270	6.8	1960	73200	7540	1500		
WQSP-3	2003	34			134000	2090	6.4	1550	82600	7870	1460		
WQSP-3	2004	38			121000	2230	6.94	2230	57400	6980	1480		
WQSP-3	2005	34			144000	2710	6.77	2490	77500	8060	1980		
WQSP-3	2006	34			140000	2280	7.03	2870	62400	8780	1340		
WQSP-3	2007	42			136000	3190	7.05	2000	96400	8580	2020		
WQSP-3	2008	32			121000	2430	6.54	2460	91100	7190	1510		
WQSP-3	2009	30.2			138000	2390	6.77	1570	75100	7950	1480		
WQSP-3	2010	30.7			140000	2490	6.77	1570	81700	8070	1520		
WQSP-3	2011	32.6			158000	2390	6.79	1420	76000	8490	1470		
WQSP-3	2012	32.8			145000	2390	6.85	1530	79200	8060	1550		
WQSP-3	2013				127000	2300	6.83	1510			1440		
WQSP-3	2014				114000	2310	6.83	1510			1390		
WQSP-3	2015				149000	2360	6.79	1520			1490		
WQSP-3	2016				133000	2210	6.85	1670			1490		
WQSP-3	2017	43			128000	2300	6.86	1420	74500	7920	1490	43	
WQSP-3	2018	37			119000	2570	6.92	1600	81000	7300	1740	37	
WQSP-3	2019	43			136000	2300	7.03	1440	75600	6900	1490	43	
WQSP-3	2020	34			134000	2430	6.84	1550	82700	7640	1560	34	
Ave.	**1995-2020**	**36**	**95**		**131656**	**2288**	**7**	**1868**	**78307**	**7543**	**1470**	**39**	
CV		**15%**	**21%**		**7%**	**11%**	**2%**	**29%**	**20%**	**7%**	**12%**	**11%**	
WQSP-4	9/28/1995	40	55.7		61200	1270	7.16	764	35900	7100	1710		
WQSP-4	5/23/1996	29	52.8		61500	1100	7.55	700	33600	6520	1570		
WQSP-4	9/12/1996	39	52		59700	1140	7.23	733	33300	6860	1590		
WQSP-4	6/5/1997	38	52.4		59500	1040	7.125	672	30800	7040	1490		
WQSP-4	9/11/1997	41	51.4		58700	1130	7.125	681	32600	6940	1480		
WQSP-4	5/6/1998	38	47.7		57100	1280	7.1	760	37300	6020	1600		
WQSP-4	9/23/1998	44	42		53000	1230	7.2	1370	31700	6000	1560		

Information Only

Well ID	Sample Date	ALKALINITY Total (mg/L)	Br	Percent Error	Cl (mg/L)	Mg (mg/L)	pH	K (mg/L)	Na (mg/L)	SO4 (mg/L)	Ca (mg/L)	Bicarbonate (HCO3-) (mg/L)	Carbonate (CO32-) (mg/L)
WQSP-4	4/21/1999	39			57000	1040	7.2	935	32900	6800	1480		
WQSP-4	10/13/1999	38	52		57000	1249	7	980	30310	6500	1640		
WQSP-4	4/12/2000	41	58		59000	1180	7.1	1180	34000	6700	1610		
WQSP-4	10/18/2000	36	46		60000	1190	7.2	1320	30700	6700	1560		
WQSP-4	4/18/2001	40	53.2		54900	1050	7.3	1020	35000	6470	1520		
WQSP-4	10/17/2001	36	82		55300	1093	7.1	1221	34100	6300	1470		
WQSP-4	4/17/2002	42			49700	1260	7.1	1220	27200	6560	1610		
WQSP-4	2003	32			54500	1160	6.8	695	32800	6930	1440		
WQSP-4	2004	38			59800	1090	7.28	1190	29000	6770	1450		
WQSP-4	2005	42			67200	1180	7.2	1320	32400	6980	1510		
WQSP-4	2006	42			66500	1400	7.36	1570	29500	7920	1870		
WQSP-4	2007	40			75600	1180	7.19	1020	39600	9130	1600		
WQSP-4	2008	40			56200	1190	7.11	1060	36200	5750	1580		
WQSP-4	2009	38.2			61700	1170	7.16	706	34400	6830	1530		
WQSP-4	2010	37			65500	1330	7.17	793	39500	7410	1670		
WQSP-4	2011	39.8			68300	1260	7.16	763	36500	7610	1620		
WQSP-4	2012	39.9			61900	1260	7.19	780	35700	7180	1750		
WQSP-4	2013				62900	1150	7.20	701			1630		
WQSP-4	2014				56300	1200	7.09	742			1630		
WQSP-4	2015				64400	1230	7.06	788			1640		
WQSP-4	2016				62600	1250	7.15	810			1580		
WQSP-4	2017	38			58500	1250	7.14	737	36800	7300	1700	38	
WQSP-4	2018	38			63100	1190	7.13	767	35000	6700	1680	38	
WQSP-4	2019	39			54700	1250	7.15	756	38000	6890	1650	39	
WQSP-4	2020	40			59900	1190	7.23	739	35800	6980	1620	40	
Ave.	**1995-2020**	**39**	**54**		**60100**	**1193**	**7**	**922**	**33950**	**6889**	**1595**	**39**	
CV		**8%**	**18%**		**8%**	**7%**	**2%**	**27%**	**9%**	**9%**	**6%**	**2%**	
WQSP-5	11/20/1995	52	21.3	5	15000	434	7.8	286	8880	5370	987		

Information Only

Well ID	Sample Date	ALKALINITY Total (mg/L)	Br	Percent Error	Cl (mg/L)	Mg (mg/L)	pH	K (mg/L)	Na (mg/L)	SO4 (mg/L)	Ca (mg/L)	Bicarbonate (HCO3-) (mg/L)	Carbonate (CO32-) (mg/L)
WQSP-5	6/6/1996	41	21	6	15700	427	7.63	290	9580	5730	1020		
WQSP-5	9/26/1996	49	43.2	6	15700	421	7.58	292	9400	5240	1010		
WQSP-5	6/19/1997	52	29.9	8	14500	452	7.535	284	9220	4460	980		
WQSP-5	9/25/1997	49	29.7	3	15300	441	7.705	282	9160	4900	986		
WQSP-5	5/20/1998	48	21.5	4	15300	485	7.7	304	10500	4970	1040		
WQSP-5	10/7/1998	48	22	8	19000	508	7.7	360	9560	5400	1100		
WQSP-5	5/5/1999	50		1	15000	474	7.6	527	9675	4900	1090		
WQSP-5	10/27/1999	44	23	4	15000	484	7.5	385	8380	4300	1071		
WQSP-5	4/26/2000	48	28	10	16000	850	7.5	594	8470	5400	1410		
WQSP-5	11/1/2000	46	19	3	16000	454	7.6	395	9040	5200	1020		
WQSP-5	5/2/2001	46	27.8	4	16100	425	7.58	474	9756	4890	1011		
WQSP-5	10/31/2001	46	21.8	9	15600	545	7.6	452	10600	4690	1090		
WQSP-5	5/1/2002	46		9	15900	451	7.6	398	8740	5230	1010		
WQSP-5	2003	50			15400	485	7.1	322	10100	4900	1130		
WQSP-5	2004	44			15100	408	7.54	412	7600	4540	924		
WQSP-5	2005	46			18100	474	7.55	539	8420	5520	1020		
WQSP-5	2006	48			15900	489	7.65	568	8180	5280	1050		
WQSP-5	2007	50			17100	431	7.23	368	10200	6410	1010		
WQSP-5	2008	60			14800	451	7.41	387	9880	4690	1020		
WQSP-5	2009	43.5			16800	456	7.42	312	10400	5330	1010		
WQSP-5	2010	45.1			16000	492	7.48	313	10200	5760	1050		
WQSP-5	2011	48			15900	480	7.49	297	9310	5480	1110		
WQSP-5	2012	52.4			16900	505	7.6	313	10900	5430	1080		
WQSP-5	2013				14300	424	7.32	313			1010		
WQSP-5	2014				14000	454	7.49	289			1030		
WQSP-5	2015				16800	586	7.53	343			1110		
WQSP-5	2016				16000	610	7.6	346			1070		
WQSP-5	2017	48			14400	608	7.54	338	11200	4570	1090	48	

Information Only

Well ID	Sample Date	ALKALINITY Total (mg/L)	Br	Percent Error	Cl (mg/L)	Mg (mg/L)	pH	K (mg/L)	Na (mg/L)	SO4 (mg/L)	Ca (mg/L)	Bicarbonate (HCO3-) (mg/L)	Carbonate (CO32-) (mg/L)
WQSP-5	2018	51			17000	578	7.51	323	10000	4700	1140	51	
WQSP-5	2019	47			15000	560	7.52	330	11000	4800	1100	47	
WQSP-5	2020	47			14000	530	7.49	310	9800	4800	1100	47	
Ave.	**1995-2020**	**48**	**26**		**15738**	**496**	**8**	**367**	**9577**	**5103**	**1059**	**48**	
CV		**7%**	**25%**		**7%**	**17%**	**2%**	**24%**	**9%**	**9%**	**8%**	**4%**	
WQSP-6	10/16/1995	52.5	11.2		15800	250	7.81	182	6070	5590	719		
WQSP-6	3/12/1996	54			6200	214	7.62	199	5540	4730	663		
WQSP-6	6/27/1996	48	9.64		6198	199	7.62	152	4470	4523	696		
WQSP-6	4/3/1997	53	9.39		5973	203	7.74	150	4280	4670	662		
WQSP-6	6/25/1997	47	13.9		5500	210	7.695	148	4210	5100	572		
WQSP-6	6/3/1998	43	8.84		6070	219	7.8	161	4890	4660	714		
WQSP-6	10/21/1998	46			6000	200	7.82	144		4800	680		
WQSP-6	5/19/1999	46	6		5900	201	7.7	215	4460	4400	675		
WQSP-6	11/3/1999	44	13		6000	214	7.7	239	4350	5000	677		
WQSP-6	5/10/2000	45			5600	222	7.7	184	4280	4700	707		
WQSP-6	11/15/2000	48	10		5500	226	7.7	224	4120	4800	747		
WQSP-6	5/16/2001	42	6.04		5140	212	7.71	208	4320	4600	663		
WQSP-6	11/7/2001	46	6.36		4970	234	7.8	278	4090	4500	672		
WQSP-6	5/15/2002	46			4990	238	7.47	221	3870	4640	738		
WQSP-6	2003	48			5410	218	7.4	175	4120	4670	662		
WQSP-6	2004	48			4950	187	7.76	177	3550	4450	606		
WQSP-6	2005	44			6140	232	7.63	275	3980	5260	736		
WQSP-6	2006	52			6250	237	7.79	288	3470	5800	766		
WQSP-6	2007	48			5930	188	7.72	180	5210	5820	679		
WQSP-6	2008	52			5030	205	7.83	184	4430	4450	672		
WQSP-6	2009	45.7			5900	213	7.69	157	4250	5000	680		
WQSP-6	2010	44.4			5510	215	7.65	155	4420	4480	671		
WQSP-6	2011	48.2			5060	222	7.64	167	4290	4490	714		

Information Only

Well ID	Sample Date	ALKALINITY Total (mg/L)	Br	Percent Error	Cl (mg/L)	Mg (mg/L)	pH	K (mg/L)	Na (mg/L)	SO4 (mg/L)	Ca (mg/L)	Bicarbonate (HCO3-) (mg/L)	Carbonate (CO32-) (mg/L)
WQSP-6	2012	45			5900	221	7.83	160	4720	4990	688		
WQSP-6	2013				5010	199	7.66	147			675		
WQSP-6	2014				5090	205	7.79	150			665		
WQSP-6	2015				5120	215	7.79	158			709		
WQSP-6	2016				5790	214	7.84	157			684		
WQSP-6	2017	53			4300	212	7.82	153	4280	4870	669	53	
WQSP-6	2018	49			5160	206	7.78	150	4300	4500	696	49	
WQSP-6	2019	48			4800	220	7.66	160	4400	4700	680	48	
WQSP-6	2020	51			5000	200	7.82	150	4600	4600	650	51	
Ave.	**1995-2020**	**48**	**9**		**5818**	**214**	**8**	**183**	**4406**	**4814**	**684**	**50**	
CV		**7%**	**27%**		**32%**	**7%**	**1%**	**22%**	**12%**	**8%**	**5%**	**4%**	

Notes:

- Where a specific Sample Date is not available, the year is provided instead.
- All data and References are summarized at file path: CVS/CVSLIB/WIPP EXTERNAL/ap194

Information Only

6 References

Abdi, H., *Coefficient of Variation*, In Neil Salkaind (Ed.), Encyclopedia of Research Design. Thousand Oaks, CA: Sage. 2010

Adams, S., Titus, R., Pietersen, K., Tredoux, G., Harris, C., 2001. *Hydrochemical characteristics of aquifers near Sutherland in the western Karoo, South Africa.* Journal Hydrology. 2001, 241, 91-103.

Alcalá, F. J. and Custodio, E. 2004. *Use of the Cl/Br ratio as tracer to identify the origin of salinity in some Spanish coastal aquifers* SWIM pp 481–97

Alcalá, F. J. and Custodio, E. 2008 *Using the Cl/Br ratio as a tracer to identify the origin of salinity in aquifers in Spain and Portugal* Journal of Hydrology. 359 189–207

Beauheim, R.L., and Holt, R. M., 1990. *Hydrogeology of the WIPP Site. Geological and Hydrological Studies of Evaporites in the Northern Delaware Basin for the Waste Isolation Pilot Plant (WIPP), New Mexico* (pp. 131–79). Geological Society of America Field Trip No. 14 Guidebook. Dallas: Dallas Geological Society.

Beauheim, R.L. 2007. Diffusivity mapping of fracture interconnections. In Proceedings of the 2007 US EPA/NGWA Fractured Rock Conference. Westerville, OH, 2007. National Ground Water Association

Bodine, M. W., Jones, B. F., 1990. *Normative analysis of groundwaters from the Rustler Formation associated with the Waste Isolation Pilot Plant (WIPP), southeastern New Mexico.* Fluid Mineral Interactions: A Tribute to H.P Eugster. The Geochemical Society, Special Publication No 2., 1990.

Braitsch, O., 1971. *Salt Deposits – Their Origin and Composition*, translators P.J. Burek and A.E.M. Nairn Berlin-Heidelberg-New York: Springer-Verlag

Bowman, D.O. 2019. *Milestone Report for WIPP Water Qualities Collected from 2017 to 2018. Milestone Report for Groundwater Sampling.* Sandia National Laboratories. Carlsbad, New Mexico. ERMS 571297

Carol, E.S., Kruse, E. E., Laurencena, P.C., Rojo, A., Deluchi, M.H., 2012. *Ionic Exchange in groundwater hydrochemical evolution. Study case: the drainage basin of El Pescado creek (Buenos Ares province, Argentina).* Environmental Earth Science (2012) 65:421-428.

Information Only

Cartwright, I, Weaver, T.R. and Keith Fifield, L. 2006. *Cl/Br ratios and environmental isotopes as indicators of recharge variability and groundwater flow: An example from the southeast Murray Basin, Australia* Chemical Geology. 231 38–56

Chadha, D.K. 1999. *A Proposed New Diagram for Geochemical Classification of Natural Waters and Interpretation of Chemical Data.* Hydrogeology Journal, 7, 431-439.

Chapman, J.B., 1988. *Chemical and Radiochemical Characteristics of Groundwater in the Culebra Dolomite, Southeastern New Mexico.* EEG-39. Albuquerque, NM: New Mexico Environmental Evaluation Group.

Combs, D.W., 1975. *The Mineralogy, Petrology and Bromine Geochemistry of Selected Samples of the Salado Salt, Lea and Eddy Counties, New Mexico – A Potential Horizon for the Disposal of Radioactive Waste.* ORNL/Sub/3670-5. University of Tennessee.

Corbet, T.F., and Knupp, P. M., 1996. *The Role of Regional Groundwater Flow in the Hydrogeology of the Culebra Member of the Rustler Formation at the Waste Isolation Pilot Plant (WIPP), Southeastern New Mexico.* SAND96-2133. Albuquerque, NM: Sandia National Laboratories.

Deocampo, D. M. and Jones, B. F., 2003. *Geochemistry of Saline Lakes.* Treatise on Geochemistry 2nd Edition. http://dx.doi.org/10.1016/B978-0-08-095975-7.00515-5

Domski, P. and Beauheim, R.L. 2008. *AP-125 Analysis Report: Evaluation of Culebra Brine Chemistry.* Sandia National Laboratories. Carlsbad, New Mexico. ERMS 549443

Eugster, H. P. and Jones, B. F., 1979. *Behavior of Major Solutes During Closed-basin Brine Evolution.* American Journal of Science, Vol. 279, June 1979, P. 609-631.

Freeman, J. T. 2007. *The use of bromide and chloride mass ratios to differentiate salt-dissolution and formation brines in shallow groundwaters of the Western Canadian Sedimentary Basin.* Hydrogeology Journal. 15 1377–85

Hansen, C., 2021. *Review of Conceptual Models for the Additional Panels Performance Assessment.* Sandia National Laboratories. Carlsbad, New Mexico. ERMS 575130

Hardie, L.A., Eugster, H. P., 1978. *Saline Lakes. In: Lerman A (ed) Lakes chemistry, geology, physics.* Springer, New York, 230 p.

Heston, D., 2015. *Using Chloride and Bromide Mass Ratios and Binary Mixing Curves to Evaluate Anthropogenic Influences on Groundwater in Lycoming and Wayne counties*, Pennsylvania

Information Only

Holt, R. M., Powers, D.W., 1988. *Facies variability and post-depositional alteration within the Rustler formation in the vicinity of the Waste Isolation Pilot Plant, Southeastern New Mexico*: WIPP-DOE-88-004. Department of Energy, Carlsbad, NM.

Holt, R.M., 1997. *Conceptual Model for Transport Processes in the Culebra Dolomite Member, Rustler Formation.* SAND-0194. Albuquerque, NM: Sandia National Laboratories

Holt, R.M., Beauheim, R.L., Powers, D.W. 2005. *Predicting Fractured Zones in the Culebra Dolomite*: SAND2005-4435 J, Sandia National Laboratories, Albuquerque, NM.

Hounslow, A.W. 1995. *Water quality data analysis and interpretation.* Lewis Publishers, Boca Raton. https://doi.org/10.1201/9780203734117

Johnson, P.B., 2015. SP 9-11 *Calculation of Densities for Groundwater in WIPP Wells.* Sandia National Laboratories, Albuquerque, NM. ERMS # 565218

Kim, K. 2002. *Plagioclase weathering in the groundwater system of a sandy, silicate aquifer* Hydrol. Process. 2002, 16, 1793-1806.

Kloppmann, W., Negrel, Ph., Cassanova, J., Klinge, H., Schelkes, K., Guerrot, C., 2001. *Halite dissolution derived brines in the vicinity of a Permian salt dome (N German Basin). Evidence from boron, strontium, oxygen, and hydrogen isotopes.* Geochimica et Cosmochimica Acta 65 (22), 4087-4101.

Kuhlman, K., and Barnhart, K.S., 2011. Hydrogeology Associated with the Waste Isolation Pilot Plant. SAND2011-0036C. Sandia National Laboratories, Carlsbad, NM.

Lak, R., Mohammadi, A., Darvishi Khatooni, J., 2022. *Lake Urmia Brine Evolution from 2007 to 2019. In: The Handbook of Environmental Chemistry.* Springer, Berlin Heidelberg. https://doi.org/10.1007/698_2021_807.

Lakshmanan, E., Kannan, R., Senthil Kumar, M., 2003. *Major ion chemistry and identification of hydrogeochemical processes of ground water in a part of Kancheepuram district, Tamil Nadu, India.* Environmental Geosciences, Vol.10, No. 4, pp.157-166.

Lambert, S.J., 1983. *Dissolution of evaporites in and around the Delaware Basin, southeastern New Mexico and west Texas*: SAND82-0461, Sandia National Laboratories, Albuquerque, NM.

Information Only

Lambert, S.J., 1991. *"Isotopic Constraints on the Rustler and Dewey Lake Groundwater Systems", in M.D. Siegel, S.J. Lambert, and K.L. Robinson, Eds., Hydrogeochemical Studies of the Rustler Formation and Related Rocks in the Waste Isolation Pilot Plant Area, Southeastern New Mexico*. SAND88-0196. Albuquerque, NM: Sandia National Laboratories

Lofton, O.W. 2021. *Milestone Report for WIPP Water Qualities Collected from 2019 to 2020. Milestone Report for Groundwater Sampling.* Sandia National Laboratories. Carlsbad, New Mexico. ERMS 576354

Malama, B., Kuhlman, K.L., James, S.C., 2013. *Core-scale solute transport model selection using Monte Carlo analysis*. Water Resources Research, Vol. 49. 3133-3147.

Park J, M., C. Bethke, T. Torgersen and T. Johnson. 2002. *Transport modeling applied to the interpretation of groundwater ^{36}Cl age*. Water Resources Research. Volume 38, Issue 5. May, 2002.

Parkhurst, D.L., and Appelo, C.A.J. 1999. *User's Guide to PHREEQCI (Version 2)—A computer program for Speciation, Batch-Reaction, One-Dimensional Transport, and Inverse Geochemical Calculations:* U.S. Geological Survey Water-Resources Investigations Report 99-4259, 312p.

Piper, A.M., 1944. *A Graphic Procedure in the Geochemical Interpretation of Water Analyses.* Transactions, American Geophysical Union. 25(6):914-923

Powers, D.W. 2007. *Analysis Report for Task 1A of AP-114: Refinement of Rustler Halite Margins Within the Culebra Modeling Domain.* ERMS# 547559. Carlsbad, NM: Sandia National Laboratories, WIPP Records Center.

Ramey, D.S. 1985, *Chemistry of Rustler Fluids*: EEG-31. Albuquerque, NM: New Mexico Environmental Evaluation Group.

Raup, O.B., and Hite, R.J. 1996. *Bromine Geochemistry of Chloride Rocks of the Middle Pennsylvanian Paradox Formation of the Hermosa Group, Pardox Basin, Utah and Colorado.* U.S. Geological Survey Bulletin 2000-M.

Reardon, A., Bowman, D.O., and Kirkes, L. 2021. *Milestone Report for WIPP Downhole Density Measurements.* Sandia National Laboratories. Carlsbad, New Mexico. ERMS 576350.

Roberts, R.M., Beauheim, R.L., and Domski, P.A., 1999. *Hydraulic Testing of Salado Formation Evaporites at the Waste Isolation Pilot Plant Site: Final Report.* SAND98-2537. Albuquerque, NM: Sandia National Laboratories.

Information Only

Sewards, T., Williams, M. L., and Keil, K. 1991. *Mineralogy of the Culebra Dolomite Member of the Rustler Formation.* SAND90-7008. Albuquerque, NM: Sandia National Laboratories.

Siegel, M.D., Lambert, S. J., and Robinson, K. L., eds. 1991. *Hydrogeochemical Studies of the Rustler Formation and Related Rocks in the Waste Isolation Pilot Plant Area, Southeastern New Mexico.* SAND88-0196. Albuquerque, NM: Sandia National Laboratories.

Sonney, R., and Vuataz, F-D., 2010. *Use of Cl/Br to Decipher the Origin of Dissolved Mineral Components in Deep Fluids from the Alps Range and Neighboring Areas.* Published in Proceedings World Geothermal Congress, session 15, 1504, 1-13, 2010.

Tay, C. K., 2021. *Hydrogeochemical framework of groundwater within the Asutifi-North District of the Brong-Ahafo Region, Ghana.* Applied Water Science (2021) 11:72.

U.S. Department of Energy Carlsbad Field Office. 2021. Waste Isolation Pilot Plant Annual Site Environmental Report for 2020 Revision 0 September 29, 2021. DOE/WIPP-21-3591.

Vento, A. and Bowman, D.O., 2019. *Milestone Report for H-6bR Water Density Stratification Investigation. Milestone Report for Groundwater Sampling.* Sandia National Laboratories. Carlsbad, New Mexico. ERMS 571997.

Walraevens, K., Bakundukize, C., Mtoni, Y.E., Van Camp, M., 2018. *Understanding the hydrogeochemical evolution of groundwater in Precambrian basement aquifers: A case study of Bugesera region in Burundi.* J. Geochem. Explor. 2018, 188, 24-42.

Wu, C., Wu, X., Lu, C., Sun, Q., He, X., Yan, L., Qin, T., 2021. *Hydrogeochemical Characterization and its Seasonal Changes of Groundwater Based on Self-Organizing Maps.* Water, 2021, 13, 3065.

Zhang, B., Zhao, D., Zhou, P., Qu, S., Liao, S., and Wang, G. 2020. *Hydrochemical Characteristics of Groundwater and Dominant Water-Rock Interactions in the Delingha Area, Qaidam Basin, Northwest China.* Water, 2020, 12, 836.doi:10.3390/w12030836.

Information Only